



12-1993

## Application of Fuzzy Logic for Performance Enhancement of Drives

Gilberto Costa Sousa  
*University of Tennessee - Knoxville*

Follow this and additional works at: [https://trace.tennessee.edu/utk\\_graddiss](https://trace.tennessee.edu/utk_graddiss)

 Part of the [Electrical and Computer Engineering Commons](#)

---

### Recommended Citation

Sousa, Gilberto Costa, "Application of Fuzzy Logic for Performance Enhancement of Drives. " PhD diss., University of Tennessee, 1993.  
[https://trace.tennessee.edu/utk\\_graddiss/3384](https://trace.tennessee.edu/utk_graddiss/3384)

This Dissertation is brought to you for free and open access by the Graduate School at TRACE: Tennessee Research and Creative Exchange. It has been accepted for inclusion in Doctoral Dissertations by an authorized administrator of TRACE: Tennessee Research and Creative Exchange. For more information, please contact [trace@utk.edu](mailto:trace@utk.edu).

To the Graduate Council:

I am submitting herewith a dissertation written by Gilberto Costa Sousa entitled "Application of Fuzzy Logic for Performance Enhancement of Drives." I have examined the final electronic copy of this dissertation for form and content and recommend that it be accepted in partial fulfillment of the requirements for the degree of Doctor of Philosophy, with a major in Engineering Science.

Bimal K. Bose, Major Professor

We have read this dissertation and recommend its acceptance:

Frederick W. Symonds, Walter L. Green, J. M. Bailey, B. R. Upadhyaya

Accepted for the Council:

Carolyn R. Hodges

Vice Provost and Dean of the Graduate School

(Original signatures are on file with official student records.)

To the graduate Council:

I am submitting herewith a dissertation written by Gilberto Costa D. Sousa entitled "Application of Fuzzy Logic for Performance Enhancement of Drives". I have examined the final copy of this dissertation for form and content and recommend that it be accepted in partial fulfillment of the requirements for the degree of Doctor of Philosophy, with a major in Electrical Engineering.

Bimal K. Bose  
Bimal K. Bose, Major Professor

We have read this dissertation  
and recommend its acceptance:

Federick W. Symonds  
Walter R. M. Dean  
J. M. Bailey  
Belle R. Upadhyaya

Accepted for the Council:

C. W. Minkel  
Associate Vice Chancellor  
and Dean of The Graduate School

**APPLICATION OF FUZZY LOGIC FOR PERFORMANCE  
ENHANCEMENT OF DRIVES**

A Dissertation

Presented for the

Doctor of Philosophy

Degree

The University of Tennessee, Knoxville

Gilberto Costa D. Sousa

December 1993



## ACKNOWLEDGMENTS

This work has been made possible due to the generosity of several people and institutions. I would like to initially thank my employer, The Federal University of Espirito Santo (UFES), and the Brazilian Council of Scientific and Technological Development (CNPq) for their invaluable financial support. I am also grateful to Research Triangle Institute (RTI) for funding part of this work.

I wish to express my deep appreciation to my advisor, Prof. B. K. Bose for his guidance and constant challenges that helped me mature in this new field. Thanks are in order to Profs. J. M. Bailey, W. L. Green, F. W. Symonds, and B. R. Upadhyaya, for their kindness in serving as my supervisory committee.

A special thank is reserved for Dr. K. S. Kim, of Goldstar Industrial Systems Co., Korea, for designing the basic vector control system and introducing me to the practical aspects of drive technology. I am also grateful to Prof. M. G. Simoes for the preliminary study on converter modeling. The support of R. L. Lambert and other Power Electronics Application Center staff members has been of great help.

Finally, I would like to express my gratitude to my wife, Loise C. P. Drumond, for her unconditional emotional support, as well as for helping me in the preparation of this manuscript.

## ABSTRACT

Fuzzy logic shows enormous potential for advancing power electronics technology. Its application to DC and AC drives control is discussed here.

Initially, a phase-controlled bridge converter DC drive was considered. Analysis of converter performance at continuous and discontinuous conduction modes was first conducted. Fuzzy control was used to linearize the transfer characteristics of the converter in discontinuous conduction mode. It was then extended to current and speed loops, replacing the conventional proportional-integral controllers. The control algorithms were developed in detail, and verified by PC-SIMNON (developed by Lund Institute of Technology, Sweden) digital simulation. Significant performance improvement was achieved over conventional control methods.

Efficiency optimization of an indirect vector controlled induction motor drive was next considered. An accurate loss model of the converter induction machine system was first developed. Steady-state fundamental and harmonics loss characteristics, besides the dynamics of the machine were analyzed and incorporated in the model, resulting in a new synchronous frame dynamic  $D^e$ - $Q^e$  equivalent circuit. The converter system has been modeled accurately for conduction and switching losses. The lossy models were then used in the validation of the fuzzy logic based on-line efficiency optimization control. At steady-state, the fuzzy controller adaptively changes the excitation current on the basis of measured input power, until the maximum efficiency point is reached. The pulsating

torque, due to flux reduction, has been compensated by an ingenious feedforward scheme. During transients, rated flux is established, to get the best transient response. After a comprehensive simulation study, an experimental 5 hp drive system was tested, with the proposed controller implemented on a Texas Instrument TMS320C25 digital signal processor, and the theoretical development was fully validated.

Finally, fuzzy logic was applied in combination with model-reference adaptive control (MRAC) technique to slip gain tuning of an indirect vector controlled induction motor drive. The MRAC methods based on reactive power and D-axis voltage were combined through a weighting factor, generated by a fuzzy controller, that ensures the use of the best method for any point in the torque-speed plane. A second fuzzy controller tunes the slip gain based on combined detuning error and its slope. The drive performance was extensively investigated through simulations and experiments. The results confirmed the validity of the proposed method.

## TABLE OF CONTENTS

1.	INTRODUCTION.....	1
1.1	Artificial Intelligence and Adjustable Speed Drives.....	1
1.2	Principles of Fuzzy Logic Control.....	3
1.3	Outline of Dissertation.....	12
2.	FUZZY CONTROL OF A DC DRIVE SYSTEM.....	15
2.1	Introduction.....	15
2.2	Fuzzy Controlled DC Drive System.....	19
2.2.1	Fuzzy Linearization of Converter Characteristics.....	24
2.2.2	Fuzzy Control of Current and Speed Loops.....	29
2.3	Simulation Study.....	34
3.	LOSS MODELING OF CONVERTER INDUCTION MACHINE SYSTEMS .....	48
3.1	Introduction.....	48
3.2	Dynamic Lossy Model for the Induction Machine.....	51
3.2.1	Induction Machine Losses.....	53
3.2.2	Temperature and Saturation Effects.....	57

3.2.3	Per-phase Harmonic Equivalent Circuit.....	59
3.2.4	Synchronous Frame Lossy Equivalent Circuit.....	62
3.2.5	Lossy Model Parameter Computation.....	68
3.3	Loss Modeling of Converter System.....	73
3.3.1	Loss Modeling of Diode Rectifier.....	73
3.3.2	Loss Modeling of PWM Inverter.....	75
3.4	Model Validation.....	85
4.	<b>FUZZY EFFICIENCY OPTIMIZATION CONTROL.....</b>	<b>95</b>
4.1	Introduction.....	95
4.2	Fuzzy Efficiency Optimization of a Vector Control Drive.....	98
4.2.1	The Efficiency Optimization Controller.....	102
4.2.2	Feedforward Pulsating Torque Compensation.....	108
4.2.3	Transition to Optimum Transient Response Mode.....	112
4.3	Simulation Program Development.....	114
4.4	Simulation Study.....	122
4.5	Hardware Circuit Design.....	127
4.5.1	Current Controller.....	129
4.5.2	Monitoring and Protection.....	129
4.5.3	Speed Measurement and Control Interface.....	132
4.5.4	DC Link Voltage and Current Sensing Interface.....	134

4.6	Real Time Software Design.....	134
4.6.1	Basic Vector Control Functions.....	137
4.6.2	Speed Computation.....	138
4.6.3	Efficiency Optimization controller.....	138
4.7	Experimental Study.....	140
5.	FUZZY LOGIC BASED SLIP GAIN TUNING.....	152
5.1	Introduction.....	152
5.2	Fuzzy Tuning Controller.....	158
5.2.1	Reactive Power and D-axis Voltage Regulators.....	160
5.2.2	Derivation of Combined Error Signal.....	162
5.2.3	Design of the Fuzzy Tuning Controller.....	164
5.3	Simulation Study.....	170
5.4	Hardware Design.....	172
5.5	Real Time Software Design Issues.....	177
5.6	Experimental Study.....	181
6.	CONCLUSIONS AND RECOMMENDATIONS FOR FUTURE RESEARCH .....	187
	REFERENCES.....	193

APPENDICES.....	200
A. SIMNON Simulation Programs Listing .....	201
A.1 DC Drive Programs .....	201
A.2 Loss Modeling and Efficiency Optimization Programs .....	209
A.3 Slip Gain Tuning Programs .....	222
B. TMS320C25 Assembly Programs Listing .....	228
B.1 Efficiency Optimization and Vector Control Programs .....	228
B.2 Slip Gain Tuning Assembly Programs .....	260
VITAE .....	285

## LIST OF TABLES

2.1	Rule base for $\Delta\alpha$ compensation.....	25
2.2	Rule base for current and speed controllers.....	32
2.3	Parameters of DC drive system.....	35
2.4	Performance comparison of fuzzy and PI controlled drive system.....	45
3.1	Power circuit parameters of the AC drive system.....	88
4.1	Rule base for the fuzzy efficiency controller.....	107
4.2	Induction machine parameters for efficiency optimization studies .....	123
5.1	Rule base for weighting factor ( $K_f$ ) calculation.....	168
5.2	Rule base for increment of slip gain ( $\Delta K_s$ ).....	171
5.3	Parameters for the induction servomotor .....	171



## LIST OF FIGURES

1.1 Representation of temperature using crisp sets and fuzzy sets .....	4
1.2 Basic operations involving fuzzy sets.....	6
1.3 Fuzzy composition method by SUP-MIN principle.....	9
1.4 Basic structure of a fuzzy controlled system.....	10
2.1 Four quadrant phase-controlled converter dc drive.....	16
2.2 Converter voltage and current waveforms.....	18
2.3 Fuzzy controlled dc drive system.....	20
2.4 Theoretical $V_d$ - $I_a$ (pu) phase plot without compensation.....	23
2.5 Membership functions for $\Delta\alpha$ compensation.....	26
2.6 Membership functions of speed and current controllers.....	31
2.7 Open loop $V_d$ step ( $\alpha = 70^\circ$ ) response without compensation.....	36
2.8 Phase plot $V_d$ - $I_a$ with $\Delta\alpha$ compensation.....	38
2.9 Open loop $V_d$ step response with $\Delta\alpha$ compensation.....	39
2.10 Current loop response of the fuzzy controller.....	40
2.11 Current loop response of the PI controller.....	41
2.12 Fuzzy control system response to a $\omega_r^*$ step and $T_L$ step.....	42
2.13 PI control system response to a $\omega_r^*$ step and $T_L$ step.....	43
2.14 Fuzzy control system response to a $\omega_r^*$ step with a new inertia of four times the original value.....	46

2.15 PI control system response to a $\omega_r^*$ step with a new inertia of four times the original value.....	47
3.1 Per-phase equivalent circuit.....	49
3.2 Standard D-Q equivalent circuits in synchronous frame.....	49
3.3 Converter-machine system for variable speed drive.....	52
3.4 Per-phase harmonic equivalent circuit of the induction motor.....	60
3.5 D <sup>s</sup> -Q <sup>s</sup> equivalent circuit with core loss resistance.....	64
3.6 D <sup>e</sup> -Q <sup>e</sup> equivalent circuit with core loss resistance.....	67
3.7 Lossy D <sup>e</sup> -Q <sup>e</sup> equivalent circuits in synchronously rotating reference frame.	69
3.8 Diode rectifier equivalent circuit.....	74
3.9 Rectifier voltage and current waves.....	74
3.10 Transistor inverter phase leg with conduction loss equivalent circuit .....	76
3.11 Pulse width modulation waves for phase leg A .....	78
3.12 Typical turn-on and turn-off switching waves for transistor Q <sub>1</sub> .....	80
3.13 Q <sup>e</sup> -axis circuit showing loops for state equations derivation.....	87
3.14 Steady state performance.....	90
3.15 Rotor flux responses at constant speed.....	91
3.16 Torque responses of the drive at rated flux.....	93
4.1 Simulation of the input power minimization process.....	97
4.2 Indirect vector controlled induction motor drive incorporating the efficiency optimization controller.....	99
4.3 Principle of efficiency optimization control with rotor flux programming...	101

4.4	Efficiency optimization control block diagram.....	103
4.5	Membership functions for the fuzzy efficiency control .....	106
4.6	Principles of feedforward torque compensation.....	109
4.7	Feedforward pulsating torque compensator block diagram.....	111
4.8	Transition between efficiency optimization and transient response optimization modes.....	113
4.9	SIMNON simulation block diagram showing I/O variables.....	115
4.10	Fuzzy efficiency optimization flowchart.....	116
4.11	Evaluation of degree of membership.....	118
4.12	Feedforward torque compensation flowchart.....	121
4.13	Time domain simulated optimum efficiency search curves .....	124
4.14	Simulated efficiency curves.....	125
4.15	Drive performance in time domain with sudden increase of load torque ...	126.
4.16	Block diagram for vector control system hardware.....	128
4.17	Hysteresis band current controller.....	130
4.18	Monitoring and protection circuit diagram.....	131
4.19	Speed sensing and control interface.....	133
4.20	DC link voltage and current sensing.....	135
4.21	Software structure of the drive system including the efficiency optimization controller.....	136
4.22	Speed computation flowchart.....	139

4.23 AC supply phase voltage and current waveforms at $\omega_r=0.75$ pu and $T_L=0.50$ pu .....	142
4.24 Machine input currents at $\omega_r=0.75$ pu and $T_L=0.50$ pu .....	142
4.25 Experimental search curves at $\omega_r=0.25$ pu and $T_L=0.10$ pu, with pulsating torque compensation .....	143
4.26 Experimental search curves $\omega_r=0.50$ pu and $T_L=0.30$ pu .....	145
4.27 Search curves at $\omega_r=0.25$ pu and $T_L=0.10$ pu without pulsating torque compensation .....	147
4.28 Drive performance in time domain with sudden changes in command speed .....	148
4.29 Experimental efficiency curves .....	150
5.1 Indirect vector controlled induction motor drive with open loop torque and flux control.....	153
5.2 Steady-state detuning effects on torque and rotor flux.....	155
5.3 Transient response for developed torque and rotor flux .....	156
5.4 Indirect vector-controlled induction motor drive showing the proposed fuzzy tuning controller.....	159
5.5 Fuzzy logic based MRAC tuning control block diagram.....	163
5.6 Normalized control loop error vs. normalized slip gain curves ( $\omega_r=0.50$ pu) .....	165
5.7 Membership functions for FLC-1 .....	167
5.8 Membership functions for FLC-2 .....	169

5.10 Performance of tuning controller to a 100% increase in rotor resistance.....	174
5.11 Voltage sensing interface.....	176
5.12 Real time software flowchart.....	178
5.13 Phase-shift compensation phasor diagram .....	180
5.14 Saturation profile for $L_\sigma$ .....	182
5.15 Experimental tuning performance at $T_L=0.1$ pu and $K_s/K_{s0}(0)=2$ .....	183
5.16 Experimental tuning performance at $T_L=0.5$ pu and $K_s/K_{s0}(0)=5$ .....	183
5.17 Speed response at no load for a square-wave torque command ( $i_{qs}^*$ ) .....	186

# **CHAPTER 1**

## **INTRODUCTION**

### **1.1 Artificial Intelligence and Adjustable Speed Drives**

Adjustable speed drive technology has evolved enormously over the past 30 years. This evolution has been made possible because of technological advances in a number of related fields, such as power semiconductor devices, converter topologies and control techniques, microprocessors and digital signal processors (DSP). More recently, the application of intelligent control technologies, such expert systems, fuzzy logic and artificial neural networks, is advancing the frontier of this technology [19].

Among the artificial intelligence (AI) techniques, fuzzy logic is perhaps the most successful one, if judged from the standpoint of the number of practical applications [10]. Compared to other AI control techniques, i.e., expert systems and neural networks, fuzzy logic controllers numerically process structured knowledge that is embedded in only a few rules; expert systems symbolically process structured knowledge defined by a larger number of rules, whereas neural networks numerically process unstructured knowledge, and heavily depend on off-line learning techniques.

Fuzzy logic was introduced by Zadeh [1] in 1965, and can be viewed as a generalization of conventional Boolean logic. Its main purpose is the mathematical representation of imprecision and non-statistical uncertainty. The key concept in this

theory is that of a fuzzy set. A fuzzy set possesses a distinct feature of allowing partial membership, with degrees of membership varying from 0 (non-member) to 1 (full member). In contrast, in a "crisp" or Boolean set, a given element is a member of the set or it is not a member at all.

A fuzzy logic controller for a given process is capable of embedding in the control strategy, the qualitative knowledge and experience that an operator or engineer has about the process. Typically, the design of a fuzzy logic controller starts with a linguistic description of the control strategy, in the form of IF-THEN rules, that relate some process states (usually error and change in error), to the appropriate control action. The next step consists in making a quantitative interpretation of the linguistic variables, in the form of fuzzy sets. This is the most difficult step in the design process, and usually requires a significant number of iterations. The design process is completed by selecting an inference method, that essentially defines how the set of control rules, i.e., the rule base, is evaluated to derive the control action for a particular process state.

Fuzzy logic control does not require an accurate model of the plant, and therefore, it suits well to a process for which a formal model is unknown or ill-defined. It also works well for complex non-linear multi-dimensional systems, systems with parameter variation problem, or where the sensor signals are not precise.

Fuzzy Logic applications to power electronics and drives are almost entirely new, and this work is one of the first attempts to systematically apply fuzzy logic to the control of DC and AC drives. Prior to 1991, Li and Lau [5] applied fuzzy logic to a microprocessor-based servomotor controller, assuming a linear power amplifier. They also

compared system performance under PID control and model-reference adaptive control (MRAC) to that obtained with fuzzy control, and demonstrated the superiority of the latter. Da Silva et al [6] developed a fuzzy adaptive controller for a four quadrant power converter. The control system possesses a three-level hierarchical structure capable of identifying the best control law for any load condition, such that robust operation is achieved even under sudden changes in load.

Fuzzy logic shows enormous potential for advancing power electronics technology. Its ability to incorporate qualitative knowledge and to deal with imprecise information makes it very attractive to power electronics systems, where non-linearity is a common feature, and a precise model is difficult to obtain. In such cases, fuzzy logic can be applied to derive a linguistic model of the system, that describes its operational behavior. This fuzzy model can then be used in the design of a fuzzy controller for the system, just as a mathematical model is helpful in the design of a conventional controller.

## **1.2 Principles of Fuzzy Logic Control**

It is appropriate to review here some basic concepts of fuzzy logic and fuzzy control. Although numerous fuzzy inference methods have been proposed in the literature [11]-[12], this discussion is based on Zadeh's [1]-[2] and Mamdani's [3] approaches.

A fuzzy set is characterized by a membership function, that associates each element in the set to a number in the real interval  $[0,1]$ , that represents its grade of membership in the set. In contrast, a Boolean or "crisp" set is defined by a characteristic function, that maps all members to logic level 1 and the non-members to 0. Fig. 1.1



difference for the case of a hypothetical temperature control system. In Fig. 1.1(a), a crisp classification is provided, such that, the temperature value  $T = 67^\circ\text{F}$  is a member of the HOT set only. In contrast, in Fig. 1.1(b) temperature is considered a fuzzy variable, and  $T = 67^\circ\text{F}$  is a partial member of both MILD and HOT fuzzy sets. Because language is the primary vehicle for conveying knowledge, fuzzy variables are usually referred to as linguistic variables, and the fuzzy sets are viewed as the mathematical representation of their linguistic values ( e.g., COLD, MILD, and HOT in Fig. 1.1). The numerical interval, that is relevant for the description of a fuzzy variable, is commonly named Universe of Discourse (in Fig. 1.1, the real interval  $[20,90]$ ).

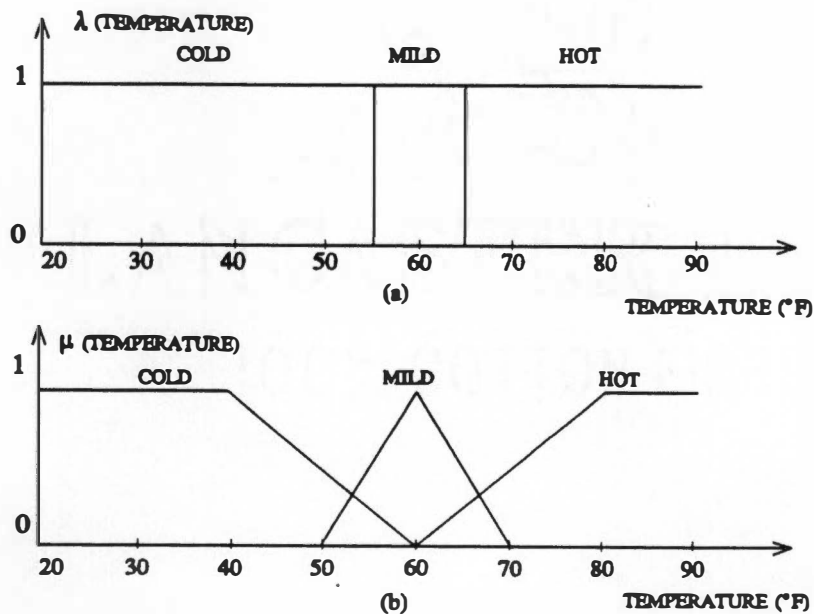


Fig. 1.1 Representation of temperature using:

(a) Crisp sets. (b) Fuzzy sets.

A few operations of Boolean set theory are also valid in fuzzy set theory, and are described below. Let  $\mu_A(x)$  denote the degree of membership of a given element  $x$  in the fuzzy set  $A$ .

Union: Given two fuzzy sets  $A$  and  $B$ , defined on a universe of discourse  $X$ , the union  $(A \cup B)$  is also a fuzzy set of  $X$ , with membership function given as

$$\mu_{A \cup B}(x) = \text{Max}[\mu_A(x), \mu_B(x)] \quad (1.1)$$

where  $x$  is any element of  $X$ .

Intersection: The intersection of two fuzzy sets  $A$  and  $B$  of the universe of discourse  $X$ , denoted by  $A \cap B$ , has the membership function given by

$$\mu_{A \cap B}(x) = \text{Min}[\mu_A(x), \mu_B(x)] \quad (1.2)$$

Compliment: The compliment of a given set  $A$  of the universe of discourse  $X$  is denoted by  $\neg A$ , and has the membership function

$$\mu_{\neg A} = 1 - \mu_A(x) \quad (1.3)$$

Fig. 1.2 illustrates these three basic properties. For fuzzy logic control, a few more concepts, such as fuzzy implication (fuzzy rules) and fuzzy composition (fuzzy inference) are important. A fuzzy rule typically has an IF-THEN format as follows:

IF (  $x$  is  $A$  AND  $y$  is  $B$  ) THEN (  $z$  is  $C$  )

where  $x$ ,  $y$  and  $z$  are fuzzy variables and  $A$ ,  $B$  and  $C$  are fuzzy sets in the universes of discourse  $X$ ,  $Y$  and  $Z$ , respectively. If the conditions expressed in the antecedent (IF portion) are met, then the action(s) specified in the consequent (THEN portion) are

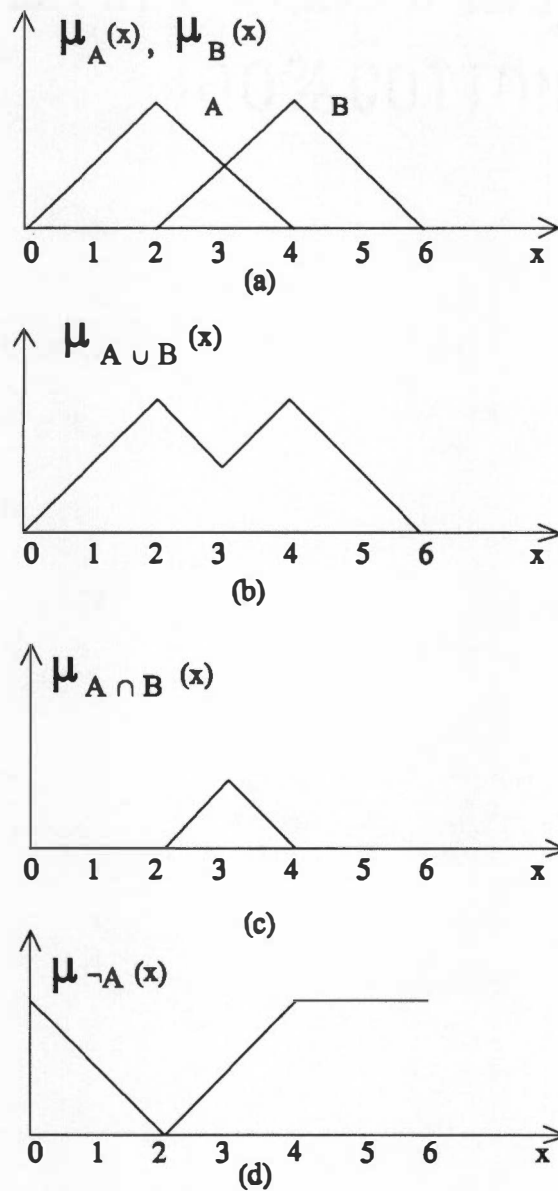


Fig. 1.2 Basic operations involving fuzzy sets.

(a) Original fuzzy sets defined on  $X$ .

(b) Union. (c) Intersection. (d) Negation.

taken. In order to design a fuzzy controller, a fuzzy rule base consisting of several rules must be constructed. For example, consider a hypothetical fuzzy speed control system for a DC motor, where the speed error (E) and change in error (CE) are used to determine changes in the control signal (DU), that in this case is the command armature current  $I_a^*$ .

A part of the rule base would be:

Rule 1: IF E is Zero AND CE is Zero THEN DU is Zero;

Rule 2: IF E is Zero AND CE is Negative Small THEN DU is Negative Small;

Rule 3: IF E is Positive Small AND CE is Negative Small THEN DU is Zero;

Here, error (E), change in error (CE) and change in control (DU) are considered fuzzy variables, with possible values given by fuzzy sets such as Positive Small, Negative Small, and so on. As illustrated in Fig. 1.1, a given numerical value can be a member of more than one fuzzy set. This means that, for a particular input pair of values (E and CE), more than one rule could be activated or "fired". Therefore, there must be a way to combine the individual control actions of the fired rule, such that a single, meaningful action is taken. In fuzzy logic terms, the composition operation is the mechanism by which such task can be performed. Although several composition principles have been proposed in the literature, the most common one is the SUP-MIN (SUPremum-MINimum) composition. In a simplistic way, given a rule base, it is possible to construct a n-dimensional fuzzy relation R (consider it as a function of n variables). The simplest case is a single input (x), single output (u) system, resulting in a two-dimensional fuzzy relation, represented by a membership function  $\mu_R(x,u)$ . For this case, the composition operation can be expressed as:

$$\mu_B(u) = \text{Sup}_x [\text{Min}(\mu_A(x), \mu_R(x, u))] \quad (1.4)$$

where A is the known fuzzy set for the input x and B is the inferred fuzzy set for the output u. In practice, the fuzzy relation R is seldom evaluated explicitly; instead, the SUP-MIN composition is applied to one rule at a time, and the individual control actions combined using the union operation. Fig. 1.3 illustrates the fuzzy composition by SUP-MIN principle for the two stated rules. Note that the output membership function of each rule is given by MIN operator whereas the combined fuzzy output is given by the SUP operator. This will be evident by the numerical example in Chapter 2.

The general structure of a fuzzy control system is given in Fig. 1.4. The control signal U is inferred from the two state variables error (e) and change in error (ce) ( de/dt for the sampling interval). The e and ce are per unit (pu) signals derived from the actual E and CE signals by dividing with the respective gain factors as shown. In a strict sense, the fuzzy controller is designed to process fuzzy quantities only. Therefore, all crisp input values must be converted to fuzzy sets before being used. This process is called fuzzification operation, and can be performed by considering the crisp input values as "singletons" (fuzzy sets that have membership value of 1 for the given input value, and 0 for all other points in the universe of discourse). In Fig. 1.3, the given input values E' and CE' were "converted" to fuzzy sets by this process, before being compared to the other fuzzy sets. In a similar way, there is a need for converting the output of the fuzzy controller (a fuzzy set) to a crisp value required by the plant. This is called defuzzification operation, and can be performed by a number of methods of which the center-of-gravity (also known as centroid) and height methods are common. The centroid defuzzification

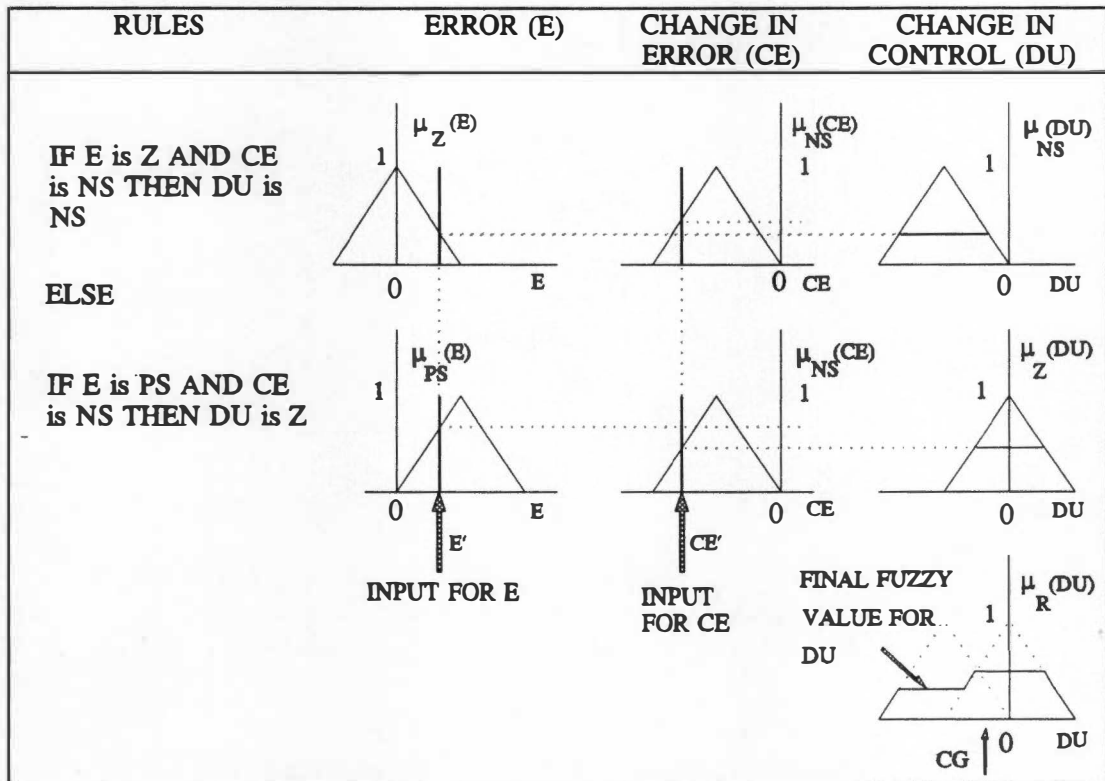


Fig. 1.3 Fuzzy composition method by SUP-MIN principle.

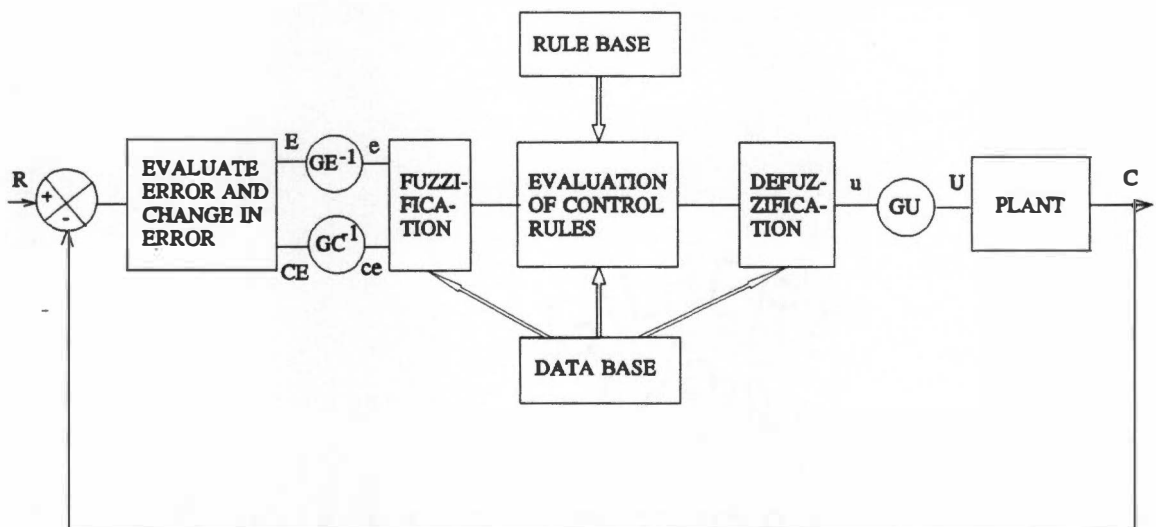


Fig. 1.4 Basic structure of a fuzzy controlled system.

method selects the output crisp value corresponding to the center of gravity of the output membership function, which is given by the expression

$$U_o = \frac{\int u \mu(u) du}{\int \mu(u) du} \quad (1.5)$$

In the height method, the centroid of each output membership function associated with every rule is first evaluated. The final output is then calculated as the average of the individual centroids, weighted by their heights (degree of membership) as

$$U_o = \frac{\sum_{i=1}^n u_i \mu(u_i)}{\sum_{i=1}^n \mu(u_i)} \quad (1.6)$$

Finally, the data base provides the operational definitions of the fuzzy sets used in the control rules, fuzzification and defuzzification operations.

Fuzzy logic controllers have been successfully applied to a number of different processes, in many cases yielding improved performance, compared to conventional control techniques. A qualitative explanation for this superior performance will now be discussed.

For a discrete PI controller, the change in control  $\Delta u(k)$  can be expressed as

$$\Delta u(k) = K_p ce(k) + K_i \Delta t e(k) \quad (1.7)$$

where  $K_p$  and  $K_i$  are the proportional and integral gains, respectively,  $e(k)$  is the control error,  $ce(k)$  ( $=e(k) - e(k-1)$ ) is the change in error, and  $\Delta t$  is the sampling interval. For a specific value of error  $e(k)$ , the control increment  $\Delta u(k)$  varies linearly with  $ce(k)$ . In other



words, the mapping produced by a PI controller results in a plane in the three-dimensional space ( $ce$ ,  $e$ ,  $\Delta u$ ). On the other hand, for a fuzzy controller, any type of mapping is theoretically possible. Again, for a given value of error  $e(k)$ , the relationship between  $\Delta u(K)$  and  $ce(k)$  is not confined to a straight line, resulting in practice, in a variable  $K_p$  gain. Of course, in order to realize the potential benefits of this highly flexible structure, a much more elaborated design process is required. In response to this challenge, significant research effort has been devoted to the development of a theory for fuzzy dynamic systems, addressing problems such as fuzzy state variables, controllability and stability [12].

### **1.3 Outline of the Dissertation**

The application of fuzzy logic to the control of both DC and AC drive systems is discussed in this work. Phase-controlled converter DC drives have been used in applications that usually require fast response, such as steel mills. Under normal conditions, the converter operates in a continuous conduction mode, in which the converter transfer characteristics are linear, and fast transient response for the current loop is obtained. However, at light load conditions, the converter tends to operate in a discontinuous conduction mode, that results in non-linear converter transfer characteristics and sluggish response of the current loop. Ultimately, the overall system performance is adversely affected. Furthermore, in many applications load disturbance is quite common, as well as parameter variation in the drive system. Consequently, fuzzy logic control can be applied with potential advantages over classical control techniques.

In Chapter 2, a speed control system that uses a phase-controlled bridge converter and a separately excited DC machine was investigated. Fuzzy control was used to linearize the transfer characteristics of the converter in discontinuous conduction mode occurring at high speed and light loads. The fuzzy control was then extended to the current and speed control loops, replacing the conventional proportional-integral (PI) control method. The compensation and control algorithms were developed in detail and verified by digital simulation using PC-SIMNON.

Vector control drives are becoming the industry standard for high performance applications [19]. Under vector control, an AC machine drive dynamic imitates that of a separately excited DC machine drive, with the advantages of ruggedness and higher torque to inertia ratio.

Most drive systems operate at rated flux, to ensure fast transient responses. However, at light loads, rated flux operation results in unnecessarily high core losses, thus impairing the efficiency of the drive. To address this problem, fuzzy logic was applied to the efficiency optimization of a speed control system, using an indirect vector controlled induction motor drive. In order to validate the new control scheme, as well as to predict system performance, an accurate loss model of the converter induction machine system was first developed, as discussed in Chapter 3. The model properly represents the loss phenomena as well as dynamic behavior of both machine and converter. After validation of the lossy models, they were used by the fuzzy logic based on-line efficiency optimization control, presented in Chapter 4. During efficiency optimization, the rotor flux is typically reduced, causing undesirable low frequency torque pulsations. To address this

problem, an innovative feedforward torque compensator is also described in Chapter 4. The drive system with the proposed efficiency optimization controller was simulated with the lossy models of converter and machine, and its performance was thoroughly investigated. An experimental 5 hp drive system, with the proposed controller implemented on a Texas Instruments TMS320C25 digital signal processor, was tested in the laboratory to validate the theoretical development.

Indirect vector control induction motor drives require the knowledge of rotor time constant, to generate the slip frequency used in the synthesis of the unit vectors. Fast dynamic response is only achieved when the slip gain used in the control matches the actual machine rotor time constant. Unfortunately, machine parameters are temperature and saturation dependent, and drive performance tends to deteriorate. Chapter 5 discusses the application of fuzzy logic to the slip gain tuning of an indirect vector controlled induction motor drive, using the standard model-reference adaptive control (MRAC) technique. The MRAC methods based on reactive power and synchronous frame D-axis voltage are combined together with a weighting factor that is generated by a fuzzy controller. The weighting factor ensures the dominant use of reactive power method in low speed high torque regions whereas the D - axis voltage method is dominant in high speed low torque regions. A second fuzzy controller tunes the slip gain based on the combined detuning error and its slope, so as to ensure fast convergence at any operating point in the torque-speed plane. Drive performance was extensively investigated, initially through PC-SIMNON simulation, and then using an experimental drive system.

## CHAPTER 2

### FUZZY CONTROL OF A DC DRIVE SYSTEM

#### 2.1 Introduction

Direct current (dc) drives have been the traditional industry option in applications that require adjustable speed, mainly due to the ease of control and fast speed response. Although in the recent years alternate current (ac) drives have gained increased popularity, and will certainly dominate the adjustable speed drive market, dc drives still constitute the majority of industrial drive systems.

The application of fuzzy logic to the control of a dc servomotor has been discussed in the literature [5]. The authors described the system performance in the presence of sudden changes in inertia, under fuzzy control as well as under PID and MRAC control, and showed the superiority of fuzzy control. In their study, however, a linear power amplifier was assumed, and consequently, the problems associated with the non-linearities of actual power converters were not addressed.

Among the dc drive systems, the phase-controlled bridge converter drive shown in Fig. 2.1 is the most popular. It is shown here in a four-quadrant speed control mode, with inner current control loop, that provides fast transient response and also limits the armature current. Traditionally, proportional-integral (PI) control is used in both speed and current loops. The firing angle  $\alpha$  is obtained from the current PI controller output  $V_s$ ,

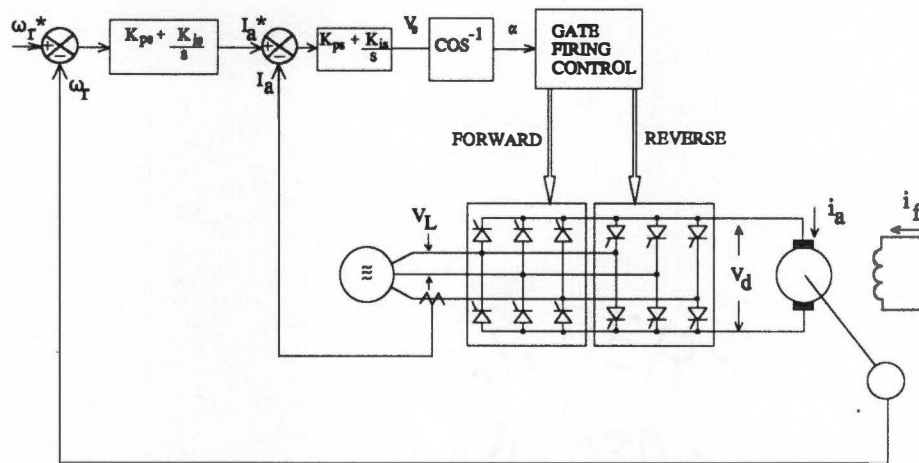


Fig. 2.1 Four quadrant phase-controlled converter DC drive.

by cosine wave crossing method, such that the converter output voltage  $V_d$  is proportional to  $V_s$ , i.e., a linear transfer characteristic is obtained for the converter system. The converter, however, may operate in either continuous or discontinuous conduction modes, as indicated by the current and voltage waveforms of Fig. 2.2. At high load torque, the difference between applied voltage  $V_d$  and the counter emf  $V_c$  is large enough such that the conduction will be continuous. However, at light load torques, this difference becomes small and the conduction tends to be discontinuous. Under discontinuous conduction, the converter characteristics is no longer linear, and the current loop response tends to deteriorate. This in turn results in a sluggish speed response, rendering the system inadequate for high performance applications. Among the number of methods suggested to linearize the converter transfer characteristics at discontinuous conduction mode, the look-up table method suggested by Ohmae et al. [15] appears to be very attractive. In this method, an auxiliary compensating  $\Delta\alpha$  angle is generated as a function of main  $\alpha$  angle and armature current  $I_a$ , and then added with  $\alpha$  to generate the actual firing angle. The two-dimensional relation of  $\Delta\alpha$  can be pre-computed for each X/R parameter and stored in the form of a look-up table for microcomputer implementation. If the parameter X/R variation is considered, and the compensating angle is needed with good accuracy, then the look-up tables memory tends to be very large.

The following sections discuss the application of fuzzy logic to a DC drive system. Initially, a fuzzy controller was designed to generated a  $\Delta\alpha$  compensating angle, that when added to the original firing angle  $\alpha$ , produces a linear characteristic for the converter system, even under discontinuous conduction mode. Next, fuzzy control was

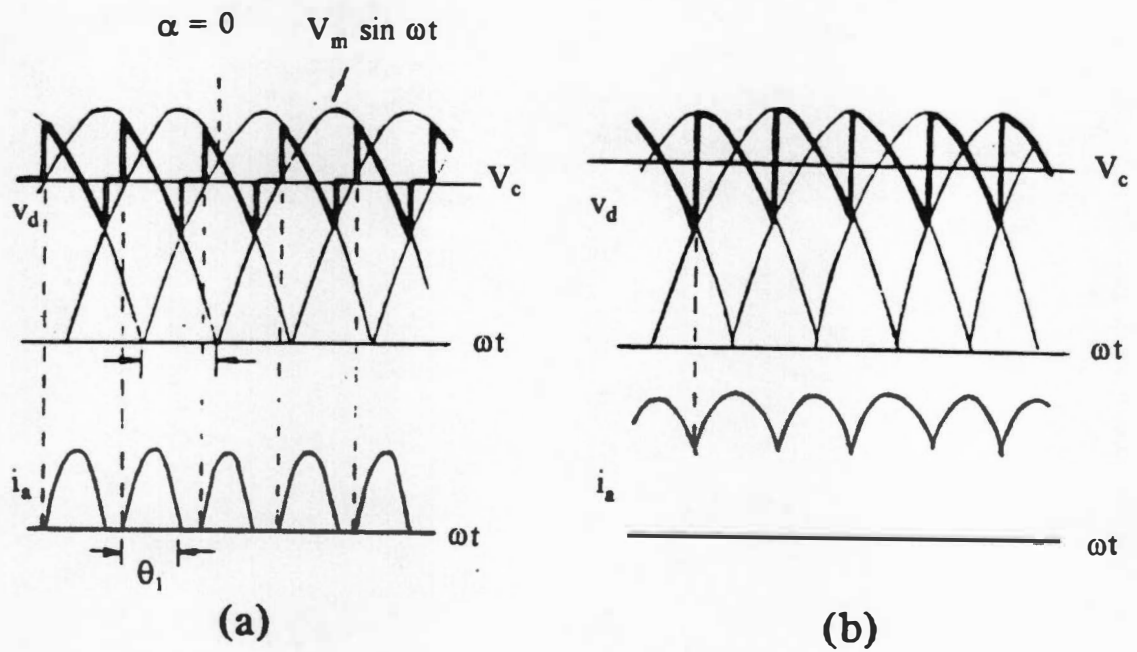


Fig. 2.2 Converter voltage and current waveforms [15].

(a) Discontinuous conduction.

(b) Continuous conduction.

extended to speed and current control loops, replacing the conventional PI control method. The compensation and control algorithms were developed in detail and verified by digital simulation of a drive system. The results were originally published at the IEEE IAS Annual Meeting, 1991 [14].

## 2.2 Fuzzy Controlled DC Drive System

The speed control system under consideration is shown in Fig. 2.3. The power circuit consists of a phase-controlled bridge converter that drives a separately excited DC motor. For simplicity, the converter is used in motoring mode only with fixed field excitation. Fuzzy controllers were used in both the speed control loop and in the inner current control loop. The current loop output  $V_s'$  is added with the estimated feed-forward counter emf signal  $\hat{V}_c$ , to generate the control signal  $V_s$ , which then generates the firing angle  $\alpha$ , by cosine wave crossing method. The feed-forward addition of counter emf gives faster loop response. The fuzzy compensator is also indicated in the figure.

As mentioned in the introduction, the converter may operate in either continuous or discontinuous conduction mode. Complete mathematical analysis of converter performance characteristics has been made for both operating modes [21], and the relevant results will be repeated here. When current is flowing into the armature, the loop equation is given by

$$L \frac{di_a}{dt} + Ri_a = V_m \sin \omega t - V_c \quad (2.1)$$

where  $V_c$  = machine counter emf,  $V_m$  = peak supply line voltage,  $i_a$  =



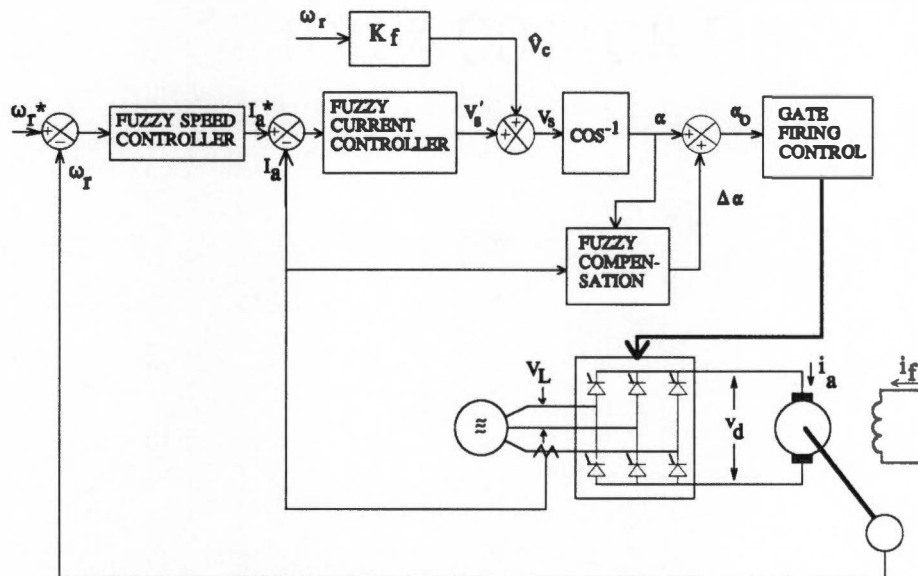


Fig. 2.3 Fuzzy controlled DC drive system.

instantaneous armature current, and  $R$  and  $L$  are , respectively, the resistance and inductance of the armature plus ac source and connections. In continuous conduction mode, the average armature current  $I_a$  and converter output voltage  $V_d$ , in normalized form can be given as follows

$$I_a(pu) = \frac{I_a}{3 V_m / \pi X} = \frac{X}{R} \left[ \cos \alpha - \frac{\pi V_c}{3 V_m} \right] \quad (2.2)$$

$$V_d(pu) = \frac{V_d}{V_m} = \frac{3}{\pi} \cos \alpha \quad (2.3)$$

where  $X$  is the armature reactance ( $\omega L$ ), and  $\alpha$  is the converter firing angle. The peak line voltage ( $V_m$ ) can essentially be considered a constant, and therefore,  $V_d$  can be controlled linearly by  $V_s$  with cosine wave crossing technique, as indicated in Fig. 2.3. In discontinuous conduction mode, the following armature circuit equations are valid

$$I_a(pu) = \frac{I_a}{3 V_m / (\pi X)} = \frac{X}{R} \left[ \cos\left(\frac{\pi}{3} + \alpha\right) - \cos\left(\frac{\pi}{3} + \alpha + \theta_1\right) - \frac{V_c}{V_m} \theta_1 \right] \quad (2.4)$$

$$V_d(pu) = \frac{V_d}{V_m} = \frac{3}{\pi} \left[ \cos\left(\frac{\pi}{3} + \alpha\right) - \cos\left(\frac{\pi}{3} + \alpha + \theta_1\right) - \frac{V_c}{V_m} \theta_1 \right] + \frac{V_c}{V_m} \quad (2.5)$$

$$\frac{V_c}{V_m} = \frac{\sqrt{1 + (X/R)^2}}{\left[1 - \exp\left(-\frac{R}{X}\theta_1\right)\right]} \left\{ \sin\left(\frac{\pi}{3} + \alpha + \theta_1 - \phi\right) - \sin\left(\frac{\pi}{3} + \alpha - \phi\right) \exp\left(-\frac{R\theta_1}{X}\right) \right\} \quad (2.6)$$

where  $\theta_1$  is the conduction angle of current pulse ( $0 < \theta_1 < \pi/3$ ), as indicated in Fig.2.2(a), and  $\phi = \tan^{-1}(X/R)$ . For a fixed  $X/R$  parameter, the equations 2.2 - 2.6 were plotted in Fig. 2.4 for different  $\alpha$  angles, which also indicates the boundary between continuous and discontinuous conduction modes. For example, at  $\alpha = 80^\circ$ , the conduction is continuous at the point A. As the machine counter emf is increased, the  $V_d$  (pu) remains constant at decreasing  $I_a$  (pu) until point B, when the conduction becomes discontinuous. Further increase of counter emf will cause increase of  $V_d$  (pu) until it reaches the point at which  $I_a(\text{pu}) \cong 0$ , if the machine is not loaded. The nonlinear  $V_d(\text{pu}) - I_a(\text{pu})$  relation adversely affects the gain characteristics of the current control loop. If, for example, the loop gain is made optimum at continuous conduction mode, the lower gain at discontinuous conduction will make the loop response sluggish. On the other hand, if the gain is optimized for discontinuous mode at a certain operating point, the loop will tend to be unstable at continuous conduction. This problem can be overcome through Fuzzy  $\Delta\alpha$  compensation. For instance, at operating point C in Fig. 2.4, if the proper  $\Delta\alpha$  angle is added to  $\alpha_o = 80^\circ$ , the compensated  $V_d$  moves to point D, that lies in the extension of the horizontal characteristics of the continuous conduction mode. As a consequence, the converter gain becomes the same as in the continuous conduction mode, and proper tuning of the current controller is now possible.

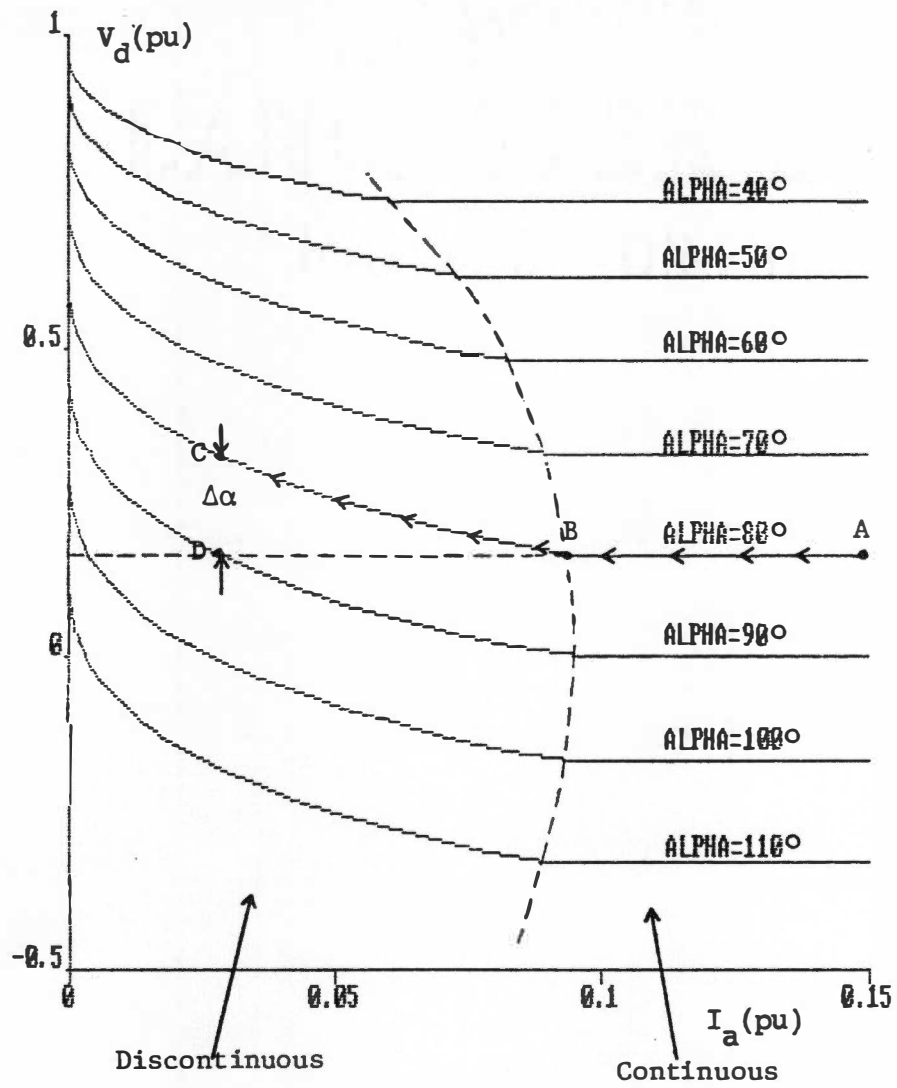


Fig. 2.4 Theoretical  $V_d$ - $I_a$  (pu) phase plot without compensation.

### 2.2.1 Fuzzy Linearization of Converter Characteristics

It was mentioned in Chapter 1 that fuzzy control is well-suited in a non-linear system, especially where parameter variation problem exists. Therefore, we applied fuzzy method of  $\Delta\alpha$  angle compensation, in order to linearize the converter transfer characteristics in discontinuous conduction mode. The special feature in fuzzy control is that the  $\Delta\alpha$  angle is expressed as a fuzzy relation of the variables  $I_a$  and  $\alpha$  angle. The set of rules for fuzzy compensation is given in matrix form in Table 2.1, where all the symbols are defined in the usual fuzzy logic terminology. A typical rule has the following structure:

**IF  $I_a$  is small negative (NS) AND  $\alpha$  is small positive (PS)**

**THEN  $\Delta\alpha$  is small negative (NS)**

The rule base was developed by heuristic from the viewpoint of practical system operation. The current  $I_a$  was represented in normalized form. Fig. 2.5 shows the membership function plots of the variables  $\alpha$ ,  $I_a(\text{pu})$  and  $\Delta\alpha$ . The universes of discourse of the variables cover the whole discontinuous conduction region. The sensitivity of a variable determines the number of fuzzy sets required to describe it. The universe of discourse of  $\alpha$  is described by five fuzzy sets, whereas  $I_a(\text{pu})$  and  $\Delta\alpha$  are described by nine and eleven sets, respectively. The linguistic terms used for the sets are for convenience only and must be interpreted in a "context free" grammar, since their conventional meaning does not correspond to the sign and numerical values of the variables. In Fig. 2.5, 50% overlap was provided for the neighboring fuzzy sets. Therefore, at any given point of the universe of discourse, no more than two fuzzy sets

Table 2.1 Rule base for  $\Delta\alpha$  compensation.

$I_a \backslash \alpha$	NB	NS	Z	PS	PB
NVB	NVB	PB	PB	PB	PB
NB	NVB	Z	Z	Z	Z
NM	NVB	NS	NVS	NVS	NVS
NS	NVB	NM	NS	NS	NS
Z	NVB	NB	NM	NM	NS
PS	NVB	NVB	NB	NM	NM
PM	NVB	NVB	NB	NB	NB
PB	NVB	NVB	NVB	NB	NB
PVB	NVB	NVB	NVB	NVB	NB

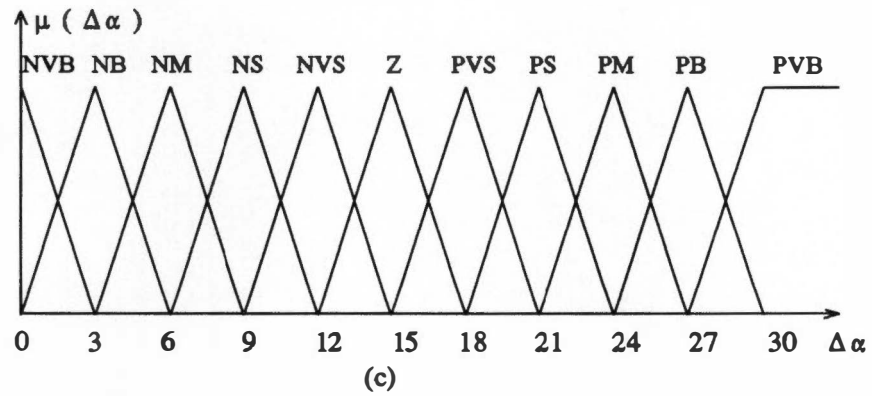
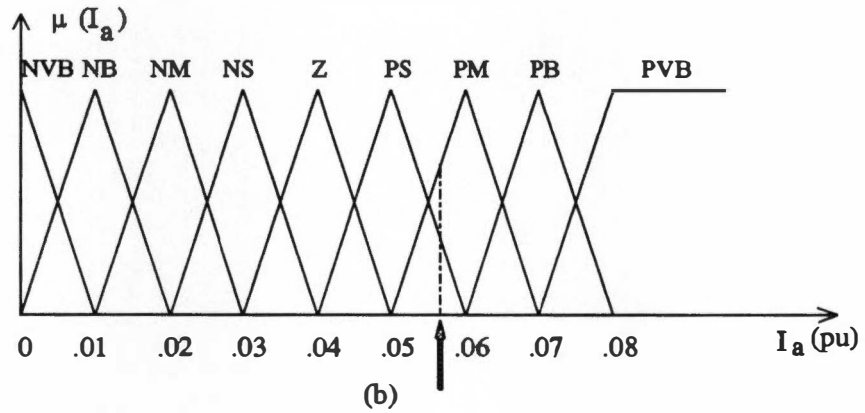
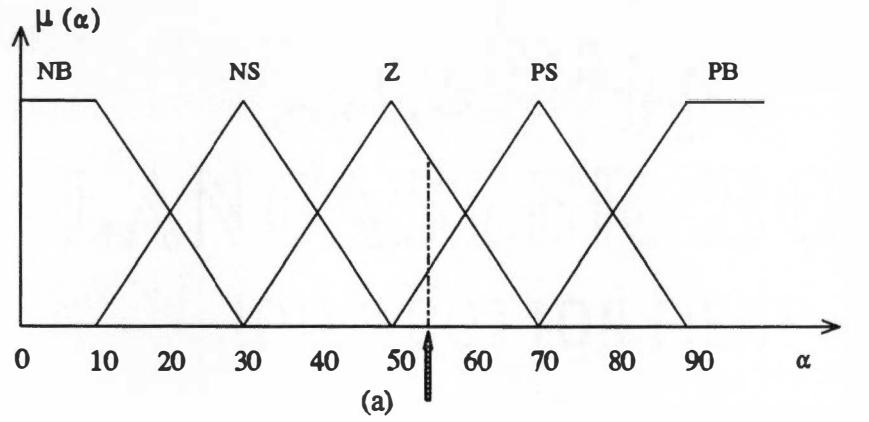


Fig. 2.5 Membership functions for  $\Delta\alpha$  compensation.

a) Firing angle ( $\alpha$ )      b) Armature current ( $I_a$ )

c) Compensating angle ( $\Delta\alpha$ )

have non-zero degree of membership. This choice of fuzzy partitioning along with the SUP-MIN composition method resulted in a simplification of the fuzzy linearization algorithm. It is evident that, for any input data of  $I_a(\text{pu})$  and  $\alpha$ , at the most four rules will be valid in the entire rule base given in Table 2.1. The algorithm for fuzzy linearization is described below, along with a numerical example, included for clarity.

1. Sample the DC current  $I_a$  and firing angle  $\alpha$  from the current control loop. Convert

$I_a$  to  $I_a(\text{pu})$ .

[Lets assume:  $I_a = 5.6 \text{ A}$ ,  $\alpha = 55^\circ$ ,  $I_{\text{base}} = 98.5 \text{ A}$  (see Table 2.1)

$$I_a(\text{pu}) = 5.6/98.5 = 0.057 ]$$

2. Calculate the interval indices I and J (that identify the interval number in the fuzzy sets) for  $\alpha$  and  $I_a(\text{pu})$ , respectively as follows:

$$I = \text{INT} ((\alpha + 10)/20)$$

$$J = \text{INT} ((I_a(\text{pu}) + 0.01)/0.01)$$

$$[ I = 3, J = 6 ]$$

3. Calculate the degree of membership of  $\alpha$  and  $I_a(\text{pu})$  for the left most fuzzy subset using I and J, respectively as follows:

$$\mu_Z(\alpha) = ( 20 I + 10 - \alpha ) / 20$$

$$\mu_{PS}(I_a(\text{pu})) = ( 0.01 I - I_a(\text{pu}) ) / 0.01$$

$$[ \mu_Z(55^\circ) = 0.75, \mu_{PS}(0.057) = 0.3 ]$$

4. Evaluate degree of membership for other sets by complement relation

$$\mu_{PS}(\alpha) = 1 - \mu_Z(\alpha)$$

$$\mu_{PM}(I_a(\text{pu})) = 1 - \mu_{PS}(I_a(\text{pu}))$$



$$[ \mu_{PS}(55^\circ) = 0.25, \mu_{PM}(0.057) = 0.7 ]$$

5. Identify the four valid rules in Table 2.1 (stored as look-up table) and calculate the degree of membership  $\mu_{R_i}$  contributed by each rule  $R_i$  [  $i = 1, 2, 3, 4$  ], using MIN operator

$$[ \mu_{R1} = \text{Min} \{ \mu_Z(\alpha), \mu_{PS}(I_a(pu)) \} = \text{Min} \{ 0.75, 0.3 \} = 0.3 ]$$

$$[ \mu_{R2} = \text{Min} \{ \mu_{PS}(\alpha), \mu_{PS}(I_a(pu)) \} = \text{Min} \{ 0.25, 0.3 \} = 0.25 ]$$

$$[ \mu_{R3} = \text{Min} \{ \mu_Z(\alpha), \mu_{PM}(I_a(pu)) \} = \text{Min} \{ 0.75, 0.7 \} = 0.7 ]$$

$$[ \mu_{R4} = \text{Min} \{ \mu_{PS}(\alpha), \mu_{PM}(I_a(pu)) \} = \text{Min} \{ 0.25, 0.7 \} = 0.25 ]$$

6. Retrieve the amount of correction  $\Delta\alpha_i$ ,  $i = 1, 2, 3, 4$  corresponding to each rule, from Table 2.1

$$\Delta\alpha_1 = (\alpha = Z, I_a(pu) = PS) \rightarrow \Delta\alpha_1 = NB = 3^\circ$$

$$\Delta\alpha_2 = (\alpha = PS, I_a(pu) = PS) \rightarrow \Delta\alpha_2 = NM = 6^\circ$$

$$\Delta\alpha_3 = (\alpha = Z, I_a(pu) = PM) \rightarrow \Delta\alpha_3 = NB = 3^\circ$$

$$\Delta\alpha_4 = (\alpha = PS, I_a(pu) = PM) \rightarrow \Delta\alpha_4 = NB = 3^\circ$$

7. Calculate the crisp value of  $\Delta\alpha$  by height defuzzification method as follows:

$$[\Delta\alpha = (0.30*3 + 0.25*6 + 0.70*3 + 0.25*3) / (0.30 + 0.25 + 0.70 + 0.25) = 3.5]$$

The strength of fuzzy compensation is that the number of rules required to express the fuzzy relation is fairly small and memory requirement is low compared to large look-up table needed in conventional method.

### 2.2.2 Fuzzy Control of Current and Speed Loops

In addition to converter linearization, fuzzy logic control was applied to the speed and current loops as well, replacing the conventional PI controllers. The objective was to explore the control robustness in the presence of parameter variation and load disturbance effect. However, both loops must satisfy the requirements of fast transient response with minimum overshoot. With converter linearization, both speed and current loops have essentially first order characteristics. Therefore, intuitively the same fuzzy control strategy should be valid for both.

The selected fuzzy controller structure possesses two input variables, namely error (E) and change in error (CE), and one output variable, the change in control setting ( $\Delta U$ ). Such controller can be viewed as a generalization of the conventional PI controller, where the effective gains  $K_p$  and  $K_i$  are dependent on the input state (E,CE). The input variables considered in the fuzzy rule base are defined as:

$$E(k) = R(k) - C(k)$$

$$CE(k) = E(k) - E(k-1)$$

where  $R(k)$  = reference signal,  $C(k)$  = output signal and  $k$  = sampling interval. The control strategy is described linguistically by rules of the following format:

$$\text{IF } E(k) \text{ is } X \text{ AND } CE(k) \text{ is } Y \text{ THEN } \Delta U(k) \text{ is } Z$$

where  $\Delta U(k)$  is the change in the control setting,  $X$ ,  $Y$  and  $Z$  are the fuzzy sets defined in the universe of discourse of  $E$ ,  $CE$  and  $\Delta U$ , respectively. The variables can be expressed as per unit quantities as follows:

$$e(\text{pu}) = E(k)/GE$$

$$ce(pu) = CE(k)/GCE$$

$$\delta u(pu) = \Delta U(k)/GU$$

where GE, GCE and GU are the respective gain factors of the controller. The gain factors are normally different for speed and current control loops. The representation of the variables in terms of per unit values permits flexibility in the design and tuning of the controller. Fig. 2.6 shows the membership functions of  $e(pu)$ ,  $ce(pu)$  and  $\delta u(pu)$  variables. Note that the fuzzy sets for each variable have asymmetrical shape causing more crowding near the origin. This permits precision control near the steady state operating point, without unduly increasing the number of sets. However, a finer partitioning for  $\delta u(pu)$  was necessary considering the sensitivity of this variable. As fuzzy controller design is based on intuition and experience, instead of the system model, the following considerations were given in the beginning:

1. If both  $e(pu)$  and  $ce(pu)$  are zero, then maintain the present control setting  $U(k)$  (i.e.,  $\delta u(pu) = 0$ );
2. If  $e(pu)$  is not zero, but is approaching this value at satisfactory rate, then maintain the present control setting  $U(k)$ ;
3. If  $e(pu)$  is growing, then change in the control signal  $\delta u(pu)$  is not zero and its value depends on the magnitude and sign of  $e(pu)$  and  $ce(pu)$  signals [7].

Table 2.2 gives the rule base matrix for current and speed controllers. A close look at the rule base indicates that the auxiliary diagonal consists of Z (zero) elements which conform to the second consideration as given above. Note that the value assigned to  $\delta u(pu)$  depends on the distance from the auxiliary diagonal. For instance, if  $e=PS$  and

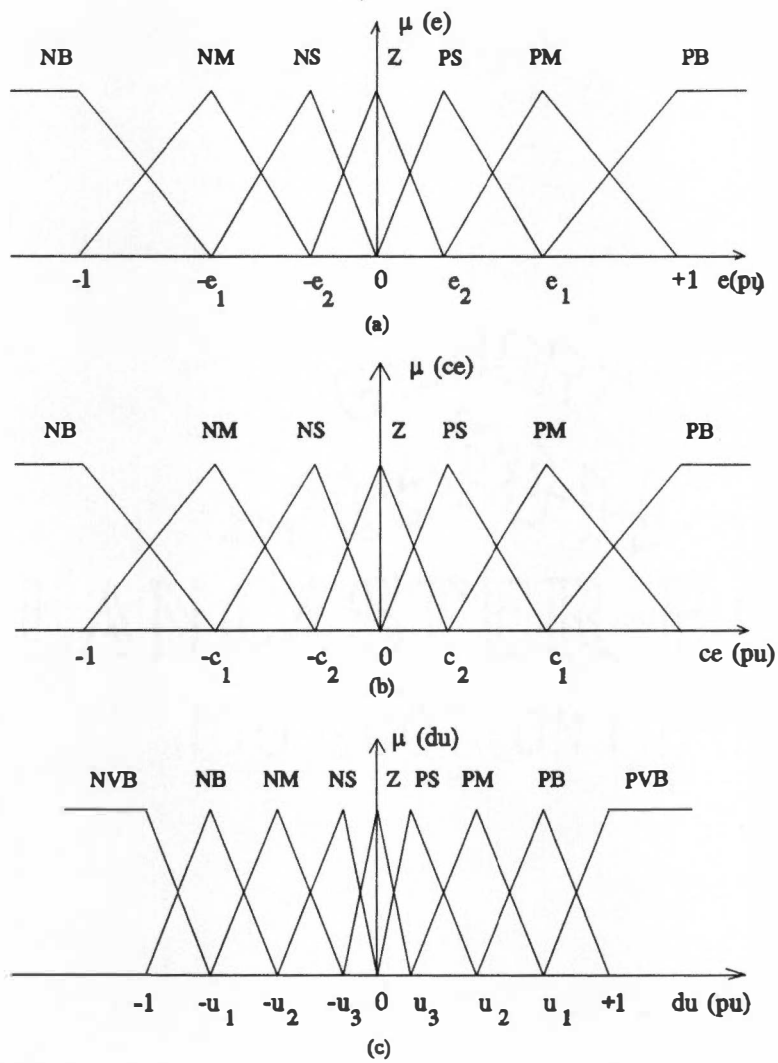


Fig. 2.6 Membership functions of speed and current controllers.

- a) Error
- b) Change in error
- c) Change in control

ce=NB, the system is approaching the steady state point ( $e=Z$ ,  $ce=Z$ ) too fast, and  $\delta u$  is made NM to prevent a large overshoot. On the other hand, if  $e=PS$  but  $ce=NS$ , the system is converging to the steady state point at the desired rate, and no change in control is required, i.e.,  $\delta u=Z$ . The control strategy is dominantly affected by changes in the rule base, and these constitute the primary means for controller tuning.

Table 2.2 Rule base for current and speed controllers.

$\begin{matrix} e \\ \backslash \\ ce \end{matrix}$	NB	NM	NS	Z	PS	PM	PB
NB	NVB	NVB	NB	NB	NM	NS	Z
NM	NB	NB	NM	NM	NS	Z	PS
NS	NB	NM	NS	NS	Z	PS	PM
Z	NB	NM	NS	Z	PS	PM	PB
PS	NM	NS	Z	PS	PS	PM	PB
PM	NS	Z	PS	PM	PM	PM	PB
PB	Z	PS	PM	PB	PM	PVB	PVB

A finer tuning was obtained by iterating the parameters  $e_1, e_2, \dots, c_1, c_2, \dots, u_1, u_2, \dots$  in Fig. 2.6, until the desired controller performance was obtained. The control procedure is essentially identical to that of  $\Delta\alpha$  compensation scheme. The steps for speed control can be summarized as follows:

1. Sample  $\omega_r^*$  and  $\omega_r$ .
2. Compute error (E), change in error (CE) and their per unit values as follows:  

$$E(k) = \omega_r^*(k) - \omega_r(k)$$

$$CE(k) = E(k) - E(k-1)$$

$$e(\text{pu}) = E(k)/GE$$

$$ce(\text{pu}) = CE(k)/GCE$$
3. Identify the interval indices I and J (1, 2, etc. shown in Fig. 2.6) for  $e(\text{pu})$  and  $ce(\text{pu})$ , respectively, by comparison method.
4. Compute the degree of membership of  $e(\text{pu})$  and  $ce(\text{pu})$  for the relevant fuzzy sets.
5. Identify the four valid rules in Table 2.2 and calculate the degree of membership  $\mu_{Ri}$  using MIN operator.
6. Retrieve  $\delta u_i$  for each rule from Table 2.2
7. Calculate the resultant crispy value of  $\delta u(\text{pu})$  by height defuzzification method.
8. Compute the next control signal as

$$U(k) = U(k-1) + GU * \delta u(\text{pu})$$

The control for the current loop is the same as above, except here the gain factors  $GE$ ,  $GCE$  and  $GU$  are different.

## 2.3 Simulation Study

In order to validate the control strategies discussed above, digital simulation studies were made using PC-SIMNON language. The phase-controlled rectifier and DC machine SIMNON models were initially developed and tested. Next, the fuzzy  $\Delta\alpha$  compensator was constructed, along with the current and speed fuzzy controllers, and integrate to the other sub-systems. All SIMNON routines are listed in the appendix. Although SIMNON is well suited for linear and non-linear systems simulation, it does not support branch instructions, what complicates the programming of fuzzy controllers. A complete description of the simulation methodology will be postponed to Chapter 4.

Table 2.3 shows the parameters of the drive system used in the simulation study. The speed and current loops of the drive were also designed and simulated with PI control, in order to compare performance with the respective fuzzy control loop. The compensation and feedback control algorithms were iterated until best simulation results were obtained.

In the beginning, the performance of the fuzzy compensation scheme was tested keeping both the speed and current loops open. Fig. 2.7 shows the voltage and current responses without compensation. Initially,  $V_s$  was set such that  $\alpha = 70^\circ$ , and then the drive simulation was enabled. With inertia load, the machine speed builds up freely with the developed torque. Initially, the conduction is continuous and  $V_d = V_d^* = KV_s$ . As speed builds up, the higher counter emf forces the converter to enter into discontinuous conduction, and  $V_d$  rises above the reference value  $V_d^*$  as shown. The experiment was then repeated with fuzzy  $\Delta\alpha$  compensation enabled, for different values of  $\alpha$  angle.

Table 2.3 Parameters of DC drive system.

<u>DC Motor:</u>		
110 V	2.5 hp	1800 rpm
$R_a = 0.6 \Omega$	$L_a = 8 \text{ mH}$	
$J = 0.0465 \text{ Kg.m}^2$	$B = 0.004 \text{ N.m.sec/rad}$	
$K_t = 0.55 \text{ V.sec/rad}$		
$I_a = 20 \text{ A (rated value)}$		
$V_L = 90 \text{ V (line voltage from transformer)}$		
$T_L = K_L \cdot \omega_r^2 \text{ (load torque)}$		
$K_L = 2.78 \cdot 10^{-4} \text{ N.m.sec}^2/\text{rad}$		



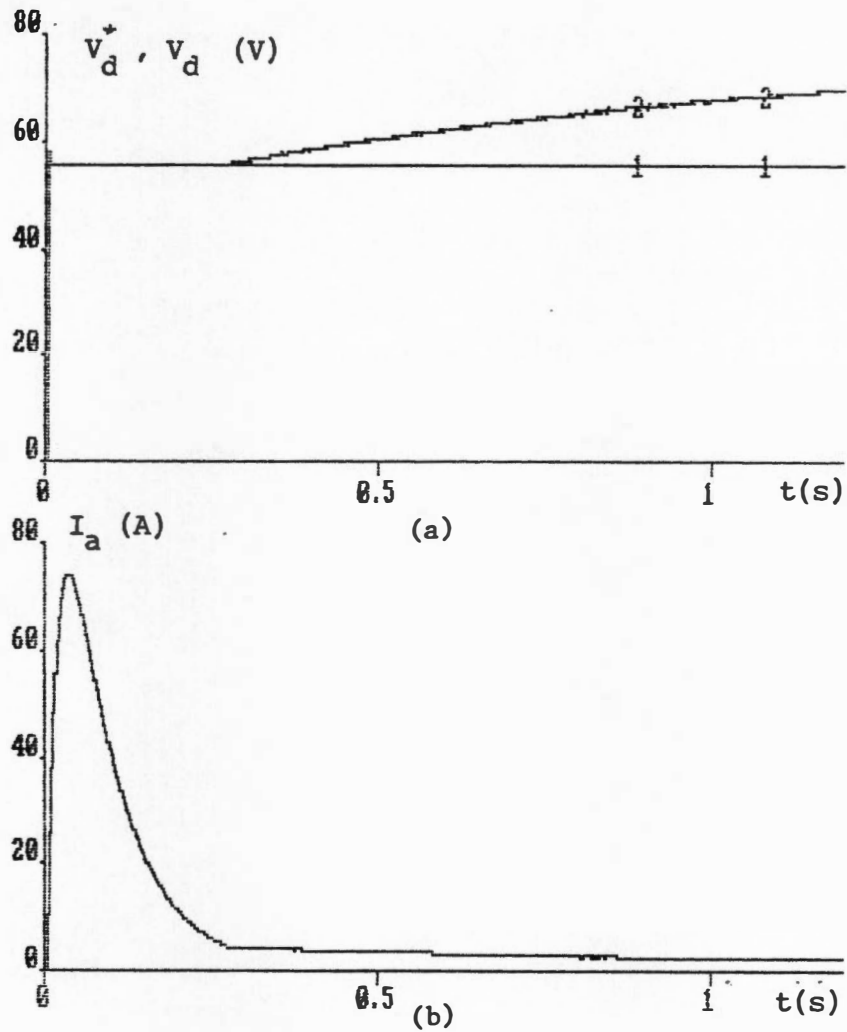


Fig. 2.7 Open loop  $V_d$  step ( $\alpha = 70^\circ$ ) response without compensation.

a) Reference (1) and actual (2) dc voltages.

b) Armature current (dc value).

The corresponding  $V_d(\text{pu}) - I_a(\text{pu})$  phase plots are given in Fig. 2.8. It is evident that with fuzzy  $\Delta\alpha$  compensation,  $V_d(\text{pu})$  at a certain angle essentially remains constant for the whole region of  $I_a(\text{pu})$ , i.e.,  $V_d$  is essentially equal to  $V_d^*$  in both continuous and discontinuous regions. Fig. 2.9 shows the corresponding time domain plot of converter DC voltage ( $v_d$ ) and armature current ( $i_a$ ) waves with  $\Delta\alpha$  compensation for  $\alpha = 70^\circ$ , where time starts at 0.46 sec.

The current control loop was then tested with the fuzzy controller with the speed loop remaining open, but the speed was locked to a fixed value by assuming a very large inertia, so as to establish the discontinuous conduction mode. Fig. 2.10(a) shows the current loop response with  $\Delta\alpha$  compensation which can be compared with Fig. 2.10(b) that gives response without compensation. In both cases, actual current waveform is shown. The boost of transient response due to converter linearization is evident. The responses of the current loop with PI control, with and without  $\Delta\alpha$  compensation, were obtained and shown in Fig. 2.11 for comparison purpose. The response improvement in Fig. 2.10 for either condition indicates the superiority of fuzzy control.

Next, the speed loop was closed, and transient response was tested with both fuzzy current and speed control at linearized converter condition. Fig. 2.12 shows the speed and current response that covers both continuous and discontinuous regions. The figure also shows the effect of 40% step load torque applied at 0.8 sec. Fig. 2.13 shows the

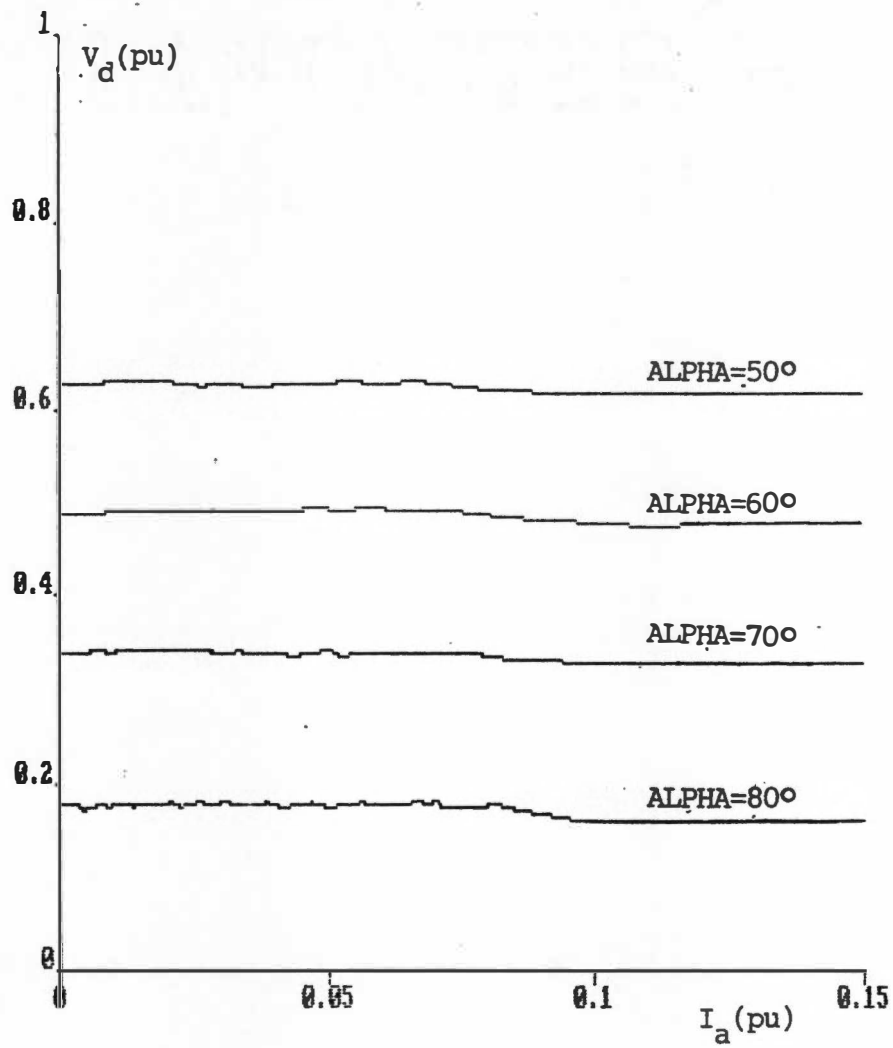


Fig. 2.8 Phase plot  $V_d$ - $I_a$  with  $\Delta\alpha$  compensation.

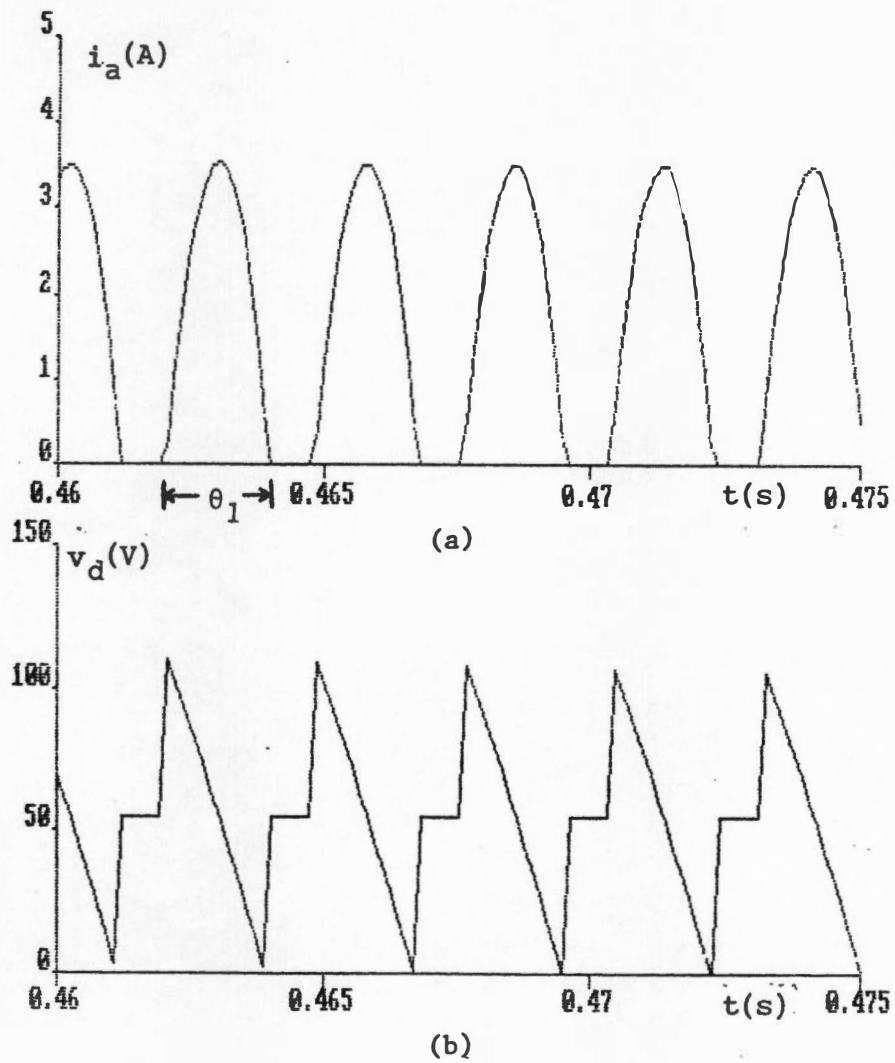


Fig. 2.9 Open loop  $V_d$  step response with  $\Delta\alpha$  compensation.

a) Armature current (actual value).

b) Converter output voltage (actual value).

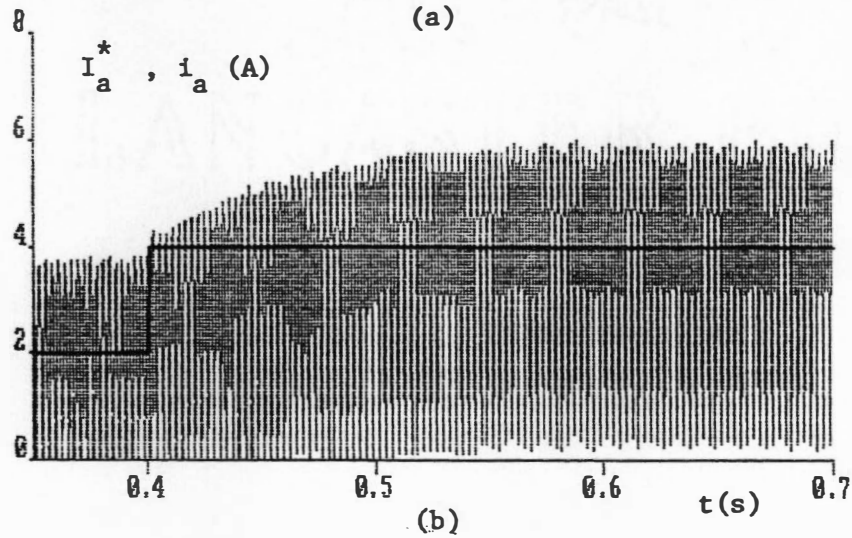
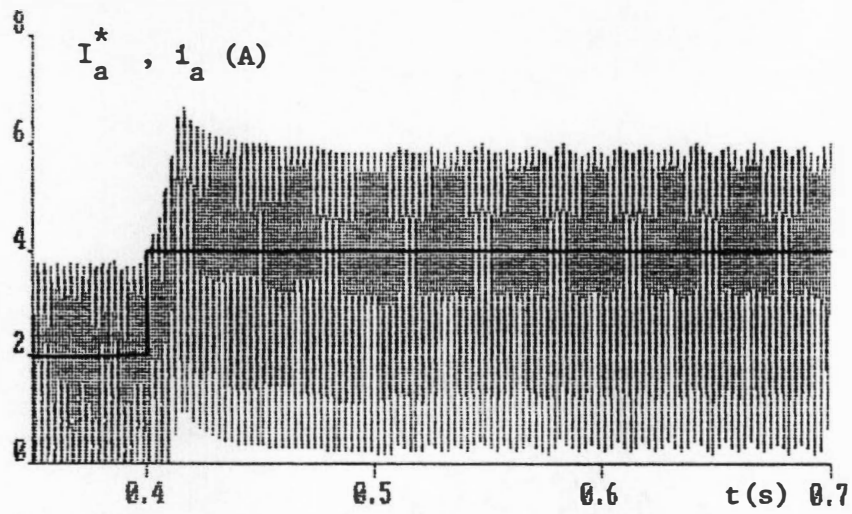


Fig. 2.10 Current loop response of the fuzzy controller.

a) With  $\Delta\alpha$  compensation.

b) Without  $\Delta\alpha$  compensation.

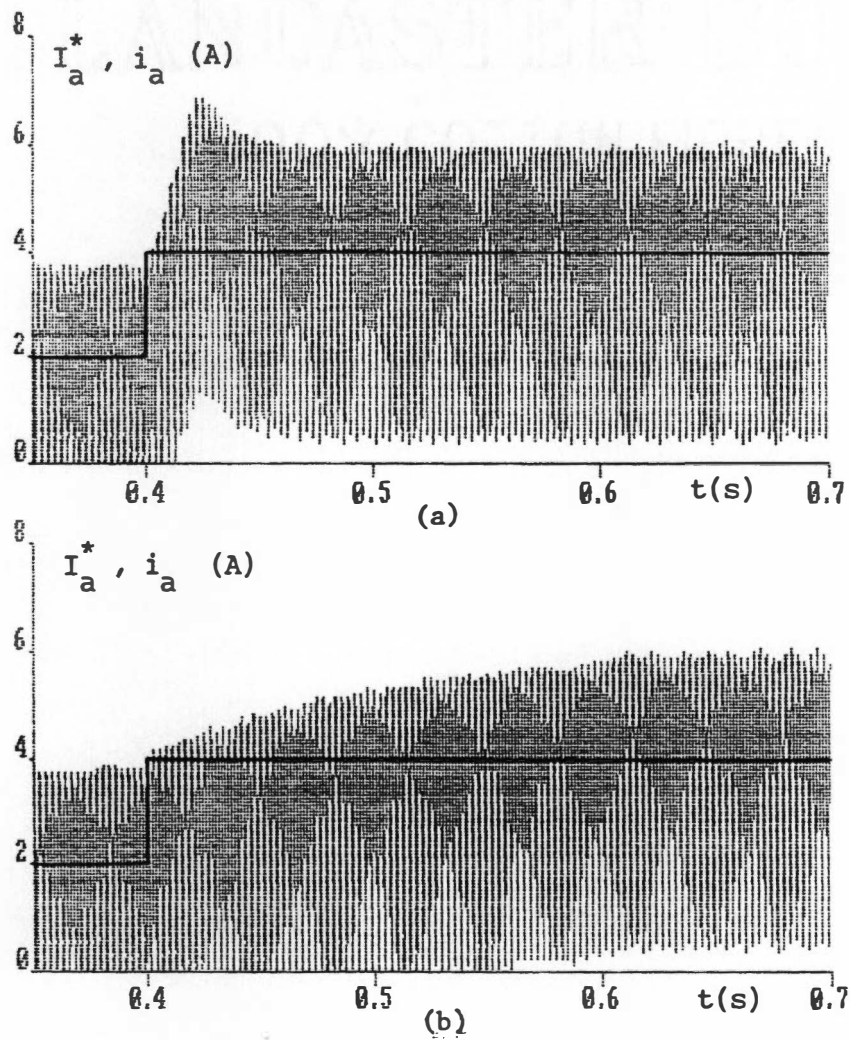


Fig. 2.11 Current loop response of the PI controller.

a) With  $\Delta\alpha$  compensation.

b) Without  $\Delta\alpha$  compensation.

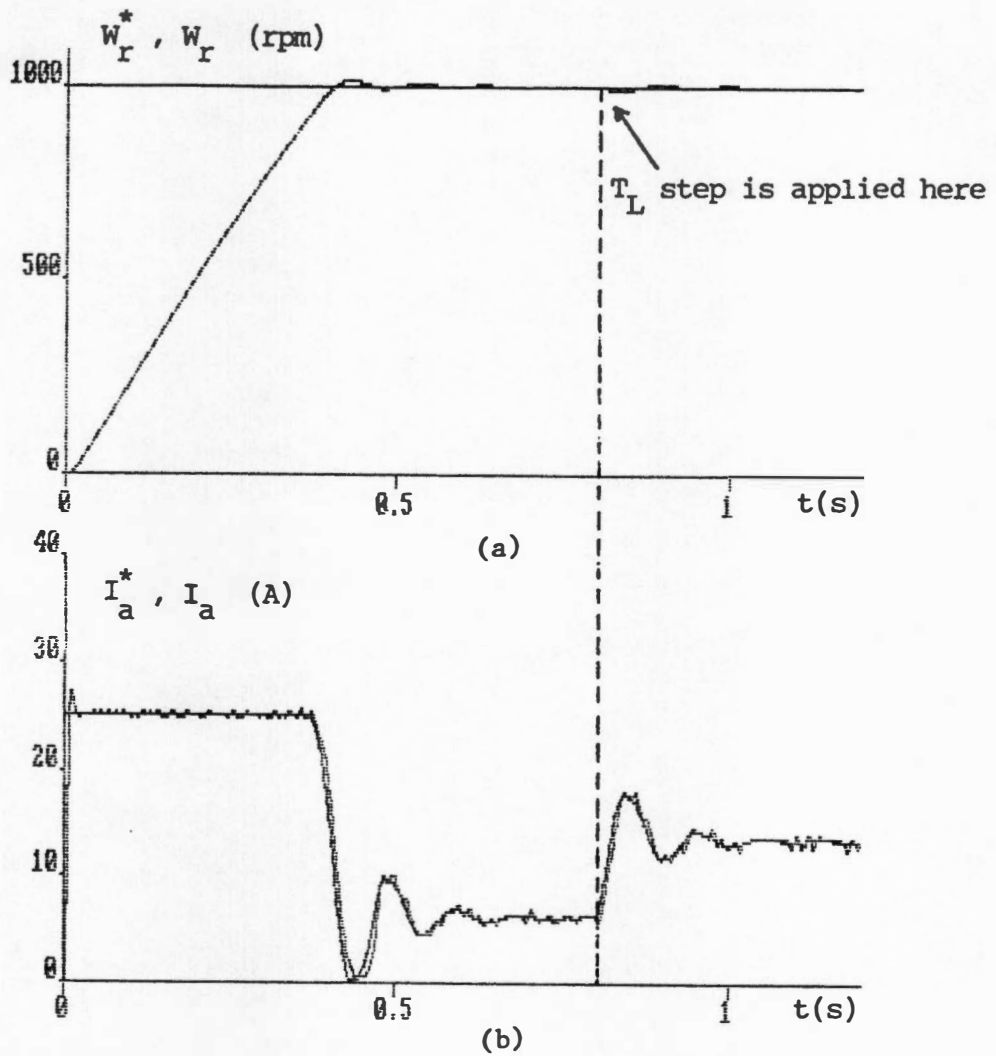


Fig. 2.12 Fuzzy control system response to a  $\omega_r^*$  step and  $T_L$  step.

a) Speed.

b) Armature currents.

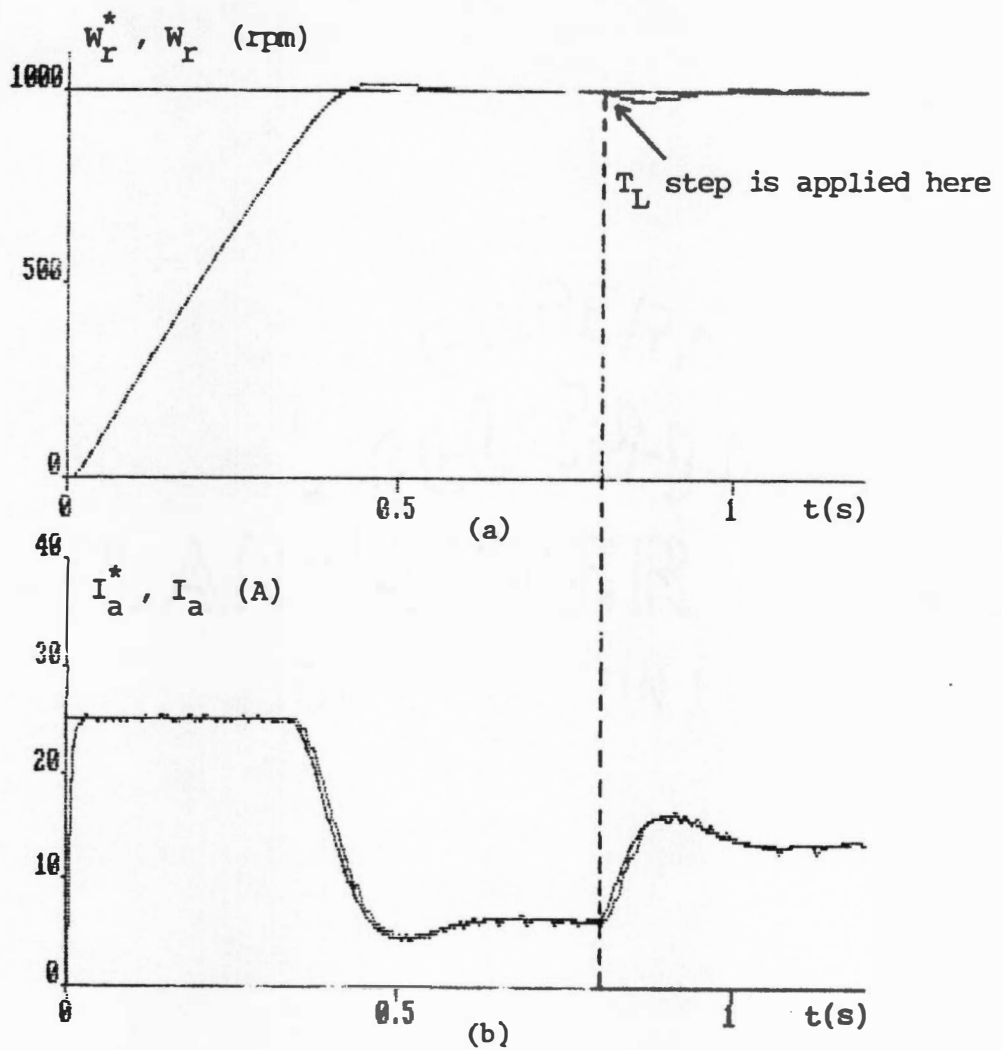


Fig. 2.13 PI control system response to a  $\omega_r^*$  step and  $T_L$  step.

a) Speed.

b) Armature currents.



corresponding system response under PI control in both loops. Table 2.4 summarizes the response improvement under fuzzy control.

Finally, the drive system was tested with  $\omega_r^*$  step at the same condition as before but with four times the effective inertia load. Fig. 2.14 shows the response with fuzzy control, and Fig. 2.15 gives the response with PI control, for comparison. Although the major portion of the rise time occurs with the current loop saturated, some improvement in rise time and overshoot under fuzzy control is evident.

In conclusion, the simulation study demonstrated the successful application of fuzzy logic to a phase-controlled converter DC drive system. The proposed fuzzy  $\Delta\alpha$  compensation scheme effectively linearizes converter characteristics at discontinuous conduction mode, and is simpler than the conventional look-up table method which requires a large memory. Fuzzy logic was also applied to the design of current and speed controllers, and the performance was compared with that of a conventional PI controlled system. The simulation study clearly indicated the superior performance of fuzzy control. The reason for superior performance of fuzzy controlled system is that basically it is adaptive in nature, and the controller is able to realize different control law for each input state (E and CE). The response of PI controlled system, on the other hand, is sensitive to model change that occurs with parameter variation. The main drawback in fuzzy control is the lack of a well defined design methodology, that results in a time consuming heuristic tuning process. Furthermore, a high speed microprocessor is needed to implement the control in real time. However, the control law is simpler to implement than expert system and neural network techniques.

Table 2.4 Performance comparison of fuzzy and PI controlled drive system.

	<u>Fuzzy</u>	<u>PI</u>
Rise time (s)	0.410	0.425
Overshoot (rpm)	13	16
Speed drop with $T_L$ (rpm)	13	25
Recovery time with $T_L$ (s)	0.09	0.20

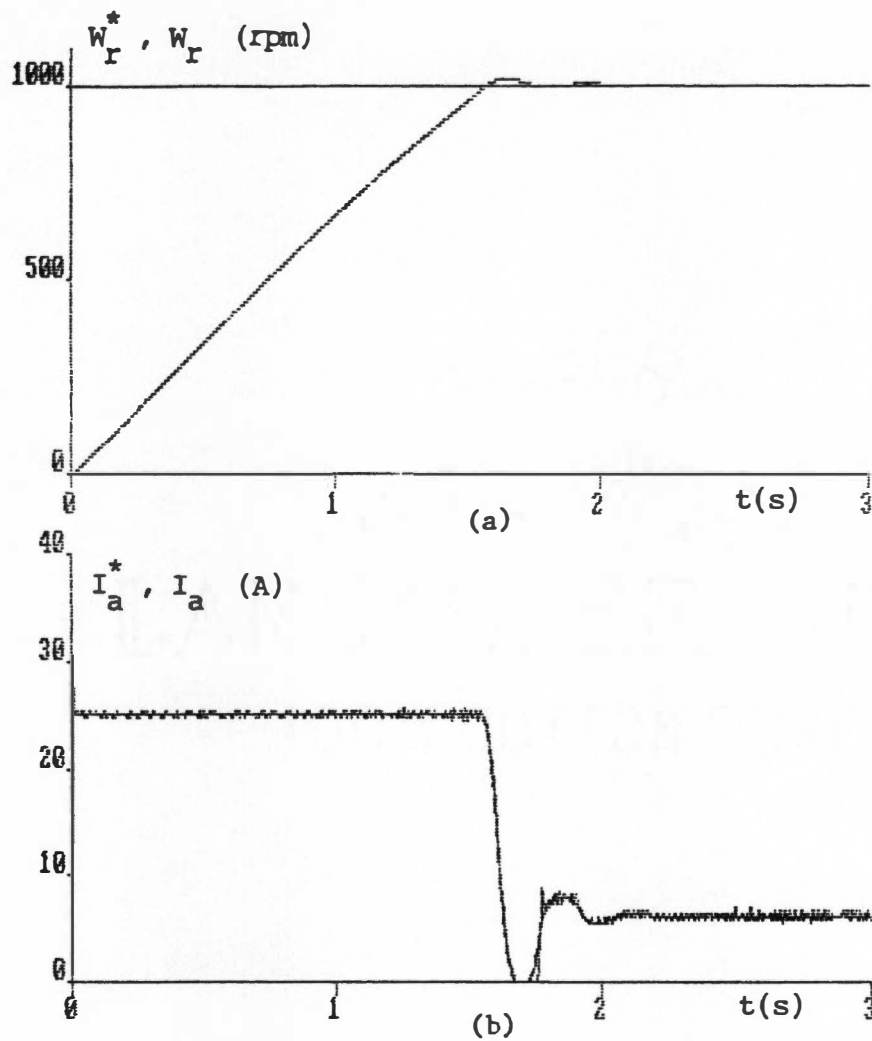


Fig. 2.14 Fuzzy control system response to a  $\omega_r^*$  step with a new inertia of four times the original value.

a) Speed.      b) Armature currents.

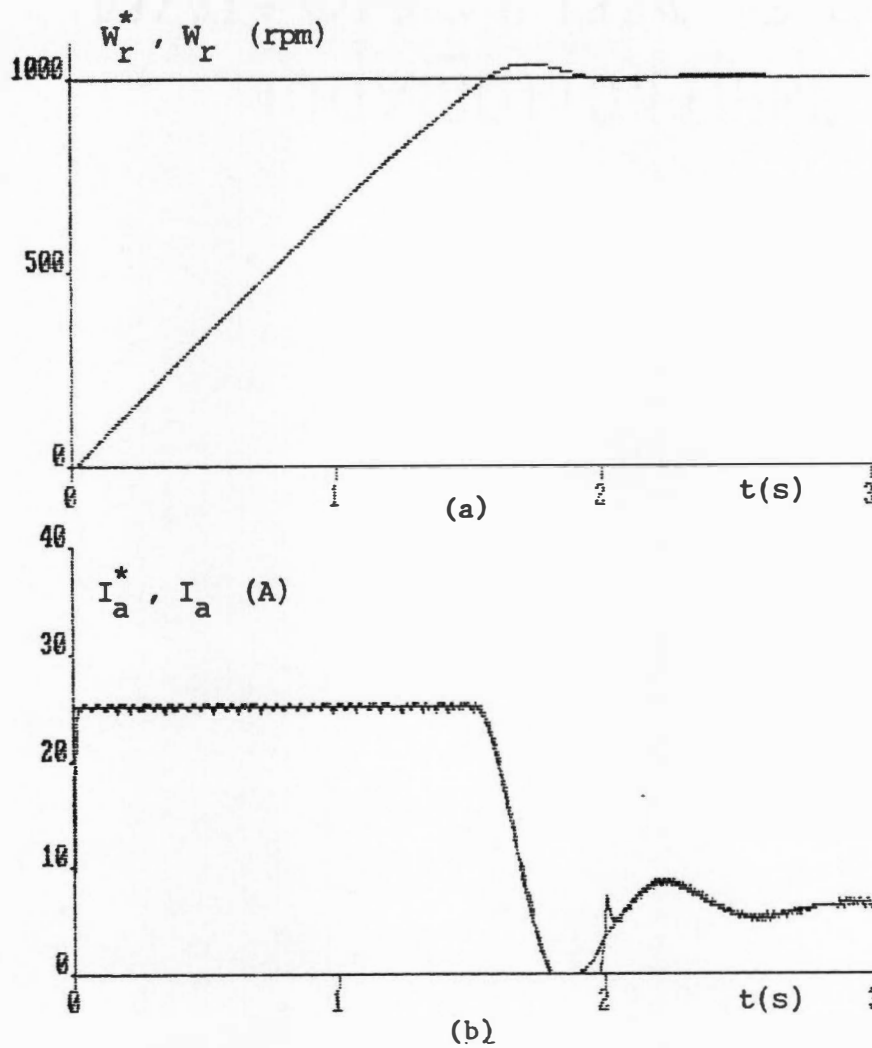


Fig. 2.15 PI control system response to a  $\omega_r^*$  step with a new inertia of four times the original value.

a) Speed.      b) Armature currents.

## CHAPTER 3

# LOSS MODELING OF CONVERTER INDUCTION MACHINE SYSTEMS

### 3.1 Introduction

Precise and reliable loss models for induction motor and converter systems are very important for performance prediction of variable speed drives. In particular, for the efficiency optimization study discussed in Chapter 4, it was realized that adequate converter and induction machine loss models were not available in the literature. In spite of the numerous studies that have been reported on the subject, in most cases the study focus on some particular aspects of interest and tend to neglect the overall picture, mainly because of the extreme complexity of the loss phenomena in induction machines. Traditionally, the machine electrical losses have been studied by using some variation of the per-phase equivalent circuit of Fig. 3.1, because the losses become primarily important at steady state condition. On the other hand, for dynamic studies, the synchronously rotating frame  $D^e$ - $Q^e$  model of Fig. 3.2 is normally used, but in this case the losses are not properly represented. Even under sinusoidal supply, a precise evaluation of machine losses is not straightforward, but it becomes much more complex when the machine is fed by a inverter, due to the wide harmonic spectrum present in the impressed voltage. Nevertheless, in order to predict the performance of the fuzzy logic based efficiency

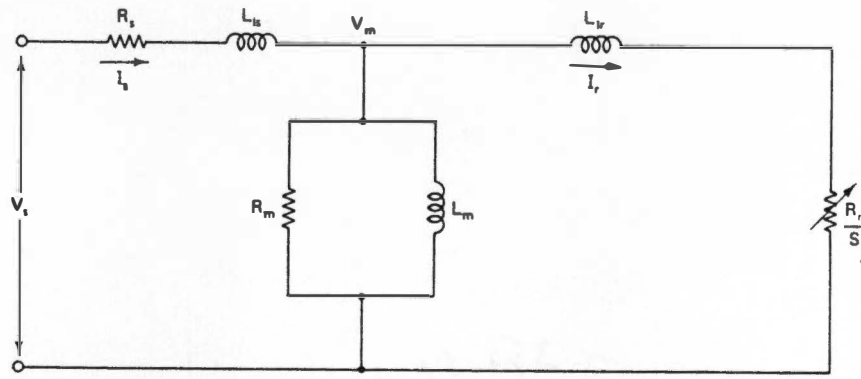


Fig. 3.1 Per-phase equivalent circuit.

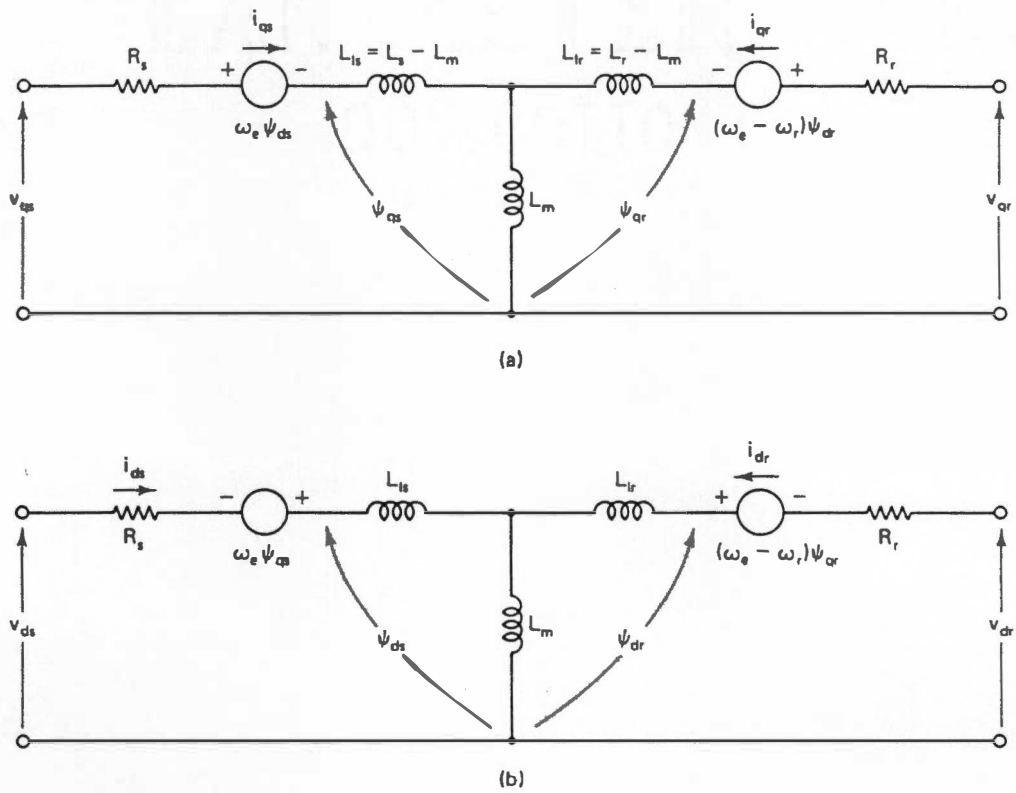


Fig. 3.2 Standard  $D^e$ - $Q^e$  equivalent circuits in synchronous frame.

a)  $Q^e$  - axis circuit.    b)  $D^e$  - axis circuit.

optimization control discussed in Chapter 4, it was necessary to derive a machine model capable of representing both the dynamic behavior and the loss characteristics of the induction machine, as well as a loss model for the converter system.

Loss modeling of induction motor has received wide attention in the literature over a number of years. Neglecting the effects of space harmonics, the machine parameters become dependent of time harmonic frequencies impressed by the inverter. Klingshirn and Jordan [30] applied superposition principle to calculate harmonic currents and the corresponding losses with per-phase equivalent circuit, where the rotor resistance and leakage inductance for each harmonic were corrected for deep bar (skin) effect. Kawagishi et al. [31] were able to verify experimentally the frequency dependency of parameter, by using a high frequency power supply, and validate some of the theoretical predictions. Honsinger [25] systematically studied the losses for a six-step inverter-fed machine and propose harmonic per-phase equivalent circuit. Since both core loss and stray load loss are basically due to hysteresis and eddy current effects, he proposed representation of stray loss by frequency dependent resistance in parallel with leakage inductance in the equivalent circuit. More recently, Udayagiri and Lipo [27] proposed a new simulation model that incorporates core loss but neglects the skin effect and leakage flux induced core loss, thereby underestimating the total loss.

In high frequency PWM inverter system, both conduction loss and switching loss are important in the loss model. The switching loss were discussed analytically by McMurray [32,] where the effects of both turn-on and turn-off snubbers were considered. Jovanovich et al. [33] made experimental evaluation of switching characteristics and

losses for a number of power devices with different base drives and load conditions. Ikeda et al. [34] have proposed loss modeling of PWM voltage-fed inverter and discussed the effect of carrier frequency on inverter losses. Circuit simulation programs, such as PSPICE that embed the detailed model of devices can give realistic lossy converter simulation. However, the drawbacks are that the losses remain somewhat transparent and can not be easily partitioned between the conduction and switching losses. Besides, such programs are not convenient for drive system simulation.

In the next sections, a unified loss model for the variable frequency drive system of Fig. 3.3 is discussed. The machine electrical losses, such as stator and rotor copper loss, core loss and stray loss, were considered for both fundamental and harmonic frequencies. Also considered were the skin effect on rotor resistance, temperature effect on both stator and rotor resistances, magnetizing inductance saturation, and friction and windage loss. All the above features were incorporated in a synchronous frame dynamic  $D^e$ - $Q^e$  equivalent circuit. The converter system, consisting of a diode rectifier and PWM transistor inverter, was modeled accurately for conduction and switching losses. Validity of the models, in both steady-state and transient conditions, was verified by simulations. These results were first presented at the 1992 international conference on industrial electronics, control and instrumentation (IECON'92), [42].

### **3.2 Dynamic Lossy Model for the Induction Machine**

The derivation of the dynamic lossy model is presented here. A discussion on machine losses is followed by the construction of a suitable harmonic equivalent circuit,



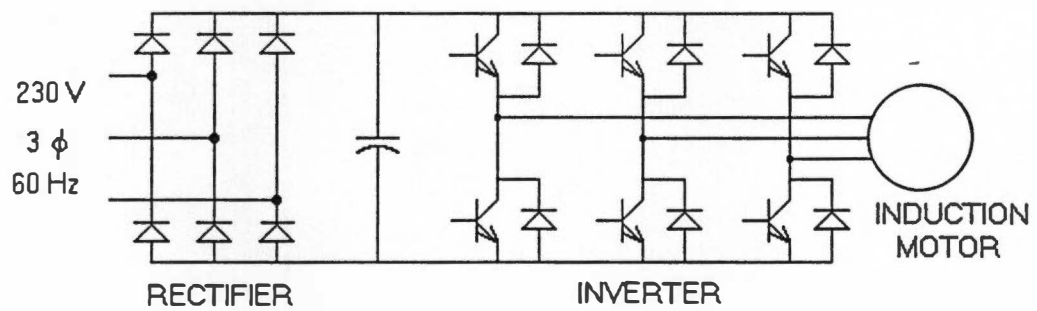


Fig. 3.3 Converter-machine system for variable speed drive.

and finally, by the derivation of the complete model through superposition principle.

### 3.2.1 Induction Machine Losses

Machine electrical and mechanical losses are examined here both qualitatively and quantitatively. The analysis follows a conventional partition of losses, encountered in the literature.

#### Copper Losses

Copper or Ohmic losses are caused by the non-ideal characteristics of the conductors employed in the stator and rotor windings, and have been modeled by

$$P_{cu} = m R I^2 \quad (3.1)$$

where  $m$  is the number of phases,  $R$  is the winding resistance and  $I$  the rms current. Proper evaluation of these losses requires the consideration of temperature effect on winding resistance, as well as its frequency dependency, commonly referred to as skin effect.

The skin effect has been widely discussed in the literature. In inverter-fed machine, the skin effect due to fundamental slip frequency can be ignored, but for the harmonic frequencies the rotor appears almost stationary, and therefore, practically all the stator harmonic currents flow in the rotor creating dominant skin effect. The rotor resistance at harmonic frequency  $f_n$  is given approximately by [29]

$$R_m = R_{rdc} (1 + c_1 d f_n^{0.5}) \quad (3.2)$$

where  $R_{rdc}$  = the dc resistance,  $d$  = bar depth, and  $c_1$  is a constant that takes into account the bar material and shape. With a number of harmonic frequencies, the superposition principle can be applied approximately by assuming that machine parameters for all harmonic frequencies are identical to those computed at carrier frequency. For a PWM inverter with sinusoidal PWM or hysteresis-band current control, the carrier frequency and the near sidebands are most dominant.

### Core Losses

Core losses consist of hysteresis and eddy-current losses, created by the time varying flux in the machine laminations. The eddy current loss may be expressed as

$$P_e = k_e f^2 \psi_m^2 \quad (3.3)$$

where  $\psi_m$  is the maximum mutual flux linkage,  $f$  the supply frequency and  $k_e$  a coefficient whose value depends on machine geometry and size, lamination thickness and resistivity of the iron. The hysteresis loss has been empirically modeled as

$$P_h = k_h f \psi_m^2 \quad (3.4)$$

where the coefficient  $k_h$  is mainly influenced by the magnetic properties of the iron and machine size. The stator core loss  $P_{cs}$  due to fundamental frequency mutual flux  $\psi_m$  can be expressed by

$$P_{cs} = k_h f \psi_m^2 + k_e f^2 \psi_m^2 \quad (3.5)$$

Under normal operation, the fundamental rotor frequency is a small fraction of the stator

frequency and the corresponding rotor core loss  $P_{cr}$  is given by

$$P_{cr} = k_h s f \psi_m^2 + k_e (s f)^2 \psi_m^2 \quad (3.6)$$

where  $f$  has been substituted for  $s f$ ,  $s$  being the per unit slip. Equations 3.5 and 3.6 can be added and rearranged to get the total fundamental core loss as

$$P_c = P_{cs} + P_{cr} = \left[ k_h \left( \frac{1+s}{f} \right) + k_e (1+s^2) \right] f^2 \psi_m^2 \quad (3.7)$$

As the mutual or air-gap flux linkage  $\psi_m$  is related to air-gap voltage  $V_m$  by

$$\psi_m = \sqrt{k_c} \frac{V_m}{f} \quad (3.8)$$

(3.7) can be rewritten as

$$P_c = k_c \left[ k_h \left( \frac{1+s}{f} \right) + k_e (1+s^2) \right] V_m^2 \quad (3.9)$$

The equivalent core loss resistance  $R_m$  can then be derived as

$$R_m = \frac{1}{k_c \left[ k_h \left( \frac{1+s}{f} \right) + k_e (1+s^2) \right]} \quad (3.10)$$

Assuming that the core losses due to mutual harmonic flux are governed by the same principles that control the fundamental losses, the coefficients  $k_h$  and  $k_e$  remain the same at harmonic frequency, and since harmonic slip  $s_n \approx 1$ , the equivalent core loss resistance  $R_{mn}$  at frequency  $f_n$  can be obtained from (3.10) as

$$R_{mn} = \frac{0.5}{k_c \left[ \frac{k_h}{f_n} + k_e \right]} \quad (3.11)$$

## Stray Losses

The stray losses by definition are the excess of the total losses actually occurring in a motor at a given load current, over the sum of the calculated copper losses, the no-load core loss, and the friction and windage loss, according to Alger et al. [35]. They used empirical equations to evaluate each individual loss component, what requires the knowledge of machine dimensions, type of core material, lamination thickness, winding geometry, etc. In this work, however, instead of evaluating stray loss individually, we treated them as a whole. The fundamental idea is that, the stray loss is essentially due to eddy current and hysteresis losses, induced by various types of leakage fluxes in the laminations and other structural parts of the machine. Therefore, the stray loss can be modeled in a way similar to that used for core loss modeling. The stator per phase stray loss at harmonic frequency  $f_n$  can be given as

$$P_{sln} = k_{sln} \left[ \frac{k_h}{f_n} + k_e \right] V_{sln}^2 \quad (3.12)$$

where  $V_{sln}$  is the voltage across the stator leakage inductance and  $k_{sln}$  the stray loss constant. Therefore, the stray loss can be represented by an equivalent resistance  $R_{sln}$  in parallel with the leakage inductance as

$$R_{sln} = \frac{1}{k_{sln} \left[ \frac{k_h}{f_n} + k_e \right]} \quad (3.13)$$

A similar expression was derived for rotor harmonic stray loss. The stray loss due to fundamental current is essentially concentrated in the stator, and an equation similar to (3.13) could also be used. However, the fundamental stray loss was represented by a

resistance in series with the stator leakage reactance  $X_{ls}$ , for reasons that will become clear later. The fundamental voltage drop  $V_{sl}$  across the leakage reactance  $X_{ls}$  can be expressed as  $(2\pi f L_{ls} I_{sl})$ , where  $I_{sl}$  is the fundamental stator current. It can be substituted into (3.12) to derive fundamental per-phase stray loss  $P_{sl}$  as

$$P_{sl} = k_{sl} [k_h f + k_e f^2] I_{sl}^2 = R_{sl} I_{sl}^2 \quad (3.14)$$

where  $R_{sl}$  is the equivalent series resistance. From this expression,  $R_{sl}$  is given as

$$R_{sl} = k_{sl} [k_h f + k_e f^2] \quad (3.15)$$

### Friction and Windage Losses

The friction and windage losses are essentially a function of motor speed  $\omega_r$  and does not depend on the type of power supply. It can be expressed as

$$P_{fw} = k_{fw} \omega_r^3 \quad (3.16)$$

### 3.2.2 Temperature and Saturation Effects

The preceding discussion on machine losses did not include the effects of temperature on winding resistances, nor the saturation effects on machine inductances. These effects will now be considered.

## Temperature Effects

Both stator and rotor resistances increase with temperature. The stator temperature can be monitored and approximate correction factor can be applied, but there is no easy way to measure or estimate the rotor temperature. Precise prediction of temperature in each part of the machine requires detailed dynamic thermal model that depends on machine geometry, material characteristics, cooling effects, etc, and is extremely difficult to estimate. The machine transient thermal response can be given approximately by a first order model, where the temperature rise  $\Delta T$  is expressed as

$$\Delta T = \frac{P_{\text{tl}}}{\theta (1 + \tau s)} \quad (3.17)$$

where  $P_{\text{tl}}$  is the total machine loss,  $\theta$  is the steady-state thermal resistance, and  $\tau$  is the thermal time constant. The  $\theta$  and  $\tau$  parameters can be estimated approximately by experimentation. Both rotor and stator resistances were corrected for temperature effects by using the well known formula

$$R_{T_2} = R_{T_1} (1 + \alpha_{T_1} (T_2 - T_1)) \quad (3.18)$$

where  $\alpha_{T_1}$  = temperature coefficient (usually at  $T_1=25^\circ\text{C}$ ), and  $\Delta T = (T_2 - T_1)$ . The temperature corrected resistances were then used to calculate fundamental and harmonic copper losses. For harmonic rotor losses, the skin effect was superimposed on the temperature effect.

## Saturation Effects

Although saturation is strictly present in both leakage and magnetizing inductances, it was ignored in the former, and represented in the magnetizing inductance  $L_m$  by a piece-wise linear function of magnetizing current  $I_m$  as

$$\begin{aligned} L_m &= L_{m0} & , \text{ if } I_m \leq I_{m0} \\ &= L_{m0} - m (I_m - I_{m0}) & , \text{ if } I_m > I_{m0} \end{aligned} \quad (3.19)$$

where  $L_{m0}$  is the unsaturated inductance and  $I_m$  is the magnetizing current at the start of saturation. The saturation coefficient  $m$  was selected to best fit the actual saturation curve of the machine.

### 3.2.3 Per-phase Harmonic Equivalent Circuit

The effects of time harmonics have been traditionally investigated by solving the per-phase equivalent circuit [25] shown in Fig. 3.4(a), where the harmonic stray losses are represented by shunt resistances ( $R_{ssn}$  and  $R_{tsn}$ ). For each harmonic component, the circuit is solved, and superposition principle is applied to get the overall harmonic effect [25]. In this way, the frequency dependence of machine parameters can be taken into account precisely. The following simplifying assumptions can be made at this point:

- For sinusoidal PWM or hysteresis-band current-controlled inverter, only the carrier frequency is considered for computation of frequency dependent parameters, and the resulting circuit can be used to compute the effect of all the harmonics with little loss of precision.
- The harmonic frequencies are sufficiently high such that the harmonic slip  $s_n$  is essentially one.



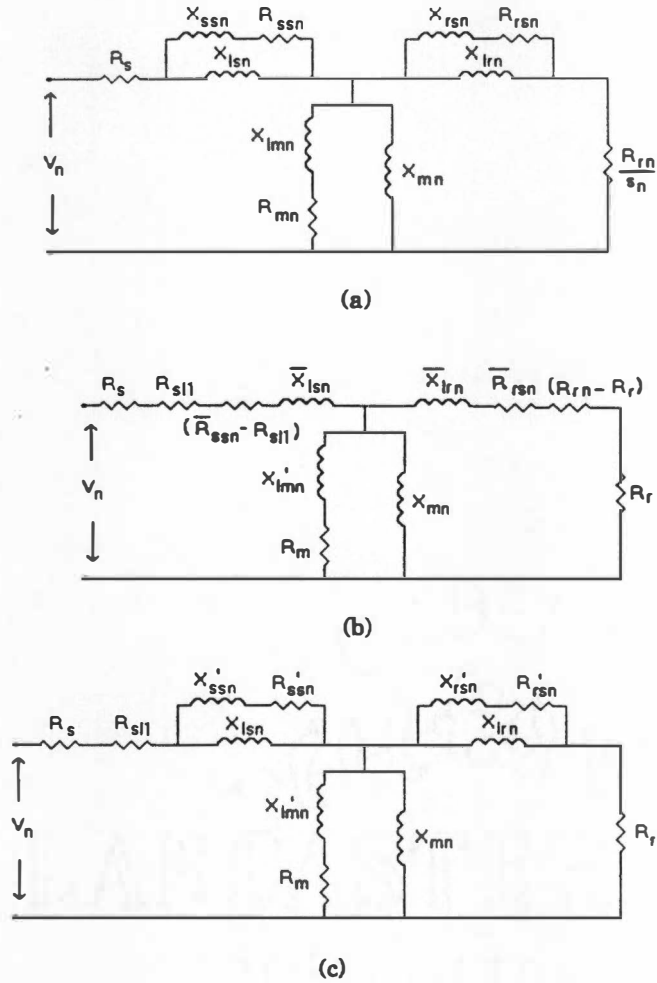


Fig. 3.4 Per phase harmonic equivalent circuit of the induction motor.

- a) Generic circuit for harmonic of order  $n$ .
- b) "Series" equivalent form of circuit (a).
- c) Modified "shunt" equivalent form of circuit (b).

By applying these assumptions, Fig 3.4(a) was converted to the series equivalent form of Fig. 3.4(b). The barred parameters are simply the series equivalents of the corresponding original parameters. For example, the series equivalent stator stray loss resistance can be expressed as

$$\bar{R}_{ssn} = \frac{R_{ssn} X_{ssn}^2}{R_{ssn}^2 + (X_{ssn} + X_{lsn})^2} \approx \frac{R_{ssn} X_{ssn}^2}{R_{ssn}^2 + X_{lsn}^2} \quad (3.20)$$

since the secondary leakage reactance  $X_{ssn}$  is very small. The harmonic rotor resistance  $R_m$  is shown split into fundamental rotor resistance  $R_r$  and  $(R_m - R_r)$ . Similarly,  $R_{ssn}$  is shown as the sum of the fundamental frequency stray loss resistance  $R_{sl1}$  and  $(R_{ssn} - R_{sl1})$ . The harmonic core loss resistance  $R_{mn}$  was substituted in Fig. 3.4(b) by a series combination of the fundamental core loss resistance  $R_m$  and a modified secondary magnetizing reactance  $X'_{lmn}$ , so as to ensure constancy of harmonic core loss  $P_{cln}$ . From Fig. 3.4(a), the harmonic core loss  $P_{cln}$  (neglecting small  $X_{lmn}$ ) is given as

$$P_{cln} = \frac{3 V_{mn}^2}{R_{mn}} \quad (3.21)$$

where  $V_{mn}$  is the rms harmonic airgap voltage. From Fig. 3.4(b),  $P_{cln}$  is given by

$$P_{cln} = \frac{3 V_{mn}^2 R_m}{R_m^2 + X_{lmn}'^2} \quad (3.22)$$

In order to keep the harmonic core loss invariant, the two equations must yield the same result. By equating the two expressions, the modified secondary magnetizing reactance was derived as follows:

$$X_{lmn}' = \sqrt{R_{mn} R_m - R_m^2} \quad (3.23)$$

The circuit of Fig. 3.4(b) was next transformed into the modified "shunt" form of Fig. 3.4(c). The final values of the harmonic stray loss resistances  $R_{ssn}'$  and  $R_{rsn}'$  were obtained by equating the corresponding resistive terms in Figs. 3.4(b) and 3.4(c). Neglecting the small  $X_{rsn}'$  the following expression was derived:

$$\frac{R_{rsn}' X_{lrn}}{R_{rsn}'^2 + X_{lrn}^2} = R_{rle} \quad (3.24)$$

where  $R_{rle} = R_{rsn} + (R_m - R_r)$ . Solving for  $R_{rsn}'$ ,

$$R_{rsn}' = \frac{X_{lrn}^2 \pm \sqrt{\left(\frac{X_{lrn}^2}{R_{rle}}\right)^2 - 4 X_{lrn}^2}}{2} \quad (3.25)$$

For most practical drives,  $R_{rsn} > X_{lrn}$  and therefore, the plus sign is considered in the above equation. With a similar procedure, the expression for  $R_{ssn}'$  was also derived. In practice, the value of  $R_{sll}$  is very small compared to  $R_{ssn}$ . Therefore,  $R_{ssn}'$  could be taken equal to  $R_{ssn}$ . Note that  $R_{rsn}'$  represents not only the rotor harmonic stray loss, but also the additional harmonic copper loss due to skin effect.

### 3.2.4 Synchronous Frame Lossy Equivalent Circuits

The per-phase equivalent circuit derived in Fig. 3.4(c) is only valid for steady-state operation, and can not be used for dynamic performance study. Usually, synchronously rotating frame  $D^e$ - $Q^e$  equivalent circuits are used for dynamic study. The standard  $D^e$ - $Q^e$  equivalent circuits can not directly incorporate a core loss resistor in parallel with magnetizing inductance because DC current (equivalent fundamental frequency current)

will not flow through it. In this section, it is described how these circuits were modified to incorporate the core loss resistor, and then how the harmonic equivalent circuits were superimposed to them to derive the unified lossy equivalent circuits.

### D<sup>e</sup>-Q<sup>e</sup> Equivalent Circuits with Core Loss Resistor

The stationary frame D<sup>s</sup>-Q<sup>s</sup> equivalent circuits can easily incorporate core loss resistance in parallel with magnetizing inductance, as shown in Fig. 3.5. With this modifications the following equations can be readily written:

$$R_s \begin{pmatrix} i_{qs}^s \\ i_{ds}^s \end{pmatrix} + L_s \frac{d}{dt} \begin{pmatrix} i_{qs}^s \\ i_{ds}^s \end{pmatrix} + R_m \begin{pmatrix} i_{qrm}^s \\ i_{drm}^s \end{pmatrix} = \begin{pmatrix} v_{qs}^s \\ v_{ds}^s \end{pmatrix} \quad (3.26)$$

$$-L_m \frac{d}{dt} \begin{pmatrix} i_{qm}^s \\ i_{dm}^s \end{pmatrix} + R_m \begin{pmatrix} i_{qrm}^s \\ i_{drm}^s \end{pmatrix} = \begin{pmatrix} 0 \\ 0 \end{pmatrix} \quad (3.27)$$

$$-\omega_r \begin{pmatrix} \Psi_{dr}^s \\ \Psi_{qr}^s \end{pmatrix} + R_r \begin{pmatrix} i_{qr}^s \\ i_{dr}^s \end{pmatrix} + L_r \frac{d}{dt} \begin{pmatrix} i_{qr}^s \\ i_{dr}^s \end{pmatrix} + L_m \frac{d}{dt} \begin{pmatrix} i_{qm}^s \\ i_{dm}^s \end{pmatrix} = \begin{pmatrix} v_{qr}^s \\ v_{dr}^s \end{pmatrix} \quad (3.28)$$

Synchronous frame quantities are related to their stationary frame counterparts by a transformation matrix T, defined as

$$T = \begin{bmatrix} \cos \omega_e t & \sin \omega_e t \\ -\sin \omega_e t & \cos \omega_e t \end{bmatrix} \quad (3.29)$$

where  $\omega_e$  is the synchronous frequency,  $\cos \omega_e t$  and  $\sin \omega_e t$  are the unit vectors. For the stator currents, the relationship can be expressed as

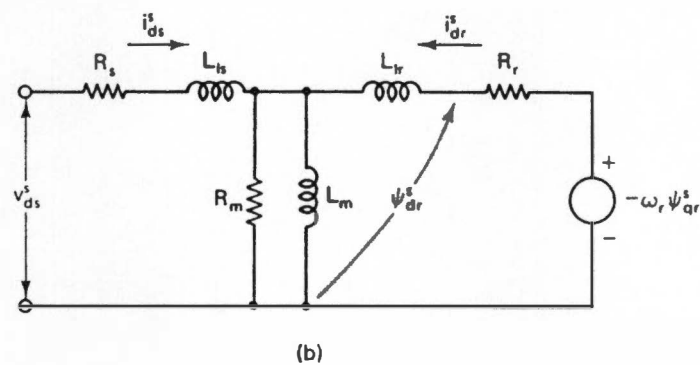
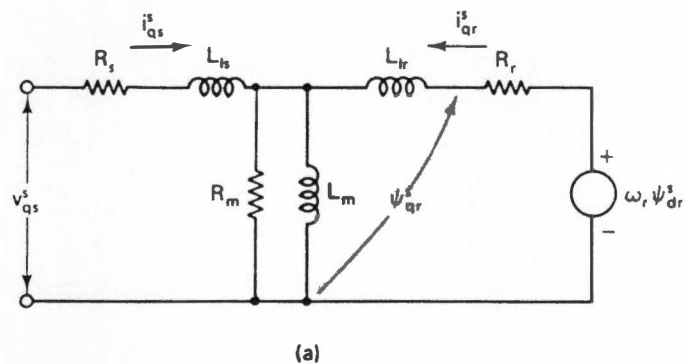


Fig. 3.5  $D^s$ - $Q^s$  equivalent circuit with core loss resistance.

$$\begin{pmatrix} i_{qs}^s \\ i_{ds}^s \end{pmatrix} = T \begin{pmatrix} i_{qs} \\ i_{ds} \end{pmatrix} \quad (3.30)$$

Substitution of (3.30) and similar relations for the remaining variables into (3.26) results in

$$R_s T \begin{pmatrix} i_{qs} \\ i_{ds} \end{pmatrix} + L_s \frac{d}{dt} \left[ T \begin{pmatrix} i_{qs} \\ i_{ds} \end{pmatrix} \right] + R_m T \begin{pmatrix} i_{qrm} \\ i_{drm} \end{pmatrix} = T \begin{pmatrix} v_{qs} \\ v_{ds} \end{pmatrix} \quad (3.31)$$

Pre-multiplying (3.31) by the inverse transformation  $T^{-1}$  yields

$$R_s \begin{pmatrix} i_{qs} \\ i_{ds} \end{pmatrix} + L_s T^{-1} \frac{d}{dt} \left[ T \begin{pmatrix} i_{qs} \\ i_{ds} \end{pmatrix} \right] + R_m \begin{pmatrix} i_{qrm} \\ i_{drm} \end{pmatrix} = \begin{pmatrix} v_{qs} \\ v_{ds} \end{pmatrix} \quad (3.32)$$

As  $T$  is a function of time, the product rule must be used to evaluate the derivative, and the second term can be rewritten as

$$\begin{aligned} L_s T^{-1} \frac{d}{dt} \left[ T \begin{pmatrix} i_{qs} \\ i_{ds} \end{pmatrix} \right] &= L_s \left\{ T^{-1} \frac{dT}{dt} \begin{pmatrix} i_{qs} \\ i_{ds} \end{pmatrix} + T^{-1} T \frac{d}{dt} \begin{pmatrix} i_{qs} \\ i_{ds} \end{pmatrix} \right\} \\ &= L_s \left\{ \begin{pmatrix} 0 & \omega_e \\ -\omega_e & 0 \end{pmatrix} \begin{pmatrix} i_{qs} \\ i_{ds} \end{pmatrix} + \frac{d}{dt} \begin{pmatrix} i_{qs} \\ i_{ds} \end{pmatrix} \right\} \\ &= L_s \omega_e \begin{pmatrix} i_{ds} \\ -i_{qs} \end{pmatrix} + L_s \frac{d}{dt} \begin{pmatrix} i_{qs} \\ i_{ds} \end{pmatrix} \end{aligned} \quad (3.33)$$

Substitution of the last form of (3.33) into (3.32) produces

$$R_s \begin{pmatrix} i_{qs} \\ i_{ds} \end{pmatrix} + \omega_e \begin{pmatrix} \psi_{ds} \\ -\psi_{qs} \end{pmatrix} + L_{ls} \frac{d}{dt} \begin{pmatrix} i_{qs} \\ i_{ds} \end{pmatrix} + R_m \begin{pmatrix} i_{qrm} \\ i_{drm} \end{pmatrix} = \begin{pmatrix} v_{qs} \\ v_{ds} \end{pmatrix} \quad (3.34)$$

where  $\psi_{dls} = L_{ls} i_{ds}$  and  $\psi_{qls} = L_{ls} i_{qs}$  are the stator leakage fluxes, and the new terms  $\omega_e \psi_{dls}$  and  $-\omega_e \psi_{qls}$  represent the speed voltages due to rotation of the reference axes. By applying the same methodology to (3.27) and (3.28), their synchronous frame counterparts can be obtained as

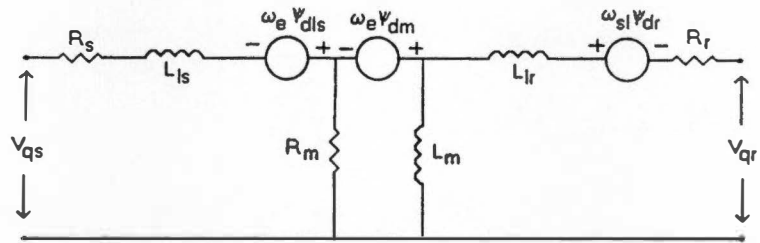
$$\omega_e \begin{pmatrix} \psi_{dm} \\ \psi_{qm} \end{pmatrix} + L_m \frac{d}{dt} \begin{pmatrix} i_{qm} \\ i_{dm} \end{pmatrix} - R_m \begin{pmatrix} i_{qrm} \\ i_{drm} \end{pmatrix} = \begin{pmatrix} 0 \\ 0 \end{pmatrix} \quad (3.35)$$

$$(\omega_e - \omega_r) \begin{pmatrix} \psi_{dr} \\ \psi_{qr} \end{pmatrix} + R_r \begin{pmatrix} i_{qr} \\ i_{dr} \end{pmatrix} + L_{lr} \frac{d}{dt} \begin{pmatrix} i_{qr} \\ i_{dr} \end{pmatrix} + L_m \frac{d}{dt} \begin{pmatrix} i_{qm} \\ i_{dm} \end{pmatrix} = \begin{pmatrix} v_{qr} \\ v_{dr} \end{pmatrix} \quad (3.36)$$

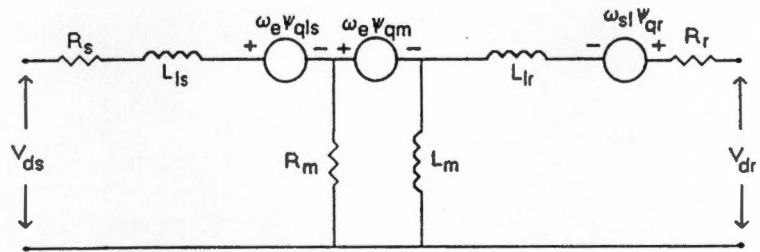
Equation 3.34 through 3.36 can be represented by the equivalent circuits of Fig.3.6, where  $\psi_{dm} = L_m i_{dm}$  and  $\psi_{qm} = L_m i_{qm}$  are the air-gap fluxes,  $\psi_{dr} = \psi_{dm} + L_{lr} i_{dr}$  and  $\psi_{qr} = \psi_{qm} + L_{lr} i_{qr}$  are the rotor fluxes.

### D<sup>e</sup>-Q<sup>e</sup> Equivalent Circuits with Core Loss and Harmonic Loss

Although the harmonic equivalent circuit of Fig. 3.4(c) is a per phase stationary frame circuit, it can be used in the synchronously rotating frame as well, with little loss of precision, because the axes rotation will have the effect of adding (or subtracting) the fundamental frequency to the particular harmonic frequency. Consequently, under the assumption  $f_n \gg f$ , the effect of axes rotation is negligible. The circuit of Fig. 3.4(c) was therefore, superimposed on the synchronously rotating frame D<sup>e</sup>-Q<sup>e</sup> equivalent circuits with core loss resistance of Fig. 3.6, resulting in the complete lossy dynamic D<sup>e</sup>-Q<sup>e</sup>



(a)



(b)

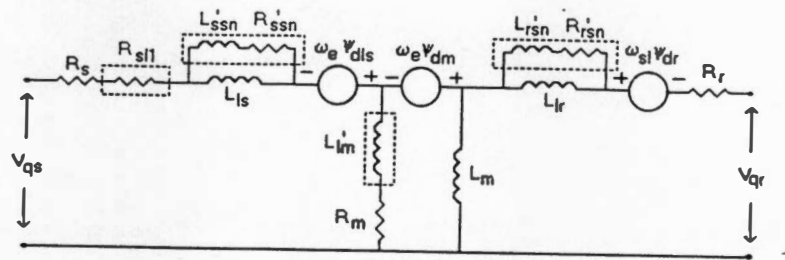
Fig. 3.6 D<sup>c</sup>-Q<sup>c</sup> equivalent circuit with core loss resistance.



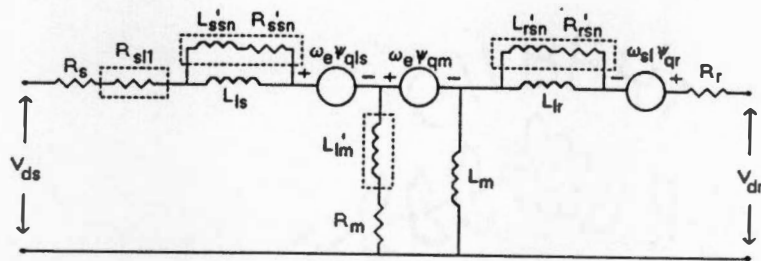
equivalent circuits shown in Fig. 3.7. The model represents true physical behavior of the machine, and can be used for evaluation of fundamental and harmonic losses, as well as for dynamic studies. Since at steady-state conditions all fundamental variables appear as DC quantities, the fundamental current will not flow through  $R'_{ssn}$  and  $R'_{rsn}$ , i.e., the harmonic stray loss shunt terms have no effect on fundamental losses. Similarly, the presence of the secondary magnetizing inductance  $L'_{lm}$  has no effect on fundamental core loss. For harmonic losses, the circuits of Fig. 3.7 give almost the same result as that of Fig. 3.4(c). This follows from the fact that the harmonic fluxes are very small, and therefore, the corresponding harmonic voltages present in the dependent voltage sources are negligible, i.e., the terms such as  $\omega_e \psi_{dm}$  essentially represent fundamental counter emf. During transient operations, some amount of fundamental current will flow through the shunt stray loss resistances, and this is theoretically coherent, because a change in fundamental leakage flux induces extra stray losses both in the stator and the rotor. During the transient, the effective rotor resistance seen by the fundamental current increases and the effective inductance decreases, and this is also consistent with the theory, because the skin effect is present during sinusoidal transients.

### 3.2.5 Lossy Model Parameter Computation

In order to use the equivalent circuits of Fig. 3.7, it was necessary to evaluate the parameters for the particular machine. The fundamental frequency parameters can be easily obtained from standard tests, but harmonic frequency parameters are much more difficult to obtain experimentally [28]. On the other hand, accurate theoretical prediction



a)



b)

### 3.7 Lossy D<sup>c</sup>-Q<sup>c</sup> equivalent circuits in synchronously rotating reference frame.

a) Q<sup>c</sup>-axis circuit      b) D<sup>c</sup>-axis circuit

of harmonic frequency parameters also constitutes a formidable task. In this work, the standard fundamental frequency parameters were taken from literature [39], and the remaining parameters were estimated from practical considerations [31], as discussed below.

The fundamental stray load loss  $P_{sl1}$  at rated conditions amount to a few percent (typically 1% to 3%) of the rated machine power  $P_o$  [35]. Let  $\epsilon_{sl}$  be the selected (or measured) percentage for a particular machine with a rated current  $I_s$ . The stray loss resistance  $R_{slb}$ , at base frequency  $f_b$  is given by

$$R_{slb} = \frac{\epsilon_{sl} P_o}{3 I_s^2} \quad (3.37)$$

At any other fundamental frequency  $f$ , the fundamental stray loss resistance of (3.15) can be rewritten as a function of  $R_{slb}$

$$R_{sl1} = R_{slb} \left( \frac{f}{f_b} \right) \left( \frac{1 + \gamma_1 f}{1 + \gamma_1 f_b} \right) \quad (3.38)$$

where  $\gamma_1 = K_e/k_h$ .

Although the core loss resistance  $R_m$  at base 60 Hz frequency can be easily computed from standard machine tests, the estimation of eddy current coefficient  $k_e$  and hysteresis loss coefficient  $k_h$  requires the breakdown of total core loss  $P_c$  into its eddy current  $P_e$  and hysteresis  $P_h$  components. Usually, the eddy current loss  $P_e$  amounts to 20% - 50% of total core loss. Let  $\epsilon_{ec}$  be the assumed  $P_e/P_c$  ratio. The corresponding relation between eddy current and hysteresis losses becomes

$$P_e = \frac{\epsilon_{ec}}{1 - \epsilon_{ec}} P_h \quad (3.39)$$

Substituting (3.3) and (3.4) into (3.39) leads to

$$k_e = \frac{k_h}{f} \frac{\epsilon_{ec}}{1 - \epsilon_{ec}} \quad (3.40)$$

At no load, the per unit slip  $s$  is practically zero, and (3.10) can be rewritten as

$$\frac{k_h}{f} + k_e = \frac{(2\pi)^2}{R_m} \quad (3.41)$$

where  $(2\pi)^2$  has been substituted for  $k_e$ . Finally, solving (3.40) and (3.41) results in

$$k_e = \frac{(2\pi)^2 \epsilon_{ec}}{R_m} \quad (3.42)$$

$$k_h = \frac{(2\pi)^2 (1 - \epsilon_{ec}) f}{R_m} \quad (3.43)$$

The harmonic frequency stray loss resistances will now be discussed. Kawagishi et al. [31] have indicated that the efficiency of an induction machine fed by a 5 KHz sinusoidal PWM inverter is nearly 99% of that attainable under a 60 Hz AC supply. Their findings were also confirmed by Bausch et al. [59] for a much larger machine, operating from a hysteresis band PWM inverter. It can be assumed, therefore, that the harmonic stray losses  $P_{slh}$  of an induction motor fed by a 5 KHz PWM inverter is a percentage  $\epsilon_{slh}$  ( $\approx 1\%$ ) of the rated output power  $P_o$ . From Fig. 3.4(a) it is clear that, essentially all harmonic voltage will appear across the leakage reactances  $X_{lsn}$  and  $X_{lm}$ , since they are much larger than the resistive terms  $R_s$  and  $R_r$ . Neglecting the small

secondary leakage reactance terms  $X_{ssn}$  and  $X_{rsn}$ , the total harmonic stray loss resistance  $R_{slh}$  can be obtained from

$$R_{slh} = \frac{3V_h^2}{\epsilon_{slh}P_o} \quad (3.44)$$

where  $V_h$  is total rms harmonic phase voltage. For a given PWM inverter,  $V_h$  can be obtained from simulation, or computed from the harmonic spectrum, if known. Distribution of  $R_{slh}$  into rotor and stator components is accomplished by assuming a partition proportional to the respective leakage inductances as

$$R_{rsb} = R_{slh} \frac{L_r}{L_r + L_s} \quad (3.45)$$

$$R_{ssb} = R_{slh} \frac{L_s}{L_r + L_s} \quad (3.46)$$

The actual harmonic stray loss resistances  $R_{ssn}$  and  $R_{rsn}$ , at any other carrier frequency  $f_c$  are obtained from (3.13) as

$$R_{rsn} = R_{ssb} \left( \frac{f_c}{f_{cb}} \right) \left( \frac{1 + \gamma_h f_{cb}}{1 + \gamma_h f_c} \right) \quad (3.47)$$

$$R_{rsn} = R_{rsb} \left( \frac{f_c}{f_{cb}} \right) \left( \frac{1 + \gamma_h f_{cb}}{1 + \gamma_h f_c} \right) \quad (3.48)$$

where  $\gamma_h = k_{eh}/k_{hh}$  is assumed to be identical to  $\gamma_1$ , and  $f_{cb}$  is the base carrier frequency (5 KHz, in this discussion).

The secondary leakage inductances  $L_{ssn}$  and  $L_{rsn}$ , due to eddy current fluxes, are small compared to the conventional leakage inductances [25]. In the simulation study

discussed later, they were taken as 5% of the corresponding leakage inductances. Their presence in the equivalent circuit is mainly to ensure consistency of the dynamic behavior of the model. In fact, without them the equivalent circuit would become purely resistive at infinite frequency, whereas the actual induction motor becomes purely inductive.

### 3.3 Loss Modeling of Converter System

While for a diode rectifier only the conduction loss need to be considered, for a PWM inverter both switching loss and conduction loss are relevant.

#### 3.3.1 Loss Modeling of Diode Rectifier

The three-phase diode rectifier with capacitor filter of Fig. 3.3 conducts discontinuously, and it can be shown that only two diodes (one in the upper group and one in the lower group) conduct at any instant. Fig. 3.8 shows the Thevenin equivalent circuit, where  $V_r$  is the ideal rectifier voltage profile, and the DC link inductance is  $L_d = 2 L_{sl}$ , where  $L_{sl}$  is the per-phase source leakage inductance. The typical DC link voltages and current waves are shown in Fig.3.9. The diodes conduct a current pulse  $i_d$  when  $V_r > (V_d + V_f)$ , but conduction ceases sometime after  $V_r < (V_d + V_f)$ , due to  $L_d$  effect. The two conducting diodes can be modeled by an off-set voltage  $V_f$  in series with a nonlinear resistance  $R$  as indicated. From the conduction characteristics of a particular diode, the voltage drop equation can be derived by using the software TABLE-CURVE [36]. The software takes a set of (x,y) coordinate pairs as input and calculates the equation of the best fitting curve as given by

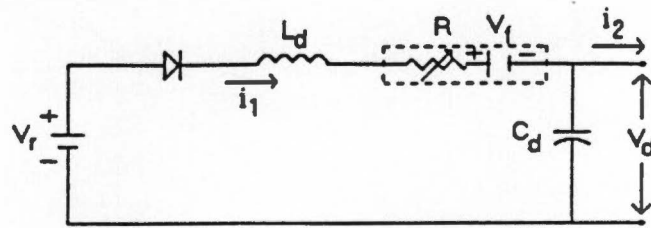


Fig. 3.8 Diode rectifier equivalent circuit.

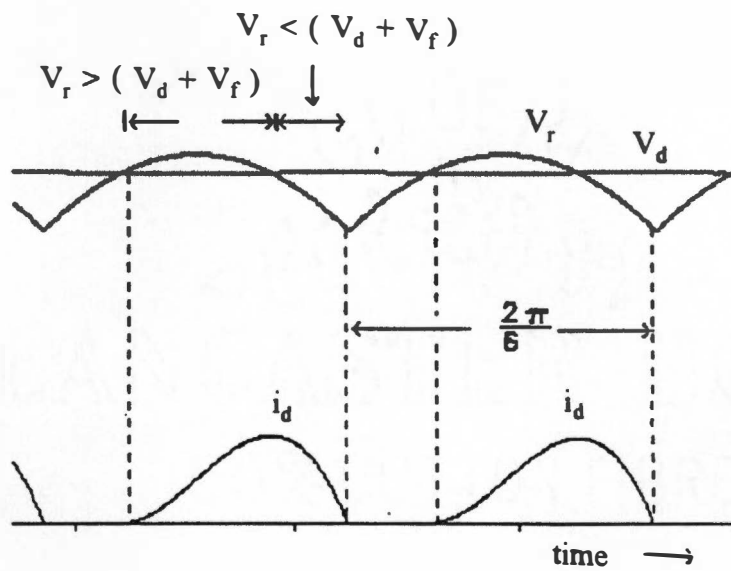


Fig. 3.9 Rectifier voltage and current waves

$$v_{dd} = v_{do} + K i_d^m \quad (3.49)$$

where  $v_{do}$  is the offset voltage, and  $m$  the resistive drop exponent. The instantaneous conduction loss  $P_{ild}$  for the diode bridge can then be given as

$$P_{ild} = 2 v_{dd} i_d \quad (3.50)$$

Similarly, the instantaneous rectifier input power  $P_{iir}$  and output power  $P_{ior}$  can be expressed as

$$P_{iir} = V_r i_d \quad (3.51)$$

$$P_{ior} = V_d i_d \quad (3.52)$$

In the simulation program these expressions are integrated and averaged over a  $60^\circ$  interval to get the corresponding average values, required for efficiency computations.

### 3.3.2 Loss Modeling of PWM Inverter

For a PWM inverter, both conduction and switching losses should be considered. The conduction loss, in turn, is distributed between transistors and feedback diodes.

#### Conduction Loss

A typical inverter phase leg, with feedback diodes and polarized snubbers, is shown in Fig. 3.10(a). The conduction loss equivalent circuit is shown in Fig. 3.10(b), where each conduction drop has been modeled by a resistance in series with an offset voltage. Again, from the transistor saturation characteristics, the following linear voltage drop equation was derived with the help of TABLE-CURVE as shown in (3.53).



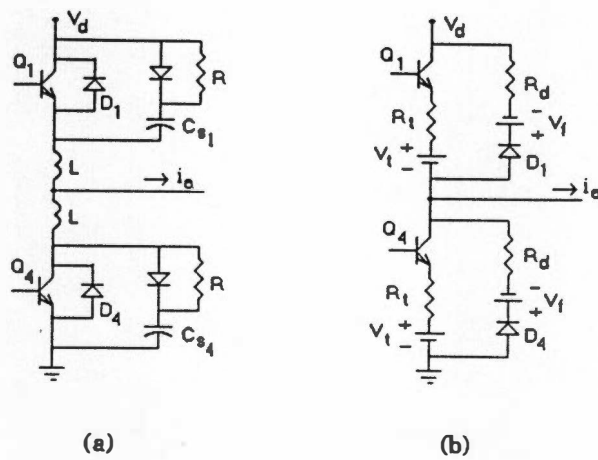


Fig. 3.10 (a) Transistor inverter phase leg.

(b) Conduction loss equivalent circuit.

$$v_{ud} = v_{u0} + R_i i_c \quad (3.53)$$

For the feedback diodes, the voltage drop eqn. (3.48) is valid for the particular devices.

It is important to observe that, for the positive half cycle of phase current  $i_a$ , only transistor  $Q_1$  or feedback diode  $D_4$  conducts, whereas for the negative half cycle,  $Q_4$  or  $D_1$  conducts. Let  $G_A$  be the logic signal from the PWM control, such that, if  $G_A=1$  the upper transistor  $Q_1$  conducts and conversely, if  $G_A=0$ ,  $Q_4$  conducts. The leg voltage with respect to "ground",  $v_{ag}$ , can be derived from the equivalent circuit as follows

$$\begin{aligned} v_{ag} &= V_d - v_{ida} ; \text{ if } i_a > 0 \text{ and } G_A = 1 \\ &= -v_{dda} ; \text{ if } i_a > 0 \text{ and } G_A = 0 \\ &= V_d + v_{dda} ; \text{ if } i_a < 0 \text{ and } G_A = 1 \\ &= v_{dda} ; \text{ if } i_a < 0 \text{ and } G_A = 0 \end{aligned} \quad (3.54)$$

Conversely, the instantaneous conduction loss in phase leg A can be expressed as

$$\begin{aligned} P_{cla} &= (V_d - v_{ag}) i_a ; \text{ if } G_A = 1 \\ &= -v_{ag} i_a ; \text{ if } G_A = 0 \end{aligned} \quad (3.55)$$

Similar expressions can be written for the other two phase legs, and the total instantaneous conduction loss  $P_{icli}$  obtained as the sum of the three components.

### Switching Losses

Proper computation of switching losses requires careful analysis of inverter operation, as illustrated in Fig. 3.11 by the PWM waves for phase leg a. Assume, for example, that  $i_a$  is positive and  $Q_1$  is initially ON, such that current flows through it.

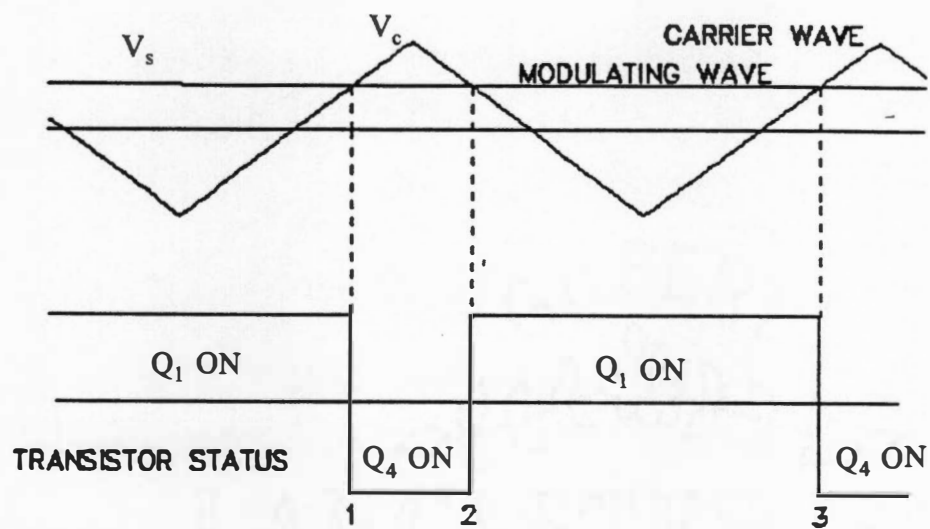


Fig. 3.11 Pulse width modulation waves for phase leg A.

At instant 1,  $Q_1$  is turned OFF and  $Q_4$  is turned ON, the energy stored in  $C_{s4}$  is dissipated across the series resistor, and  $Q_1$  goes through a turn-off switching loss. However, as the current is now actually flowing through  $D_4$ , no turn-on loss occurs in  $Q_4$ . Similarly, at instant 2, when  $Q_1$  is again turned ON,  $C_{s1}$  discharges and at the same time the device has a turn-on loss, but no loss occurs in  $Q_4$ , since it was not carrying current. Typical turn-on and turn-off switching waves are shown in Fig. 3.12. The energy loss during switchings can be related to the area of the product curve  $v_{CE} i_C$  (not shown). Summarizing, at every period of the carrier wave, the switching losses per phase leg are:

- Two discharges of capacitor snubbers;
- One turn-on loss;
- One turn-off loss.

### Shunt Snubber Loss

After the qualitative discussion above, loss expressions will be derived. The energy loss associated with one snubber capacitor  $C_s$  discharge is

$$W_1 = \frac{1}{2} C_s V_d^2 \quad (3.56)$$

The total snubber energy loss of the inverter, in one fundamental period  $T$ , can be represented as

$$W_t = 3N_s W_1 = \frac{3}{2} N_s C_s V_d^2 \quad (3.57)$$

where  $N_s$  is the number of switchings (on-and-off) of a phase leg in one fundamental period  $T$ . Consequently, the average power loss due to snubber discharge is

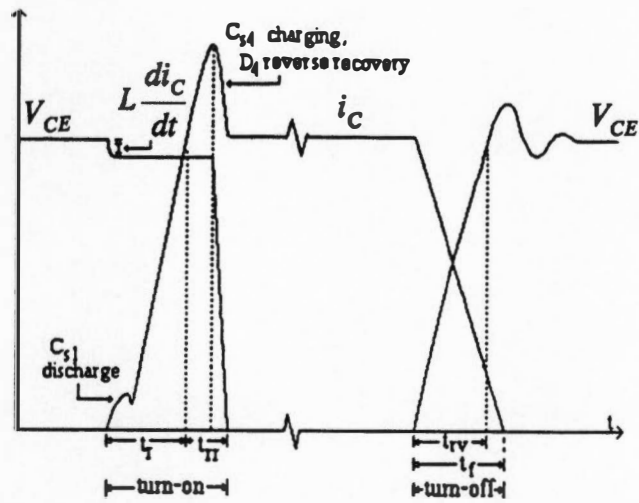


Fig. 3.12 Typical turn-on and turn-off switching waves for transistor  $Q_1$ .

$$P_s = \frac{3}{2} \frac{N_s C_s V_d^2}{T} \quad (3.58)$$

This loss can be represented by an equivalent shunt resistance  $R_s$  across the DC bus as

$$R_s = \frac{2}{3fN_s C_s} \quad (3.59)$$

where  $f = 1/T$  is the fundamental frequency. For a sinusoidal PWM, the quantity  $N_s$  is a constant, whereas for a hysteresis band PWM it can be easily counted.

### Turn-off Switching Loss

Turn-off and turn-on switching losses have been discussed and mathematically analyzed in detail by Mc Murray [32], for a DC chopper. The same formulation was extended here for the case of inverter design.

The selection of snubber capacitor typically takes into account a number of factors, such as the maximum  $dV/dt$  that the transistor can withstand, the allowable voltage overshoot during turn-off, and the turn-off switching losses. However, only the loss aspect was considered here. It can be shown [32] [37] that, for minimum total switching loss (snubber loss + turn-off loss), the value of snubber capacitor  $C_s$  is usually small, such that, during turn-off the collector-emitter voltage rise time  $t_{rv}$  is smaller than the collector current fall time  $t_f$ , as indicated in Fig. 3.12. Besides the assumption of a small  $C_s$ , another one is made in the following analysis [32]:

"During turn-off, the current fall is a linear time function completely determined

by the transistor characteristics, while the voltage rise is determined by the resulting action of the shunt snubber".

By applying this simplifying assumption, the transistor action during a turn-off can be expressed as

$$i_c = I_L \left( 1 - \frac{t}{t_f} \right) \quad ; \quad 0 \leq t \leq t_f \quad (3.60)$$

where  $I_L$  is the load current,  $i_c$  is the transistor collector current, and  $t_f$  the current fall time, as indicated in Fig. 3.12. Similarly, the transistor collector-emitter voltage  $v_{CE}$  is governed by the snubber action as

$$v_{CE} = \frac{1}{C_s} \int_0^t (I_L - i_c) dt \quad (3.61)$$

Substituting (3.60) into (3.61) and solving the integral leads to

$$v_{CE} = \frac{I_L t^2}{2C_s t_f} \quad ; \quad 0 \leq t < t_{rv} \quad (3.62)$$

The  $v_{CE}$  rise time  $t_{rv}$  can be obtained from (3.62) by applying the end condition  $v_{CE} = V_d$ :

$$t_{rv} = \sqrt{\frac{2C_s V_d t_f}{I_L}} \quad (3.63)$$

Neglecting the small voltage ringing, the transistor power dissipation can be expressed as:

$$p_{t1} = \frac{I_L^2}{2C_s} \left( 1 - \frac{t}{t_f} \right) \frac{t^2}{t_f} \quad ; \quad 0 \leq t < t_{rv} \quad (3.64)$$

$$p_{t2} = V_d I_L \left( 1 - \frac{t}{t_f} \right) \quad ; \quad t_{rv} \leq t < t_f \quad (3.65)$$

Correspondingly, the transistor energy loss in one turn-off is

$$W_t = \int_0^{t_{rv}} p_{t1} dt + \int_{t_{rv}}^{t_f} p_{t2} dt \quad (3.66)$$

Equation 3.63 to 3.66 indicate that the transistor turn-off loss decreases as the snubber capacitance is increased, at the expenses of augmented snubber loss. For an inverter, the load current  $I_L$  is nearly sinusoidal, and a precise computation of switching losses would require the solution of the preceding equations at every switching. By using the absolute value of the half-cycle average  $I_{av}$  of the load current in place of  $I_L$ , a good estimate of switching loss can be produced, with significant reduction in computation time. As a result, the average transistor turn-off power loss for all three phase legs  $P_{toff}$  can be expressed as

$$P_{toff} = 3 K_{off} V_d (N_s/2) I_{av} f \quad (3.67)$$

where  $N_s/2$  is the number of lossy turn-offs per converter leg in one cycle of fundamental frequency  $f$ , and the turn-off parameter  $K_{off}$  is given by

$$K_{off} = \frac{t_f}{2} \left( 1 - \frac{4}{3} \frac{t_{rv}}{t_f} + \frac{1}{2} \left( \frac{t_{rv}}{t_f} \right)^2 \right) \quad (3.68)$$

From (3.67) it can be seen that the transistor turn-off loss can be represented by an equivalent DC link shunt resistance as

$$R_{toff} = \frac{V_d}{3 K_{off} (N_s/2) I_{av} f} \quad (3.69)$$



### Turn-on Switching Loss

For a transistor inverter, no snubber inductance  $L$  as indicated in Fig. 3.10 is normally used. The stray inductance due to the wiring between the DC link capacitor and the transistor acts as a parasitic inductance for turn-on snubber. The operation of the parasitic series snubber is dual to that of the shunt snubber, and by using a procedure similar to that used for turn-off loss computation, the transistor turn-on power loss can be given as [32]

$$\begin{aligned} P_{ton} &= 3 K_{on} V_d (N_s/2) I_{av} f \\ &= \frac{V_d^2}{R_{ton}} \end{aligned} \quad (3.70)$$

where the turn-on constant  $K_{on}$  is defined as

$$K_{on} = \frac{t_{fv}}{2} \left( 1 - \frac{4}{3} \frac{t_r}{t_{fv}} + \frac{1}{2} \left( \frac{t_r}{t_{fv}} \right)^2 \right) \quad (3.71)$$

where  $t_r$  is the collector current rise time and  $t_{fv} = t_r + t_{\pi}$  is the  $v_{CE}$  voltage fall time.

Again,  $t_r$  is given by

$$t_r = \sqrt{\frac{2 L t_{fv} I_{av}}{V_d}} \quad (3.72)$$

From eqn. 3.70, the transistor turn-on loss can be represented by an equivalent DC link shunt resistance as

$$R_{ton} = \frac{V_d}{3 K_{on} (N_s/2) I_{av} f} \quad (3.73)$$

Equations 3.70 to 3.72 indicate that the turn-on loss decreases as the inductance  $L$  is increased.

### 3.4 Model Validation

Both the converter and machine models, as discussed before, were simulated in detail, using PC-SIMNON, for a 10 HP drive with indirect vector control, with all the routines included in the Appendix. The diode rectifier routine is a direct translation of the mathematical model of Section 3.3.1. The inverter model uses hysteresis-band current control (HBPWM), and some implementation details will be now discussed. For phase leg A, a logic state variable  $A$  is defined such that, if  $A=1$  the upper transistor ( $Q_1$ ) conducts, whereas if  $A=0$ , the lower transistor is turned on. The new state of the variable ( $NA$ ) is defined as

$$NA = \text{If } I_{ae} > HB \text{ Then } 1 \text{ Else If } I_{ae} < -HB \text{ Then } 0 \text{ Else } A$$

where  $I_{ae}$  is the current error ( $= I_a^* - I_a$ ) and  $HB$  is the amplitude of the hysteresis band. The phase A voltage with respect to "ground" ( $v_{ag}$ ) is obtained from (3.54). The actual phase to neutral voltage ( $v_{an}$ ), is given by [17]:

$$v_{an} = \frac{2}{3} v_{ag} - \frac{1}{3} v_{bg} - \frac{1}{3} v_{cg} \quad (3.74)$$

The number of switchings per cycle  $N_s$  is computed by counting the transitions in the logic state variable  $A$ . The carrier frequency  $f_c$  is directly obtained by the product of  $N_s$  and the fundamental frequency  $f$ . These variables are then used in the computation of converter and machine frequency dependent parameters. Converter conduction and switching loss computation closely follows the mathematical formulation presented in

### Section 3.3.

The equivalent circuits of Fig. 3.7 were used in the derivation of machine state equations. For convenience, the  $Q^e$ -axis circuit is reproduced in Fig. 3.13, indicating the selected state variables. For each axis, five state variables were selected, in this case the currents through the inductances  $L_{ls}$ ,  $L_{ssn}$ ,  $L_m$ ,  $L_{lr}$  and  $L_{rsn}$ . The current through  $L_{lm}$  ( $i_{qrm}$ ) does not constitute an independent state variable, since the following nodal equation must hold:

$$i_{qsl} = -i_{qsr} + i_{qrm} + i_{qm} - i_{qrl} - i_{qrr} \quad (3.75)$$

The above equation can also be written in terms of current derivatives:

$$\frac{d}{dt}i_{qsl} = -\frac{d}{dt}i_{qsr} + \frac{d}{dt}i_{qrm} + \frac{d}{dt}i_{qm} - \frac{d}{dt}i_{qrl} - \frac{d}{dt}i_{qrr} \quad (3.76)$$

In order to obtain a valid SIMNON model, the system must be described in a state equation format. To avoid unnecessary coupling among the state variables derivatives, the loop equations were carefully selected, as shown in Fig. 3.13, such that the inductance  $L_{ls}$  is present in every loop. For example, the loop through  $L_{ssn}$  yields:

$$\frac{d}{dt}i_{qsr} = \frac{1}{L_{ssn}} \left[ L_{ls} \frac{d}{dt}i_{qsl} - R'_{ssn} i_{qsr} \right] \quad (3.77)$$

Substitution of (3.77) along with the other loop equations into (3.76) produced the state equation for  $i_{qsl}$ . The remaining state equations were readily obtained by further substitution of the right side of  $di_{qsl}/dt$  into the corresponding loop equations.

Both steady-state and transient conditions of the system were considered in the validation process of the models. Table 3.1 shows the complete power circuit parameters of the drive. The steady-state system performance was initially investigated, for various

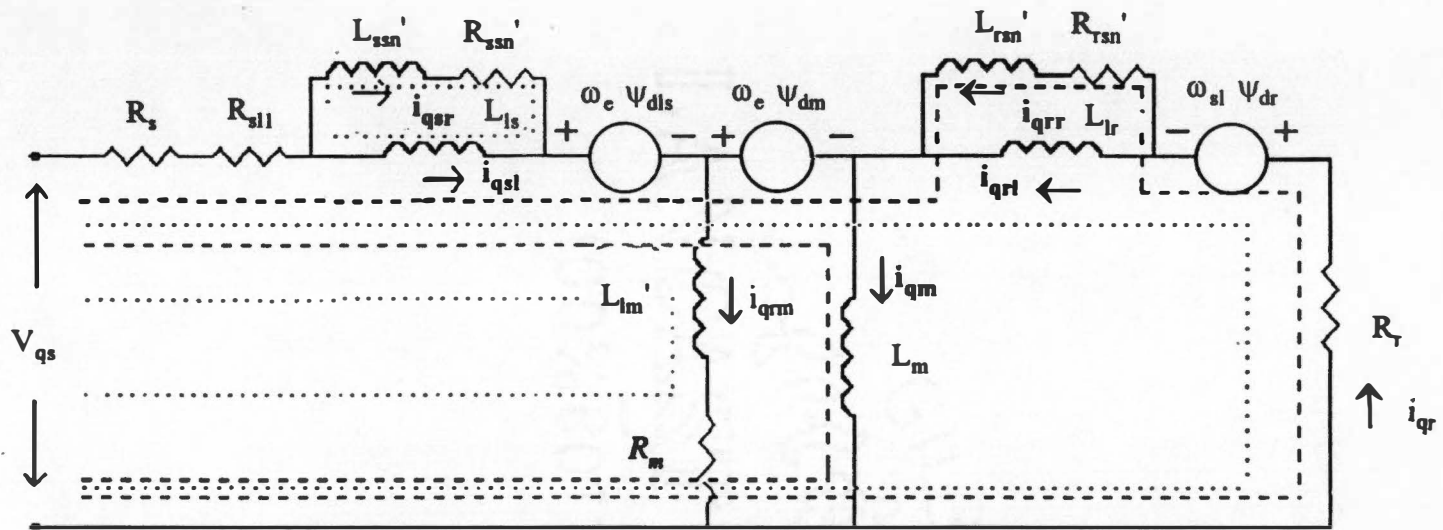


Fig. 3.13  $Q^e$ -axis circuit showing loops for state equations derivation.

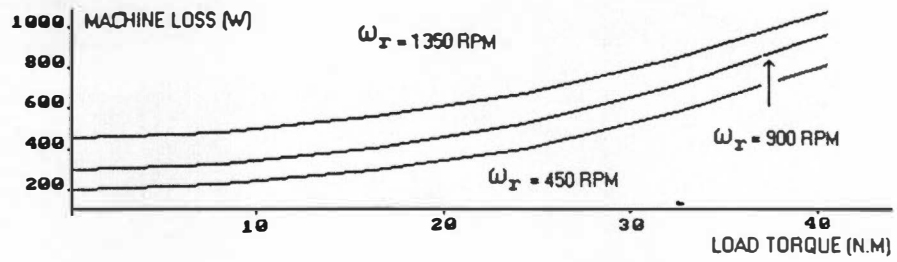
Table 3.1 Power circuit parameters of the AC drive system.

<b>Machine:</b> 10 hp 230 / 460 V 27/13.5 A 1755 rpm 60 Hz Class B 1.15 SF		
<u>D<sup>c</sup>-Q<sup>c</sup> equivalent circuit parameters</u>		
$R_s=0.2264 \Omega$	$R_r=0.1256 \Omega$	$R_m=129.06 \Omega$
$L_{ls}=0.00155 \text{ H}$	$L_{lr}=0.00193 \text{ H}$	$L_m=0.0275 \text{ H}$
$R_{sll}=0.0341 \Omega$	$R_{ssn}'=146.52 \Omega$	$R_{rsn}'=169.63 \Omega$
$L_{lm}'=0.0032 \text{ H}$	$L_{ssn}=7.75 \cdot 10^{-5} \text{ H}$	$L_{rsn}=9.65 \cdot 10^{-5} \text{ H}$
<b>Diode:</b> POWEREX CD 411230 Dual diode module 30 A / 1200 V		
<u>Drop equation parameters:</u>		
$v_{d0}=0.8 \text{ V}$	$K=0.052$	$m=0.585$
<b>Transistor:</b> POWEREX KS 524503 Single Darlington transistor module, 30 A / 600 V		
<u>Drop equation parameters:</u>		
$v_{t0}=0.7 \text{ V}$	$R_t=0.020$	

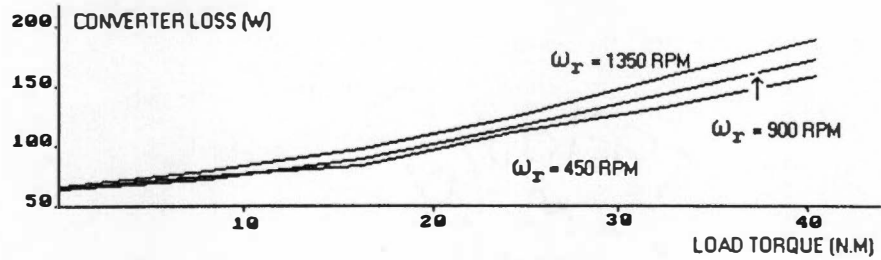
load torque and speed conditions, and the results are shown in Fig.3.14. From the machine loss profiles of Fig. 3.14(a) it can be seen that, for given speed, the total loss increases with torque, primarily due to increased fundamental copper and stray load losses. For a constant load torque, the losses increase with speed, mainly because of additional core loss and friction and windage losses. Fig. 3.14(b) shows the corresponding total converter loss for the same load torque and speed conditions. It can be seen that the converter loss is more affected by an increase in load torque at constant speed, rather than by increase of machine speed at constant load torque. This can be explained as follows:

With rated flux, the machine current is essentially a function of load torque and is practically independent of speed. Therefore, the inverter losses, that basically depend on machine current, is dominantly influenced by load torque. On the other hand, the diode rectifier loss is a function of DC link current, that increases with converter output power. Therefore, the rectifier loss is influenced by both speed and torque of the machine. Fig. 3.14(c) shows the total system efficiency at various torque and speed conditions. It can be noticed that the point of maximum efficiency moves toward the rated torque, as the speed increases, since the machine is designed to yield maximum efficiency at rated torque and speed. The upper speed used in the study is less than the base value of 1800 rpm, because the DC link voltage is not sufficiently high to enforce pure PWM operation near base speed, what is required for correct operation of the vector control system.

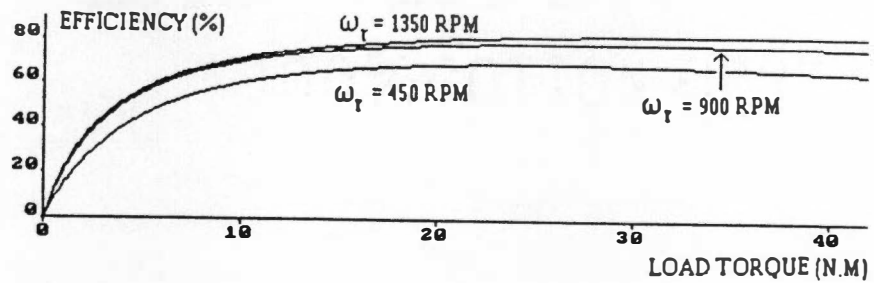
The transient performance will now be discussed. Fig. 3.15(b) and (c) show the flux responses to the magnetizing command current  $i_{ds}^*$  step of Fig. 3.15(a). The response



(a)



(b)



(c)

Fig. 3.14 Steady state performance.

- a) Machine loss at various torques and speeds.
- b) Converter loss at various torques and speeds.
- c) System efficiency at various torque and speed.

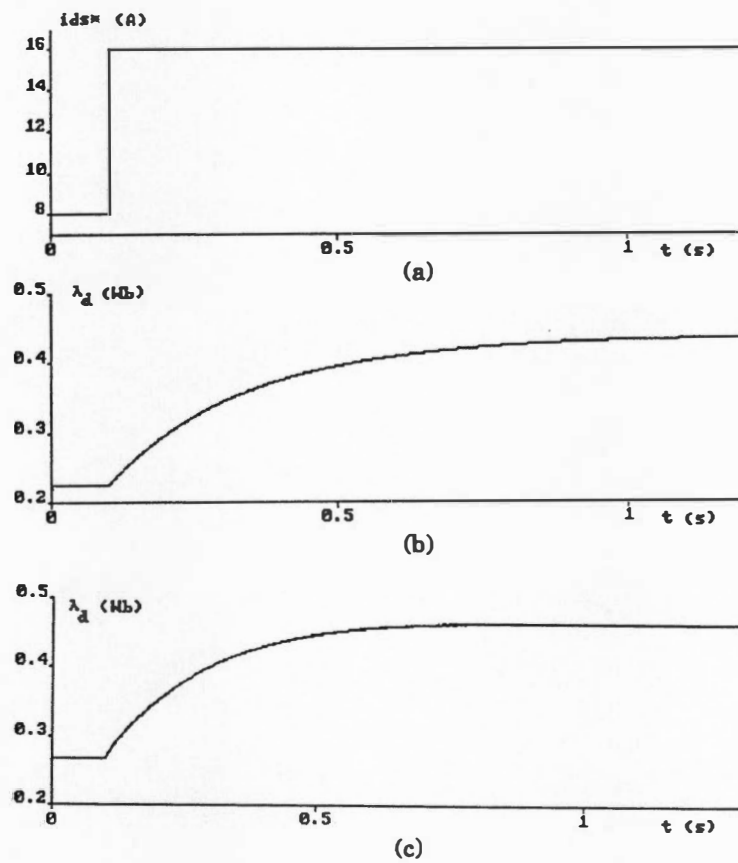


Fig. 3.15 Rotor flux responses at constant speed.

- a) Command current step.
- b) Standard  $D^e$  -  $Q^e$  model response.
- c) Lossy  $D^e$  -  $Q^e$  model response.



of the standard  $D^e - Q^e$  model of Fig. 3.2 is initially shown in Fig. 3.15(b), whereas that of the lossy model of Fig. 3.7 is presented in Fig. 3.15(c). It can be seen that the response of the proposed model has a smaller rise time than that of the standard model. This is caused by the following factors:

- . There is an increase in rotor resistance due to temperature effect, included in the proposed model, but neglected in the standard model.
- . The shunt branches that represent core loss and rotor stray loss have a transient effect of increasing the effective rotor resistance while decreasing the equivalent rotor leakage inductance. Both factors combine to reduce the effective rotor time constant ( $\tau_r = L_r/R_r$ ). While the amount of reduction in  $\tau_r$  is dependent on the proper estimation of machine parameters, it is consistent from a theoretical point of view.

Another aspect that can be observed is that, the steady-state value of rotor flux is somewhat smaller for the proposed model. This reflects the saturation effect on the magnetizing inductance, included in the proposed model, but ignored in the standard model.

Finally, the transient torque response of an indirect vector-controlled drive was investigated at constant speed, as indicated in Fig. 3.16, to study possible effect for  $D^e$ - $Q^e$  equivalent circuits modification. Fig. 3.16(a) shows the step in the torque component of current ( $i_{qs}^*$ ) at the rated flux condition. Fig. 3.16(b) shows the corresponding torque response for lossless converter and ideal  $D^e$ - $Q^e$  machine model with slip gain parameter tuned with the nominal machine parameters. The observed rise time is essentially due to

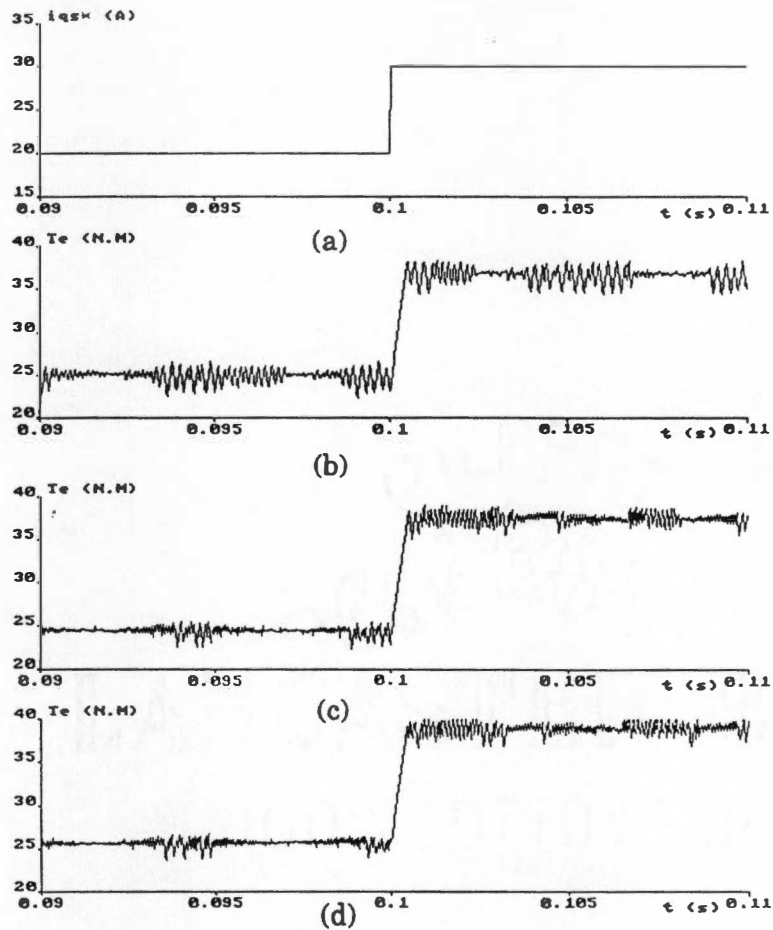


Fig. 3.16 Torque responses of the drive at rated flux (speed = 900 RPM).  
a) Command current step.  
b) Ideal and lossless converter-machine model (slip gain parameters are nominal machine parameters).  
c) Lossy converter-machine model (slip gain parameters are nominal machine parameters).  
d) Lossy converter-machine model (slip gain parameters track with machine parameters).

intrinsic delay of hysteresis-band current controller. Fig. 3.16(c) shows the response for lossy converter machine model, with nominal machine parameters used in the slip gain, whereas in Fig. 3.16(d) the same model was used, except for the slip gain, that is tuned for the actual machine parameters at the particular operating condition. The responses for all the three conditions are practically identical, what reflects a small mismatch between actual and nominal machine parameters used in the slip gain computation, for this particular operating condition.

In conclusion, the loss modeling of converter induction machine system proposed here takes into consideration the relevant losses occurring in a practical drive system. The simulation study has demonstrated the coherent system behavior at both steady-state and dynamic conditions. The actual accuracy of the models is dependent on the precision with which the machine and converter parameters can be obtained. However, the topic of parameter measurement or estimation is beyond the scope of this work.

## **CHAPTER 4**

### **FUZZY EFFICIENCY OPTIMIZATION CONTROL**

#### **4.1 Introduction**

Efficiency improvement in variable frequency drives is getting a lot of attention in the recent years. Higher efficiency is important not only from the viewpoints of energy saving and its obvious financial payoff, but also from the broad perspective of environmental pollution control. In fact, as the use of variable speed drives continues to increase in areas traditionally dominated by constant speed drives, motivated by the quest for increased productivity, the financial and environmental payoffs reach new importance.

The efficiency of a drive system is a complex function of the type of machine used, converter topology, type of power semiconductor switches and the selected PWM algorithm. In addition, the control system has profound effect on the drive efficiency. A drive system normally operating at rated flux gives the best transient response. However, at light loads, rated flux operation causes excessive core loss, compared to copper loss, thus impairing the efficiency of the drive. Since drives operate at light load most of the time, optimum efficiency can be obtained by flux control.

A number of methods for efficiency improvement through flux control have been proposed in the literature, since its principle was first introduced by Nola [38]. They can be classified into three basic types:

- 1) The simple pre-computed flux program as a function of torque, that is widely used for light load efficiency improvement. The scheme can be improved by generating the flux program at discrete speeds, to take the frequency dependency into consideration. This method, however, yields only a partial improvement in the system efficiency.
- 2) The real time computation of losses and corresponding selection of flux level that results in minimum losses is quite elegant. However, as the loss computation is based on a machine model, parameter variations caused by temperature and saturation effects tend to yield sub-optimal efficiency operation [60].
- 3) The on-line efficiency optimization control [39]-[41] on the basis of search, in which the flux is reduced in steps until the measured input power settles down to the lowest value. The control does not require the knowledge of machine parameters, is completely insensitive to parameter changes, and the algorithm is applicable universally to any arbitrary machine.

Induction motors are by far the most used among all electric motors, and are responsible for the consumption of a large fraction of the total electric energy produced. It is, therefore, natural that they have been the primary focus of the efficiency improvement studies. Part of this effort has been dedicated to vector controlled induction motor drives, since they possess inherent decoupling of flux and torque control loops, making them well suited for efficiency optimization control. In fact, Kirschen [40] investigated such system, using on line search method. Fig. 4.1 shows a typical power minimization process for a partial load condition. As the command flux is decreased, the

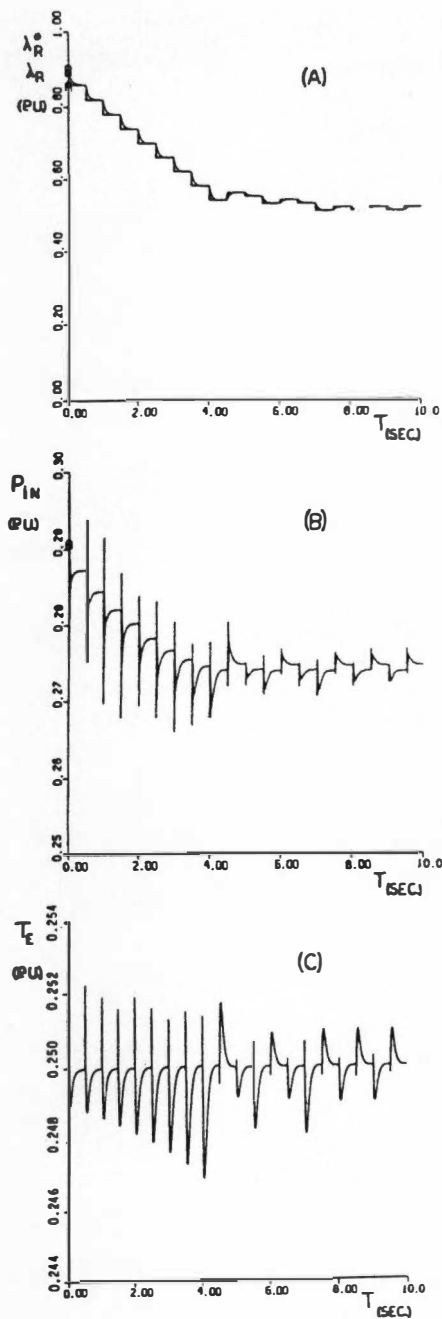


Fig. 4.1 Simulation of the input power minimization process [40].

input power initially decreases and then settles to the minimum value. There is, however, an undesirable side effect: as the flux is reduced, the developed torque is also affected, as demonstrated by the torque pulses of Fig. 4.1(c). If the load inertia is small, the low frequency torque pulsation will translate in speed fluctuation, that can eventually lead to mechanical resonance.

In this chapter, a fuzzy logic based on-line efficiency optimization control for an indirect vector controlled drive system is discussed. Fast convergence has been achieved by using adaptive step size of the excitation current. The low frequency pulsating torque generated by the efficiency controller has been suppressed by a feed-forward compensation algorithm. Both simulation and experimental studies were performed to validate the theoretical development. A paper on this subject [62] has been accepted for presentation at the 1993 international conference on industrial electronics, control, and instrumentation, IECON' 93.

## 4.2 Fuzzy Efficiency Optimization of a Vector Control Drive

An indirect vector controlled induction motor drive incorporating the proposed efficiency optimization controller is shown in Fig. 4.2. It consists of a diode rectifier and a hysteresis band PWM transistor inverter. All the control functions indicated by the dashed outline are implemented in real time by a single digital signal processor (TMS320C25 from Texas Instrument, Inc.). The feedback speed control loop generates the active or torque current command  $i_{qs}^*$ , as indicated. The vector rotator receives the torque and excitation current commands  $i_{qs}^*$  and  $i_{ds}^*$ , respectively, from the two positions

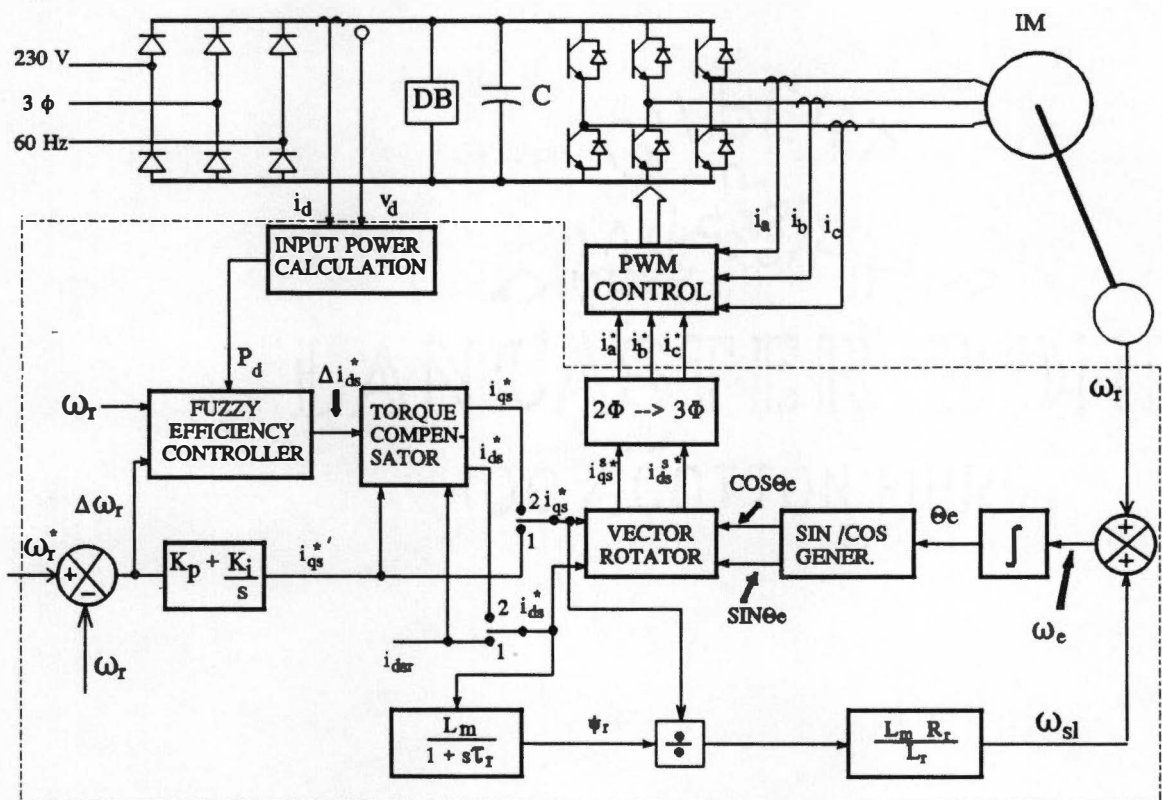


Fig. 4.2 Indirect vector controlled induction motor drive incorporating the efficiency optimization controller.



of a switch: the transient position (1), where the excitation current is established to the rated value  $i_{dsr}$  and the speed loop feeds the torque current; and the steady-state position (2), where the excitation and torque currents are generated by the fuzzy efficiency controller and feedforward torque compensator which will be explained later. The fuzzy controller becomes effective at steady-state condition, i.e., when the speed loop error  $\Delta\omega_r$  approaches zero. Note that the DC link power  $P_d$ , instead of input power, has been considered for the fuzzy controller since both follow symmetrical profiles. This can be demonstrated as follows:

- . Minimization of  $P_d$  translates into minimization of DC link current  $i_d$ , since the DC link voltage  $v_d$  is essentially constant;
- . Rectifier loss are proportional to  $i_d$ , (Eqn. 3.50);
- . Minimum  $i_d$  yields minimum rectifier loss, and consequently, minimum input power.

The principle of efficiency optimization control with rotor flux programming at a steady-state torque and speed condition is explained in Fig. 4.3. The rotor flux is decreased by reducing the magnetizing current, which ultimately results in a corresponding increase in the torque current, normally by action of the speed controller, such that the developed steady-state torque remains constant. As the flux is reduced, the iron loss decreases with the attendant increase of copper loss. However, the total system loss (converter and machine) decreases, resulting in a reduction of DC link power. The search is continued until the system settles down at the minimum input power point A, as indicated. Any excursion beyond the point A will force the controller to return to the

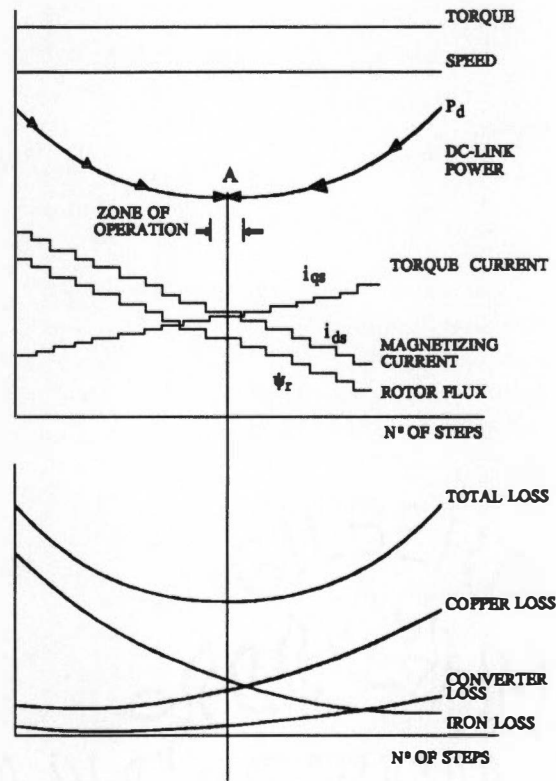


Fig. 4.3 Principle of efficiency optimization control with rotor flux programming.

minimum power point.

#### 4.2.1 The Efficiency Optimization Controller

The fuzzy efficiency controller operation is explained in Fig. 4.4. The DC link power is sampled and compared with the previous value to determine the increment  $\Delta P_d$ . In addition, the last excitation current decrement  $L\Delta i_{ds}$  is reviewed. On these basis, the decrement step of  $\Delta i_{ds}^*$  is generated from fuzzy rules through fuzzy inference and defuzzification [14], as indicated. The adjustable gains  $P_b$  and  $I_b$ , generated by the scaling factors computation block, convert the input variable and control variable, respectively, to per unit values, such that a single fuzzy rule base can be used for any torque and speed condition. The input gain  $P_b$  as a function of machine speed  $\omega_r$  can be given as

$$P_b = a \omega_r + b \quad (4.1)$$

The output gain  $I_b$  is computed from the machine speed and an approximate estimate of machine torque  $\hat{T}_e$  as

$$I_b = c_1 \omega_r - c_2 \hat{T}_e + c_3 \quad (4.2)$$

where

$$\hat{T}_e = K_t' i_{ds}^* i_{qs}^* \quad (4.3)$$

The appropriate coefficients  $a$ ,  $b$ ,  $c_1$ ,  $c_2$ , and  $c_3$  were derived from simulation studies as follows:

- . Using simplified models, the approximated optimum magnetizing current  $i_{dso}$  was determined for selected operating points in the torque-speed plane;

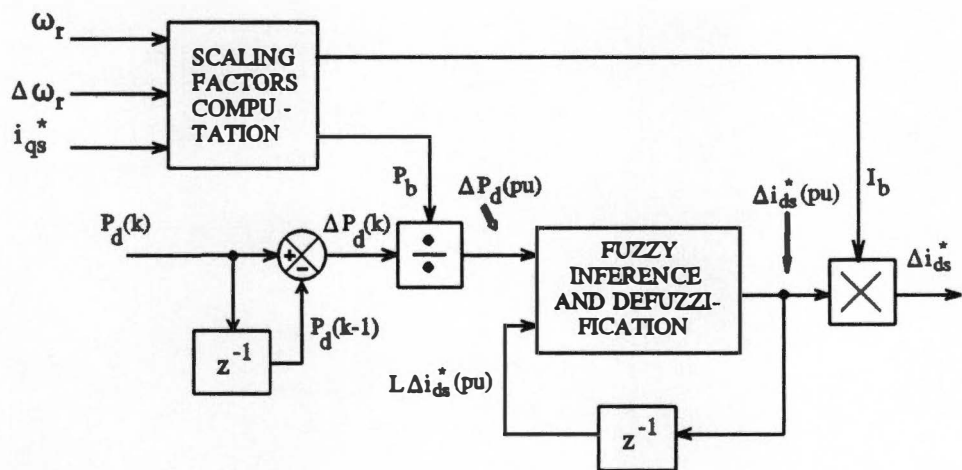


Fig. 4.4 Efficiency optimization control block diagram.

- . Least-square estimation was used to obtain a linear representation of  $i_{dso}$  as a function of machine torque  $T_e$  and speed  $\omega_r$ ;
- . The output gain expression (4.2) was defined as one third of the distance between rated magnetizing current  $i_{dsr}$  and approximate optimum  $i_{dso}$ .
- . A new set of simulations was performed, for a load torque of 0.1 pu and different speeds. The magnetizing current was reduced by a step size  $I_b$  given by (4.2), and the corresponding reduction in input power  $\Delta P$  was obtained.
- . The input power expression (4.1) was defined as the linear representation of  $\Delta P^{-1}$  as a function of speed, derived by least square estimation.

A few words on the importance of the input and output gains are appropriate here.

In the absence of input and output gains, the efficiency optimization controller would react equally to a specific value of  $\Delta P_d$ , resulting from a past action  $\Delta i_{ds}^*(k-1)$ , irrespective of operating speed. Since the optimal efficiency point A (Fig. 4.3) is speed dependant, the control action could easily be either too conservative, resulting in slow convergence, or excessive, yielding an overshoot in the search process, with possible adverse impact on system stability. As both input and output gains are functions of speed, this problem does not arise. Eqn. 4.2 also incorporates the "a priori" knowledge that the optimum value of  $i_{ds}^*$  is a function of torque as well as machine speed. In this way, for different speed and torque conditions, the same  $\Delta i_{ds}^*(pu)$  will result in different  $\Delta i_{ds}^*$ , ensuring a fast convergence. One additional advantage of per unit basis operation is that the same fuzzy controller can be applied to any arbitrary machine, by simply changing the coefficients of input and output gains.

The membership functions for the fuzzy efficiency controller are shown in Fig. 4.5. Due to the use of input and output gains, the universe of discourse for all variables are normalized in the  $[-1,1]$  interval. It was verified that, while the control variable  $\Delta i_{ds}^*$  required 7 fuzzy sets to provide good control sensitivity, the past control action  $L\Delta i_{ds}^*$ , i.e.,  $\Delta i_{ds}^*(k-1)$ , needed only 2 fuzzy sets, since the main information conveyed is the sign. The small overlap of the positive (P) and negative (N) membership functions is required to ensure proper operation of the height defuzzification method, i.e., to prevent indeterminate result in case  $L\Delta i_{ds}^*$  approaches zero.

The rule base for fuzzy control is given in Table 4.1. An example fuzzy rule can be given as:

**IF the power increment ( $\Delta P_d$ ) is negative medium (NM) and the last  $\Delta i_{ds}^*$  ( $L\Delta i_{ds}^*$ ) is negative (N), THEN the new excitation increment ( $\Delta i_{ds}^*$ ) is negative medium (NM).**

The basic idea is that, if the last control action indicated a decrease of DC link power, proceed searching in the same direction, and the control magnitude should be somewhat proportional to the measured DC link power change. In case the last control action resulted in an increase of  $P_d$  ( $\Delta P_d > 0$ ), the search direction is reversed, and the  $\Delta i_{ds}^*$  step size is reduced to attenuate oscillations in the search process.

As the optimum point varies with speed and load conditions, and is also affected by changes in machine parameters, the fuzzy logic search controller constitutes a natural choice for this problem. Initially, a linguistic description of the control strategy could be easily obtained. Fuzzy logic then provided the appropriate mathematical framework for the derivation of the actual controller. The fine tuning process was, nevertheless,

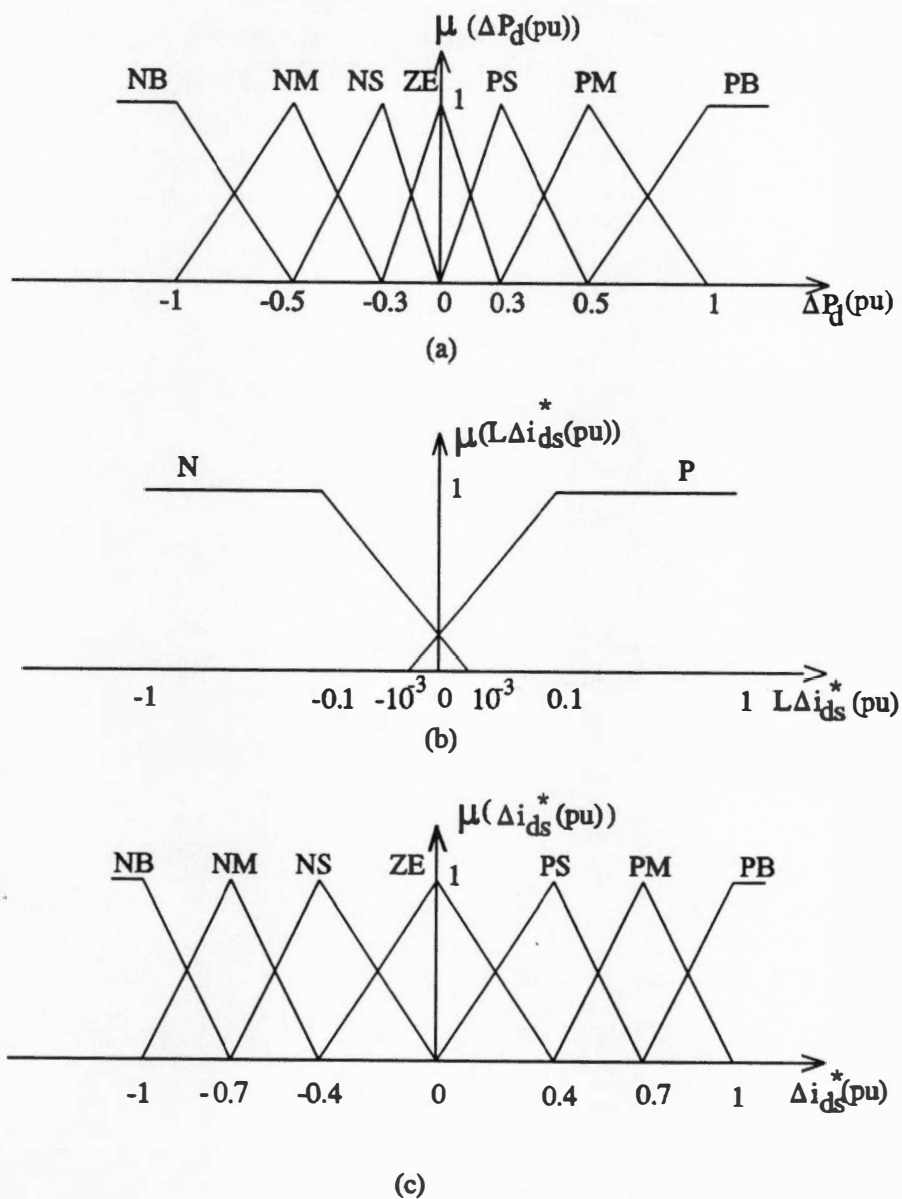


Fig. 4.5 Membership functions for the fuzzy efficiency control.  
 (a) Change in DC link power ( $\Delta P_d(\text{pu})$ ).  
 (b) Last change in magnetizing current ( $L\Delta i_{ds}^*(\text{pu})$ ).  
 (c) Magnetizing current increment ( $\Delta i_{ds}^*(\text{pu})$ ).

Table 4.1 Rule base for the fuzzy efficiency controller.

$L\Delta i_{ds}(pu)$ $\Delta P_d(pu)$	N	P
PB	PM	NM
PM	PS	NS
PS	PS	NS
ZE	ZE	ZE
NS	NS	PS
NM	NM	PM
NB	NB	PB



somewhat time consuming.

#### 4.2.2 Feed-forward Pulsating Torque Compensation

As the excitation current is reduced in adaptive steps by the fuzzy controller, the rotor flux  $\psi_r$  decreases exponentially [17], which is given by

$$\frac{d}{dt}\psi_r = \frac{L_m i_{ds} - \psi_r}{\tau_r} \quad (4.4)$$

where  $\tau_r (= L_r/R_r)$  is the rotor time constant and  $L_m$  the magnetizing inductance. The decrease of flux causes loss of torque, which normally is compensated slowly by the speed control loop. Such pulsating torque at low frequency is very undesirable because it causes speed ripple and may create mechanical resonance. To prevent these problems, a feed-forward pulsating torque compensator is proposed here.

Under correct field orientation control, the developed torque is given by

$$T_e = K_t i_{qs} \psi_r \quad (4.5)$$

For an invariant torque, the torque current  $i_{qs}$  should be controlled to vary inversely with the rotor flux  $\psi_r$ . A practical implementation of this concept is illustrated in Fig. 4.6. A compensating signal  $\Delta i_{qs}^*(t)$  is added to the original  $i_{qs}^*$  to counteract the decrease in flux  $\Delta\psi_r(t)$ , where  $t \in [0, T]$  and  $T$  is the sampling period for efficiency optimization control. Let  $i_{qs}(0)$  and  $\psi_{dr}(0)$  be the initial values for  $i_{qs}$  and  $\psi_{dr}$ , respectively, for the  $k$ -th step change of  $i_{ds}^*$  ( $k=2$  in Fig. 4.6.) For a perfect compensation, the developed torque must

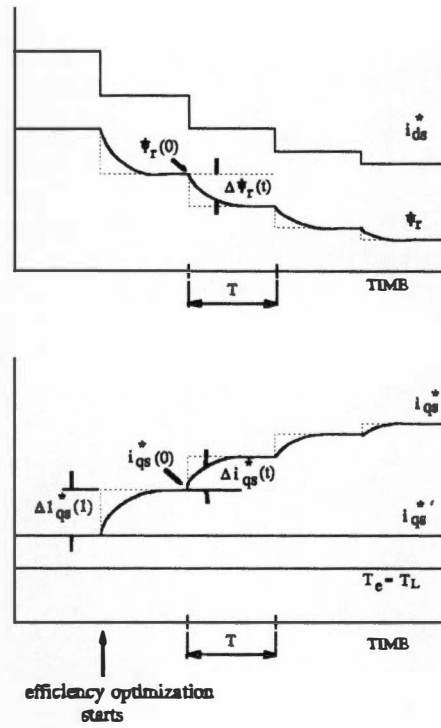


Fig. 4.6 Principles of feedforward torque compensation.

remain constant, and the following equality holds

$$[\psi_r(0) + \Delta\psi_r(t)][i_{qs}(0) + \Delta i_{qs}(t)] = \psi_r(0) i_{qs}(0) \quad (4.6)$$

Solving for  $\Delta i_{qs}(t)$  yields

$$\Delta i_{qs}(t) = \frac{-\Delta\psi_r(t) i_{qs}(0)}{\psi_r(0) + \Delta\psi_r(t)} \quad (4.7)$$

where  $\Delta\psi_r(t)$  is governed by eqn. 4.4, with  $\Delta i_{ds}$  substituted for  $i_{ds}$ . To implement such compensation, eqn. 4.7 is adapted to produce  $\Delta i_{qs}^*(t)$ , using flux estimate  $\hat{\psi}_r$  and command  $i_{qs}^*$  in place of actual signals. A good approximate solution for  $\Delta i_{qs}^*(t)$  can be obtained by replacing the denominator of (4.7) by its estimated steady-state value  $\hat{\psi}_r(T) [= L_m i_{ds}^*(T)]$ . In this case, the compensation can be implemented in two steps as shown in Fig. 4.7. First, the value for the compensating current step is computed by discrete eqn. 4.8.

$$\Delta I_{qs}^*(k) = \frac{\hat{\psi}_r(k-1) - \hat{\psi}_r(k)}{\hat{\psi}_r(k)} i_{qs}^*(k-1) \quad (4.8)$$

Next, the current step is processed through a first order low pass filter of rotor time constant, and then added to the previous compensating steps, as also illustrated in Fig. 4.6. This current is added to the original speed loop generated current  $i_{qs}^*$ , so that, at any instant the product  $i_{qs} \psi_r$  remains essentially constant. It may be noted, however, that the actual rotor time constant of the machine may vary, giving somewhat imperfect pulsating torque compensation.

To ensure adequate compensation, magnetizing inductance saturation effects were taken into account using a piece-wise linear model, similar to that developed for the induction machine model. The magnetizing inductance  $L_m$  is estimated on line from the



command  $i_{ds}^*$  as

$$\begin{aligned} L_m &= L_{m0} & , \text{if } i_{ds}^* \leq i_{ds0} \\ L_m &= L_{m0} - m_d (i_{ds}^* - i_{ds0}) & , \text{if } i_{ds}^* > i_{ds0} \end{aligned} \quad (4.9)$$

where  $L_{m0}$  is the non-saturated value of  $L_m$ ,  $i_{ds0}$  is the linear region breakpoint, and  $m_d$  is a saturation coefficient. All parameters are obtainable from a standard no-load test.

#### 4.2.3 Transition to Optimum Transient Response Mode

It may be noted from the preceding discussion that efficiency optimization control is only effective at steady-state condition. A disadvantage of this control mode is that the transient response becomes sluggish, because the weaker flux reduces the maximum torque capability, as indicated by eqn. 4.5. For any change in load torque or speed command, fast transient response capability of the drive can be restored by establishing the rated flux. Fig. 4.8 shows the criteria for transition between efficiency optimization (Mode 2) and transient response optimization (Mode 1). The system starts in Mode 1 and then switches to Mode 2 when the steady-state criteria is met. In the event of a load disturbance or a change in set speed, the system switches back to Mode 1 by establishing the rated magnetizing current.

At steady-state, current must be kept within the thermal limits of the machine and inverter, that is usually the rated machine current. During a transition from Mode 2 to Mode 1, this limit can be temporarily increased, (typically by 50% for 60 secs.) such that more torque is available to meet the acceleration / deceleration demand. This constraint is given by the relation

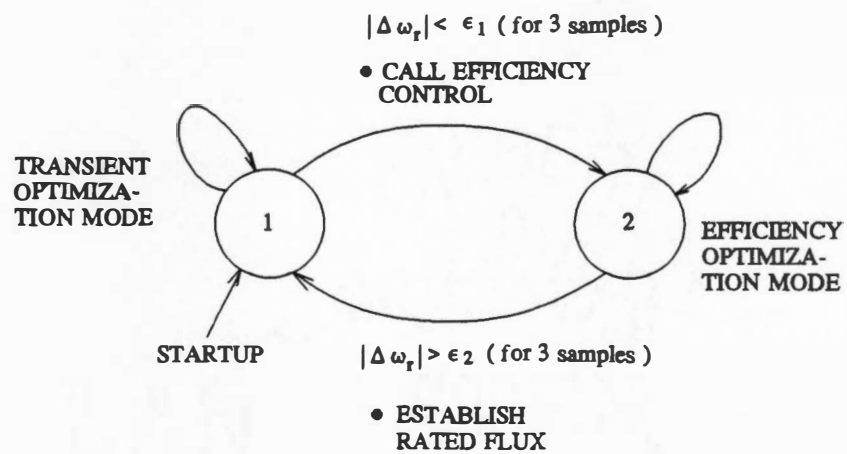


Fig. 4.8 Transition between efficiency optimization and transient response optimization modes.

$$\sqrt{i_{ds}^{*2} + i_{qs}^{*2}} < I_{lim} \quad (4.10)$$

where  $I_{lim} = 1.5 I_{sr}$ , and  $I_{sr}$  is the rated stator current.

Notice that, as the rotor flux does not change instantly, the maximum torque capability following a transition might not be enough to overcome the torque demand, even with the relaxed current limit. In such scenario, there is a possibility that the drive will stall, and preventive measures should be taken. One simple solution consists in imposing a minimum value for  $i_{ds}^*$ , during Mode 2, that would keep the maximum torque capability at a safe level, at the expenses of suboptimum efficiency operation.

### 4.3 Simulation Program Development

In chapter 3, SIMNON routines for converter and induction motor lossy models were developed and integrated to a speed control system, using indirect vector control. In this section the Fuzzy Efficiency Optimization Routine (FEOPT) and Feed Forward Torque Compensation Routine (FFTC) development will be discussed. The simulation block diagram of Fig. 4.9 shows the various routines used in the study, and the associated input/output variables for every subsystem. Discrete subsystems are identified by a D whereas continuous subsystems are marked with a C.

The flowchart of Fig. 4.10 shows the structure of the FEOPT routine. For convenience, the determination of the operating mode (Mode 1 or Mode 2 of Fig. 4.8 ) is included in the FEOPT routine. First, the program checks the previous operating mode and verifies if any transition is required. If after the tests the system is found to be in the

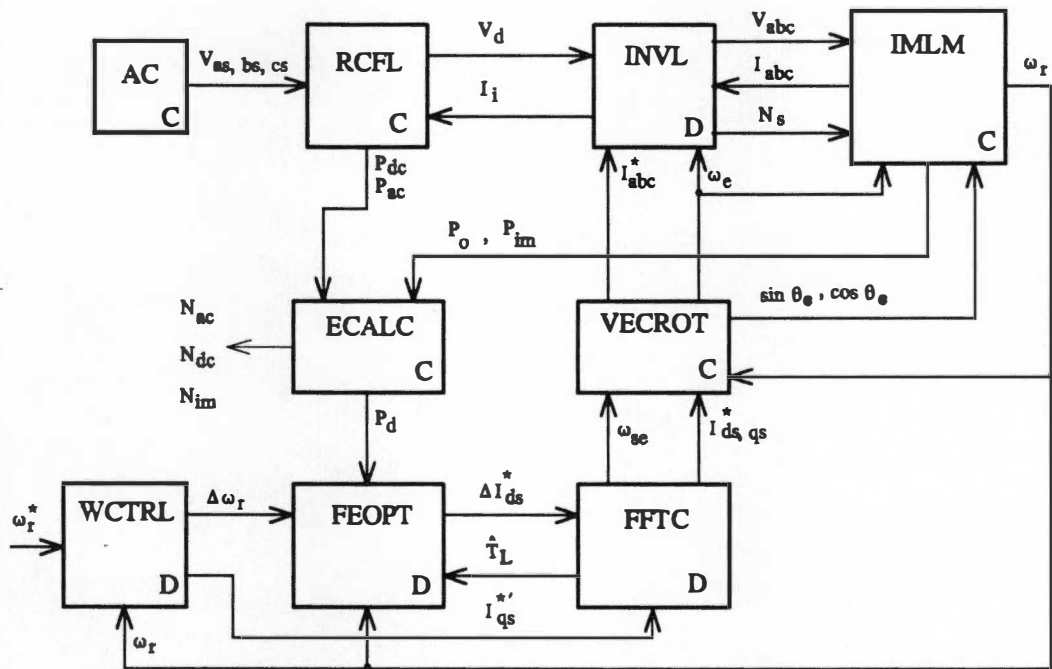


Fig. 4.9 SIMNON simulation block diagram showing I/O variables.



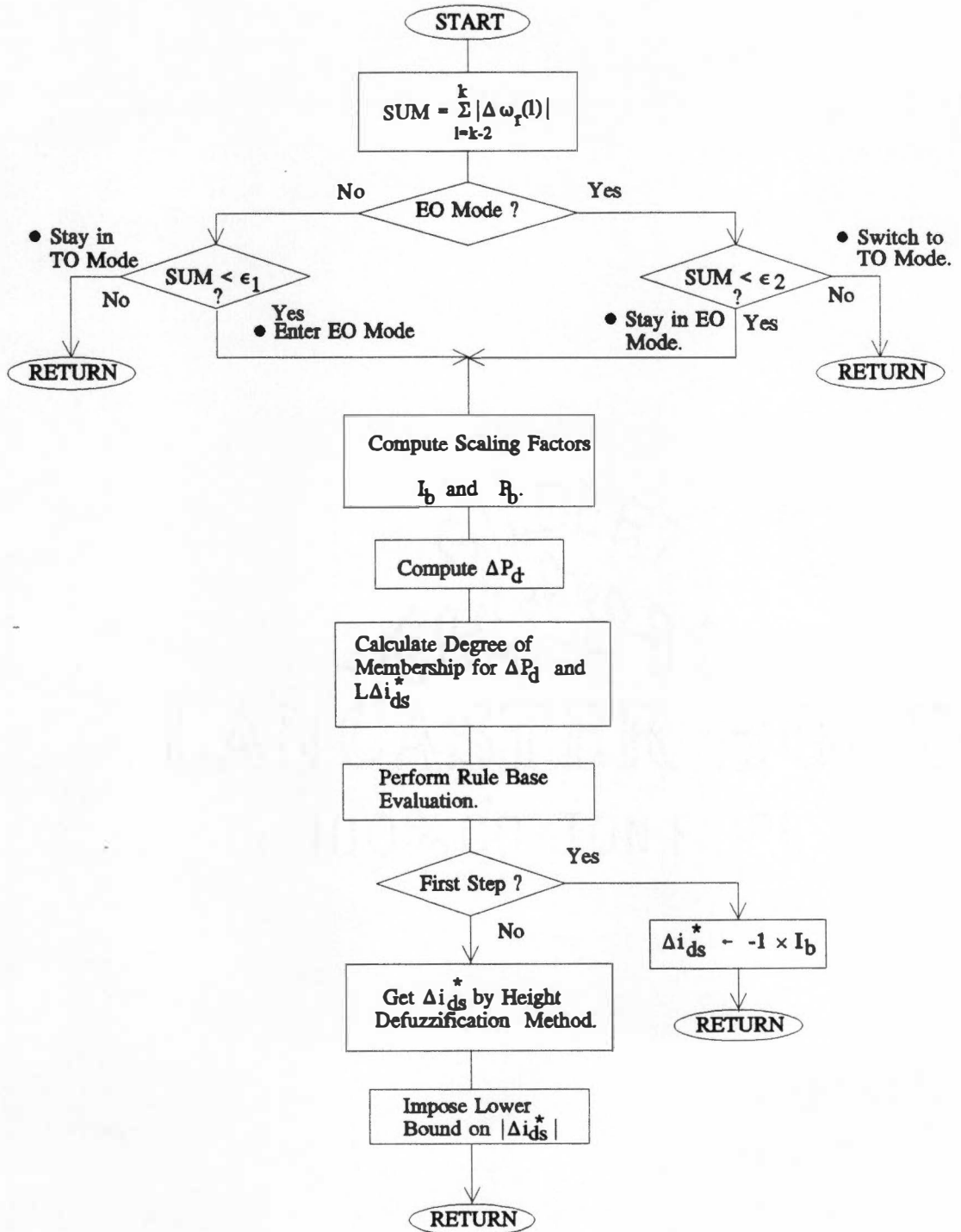


Fig. 4.10 Fuzzy efficiency optimization flowchart.

efficiency optimization (EO) mode, then the program proceeds to the tasks actually related to the efficiency optimization process, as indicated in the flowchart. In order to initiate the efficiency optimization process, following a Mode 1 to Mode 2 transition the first  $\Delta i_{ds}^*$  is set to -1 pu. The actual value in Amperes is determined by the output scaling factor  $I_b$ . From the second iteration on,  $\Delta i_{ds}^*$  value is truly derived from the fuzzy controller. After the optimum point is reached, a minimum (non-zero) value is imposed to  $\Delta i_{ds}^*$ , to keep the search process active, and ensure true optimum operation in case of parameter variation or small change in load condition.

The algorithm for fuzzy control implementation has already been described in detail in Section 2.2.1, for the case of fuzzy  $\Delta\alpha$  compensation. However, its implementation using SIMNON language is somewhat complicated, mainly because SIMNON does not support branch instructions. Furthermore, the order of program execution is not completely controlled by the user, since during compilation the program sorts the instructions to optimize for execution time.

The methodology used in the actual derivation of fuzzy efficiency optimization SIMNON routine is explained here with the help of Fig. 4.11.

1. Compute input and output scaling factors,  $P_b$  and  $I_b$ , respectively, and the change in input power,  $\Delta P_d$  (pu);
2. Make a preliminary computation of degree of membership for all fuzzy sets. For instance, the degree of membership of  $\Delta P_d$  (k) in the fuzzy set PM, shown in Fig. 4.11 is given by:

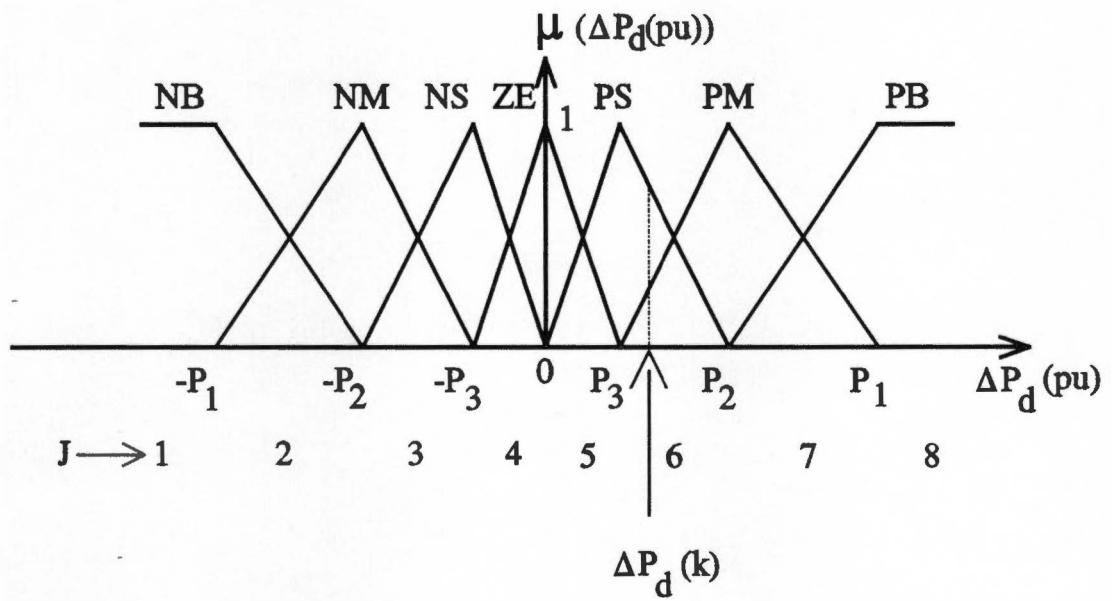


Fig. 4.11 Evaluation of degree of membership.

$$\mu_{PM}(\Delta P_d(k)) = \frac{\Delta P_d(k) - P_3}{P_2 - P_3} \quad (4.11)$$

3. Define the interval index J that identifies which fuzzy sets possess non zero degree of membership. SIMNON supports the conditional assignment of value to a variable, but does not allow a continuation line. This problem can be solved by defining some auxiliary variables ( $J_1, J_2, \dots$ ) as indicated below:

$J = \text{If } \Delta P_d < -P_1 \text{ Then } 1 \text{ Else If } \Delta P_d < -P_2 \text{ Then } 2 \text{ Else } J_1$

$J_1 = \text{If } \Delta P_d < -P_3 \text{ Then } 3 \text{ Else If } \Delta P_d < 0 \text{ Then } 4 \text{ Else } J_2$

...

4. Evaluate the degree of membership for the relevant fuzzy sets:

$\mu_{P1} = \text{If } J < 3 \text{ Then } \mu_{NB} \text{ Else If } J < 4 \text{ Then } \mu_{NM} \text{ Else... Else } \mu_{PB}$

$\mu_{P2} = 1 - \mu_{P1}$

For the situation illustrated in Fig. 4.11,  $\mu_{P1} = \mu_{PS}$  and  $\mu_{P2} = \mu_{PM}$ .

5. Apply similar procedure to compute degrees of membership  $\mu_{I1}$  and  $\mu_{I2}$ , for the second input variable,  $L\Delta i_{ds}^*(pu)$ .
6. Evaluate the antecedent of the relevant rules, using MIN operator. Typically, four rules are fired. The first rule is illustrated here:

$\mu_{RA} = \text{MIN} (\mu_{P1}, \mu_{I1})$

7. Retrieve the contribution of each fired rule, from the rule base:

$\Delta I_a = \text{If } J < 3 \text{ Then } I_1 \text{ Else If } J < 4 \text{ Then } I_2 \text{ Else...}$

Due to the symmetry of this particular rule base,  $\Delta I_b = -\Delta I_a$ .

8. Calculate the new  $\Delta i_{ds}^*$  by height defuzzification method.

$$\Delta i_{ds}^*(pu) = \frac{\mu_{RA} \Delta I_a + \dots + \mu_{RD} \Delta I_d}{\mu_{RA} + \dots + \mu_{RD}} \quad (4.12)$$

The feed forward torque compensation (FFTC) routine operation is explained by the flowchart of Fig. 4.12. Its principle has already been discussed in section 4.2.2, and therefore, only some relevant aspects will be discussed here. During the search process (EO mode), the test for maximum stator current is based on the steady-state limit  $I_{lim1}$ , that corresponds to the rated motor current. If it is detected that the new control action  $\Delta i_{ds}^*$  would result in a violation of such limit, the new magnetizing current  $i_{ds}^*(k)$  is reset to its previous value  $i_{ds}^*(k-1)$ , and similarly, no correction is made in  $i_{qs}^*(k)$ . If the program detects that the system has switched to a TO mode (Mode 1), rated  $i_{ds}^*$  is reestablished and the accumulated compensating signal  $\Sigma \Delta i_{qs}^*(k)$  is reset to zero. The actual compensating signal  $\Sigma \Delta i_{qs}$  will approach zero following the first order filter dynamics. This action ensures that no sudden change in machine torque will take place, following transition in operating mode. Furthermore, as the original torque current command  $i_{qs}^*$  from the speed controller immediately affects  $i_{qs}^*$ , proper control action to any disturbance is ensured. For the TO mode, the stator current limit is set to 50% higher than its steady-state value, as mentioned before. Besides the functions related to torque compensation, the routine also computes rotor flux estimate, performs slip frequency calculation and is also responsible for approximate machine torque estimation, required by the FEOPT routine.

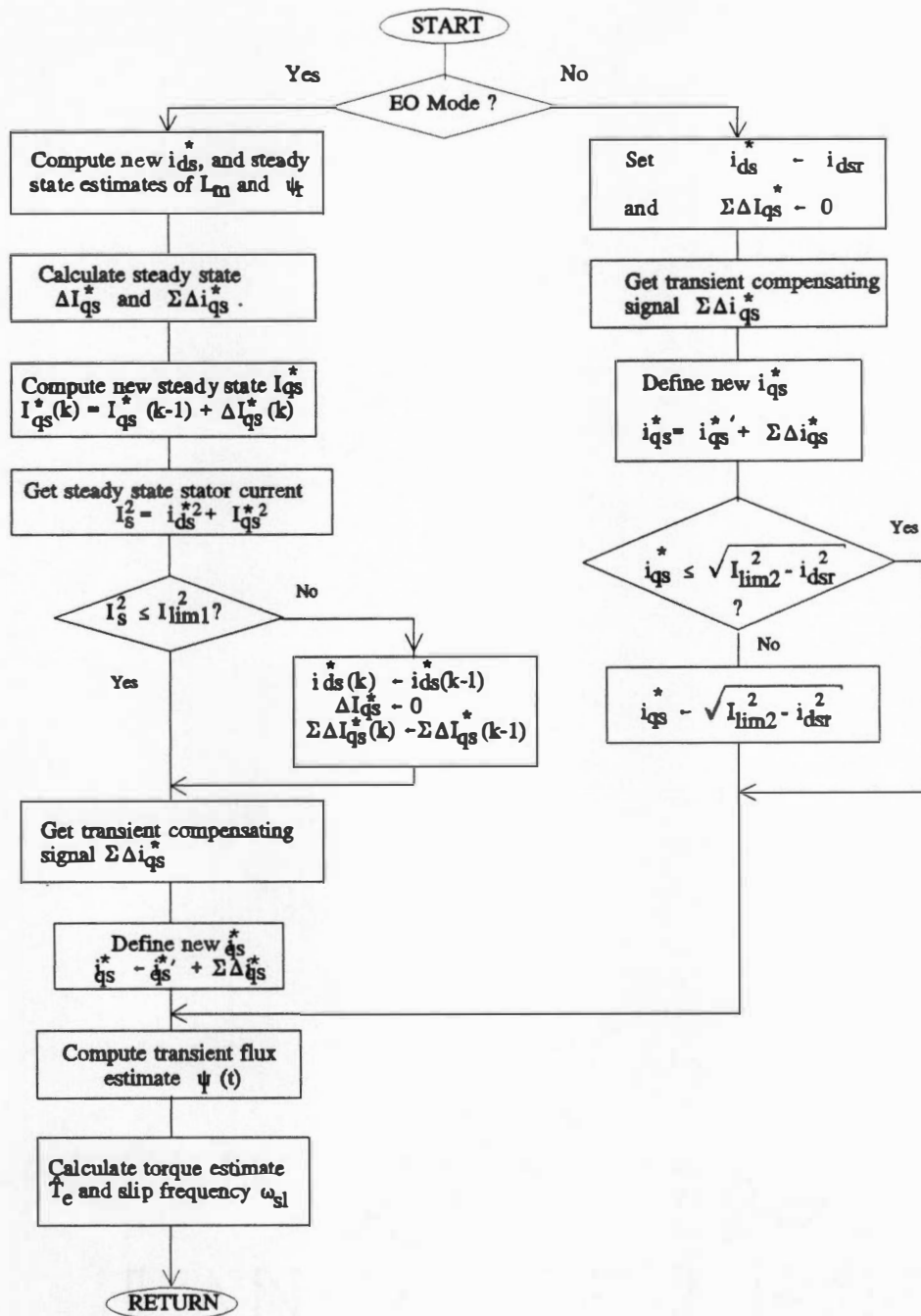


Fig. 4.12 Feedforward torque compensation simulation flowchart.

## 4.4 Simulations Study

After the development and tests of the SIMNON routines, a detailed performance evaluation study was conducted, using the machine parameters given in Table 4.2. Fig. 4.13 shows the time domain optimum efficiency search curves at speed  $\omega_r = 0.25$  pu and load torque  $T_L = 0.1$  pu. The optimum flux level is achieved in only four steps of  $i_{ds}^*$ . The search algorithm, however, imposes a minimum non-zero step size of  $\Delta i_{ds}^*$  when  $\Delta P_d$  approaches zero, in order to ensure true optimum operation for parameter variation or small change in load condition. The effectiveness of the pulsating torque compensation is evident from the torque profile of Fig. 4.13(d) and speed response of Fig. 4.13(e). Fig. 4.14 gives efficiency curves at different operating points on torque - speed plane, with and without efficiency optimization control. As the class B induction machine was designed for 230 V, 60 Hz operation, the highest speed was limited to 0.75 pu (1350 rpm), because the DC link voltage is not high enough to enforce current regulation at higher speeds, under rated flux conditions. As expected, maximum efficiency gains occur at light load, where the rated flux core losses are very dominant. Fig. 4.15 illustrates system performance during operating mode transitions. The system is initially at steady-state and the E.O. mode is activated. At  $t=3$  sec. the system has reached the optimum efficiency point, when the load torque is suddenly increased from 0.1 pu to 0.5 pu, causing a speed droop (Fig. 4.15(d)), that in turn forces a transition to TO mode (Mode 1). The rated  $i_{ds}^*$  is readily reestablished, and the speed controller increased  $i_{qs}^*$ , bringing the speed back to its command value in less than 0.3 sec. Once the system reaches a steady-state condition, it switches back to EO mode (Mode 2) and a new search is initiated. Due to

Table 4.2 Induction machine parameters for efficiency optimization studies.

5 hp 4 poles	230/460 V 1710 rpm	13.4/6.7 A NEMA class B
<u>D<sup>e</sup>-Q<sup>e</sup> equivalent circuit parameters:</u>		
$R_s=0.406 \ \Omega$	$R_r=0.478 \ \Omega$	
$L_{ls}=0.00213 \text{ H}$	$L_{lr}=0.00213 \text{ H}$	
$L_m=0.0494 \text{ H}$		



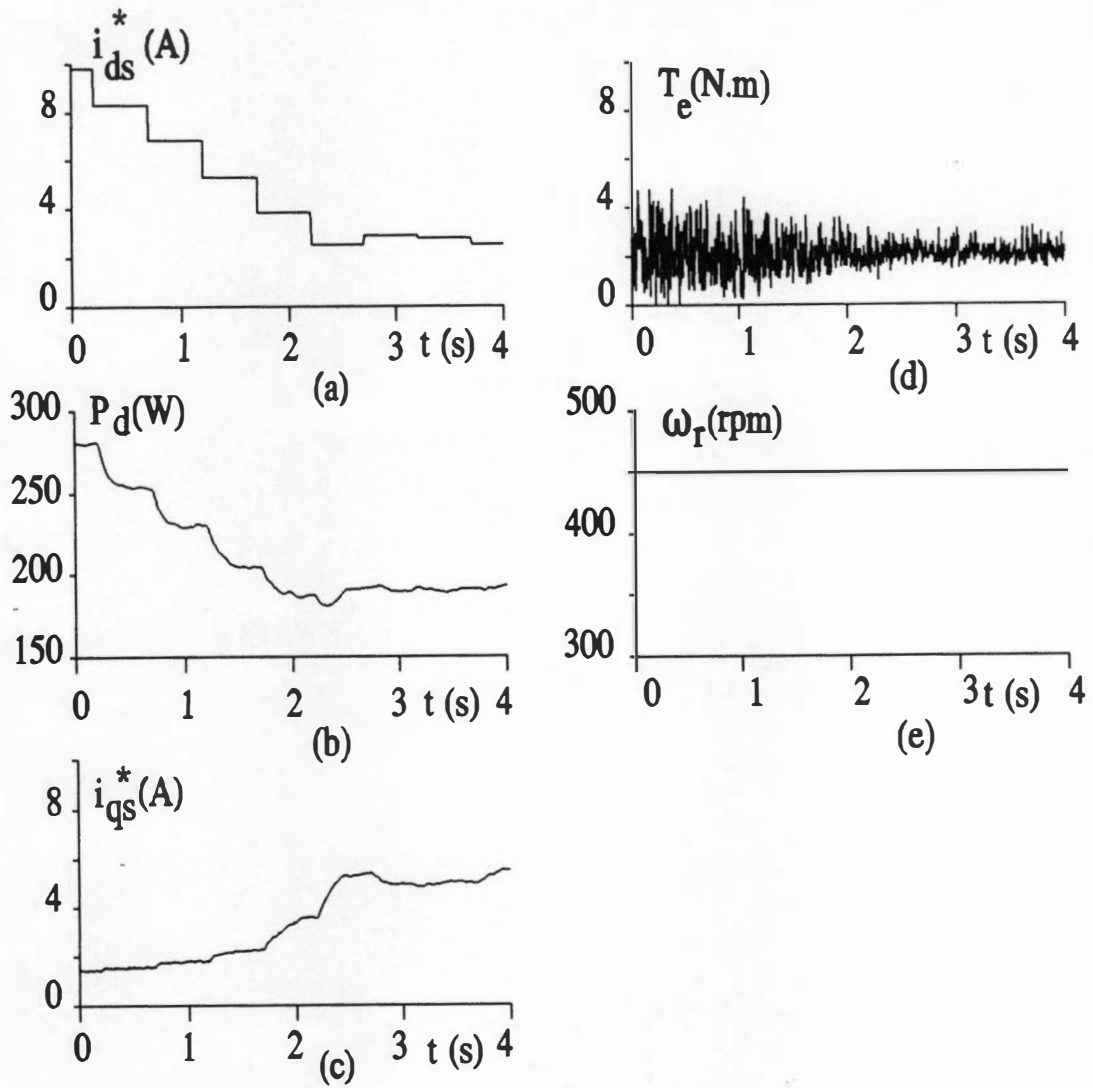


Fig. 4.13 Time domain simulated optimum efficiency search curves at  $\omega_r = 0.25$  pu and  $T_L = 0.1$  pu. (a) Magnetizing current ( $i_{ds}^*$ ). (b) DC link power ( $P_d$ ). (c) Torque current ( $i_{qs}^*$ ). (d) Machine torque ( $T_e$ ). (e) Speed ( $\omega_r$ )

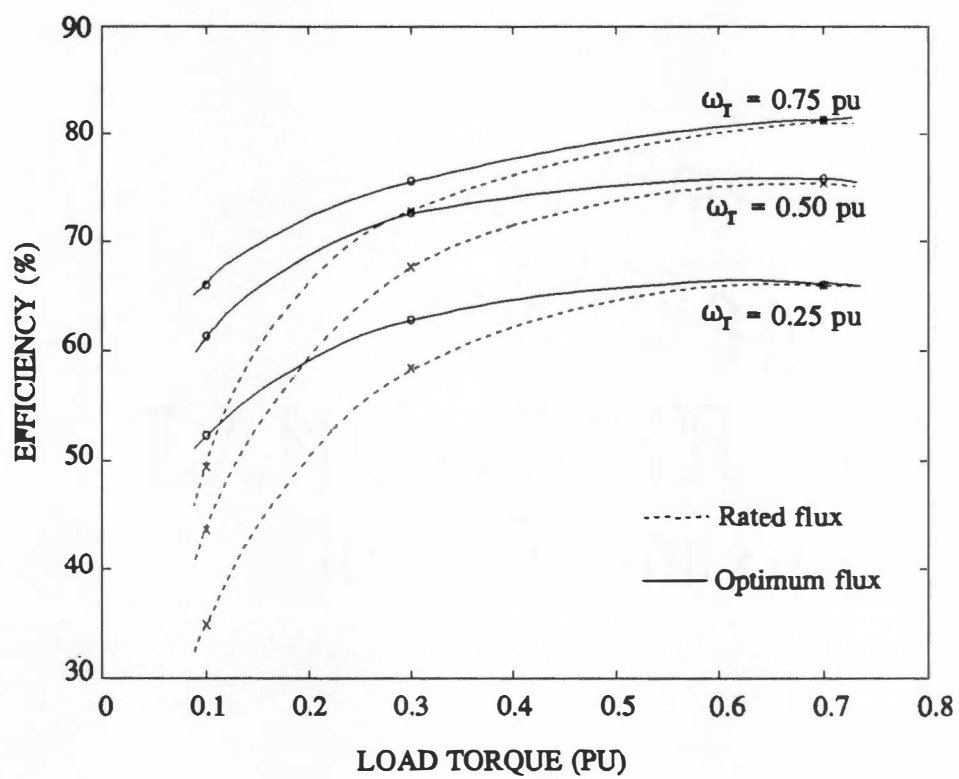


Fig. 4.14 Simulated efficiency curves.

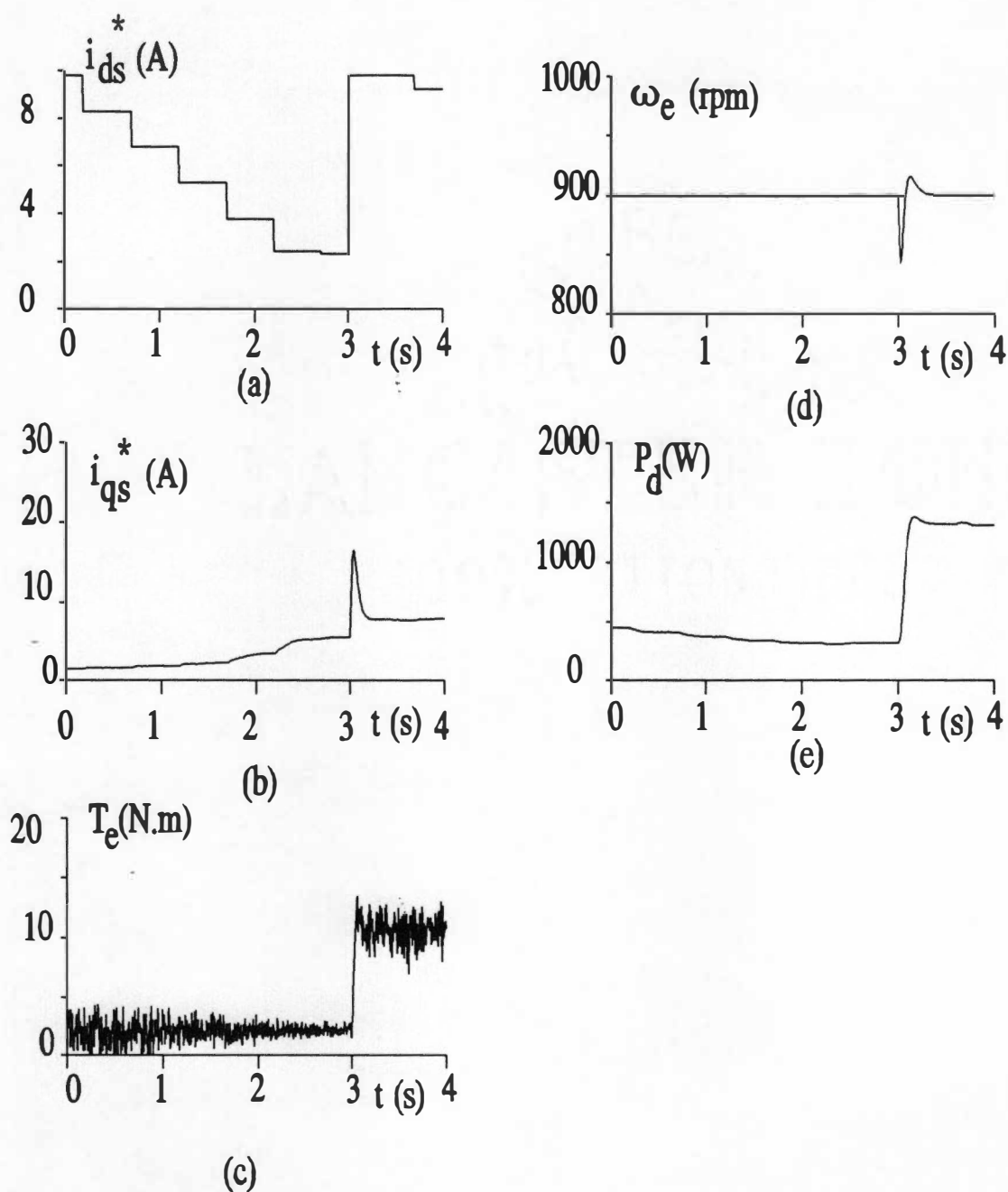


Fig. 4.15 Drive performance in time domain with sudden increase of load torque (transition to transient response optimization mode).

higher load torque the output gain  $I_b$  (in FEOPT) is reduced, what results in a smaller first step for the new search, as indicated in Fig. 4.15(a).

#### **4.5 Hardware Circuit Design**

The vector control system used in the experimental study was derived from an AC200 servo drive system, from General Electric Company. The modular servo system originally had the following components:

- **Servo System Rack.**

The rack is constructed with two receptacles to receive the plug in servo module and the power supply module. The rack has integrated cooling fan and DC link capacitor bank.

- **Power Supply.**

This module contains a power diode rectifier, rated at 230 V AC input, 325 V DC output. It also contains a low voltage, 80 KHz, auxiliary power supply for the control circuitry of the servo module. The control circuitry for dynamic braking is also included, that automatically connects an external resistor across the DC bus, whenever the DC bus voltage reaches 385 Volts. In this way, the energy recovered from the deceleration of the drive is properly dumped, and dangerous DC voltage levels are prevented.

- **Servo Module.**

This module comes with a three-phase power transistor inverter and associated base drive and control circuit boards. The system originally used a sinusoidal

PWM current control, and had all the vector control functions implemented in dedicated hardware. As the system control board was missing, a new control board was designed.

The structure of the vector control system hardware is presented in Fig. 4.16. Its major component is a DSP-16 control board, from Ariel Corporation, based on Texas Instruments TMS320C25 DSP. The board is internally mounted on an IBM 286 compatible host computer, that serves as a development and debugging environment, as well as user interface during normal operation. The control board comes with two D/A channels, used to pass command currents  $i_a^*$ ,  $i_b^*$  to the current controller, and two A/D channels, required for DC link voltage and current sensing. The speed interface is directly connected to the TMS320C25 data, address and control buses, and operates as a parallel peripheral of the DSP. The system is designed with basic protection and monitoring functions.

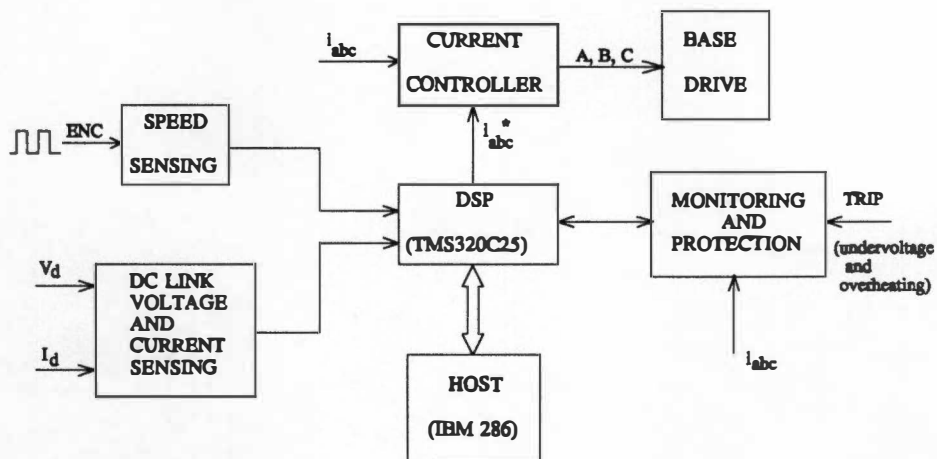


Fig. 4.16 Block diagram for vector control system hardware.

#### 4.5.1 Current Controller

A hysteresis band current controller (HBPWM) was selected, because of its simplicity and robustness. Fig. 4.17 shows the circuit diagram of the proposed controller. Only two D/A channels are available; consequently, the reference current for phase c,  $i_c^*$ , is obtained by addition of  $i_a^*$  and  $i_b^*$ . After some very small filtering and scaling, the actual machine current  $i_a$  is subtracted from the command value  $i_a^*$ . The error is next compared to the hysteresis band to determine the state of phase leg A switches. Notice that, by using isolating diodes the hysteresis band for the three phases are controlled by a single trimpot. Identical circuits are used for phases b and c, and therefore, not shown here in detail.

#### 4.5.2 Monitoring and Protection

Fig. 4.18 shows the circuit diagram for monitoring and protection. The system comes with built in inverter temperature sensor and under voltage protection, that are combined into a single trip signal (TRIP). Over current (OC) protection is obtained by extracting the positive and negative current profiles from the feedback current signals and comparing with pre-set limits. A small delay is introduced to prevent noise related false tripping. An emergence stop (E/S) push button is included for added safety. At power on, the delay circuits ensure a disable state for the drive circuit, and this must be cleared by the RESET push button. With all the protection circuitry enabled, a RUN command must be issued from the control software to effectively enable the base drive (STOP/RUN signal). LED lamps are associated with every trip/control signal for monitoring purpose.

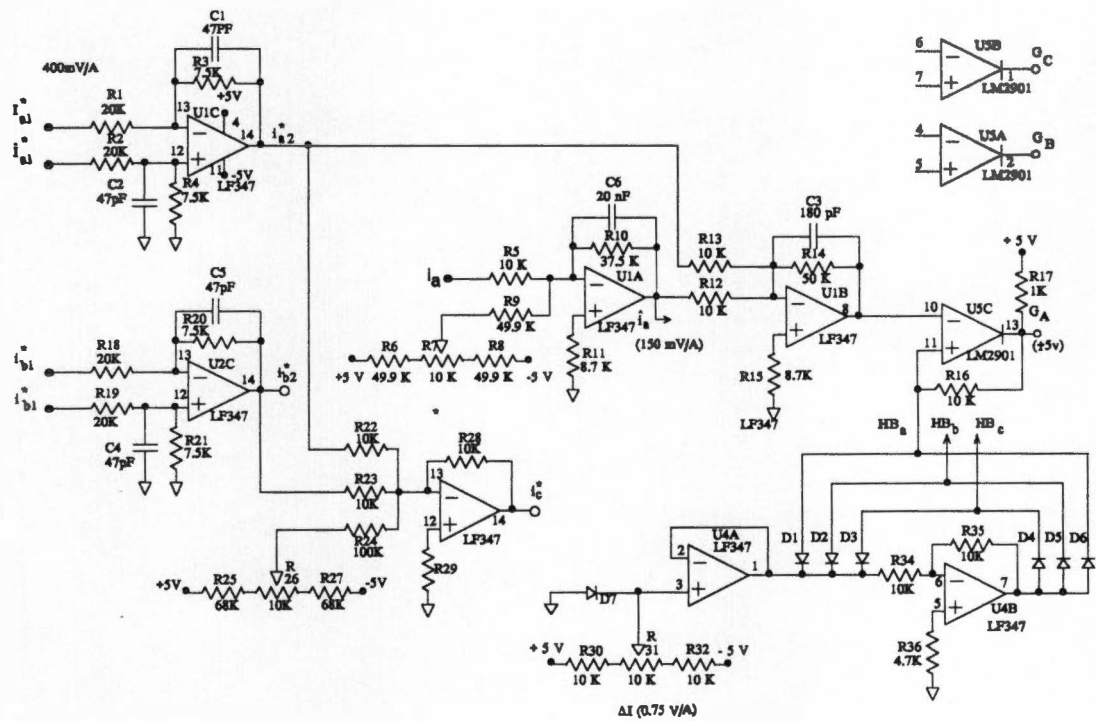


Fig. 4.17 Hysteresis band current controller.





### 4.5.3 Speed Measurement and Control Interface

Precise speed sensing is very important for proper operation of vector control systems. In fact, an error of 1% in speed measurement can result in severe degradation of drive performance.

The M/T method discussed in this section is characterized by very high precision in all speed range. Its implementation is shown in the circuit diagram of Fig. 4.19. Basically, it consists in counting pulses from an encoder (ENC) and from a high frequency clock (CLK). Speed information is obtained in software, by dividing the encoder counter increment ( $\Delta M$ ) by the clock counter increment ( $\Delta T$ ), with proper scaling, what will be explained later. Two 8-bit binary counters with output register (74ALS590) are used in cascade, for both ENC and CLK counters. The counter state is passed to the output register only at the positive edge of the register clock (RCK). By using the ENC pulse as the RCK signal of both counters, the contents of the output registers precisely reflects the actual speed.

A 3 to 8 decoder (74ALS138) is used to properly interface the counters to the DSP. Although the 74ALS590 output registers are directly connected to the DSP data bus, they are normally in a high impedance state, until the output enable pin (G) is asserted low by the 74ALS138 decoder. The output register content is then latched into the DSP.

The direction of rotation (DIR) and FAULT signals are similarly passed to the DSP through an octal bus transceiver (74ALS245). Finally, the START/STOP and counter clear CCLR signals are sent from the DSP to the control board through a dual 4-bit D flip-flop.



#### 4.5.4 DC Link Voltage and Current Sensing Interface

Adequate DC link voltage  $V_d$  and current  $I_d$  sensing is crucial for DC link power  $P_d$  computation, and consequently, for the correct operation of the efficiency controller.

DC link voltage sensing is shown in Fig. 4.20(a). A potential divider is initially used to bring the DC bus voltage to an adequate level and is next fed to an isolation amplifier (AM227), that ensures complete isolation between power and signal circuits. Its output is directly connected to the A/D input.

DC current sensing is performed by a high precision hall effect sensor (LEM LF 50-P), as indicated in Fig. 4.20(b). The sensor is placed between rectifier output and the DC capacitor bank. This location ensures that the PWM current harmonics generated by the inverter operation are filtered out by the DC link capacitor, resulting in an  $I_d$  waveform consisting of 6 pulses per period of 60 Hz supply. The LEM module works as a current transformer with a 1000:1 ratio, and with a  $50\Omega$  load resistor, a 50 mV/A gain is obtained. To ensure a better utilization of the A/D dynamic range, a low pass filter with a 3.81 gain is used. The reduction in DC link current bandwidth has no detrimental impact on  $P_d$  computation, since only its average value is relevant. In fact, as  $V_d$  is essentially constant, the average of  $P_d$  closely follows  $I_d$  average.

#### 4.6 Real Time Software Design

The complete drive control system, including the fuzzy efficiency controller and pulsating torque compensator, was implemented in assembly language in a TMS320C25 DSP based control board from Ariel Corporation. Figure 4.21 shows the software structure

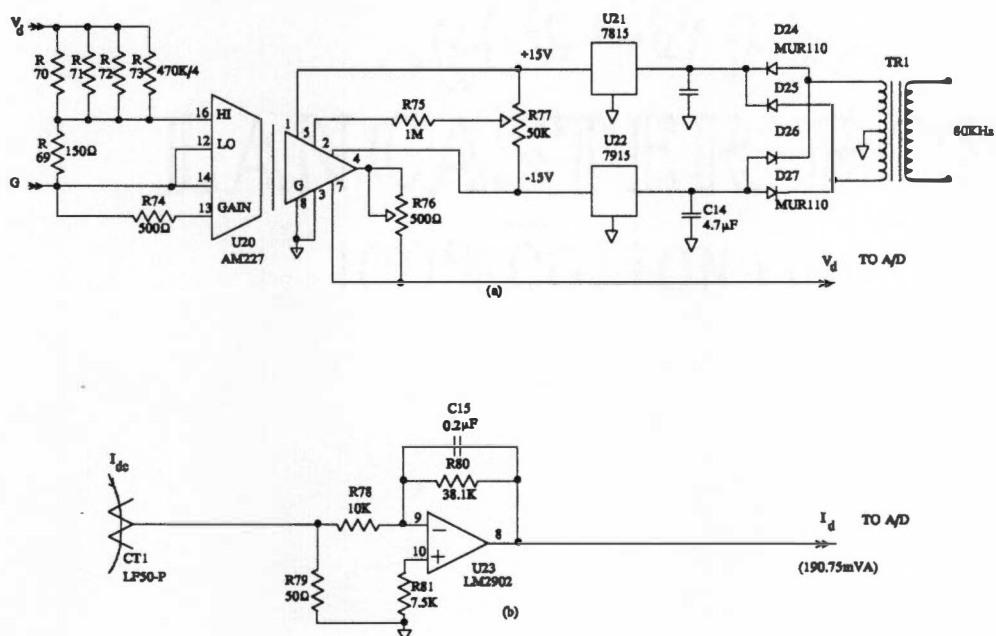


Fig. 4.20 DC link voltage and current sensing.

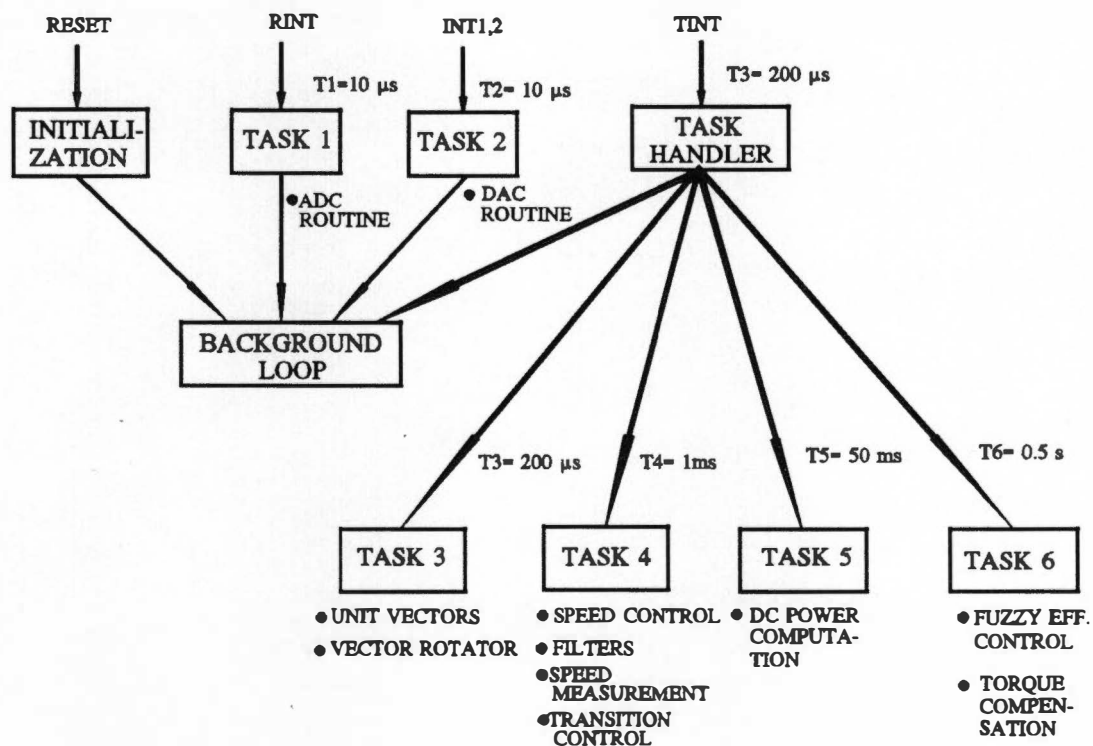


Fig. 4.21 Software structure of the drive system including the efficiency optimization controller

of the entire control system. Both the A/D and D/A converters operation are interrupt driven, and the maximum sampling frequency of 50 KHz per channel was selected, to benefit from the embedded 20 KHz bandwidth input and output filters.

The timer interrupt (TINT) was set to 200  $\mu$ s, that is the sampling time of the vector control routines. The remaining routines are executed at lower sampling frequency, and controlled by software timers.

#### 4.6.1 Basic Vector Control Functions

As previously indicated in the block diagram of Fig. 4.2, the implementation of the indirect vector control requires the generation of unit vectors  $\sin \theta_e$  and  $\cos \theta_e$ , from the speed signal  $\omega_r$  and slip frequency  $\omega_{sl}$ . The value of  $\theta_e$  is obtained by discrete integration of  $\omega_e$ , using double precision to ensure accurate computation at low speeds. A sine table with a resolution of 5.689 bits per degree was initially constructed and stored in program memory. The  $\sin \theta_e$  and  $\cos \theta_e$  values are obtained by simply scaling down the  $\theta_e$  value to the interval  $[-1024, 1024]$  bits and then retrieving the proper value from the sine table (table look-up method). The unit vectors are next used to calculate the stationary reference currents  $i_{qs}^*$  and  $i_{ds}^*$ , from which the phase current references  $i_a^*$  and  $i_b^*$  are obtained. Phase C reference  $i_c^*$  is obtained from  $i_a^*$  and  $i_b^*$  by a summing operational amplifier (Fig.4.17).

#### 4.6.2 Speed Computation

Speed computation will be discussed in details here. The basics of the M/T method have already being explained in the discussion of the speed interface hardware. The same principles are used here, as indicated by the speed computation flowchart of Fig. 4.22. The usual sampling time of 1 ms can be extended up to 5 ms, in case of very low speed. If no change occurs in the content of the encoder pulse counter (M) within the 5 ms extended period, the algorithm assumes  $\omega_r = 0$ . Under normal operation  $M_{\text{new}} > M_{\text{old}}$  and the speed computation proceeds as indicated. For operation in both directions, the direction signal (DIR) must be probed, and the speed polarity corrected accordingly. Robust operation of the algorithm is achieved by imposing a pre-defined limit ( $\Delta\omega_{\text{max}}$ ) to the speed change ( $\Delta\omega_r = \omega_{\text{new}} - \omega_{\text{old}}$ ). This protects the system against eventual malfunction of the hardware interface or encoder failure. Furthermore, by selecting  $\Delta\omega_{\text{max}}$  slightly larger than the maximum possible speed change under normal operation, no delay is introduced in the system, as would occur if a low pass filter were used.

#### 4.6.3 Efficiency Optimization Controller

The real time fuzzy efficiency controller uses the same algorithm described in the simulation study. Consequently, only some implementation aspects will be discussed here.

The algorithm basically derives the next control action ( $\Delta i_{ds}^*(k)$ ) from the measured change in input power ( $\Delta P_d(k)$ ) and the last control action ( $L\Delta i_{ds}^*(k)$ ). Initially, the interval index for each input variable is determined, thus defining the membership

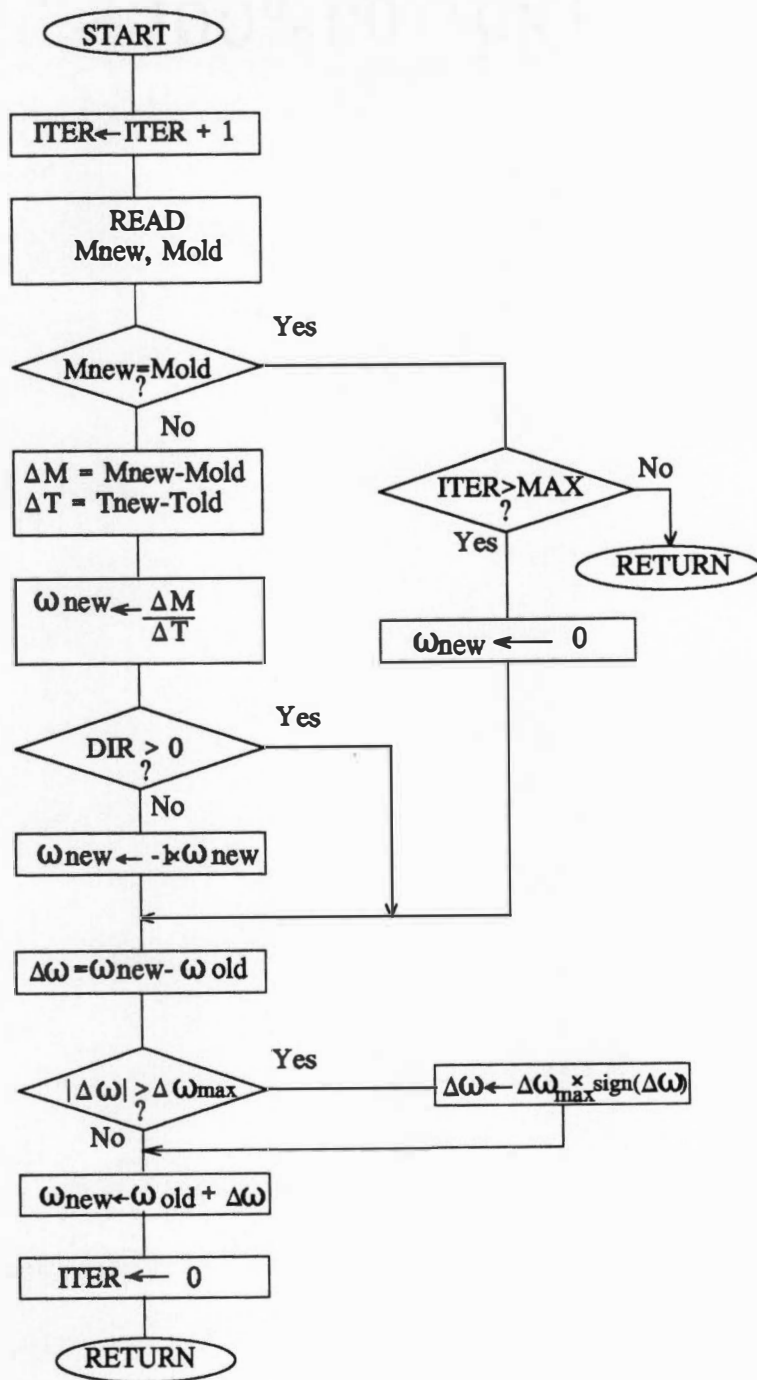


Fig. 4.22 Speed computation flowchart.



functions with non-zero degree of membership, as previously indicated in Fig. 4.11, for the case of  $\Delta P_d$ .

Because the DSP does not have a division instruction, whenever possible a division operation is replaced by a multiplication. This approach is used in the computation of the degree of membership. For the particular value of  $\Delta P_d(k)$  shown in Fig. 4.11, we have

$$\mu_{PM}(\Delta P_d) = (\Delta P_d(k) - P_3) (P_2 - P_3)^{-1} \quad (4.11)$$

As  $P_2$  and  $P_3$  are constants,  $(P_2 - P_3)^{-1}$  is pre-computed and stored in data memory.

The rule base evaluation requires the retrieval of the control signal associated with every fired rule. This task is readily accomplished by the use of interval indices and a look up table containing the rule base. Let  $J$  be the index for  $\Delta P_d$ ,  $I$  the index for  $L\Delta i_{ds}^*$ ,  $M$  and  $N$  the number of fuzzy sets for  $\Delta P_d$  and  $L\Delta i_{ds}^*$ , respectively. The relative position (POS) of the first fired rule within the look up table is given by

$$POS = (J - 1) M + I \quad (4.12)$$

The second rule is located at  $POS+1$ , the third one at  $POS+N$ , and the last one at  $POS+N+1$ . Once the rule base evaluation is performed, the new control action is computed by the height defuzzification method.

#### 4.7 Experimental Study

After careful software and hardware systems integration and debugging, the drive system was tested with a standard 5 hp NEMA class B induction machine, rated at 1710

rpm, 230 V, whose parameter were given on Table 4.2.

Typical AC supply phase voltage and current waveforms are shown in Fig. 4.23 for phase A, when the drive system was operating under rate flux, at a speed of 1350 rpm (0.75 pu) and a load torque of 7.68 lbf ft (0.5 pu). As discussed in Chapter 3, the diode rectifier conducts discontinuously, and therefore, significant amounts of harmonic currents are injected into the AC supply. The small unbalance in line voltages produces current pulses of varying amplitude, as shown. Some distortion in supply voltage waveform is also observable, generated by the harmonic current flow through the AC source impedance.

The machine input currents are shown in Fig. 4.24, when the drive was operating under rated flux, at 1350 rpm (0.75 pu) and delivering a load torque of 10.75 lbf ft (0.70 pu). The intrinsic operations of the hysteresis band PWM insures that the actual currents closely follow the sinusoidal command currents.

The operation of the fuzzy efficiency controller is illustrated in Fig. 4.25. The drive system was initially in a steady-state condition, at a speed  $\omega_r = 450$  rpm (0.25 pu) and load torque  $T_L = 1.54$  lbf ft (0.10 pu). At  $t = 0$  the efficiency controller was enabled, and the magnetizing current command  $i_{ds}^*$  was adaptively reduced on the basis of measured DC link power as shown in Fig. 4.25(a). The optimum operating point was achieved in only six steps. After that, the search algorithm remained active, with small  $\Delta i_{ds}^*$  steps, to ensure proper tracking in case the optimum point shifts due to parameter variation or slow changes in load torque. The operation of the pulsating torque compensation scheme is illustrated in Fig. 4.25(b). The bottom trace shows the

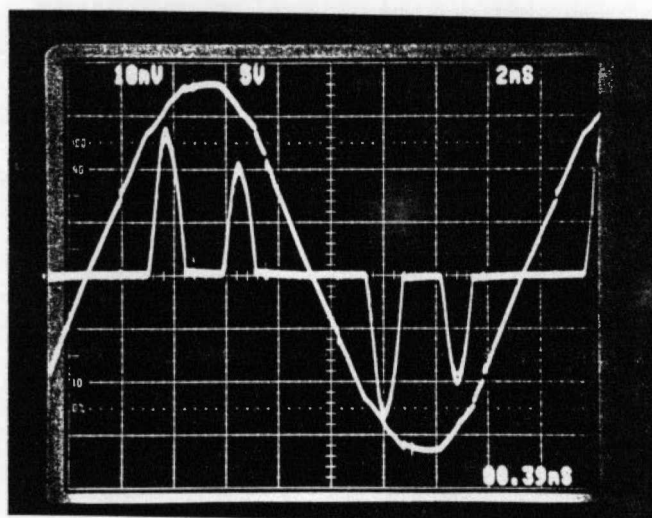


Fig. 4.23 AC supply phase voltage and current waveforms at  $\omega_r=0.75$  pu and  $T_L=0.50$  pu. Scales: 50 V/div., 10 A/div., 2 msec./div.

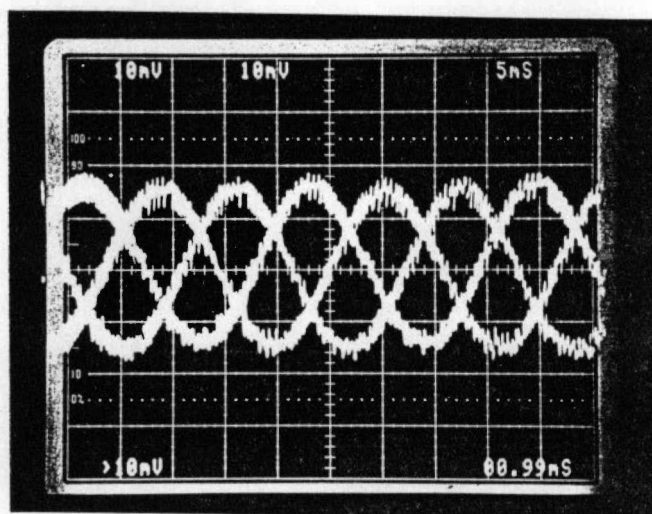
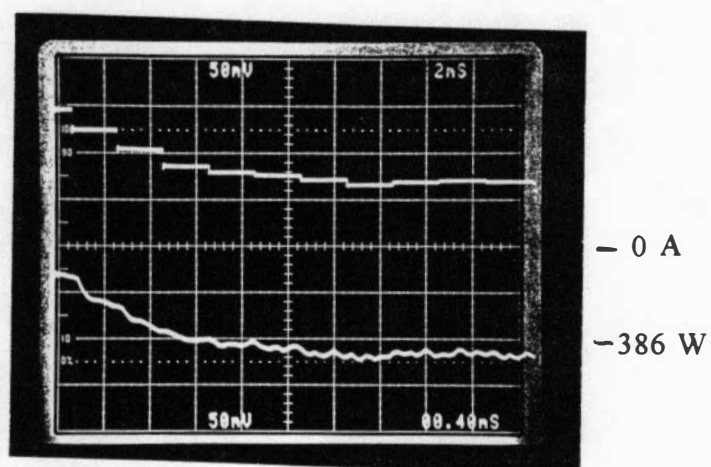
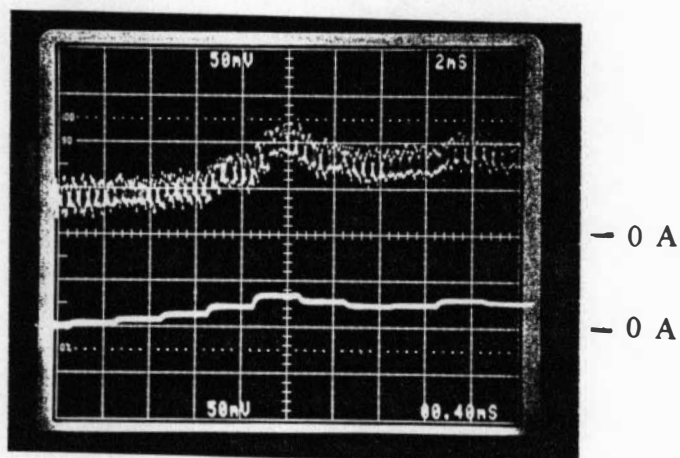


Fig. 4.24 Machine input currents at  $\omega_r=0.75$  pu and  $T_L=0.70$  pu. Scales: 10 A/div., 2 msec./div.

(a)



(b)



(c)

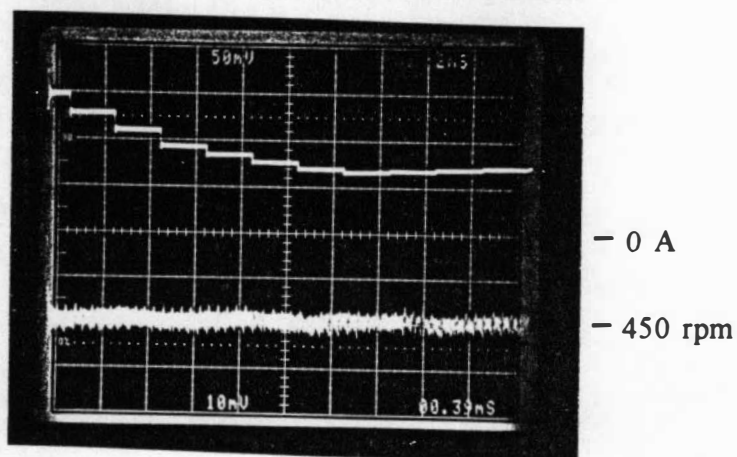


Fig. 4.25 Experimental search curve at  $\omega_r=0.25$  pu and  $T_L=0.10$  pu.

(a) Top:  $i_{ds}^*$  (3.33 A/div.); Bottom:  $P_d$  (58.5 W/div.).

(b) Top:  $i_{qs}^*$  (1.67 A/div.); Bottom:  $\Sigma \Delta i_{qs}^*$  (1.67 A/div.).

(c) Top:  $i_{ds}^*$  (3.33 A/div.); Bottom:  $\omega_r - \omega_r^*$  (61 rpm/div.).

Time scale: 2 sec./div.

compensating signal,  $\Sigma \Delta i_{qs}^*$ , whereas the upper trace represents the final torque current command,  $i_{qs}^*$ . It can be seen that both signals follow similar profiles, demonstrating that the output of the speed controller ( $i_{qs}^{*'}$ ) remains essentially constant. The effectiveness of the torque compensation can also be observed in Fig. 4.25(c), since the drive speed (bottom trace) remains practically constant.

Another set of curves are shown in Fig. 4.26, for the case of  $\omega_r = 900$  rpm (0.5 pu) and  $T_L = 4.61$  lbf ft (0.3 pu). As expected, the optimum  $i_{ds}^*$  is higher than that of Fig. 4.25(a), due to increased load torque. Accordingly, the observed reduction in DC link power (lower trace) is smaller, confirming that less efficiency gain is attainable as the load torque increases.

The associated torque current command, pulsating torque compensating signal and speed signal have similar profiles to those shown in Fig. 4.25 (b) and (c), and are not included here.

Some small fluctuations in DC link power are observable at any load condition, even at rated flux. These are caused by several factors, such as actual fluctuations in the load (dynamometer); the small unbalance in practical motors that creates negative sequence torques; and also some eventual small speed oscillations due to closed loop system dynamics. To reduce these fluctuations and ensure proper operation of the efficiency controller, a low pass filter of time constant  $\tau = 0.5$  sec. was introduced in the DC link power measurement routine, and the sampling interval for efficiency optimization increased to 2 sec.

To further demonstrate the effectiveness of the torque compensation scheme, the

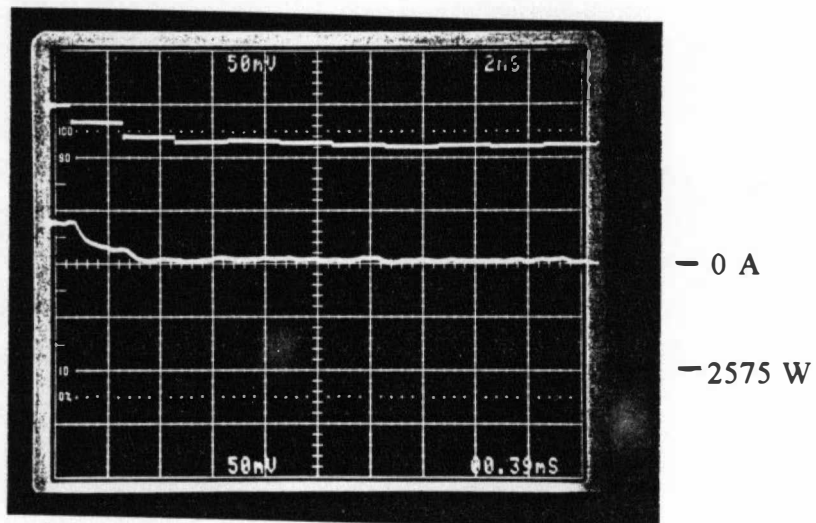


Fig. 4.26 Experimental search curve at  $\omega_r=0.50$  pu and  $T_L=0.30$  pu.  
 Top:  $i_{ds}^*$  (3.33 A/div.); Bottom:  $P_d$  (58.5 W/div.)  
 Time scale: 2 sec./div.

same operating point of Fig. 4.25 is repeated in Fig. 4.27, but with the pulsating torque compensation disabled. The flux reduction and the attendant reduction in developed torque results in larger speed drops, as shown in Fig. 4.27(a). Of course, the speed controller reacts to restore the speed to its set value. However, as shown in Fig. 4.27(b) (bottom trace), the increase in torque current command  $i_{qs}^*$  is slow, and does not prevent the speed to drop. In some applications, speed fluctuations are not permissible, and in all cases they tend to create fluctuations in DC link power, that adversely affects the operation of the efficiency controller.

In practical drive system, the operating point can vary, either by changes in load torque or in command speed. Fig. 4.28 demonstrates the ability of the proposed control strategy to cope with sudden changes in operating condition. The drive was initially operating in a steady-state mode, at  $\omega_r = 450$  rpm (0.25 pu) and  $T_L = 1.54$  lbf ft (0.10 pu), and the efficiency optimization controller brought  $i_{ds}^*$  (top trace) to its optimum value. At  $t=16$  sec. the command speed  $\omega_r^*$  was suddenly changed to 900 rpm, forcing the system to transition to a dynamic mode, where the rated  $i_{ds}^*$  was readily reestablished. At  $t = 19$  sec. the system had already reached a new steady-state mode, as indicated by the speed signal (bottom trace in Fig. 4.28(a)). A new search for the optimum efficiency point was initiated, and when it was completed, another transient was imposed by setting  $\omega_r^* = 450$  rpm once more. In any case the drive speed response was quite fast, demonstrating the adequacy of the proposed method for applications where fast transient response must be maintained. Fig. 4.28(b) shows the torque current command  $i_{qs}^*$  (lower trace) for an identical  $\omega_r^*$  profile, at same load condition. During the steady-state modes,

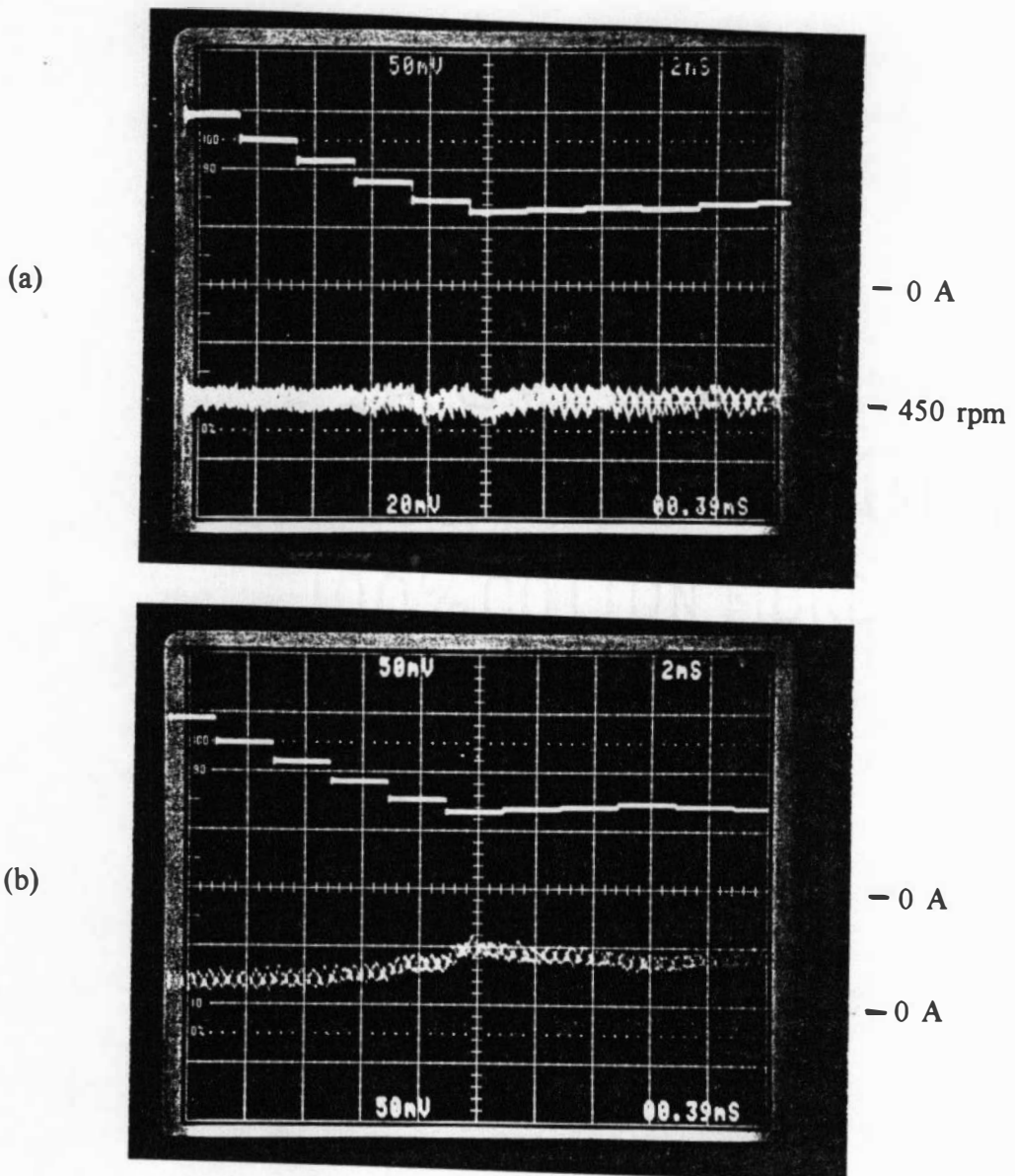
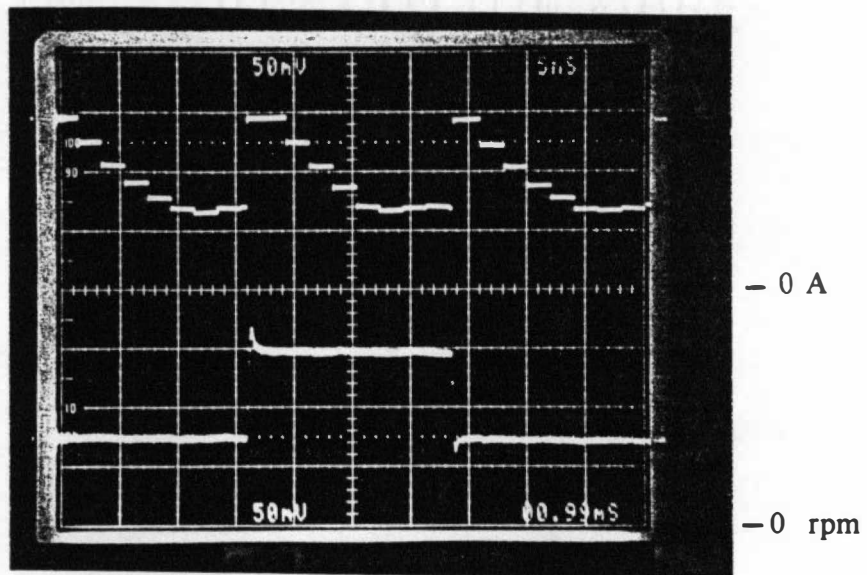


Fig. 4.27 Search curves at  $\omega_r=0.25$  pu and  $T_L=0.10$  pu, without pulsating torque compensation.  
 (a) Top:  $i_{ds}^*$  (3.33 A/div.); Bottom:  $\omega_r-\omega_r^*$ , (61 rpm/div.)  
 (b) Top:  $i_{ds}^*$  (3.33 A/div.); Bottom:  $i_{qs}^*$  (3.33 A/div.).  
 Time scale: 2 sec./div.



(a)



(b)

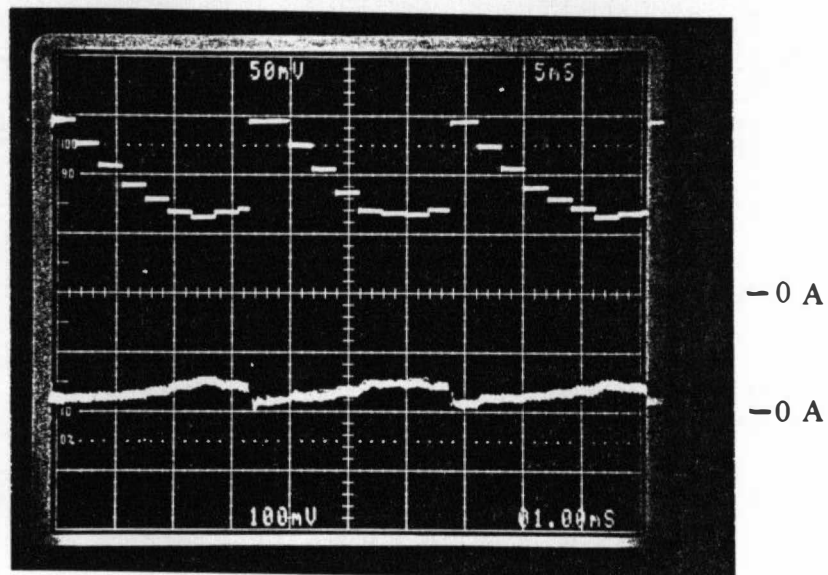


Fig. 4.28 Drive performance in time domain with sudden changes in command speed.  
(a) Top:  $i_{ds}^*$  (3.33 A/div.); Bottom:  $\omega_r$  (305 rpm/div.)  
(b) Top:  $i_{ds}^*$  (3.33 A/div.); Bottom:  $i_{qs}^*$  (3.33 A/div.).  
Time scale: 5 sec./div.

$i_{qs}^*$  changes are mainly caused by the pulsating torque compensator, whereas in the transient modes they are solely governed by the speed controller, as indicated by the spikes in  $i_{qs}^*$  waveform.

The drive system was further tested at several operating points of the torque-speed plane, both at rated and optimum flux conditions, to assess the efficiency improvements. During experimentation, it was realized that the available power measurement equipment did not have adequate bandwidth to accurately measure the system input power. On the other hand, the DC link power measurement scheme operating at 50 KHz possesses very good precision. It was then clear that the system input power could be better estimated by computing the diode rectifier loss, and then adding to the measured DC link power. However, no specifications on the power diodes were available, and consequently, the diode volt-ampere (V-I) characteristic had to be obtained experimentally. The experimental data was fed to the software TABLE-CURVE [36] to obtain the diode voltage drop equation, similar to (3.49). At every operating point, the measured DC link power and voltage were used to compute the average DC link current ( $I_{d(ave)}$ ), that in turn was substituted into (3.50) to obtain the rectifier loss.

The AC-200 system has a discharge resistor continuously connected across the DC link capacitor, such that no dangerous voltage levels remain after a few minutes the system has being shut down. However, this design feature creates extra power loss during normal operation. To make the results more general, this extra loss is deducted from the measured DC link power, prior to the diode rectifier loss and efficiency computations.

Finally, the overall system efficiency was determined, and resulting efficiency

curves are shown in Fig. 4.29. As mentioned earlier in this Chapter, the DC link power and the AC supply power follow similar profiles. Consequently, the efficiency curves of Fig. 4.29 reflect true optimum system operation. The efficiency gains are expressive, particularly at light load torques, but somewhat smaller than the predicted simulated efficiency gains. A number of factors can be enumerated to explain such differences. The most significant ones are:

- . The experimental hysteresis-band size is larger than the one used in simulations, due to lock-out time effect. This translates in lower order harmonic voltages and consequently, extra harmonic losses in the machine;

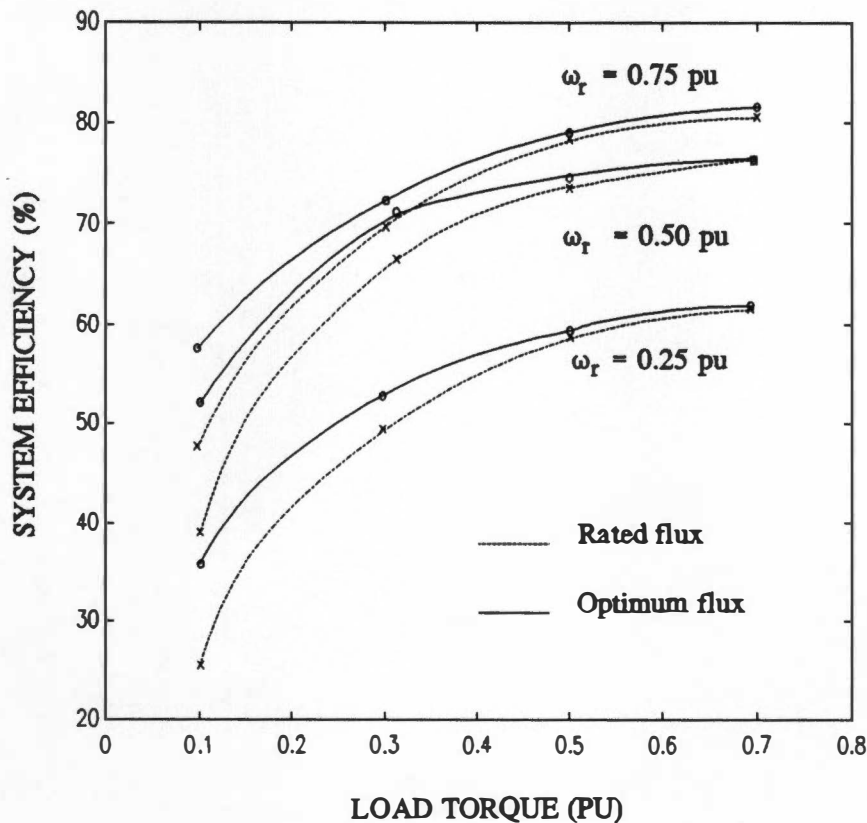


Fig. 4.29 Experimental efficiency curves.

- . The 5 hp class B motor is not perfectly symmetrical, i.e., the flux distribution in the air-gap has a negative sequence component, that in turn creates a second harmonic torque. As a consequence, the resultant torque is smaller than that of a perfectly symmetrical machine, and this leads to lower efficiencies.

Irrespective of the practical limitations of both machine and converter systems, the proposed fuzzy controller is capable of achieving the maximum possible efficiency for a given operating condition.

The technique is currently being extended to an electric vehicle drive, as part of a technology transition project for Delco-Remy company. The drive system under investigation is somewhat similar to that shown in Fig. 4.2, except that the indirect vector control operates in a torque control mode, and the inverter is fed by a battery bank. Fuzzy efficiency control is engaged when the vehicle is traveling at constant speed, i.e., when the drive system is in a steady-state mode. The system switches back to a dynamic mode, if the torque command from the vehicle driver ( $i_{qs}^*$ ) is modified, or if it is detected that a speed variation has occurred. In such cases, rated flux is promptly restored to ensure maximum torque capability. The torque compensation scheme prevents torque pulsations during efficiency optimization, that could lead to reduction in riding comfort.

## CHAPTER 5

### FUZZY LOGIC BASED SLIP GAIN TUNING

#### 5.1 Introduction

Indirect vector control is by far the most popular type of control for high performance induction motor drives. It offers the independent torque and flux control characteristics of a separately excited dc machine drive, with the advantages of lower machine cost, higher torque to inertia ratio and virtually maintenance free operation. One limitation of this control is its dependency on machine parameter, namely rotor resistance ( $R_r$ ) and rotor inductance ( $L_r$ ). It is the standard practice to use the nominal equivalent circuit parameters of the machine to compute the slip gain. For an unknown machine, the drive system can be self-commissioned, based on initial automated identification of parameters. However, machine parameters may vary widely in operating condition, due to changes in machine temperature and saturation, resulting in detuned operation.

Under detuned operation, there is a cross-coupling between flux and torque control loops, that adversely impacts their transient responses as well as results in incorrect steady state values of torque and flux. These effects will be illustrated with the help of the torque control system shown in Fig. 5.1. In this system, the flux command is kept constant at its rated value, while the torque command can be set to any value between

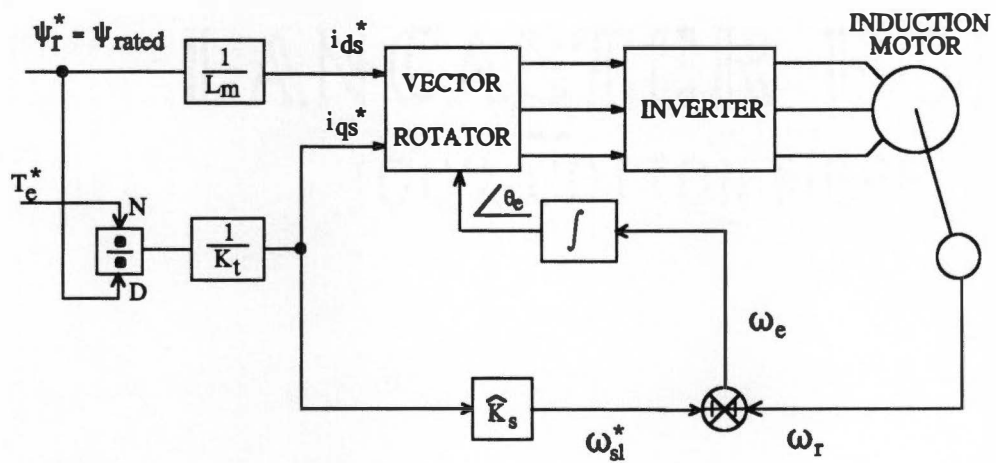


Fig.5.1 Indirect vector-controlled induction motor drive with open loop torque and flux control.

zero and the maximum torque. A fixed saturation factor is assumed, i.e., machine inductance are considered constant. The steady-state characteristics of developed torque and rotor flux are shown in Fig. 5.2, for three different values of slip gain estimate  $\hat{K}_s$ . When the slip gain estimate  $\hat{K}_s$  precisely matches the actual value  $K_{s0}$ , a linear torque transfer function is obtained, as shown by curve 2 of Fig. 5.2(a). Furthermore, the rotor flux  $\psi_r$  is unaffected by changes in torque, as indicated by curve 2 of Fig. 5.2(b). For the case  $\hat{K}_s = 0.5 K_{s0}$  (curve 1), as the torque command is increased, the insufficient slip frequency causes the magnetizing current to increase. The associated overflux forces the machine into saturation and increases the core losses, that may result in overheating of the machine. On the other hand, for  $\hat{K}_s = 2 K_{s0}$ , the opposite situation occurs. The machine is demagnetized as the torque command increases, resulting in a reduction of the maximum torque capability, that in turn might cause the drive to stall at high load torques. It is also clear the loss of linearity of the input/output torque characteristic for  $\hat{K}_s \neq K_{s0}$ .

For the case a closed loop torque control system, the torque error due to detuned operation would be corrected by action of the torque controller, such that at steady-state the torque demand would be met. However, this would require a higher stator current, that in turn would lead to extra copper losses and consequently, to a derating of the machine.

The transient effects of detuning are illustrated in Fig. 5.3. In Fig. 5.3(a) the slip gain was set to twice the correct value. The cross-coupling effect is quite evident, from higher order dynamics for torque and flux transients. The oscillatory torque response renders the system unsuitable for torque control applications. On the other hand, Fig.

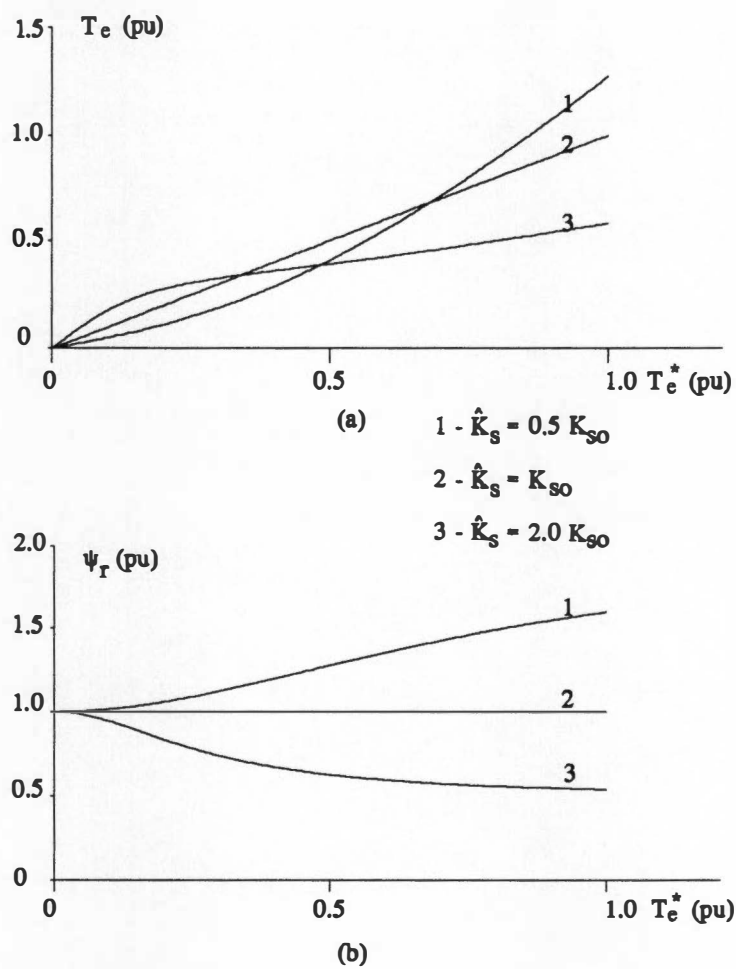


Fig. 5.2 Steady state detuning effects.  
 (a) Torque characteristics.  
 (b) Flux characteristics.



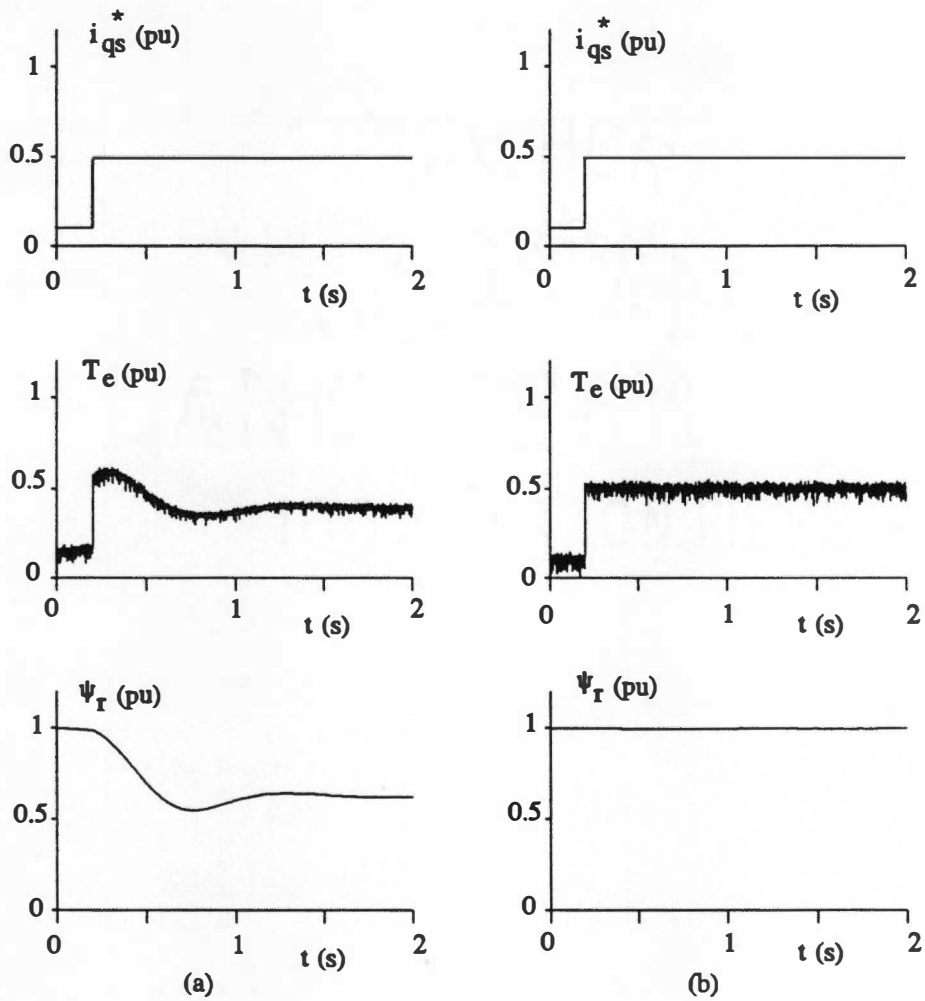


Fig. 5.3 Transient response for developed torque and rotor flux.  
 (a) Detuned condition ( $K_s / K_{s0} = 2$ .)  
 (b) Tuned condition.

5.3(b) shows the ideal transient response for torque, as well as the perfectly decoupled flux response, for the case of correct slip gain.

Various on-line slip gain tuning techniques have been reported in the literature. Slip gain adaption based on the difference between ideal machine reactive power and actual reactive power was first reported by Garces [45]. Pseudo-random binary signal injection in one axis and then tuning on the basis of the induced signal in the other axis is described by Gabriel et al. [46]. Moreira et al [47] proposed a digital deadbeat controller, that derives the corrective term  $\Delta K_s$  for the slip gain on the basis of an approximate machine inverse model and rotor flux estimates. The method, however, requires elaborated pre-computation of experimental saturation functions for air-gap flux and magnetizing inductance estimation. Zai and Lipo [50] used an extended Kalman filter to estimate the inverse rotor time constant on line, that makes use of the wide-band harmonic voltages, intrinsic to power inverters, as the random test signal. Systematic application of model-reference adaptive control (MRAC) technique based on reference torque model (ideal torque at tuned condition) and actual estimated torque for tuning the slip gain was reported in [48]. The MRAC tuning method was extended by Rowan et al. [49] to include voltage control method, which also evaluated the MRAC based torque ( $T_e$ ), reactive power ( $Q$ ), D-axis voltage ( $v_{ds}$ ), Q -axis voltage ( $v_{qs}$ ) and voltage magnitude ( $v_s$ ) control methods, at fixed speed (60 Hz), and compared their performances. The study analyzed the advantages and limitations of all the methods, and concluded that none of them can solve the tuning problem satisfactorily in all the regions of torque-speed plane. Nevertheless, it was noticed from their study that the reactive power

model possesses good convergence characteristics, except at low torques. On the other hand, the D-axis voltage model exhibits excellent sensitivity to detuning, but its implementation at low speeds is complicated by the small signal to noise ratio, inherent to PWM inverters operating at small modulation factors. Furthermore, its dependency on stator resistance tends to reduce the method's precision at high load torques. Both model characteristics are discussed in detail in section 5.2. These complementary features suggests the creation of a new hybrid method, capable of performing slip gain tuning in practically the entire torque-speed plane. Such method must be able to select the most adequate model for each particular operating point, such that convergence to correct slip gain is achieved. The application of fuzzy logic in the derivation of this new method is discussed in the following sections. The results constitute the subject of a paper [63], to be presented at the 1993 international conference. on industrial electronics, control and instrumentation, IECON'93.

## 5.2 Fuzzy Tuning Controller

Fig. 5.4 shows the simplified block diagram of the proposed tuning controller, integrated with the indirect vector controlled drive system. The close loop speed controller generates the  $i_{qs}^*$  command which then multiplies with the slip gain  $\hat{K}_s$  to generate the slip frequency command  $\omega_{sl}^*$ . The MRAC system generates the reference models ( $A^*$ ) with the help of command currents and frequency, compares with the estimated outputs of actual models ( $A$ ), and then updates the slip gain  $\hat{K}_s$  through the fuzzy tuning controller.

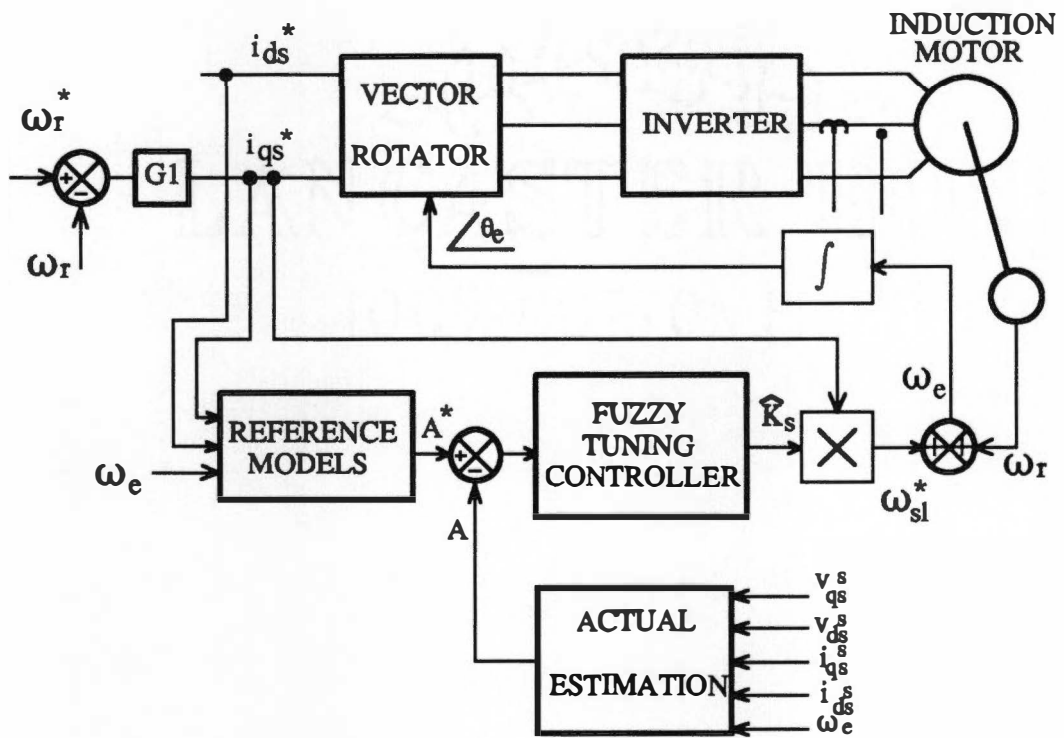


Fig. 5.4 Indirect vector-controlled induction motor drive showing the proposed fuzzy tuning controller.

The proposed method is actually based on two models, reactive power (Q) and D-axis voltage ( $v_{ds}$ ), and consequently, A and A\* are vector variables.

### 5.2.1 Reactive Power and D-axis Voltage Regulators

The derivation of reference models for reactive power ( $Q^*$ ) and D-axis voltage ( $v_{ds}^*$ ) control was based on the synchronous frame D-Q model of the induction machine, shown in Fig. 3.3. The stator voltage equations are given by

$$v_{qs} = R_s i_{qs} + \frac{d}{dt} \psi_{qs} + \omega_e \psi_{ds} \quad (5.1)$$

$$v_{ds} = R_s i_{ds} + \frac{d}{dt} \psi_{ds} - \omega_e \psi_{qs} \quad (5.2)$$

Where the stator fluxes can be expressed as

$$\psi_{qs} = L_s i_{qs} + L_m i_{qr} \quad (5.3)$$

$$\psi_{ds} = L_s i_{ds} + L_m i_{dr} \quad (5.4)$$

Under steady-state field orientation the following conditions apply [17]

$$\psi_{qr} = L_r i_{qr} + L_m i_{qs} = 0 \quad (5.5)$$

$$i_{dr} = 0 \quad (5.6)$$

From equation (5.5),  $i_{qr}$  can be expressed as

$$i_{qr} = -\frac{L_m}{L_r} i_{qs} \quad (5.7)$$

Substitution of (5.6) and (5.7) into stator flux equations 5.3 and 5.4 leads to

$$\psi_{qs} = (L_s - \frac{L_m^2}{L_r}) i_{qs} = L_\sigma i_{qs} \quad (5.8)$$

$$\psi_{ds} = L_s i_{ds} \quad (5.9)$$

Finally, substitution of (5.8) and (5.9), and the steady-state conditions of equation 5.10, into (5.1) and (5.2), results in the field oriented stator voltage equations 5.11 and 5.12.

$$\frac{d}{dt} \psi_{qs} = \frac{d}{dt} \psi_{ds} = 0 \quad (5.10)$$

$$v_{qs} = R_s i_{qs} + \omega_e L_s i_{ds} \quad (5.11)$$

$$v_{ds} = R_s i_{ds} - \omega_e L_\sigma i_{qs} \quad (5.12)$$

The steady-state reactive power of the machine [49] is expressed by

$$Q = v_{qs} i_{ds} - v_{ds} i_{qs} \quad (5.13)$$

Substituting  $v_{qs}$  and  $v_{ds}$  from (5.11) and (5.12) into equation 5.13 leads to

$$Q = \omega_e (L_s i_{ds}^2 + L_\sigma i_{qs}^2) \quad (5.14)$$

The reference quantities  $Q^*$  and  $v_{ds}^*$  are readily obtained from the field oriented equations (5.12) and (5.14) respectively as

$$v_{ds}^* = \hat{R}_s i_{ds}^* - \omega_e \hat{L}_\sigma i_{qs}^* \quad (5.15)$$

$$Q^* = \omega_e (\hat{L}_s i_{ds}^{*2} + \hat{L}_\sigma i_{qs}^{*2}) \quad (5.16)$$

Estimates of  $L_s$ ,  $L_\sigma$  and  $R_s$  are required, but no rotor parameter is involved. The feedback variables  $Q$  is computed from (5.13), and actual  $v_{ds}$  is given by

$$v_{ds} = v_{qs}^s \sin\theta_e + v_{ds}^s \cos\theta_e \quad (5.17)$$

where  $\cos\theta_e$  and  $\sin\theta_e$  are the unit vectors available in the vector controller.

### 5.2.2 Derivation of Combined Error Signal

Fig. 5.5 shows the details of the proposed control system. The scheme depends on reference model computation of reactive power ( $Q^*$ ) and D - axis voltage ( $v_{ds}^*$ ) as discussed above. The reference models are compared with the respective actual estimates of the quantities, and the corresponding loop error is divided by a base value to convert to per unit variables. Handling the variables in pu form is convenient for fuzzy controller. Besides, the same controller can be easily extended to other drive systems. The base values for the respective variables are essentially the same as reference variables, i.e.,  $Q_b = Q^* + \epsilon_1$  and  $V_b = |\omega_e L_\sigma i_{qs}^*| + \epsilon_2$ , where the parameters epsilon (a small positive constants) have been added to avoid indeterminate computation, in case the reference model approaches zero at critical conditions. Note that the reverse polarity of  $Q$  is due to opposite behavior of  $v_{ds}$  and  $Q$  with respect to  $\hat{K}_s$ , which is explained later. The first fuzzy logic controller (FLC-1) generates the weighting factor  $K_f$ , which permits

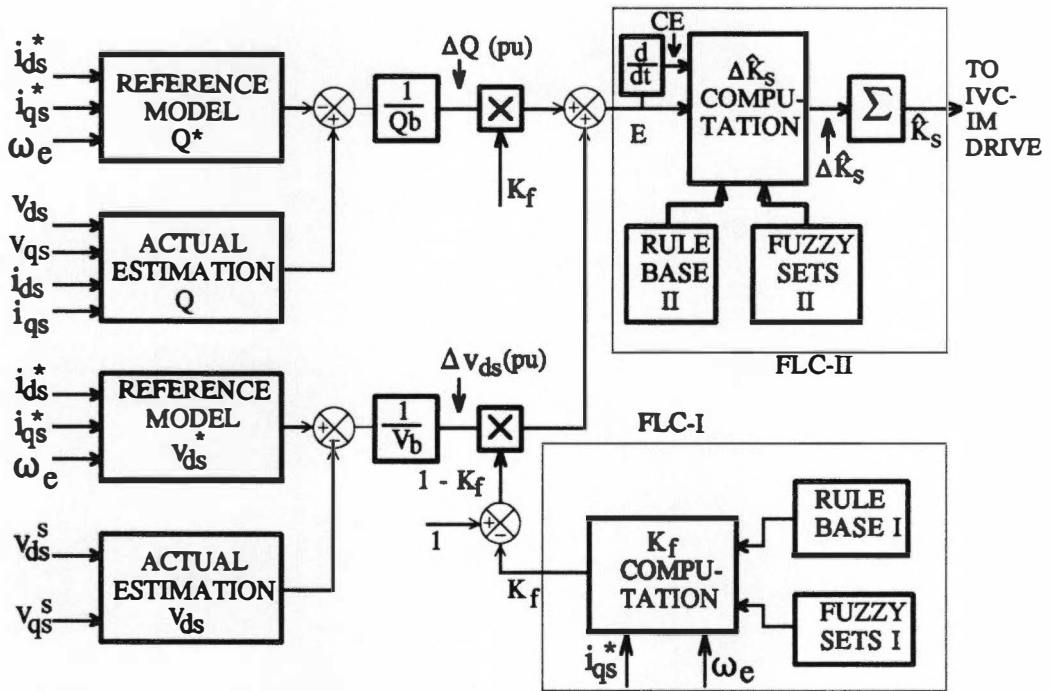


Fig. 5.5 Fuzzy logic based MRAC tuning control block diagram.



appropriate distribution of Q control and  $v_{ds}$  control on the  $i_{qs}^* - \omega_e$ , i.e., torque-speed plane. The combined error signal is defined as

$$E = \Delta Q K_f + \Delta v_{ds} (1 - K_f) \quad (5.18)$$

### 5.2.3 Design of the Fuzzy Tuning Controller

The second fuzzy controller (FLC-2) generates the corrective incremental slip gain  $\Delta \hat{K}_s$ , as shown in Fig. 5.5. As the error signal is derived from two different models, both its steady-state and dynamic characteristics vary with the operating point. Under such conditions, the use of a fuzzy controller, that inherently implements distinct control laws at different operating points, ensures fast convergence at practically any point in the torque-speed plane.

In ideally tuned condition, the signals  $\Delta Q$  and  $\Delta v_{ds}$ , and correspondingly the E signal, will be zero and the slip gain  $\hat{K}_s$  will be set to the correct value  $K_{s0}$ . If the system is detuned, for example due to change of rotor resistance, the actual Q and  $v_{ds}$  variables will deviate from the respective reference variables. The resulting error will alter the  $\hat{K}_s$  value until the system becomes tuned, i.e.,  $E = 0$ . In order to derive the knowledge required for the design of the fuzzy controllers, the static characteristics of both Q and  $v_{ds}$  loops were initially investigated through simulation. To this end, the speed control system of Fig. 5.4 was used, but with tuning algorithm disabled. The slip gain  $\hat{K}_s$  was intentionally varied from 0.5 to 2 times the correct value  $K_{s0}$ . The speed control loop ensured any steady-state operating point on torque-speed plane, even with detuned condition. Fig. 5.6 shows the normalized error relation with normalized slip gain ( $\hat{K}_s/K_{s0}$ )

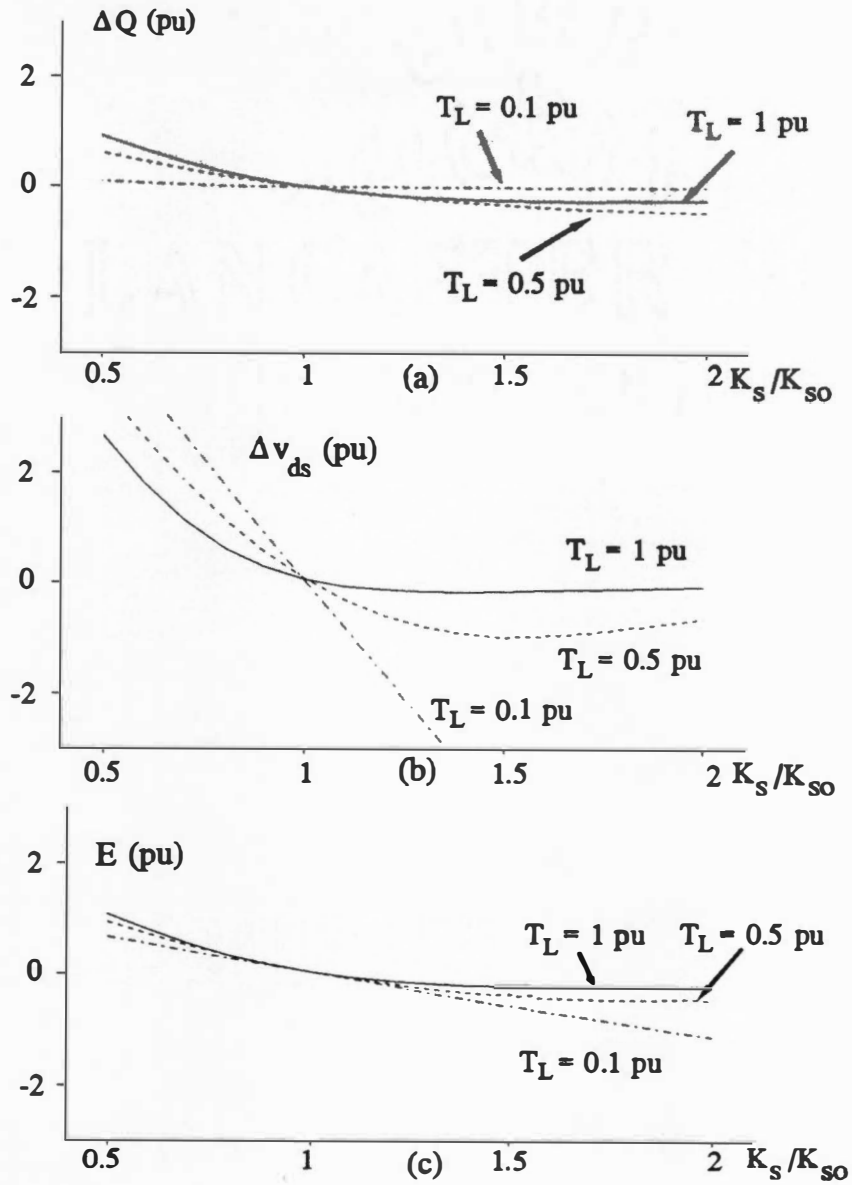


Fig. 5.6 Normalized control loop error vs. normalized slip gain curves ( $\omega_r = 0.5$  pu).

- (a) Reactive power error.
- (b) D-axis voltage error.
- (c) Combined error.

at speed  $\omega_r = 0.5$  pu, for different load torque conditions. Note that, at ideally tuned condition  $\hat{K}_s/K_{s0} = 1$ , and correspondingly  $\Delta Q$  (pu) =  $\Delta v_{ds}$ (pu) =  $E$ (pu) = 0. If the system is detuned, for example with lower  $\hat{K}_s$  (i.e., higher rotor resistance), then  $Q > Q^*$ , and the controller will raise  $\hat{K}_s$  until the tuning point is reached. Note that the loop error tends to be very small at low torque, but increases with a higher load torque. Fig. 5.6(b) shows similar curves for the voltage control loop. The voltage loop error tends to be very large at detuned condition, except at  $T_L = 1.0$  pu and  $\hat{K}_s/K_{s0} > 1$ . These characteristics indicate that the parameter  $K_r$  should be large at high torque region, but small at low torque region.

Consider now the parameter variation problem in (5.15) and (5.16). If the machine parameters deviate from those used in the reference model, the slip gain will be tuned to an incorrect value. The inductance  $L_s$  will decrease by saturation caused by air-gap flux, but its value will remain unchanged if rated flux is maintained. On the other hand, the inductance  $L_\sigma$  will vary by saturation due to stator current, i.e., is load dependant. The stator resistance in (5.16) will vary with stator temperature, but its effect can be negligible at high speed. The parameter variation effect, along with the characteristics in Fig. 5.6(a) and (b), indicate that the  $v_{ds}$  control method is better at high speed, low torque region, whereas  $Q$  control method is superior at low speed high torque region.

Fig. 5.6(c) shows the combined error  $E$  (pu) as a function of  $\hat{K}_s/K_{s0}$ , with optimum  $K_r$  distribution on torque-speed plane, obtained through FLC1. Fig. 5.7 gives the membership functions for frequency (i.e., speed), the current  $i_{qs}^*$  and the weighting factor

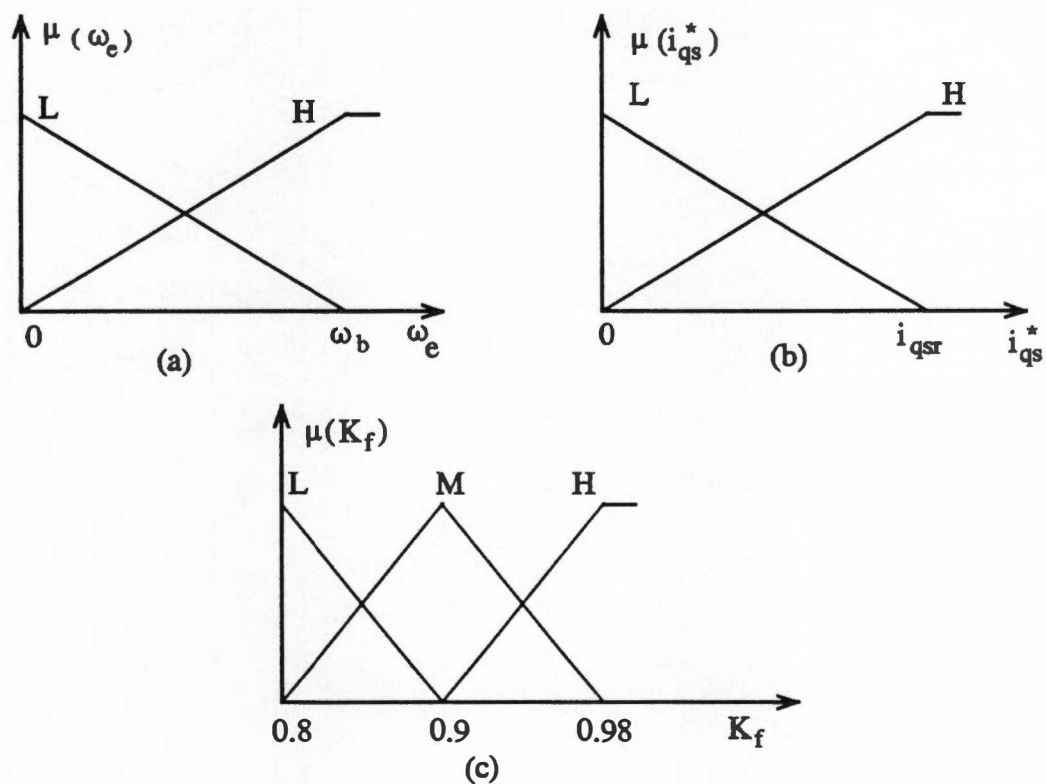


Fig. 5.7 Membership functions for FLC1.

- (a) Speed ( $\omega_e$ )
- (b) Torque current ( $i_{qs}^*$ ).
- (c) Weighting factor ( $K_f$ ).

$K_f$ , and Table 5.1 gives the corresponding rule base for fuzzy controller FLC-1. An example rule can be stated as

**IF speed ( $\omega_e$ ) is low (L) and torque ( $i_{qs}^*$ ) is high (H) THEN weighting factor ( $K_f$ ) is high (H).**

In fuzzy control, an imprecise information can be useful. For the controller FLC-1, even if the system is detuned,  $i_{qs}^*$  can still be used as a measure of torque, at approximately rated flux condition. As mentioned before, the control strategy built into Rule Base I ensures high sensitivity to detuning for any given operating condition.

Fig. 5.8 gives the membership functions for error (E), change in error (CE) and slip gain increment ( $\Delta\hat{K}_s$ ) for the controller FLC-II, where input and output gains were used to normalize the variables in the  $[-1,1]$  interval.

Table 5.1 Rule base for weighting factor ( $K_f$ ) calculation.

$i_{qs}^*$ \ $\omega_e$	H	L
H	M	H
L	L	M

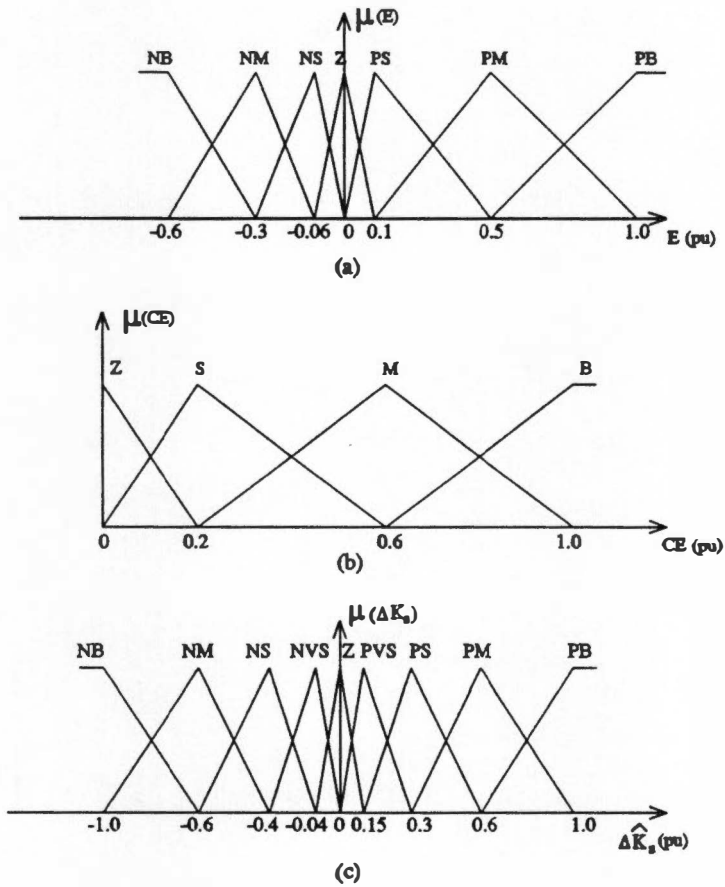


Fig. 5.8 Membership functions for FLC-2.

(a) Error (E).

(b) Change in error (CE).

(c) Increment in slip gain ( $\Delta K_s$ ).

The asymmetry of the functions gives better resolution in control, as the respective variable approaches zero. The control loop was designed to provide overdamped  $K_s$  response, and therefore, only CE magnitude was considered, resulting in simplification of the rule base, as shown on Table 5.2. Broadly speaking, the control strategy, embedded into rule base 2, consists in selecting a  $\Delta K_s$  increment that forces the combined error  $E$  to approach zero, at a desired rate CE. The final rule base is a result of a fine tuning process, that used intensive simulation of the drive system, under various operating points in the torque-speed plane.

### 5.3 Simulation Study

Once the control algorithm was formulated in detail, the complete drive system with the proposed controller, as shown in Figs. 5.4 and 5.5, was simulated in SIMNON. The system has an outer speed control loop and a hysteresis-band PWM (HBPWM) in the inner loop. Simulation studies were conducted using 5 hp induction servomotor, originally used in the General Electric AC-200 vector control system, whose parameters are given on Table 5.3.

In order to keep the simulation time small, ideal (lossless) models were used for the rectifier and inverter subsystems, and a standard synchronous frame D-Q model was selected for the machine. The fuzzy controller was implemented using the same methodology described for the fuzzy efficiency controller, but here a 1 ms sampling time was selected. All SIMNON routines are given in Appendix A.3.

Table 5.2 Rule base for increment of slip gain ( $\Delta K_s$ )

$\begin{array}{c} E \\  CE  \end{array}$	NB	NM	NS	ZE	PS	PM	PB
B	NM	NS	ZE	ZE	PVS	PM	PS
M	NB	NM	ZE	ZE	PVS	PM	PS
S	NB	NM	NVS	ZE	PVS	PB	PM
Z	NB	NB	NM	ZE	PVS	PB	PB

Table 5.3 Parameters for the induction servomotor.

5 hp 180 V 15 A		
4 poles 2200 rpm		
<u>D<sup>e</sup>-Q<sup>e</sup> equivalent circuit parameters</u>		
$R_s=0.177 \Omega$	$R_r=0.318 \Omega$	$R_m=121.4 \Omega$
$L_{ls}=0.00205 \text{ H}$	$L_{lr}=0.00130 \text{ H}$	$L_m=0.0328 \text{ H}$



As the system dynamics varies with the slip gain, performance studies were initially carried out to fine tune the membership functions as well as the rule bases of both controllers, until optimum performance was obtained in the tuning process. Fig.5.9 shows the normalized slip gain ( $\hat{K}_s/K_{s0}$ ) and error  $E(\text{pu})$  versus time, at  $\omega_r = 1100 \text{ rpm}$  ( $0.5 \text{ pu}$ ) for different load torques. The slip gain was intentionally set to an incorrect initial value, and the system was brought to a steady state condition at  $t=0$ , when the tuning algorithm was enabled. In Fig. 5.9(a), the load torque ( $T_L$ ) is small, and therefore, the voltage control is dominant. On the other hand, in Fig. 5.9(c) the high  $T_L$  results in the dominance of reactive power control. In Fig. 5.9(b) both controls contribute equally for  $E(\text{pu})$  computation. Evidently, the fuzzy controller is capable of bringing the system to a tuned condition in approximately 2 sec., in all cases. Similar convergence profiles were observed for other speed conditions, but are not shown here. Fig. 5.10 shows the tuning controller response when the drive is delivering rated torque at  $\omega_r = 0.5 \text{ pu}$ , and the rotor resistance is suddenly increased by 100% from the initially tuned condition. Actual tuning time will be much shorter, because detuning range is hardly so large. Since large thermal time constant of the machine causes slow changes of rotor resistance, this tuning time delay is perfectly acceptable.

#### **5.4 Hardware Design**

The 5 hp vector control system described in chapter 4 was adapted for the slip gain tuning experimental study, but used with the 5 hp induction servomotor, whose parameters were given on Table 5.3. The major change concerns the machine voltage

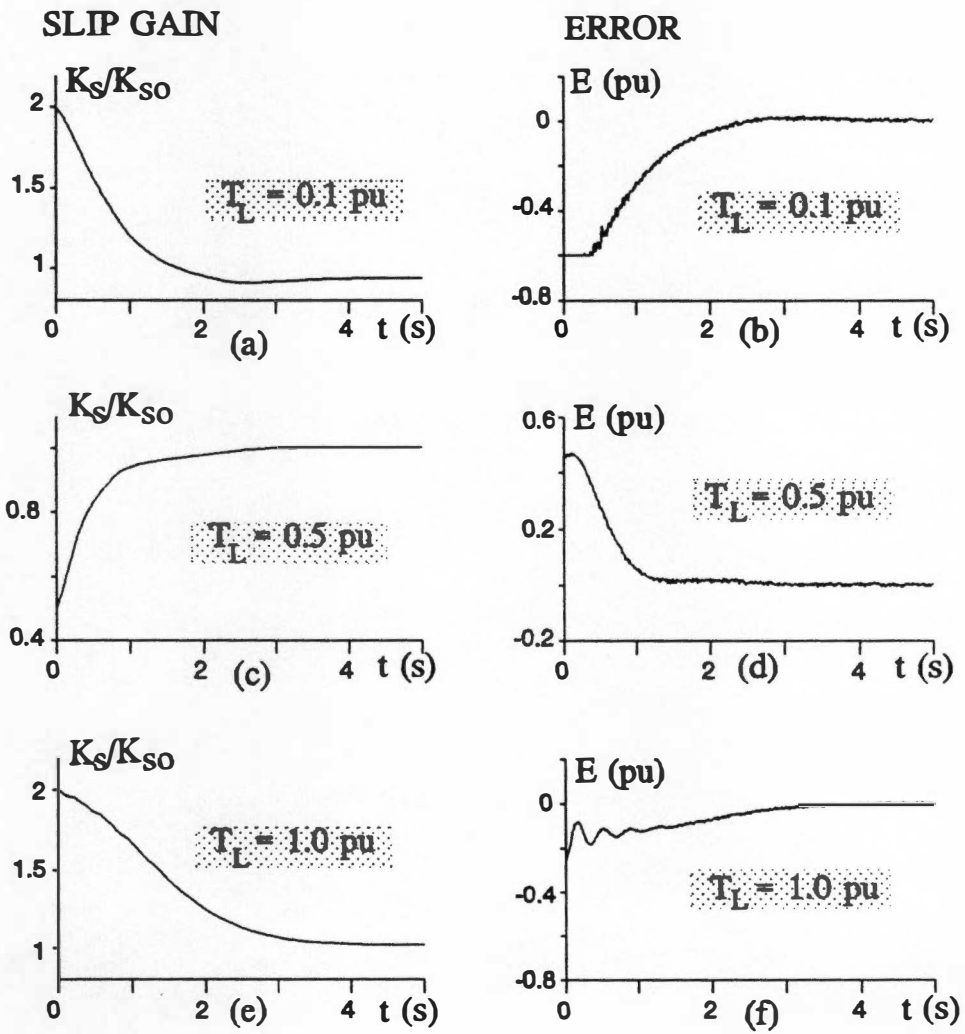


Fig. 5.9 System tuning performance at  $\omega_r=0.5$  pu and different torques.

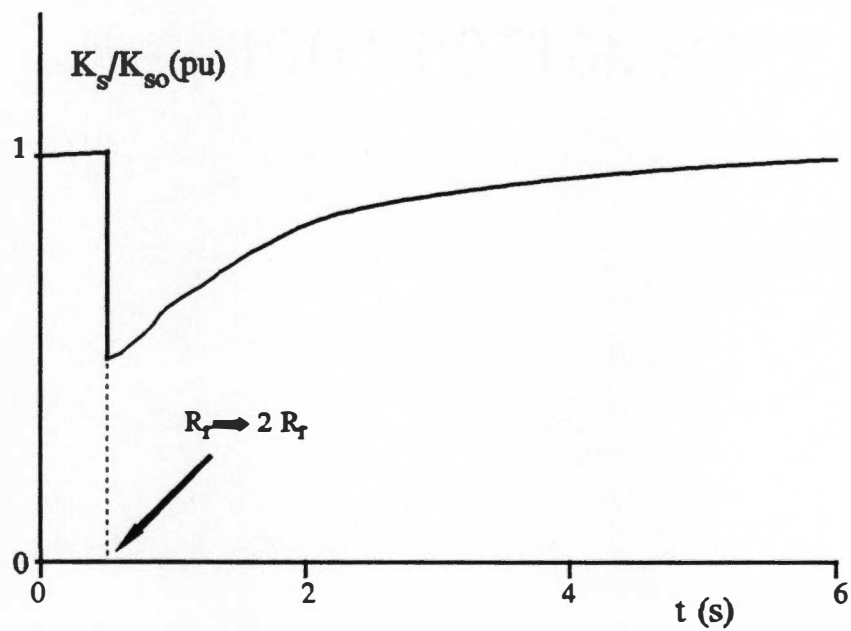


Fig. 5.10 Performance of tuning controller to a 100% increase in rotor resistance.

sensing interface, shown in Fig. 5.11. Its principal component is a 5 KHz bandwidth isolation amplifier (AD 204) from Analog Devices, Inc., that provides complete separation of power and control circuits. The line voltages  $v_{ac}$  and  $v_{cb}$  are derived by using the AD204 built in operational amplifier in a differential configuration. The large attenuation factor (80:1) of the differential amplifier brings the line voltage signal within the device's input voltage range of  $\pm 5$  V. The secondary  $v_{ac}$  and  $v_{cb}$  signals are next used to compute the stationary frame  $D^s$  -  $Q^s$  voltages  $v_{ds}^s$  and  $v_{qs}^s$ , as shown in the following development.

By definition, the  $D^s$  -  $Q^s$  voltages are obtained from the abc voltages as

$$v_{qs}^s = \frac{2}{3}v_{an} - \frac{1}{3}v_{bn} - \frac{1}{3}v_{cn} \quad (5.19)$$

$$v_{ds}^s = -\frac{v_{bn}}{3} + \frac{v_{cn}}{3} \quad (5.20)$$

Adding and subtracting  $v_{cn}$  to (5.19) and rearranging, eqn. 5.21 is obtained

$$v_{qs}^s = (2v_{ac} + v_{cb})/3 \quad (5.21)$$

Rearranging (5.20) directly yields eqn. 5.22

$$v_{ds}^s = v_{cb}/3 \quad (5.22)$$

By using (5.21) and (5.22) in place of (5.19) and (5.20), the neutral line was not required, and only two isolation amplifiers were needed. Furthermore, by performing the abc to  $D^s$ - $Q^s$  transformation in hardware, only two A/D channels were needed. Low pass filters were used both at the power and signal sides, to attenuate the PWM related harmonics, as well as to prevent aliasing in the sampling process.

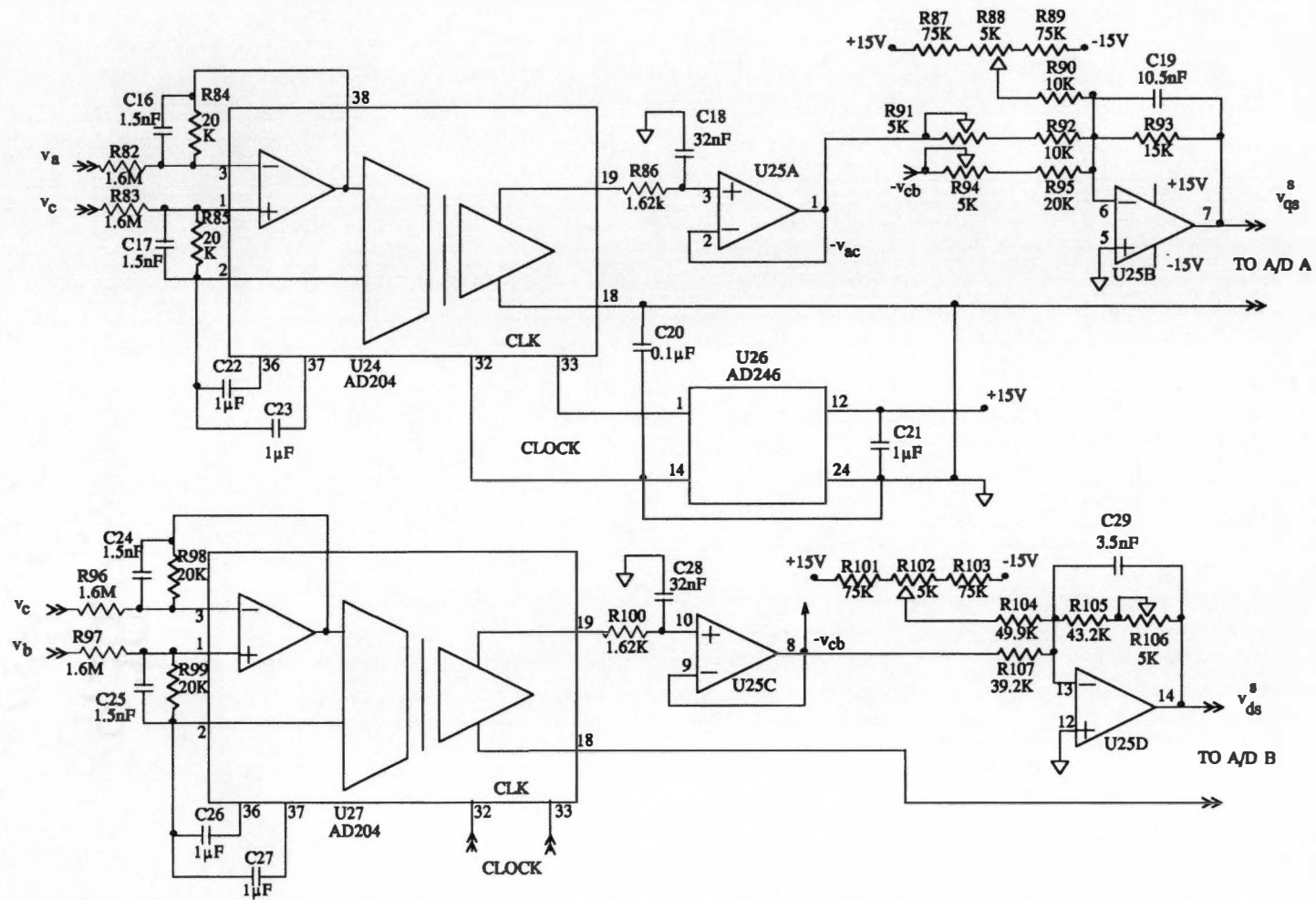


Fig. 5.11 Voltage sensing interface.

The sensing of machine current was not required, since the intrinsic operation of the HBPWM ensures that the actual currents closely track the command values. Therefore, the command currents were used also in the computation of actual  $v_{ds}$  and Q quantities.

## 5.5 Real Time Software Design Issues

The structure of the real time software related to the slip gain tuning is shown in Fig. 5.12. As the vector control routines are the same as those for the efficiency optimization study, they are not shown in the figure.

Proper operation of the tuning controller requires accurate measurement of the machine fundamental voltage. This task is complicated by the variable switching frequency, intrinsic to hysteresis band PWM control operation. This fact led to a conservative design of the analog low pass filters, required by the limited sampling frequency of the DSP. For the particular experimental system used, a cut-off frequency of approximately 1 KHz was selected, that has a negligible impact on the amplitude of the fundamental component, but introduces some amount of phase lag. Without any correction, the phase lag would translate into incorrect values for the synchronous frame voltages, particularly for the  $v_{ds}$  signal, that usually has small amplitude. This in turn would cause improper operation of the tuning controller.

A simple steady-state compensation scheme was derived for this problem. For a first order analog low-pass filter of time constant  $\tau$ , the transfer function is given by

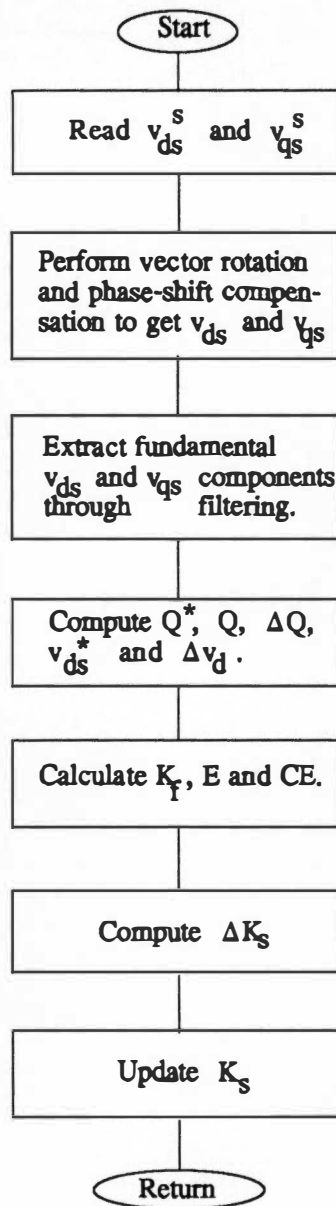


Fig. 5.12 Real time software flowchart.

$$G(s) = \frac{1}{1 + \tau s} \quad (5.23)$$

The phase shift  $\theta_{ps}$  introduced at frequency  $s=j\omega_e$  is determined by

$$\theta_{ps} = \tan^{-1}(\omega_e \tau) \quad (5.24)$$

For small  $\theta_{ps}$ ,  $\tan \theta_{ps} \approx \theta_{ps}$ , and therefore,  $\theta_{ps} \approx \omega_e \tau$ . For the case of higher order filters, the same principle can be applied, by computing the equivalent time constant  $\tau_{eq} (= \sum \tau_i)$ , as long as the overall phase shift remains small. The mechanism of phase shift compensation is illustrated on Fig. 5.13, where only the  $v_{qs}^s$  component of stator voltage is considered, for simplicity. As indicated, the measured  $\hat{v}_{qs}^s$  lags the correct value by  $\theta_{ps}$ . By subtracting the estimated  $\theta_{ps}$  from the original angle  $\theta_e$ , the  $q^e$ -axis is also shifted backwards, and correct phase relationship between  $\hat{v}_{qs}^s$  and  $q^e$ -axis is restored. The  $v_{ds}$  and  $v_{qs}$  equations then become

$$v_{ds} = v_{qs}^s \sin(\theta_e - \theta_{ps}) + v_{ds}^s \cos(\theta_e - \theta_{ps}) \quad (5.25)$$

$$v_{qs} = v_{qs}^s \cos(\theta_e - \theta_{ps}) - v_{ds}^s \sin(\theta_e - \theta_{ps}) \quad (5.26)$$

The parameter variation problem in the reference models given in (5.15) and (5.16) is important, since incorrect reference models would try to establish wrong slip gain  $\hat{K}_s$ . The parameter  $L_s$  is susceptible to magnetic saturation, as mentioned before. Even at constant flux command ( $i_{ds}^* = i_{dsr}$ ), use of incorrect slip gain would result in overfluxing



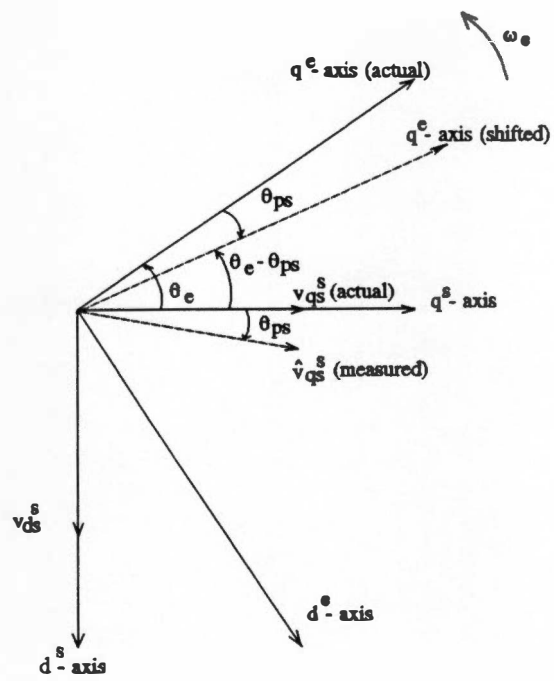


Fig. 5.13 Phase-shift compensation phasor diagram.

(for  $\hat{K}_s < K_{s0}$ ) or underfluxing (for  $\hat{K}_s > K_{s0}$ ), causing variation on  $L_s$ . However, as long as the tuning algorithm possess sufficiently high sensitivity to detuning (as in the proposed method), the error polarity for a large detuning will be coherent, and the controller will drive the estimate  $\hat{K}_s$  towards  $K_{s0}$ , and consequently, force machine flux towards its correct value. This translates into a self correcting effect for  $L_s$ , i.e., it will automatically approach its rated value, used in the reference model. It was verified during initial experimentation that the inductance  $L_\sigma$  exhibited significant variation with load torque. To enhance the performance of the controller, this saturation effect was modeled by a quadratic function of the stator current command  $I_s^*$ , obtained by least square estimation of the measured saturation profile, as shown in Fig. 5.14. The stator resistance  $R_s$  essentially varies linearly with stator temperature, and can be corrected by measurement or estimation of stator temperature. However, no compensation has been provided for this parameter.

## 5.6 Experimental Study

Experimental performance of the fuzzy tuning controller was thoroughly investigated at various torques and speeds. Prior to the actual tests, the correct slip gain value  $K_{s0}$  was determined by off-line tests. The controller performance was primarily evaluated by intentionally initializing the slip gain estimate ( $\hat{K}_s$ ) to an incorrect value, activating the tuning controller, and then observing the time domain  $\hat{K}_s$  and Error (E) responses. Fig. 5.15 shows the normalized slip gain ( $\hat{K}_s/K_{s0}$ ) and error (E) responses for  $T_L = 0.1$  pu, when  $\hat{K}_s$  is initialized to twice the correct value  $K_{s0}$ , and the tuning algorithm

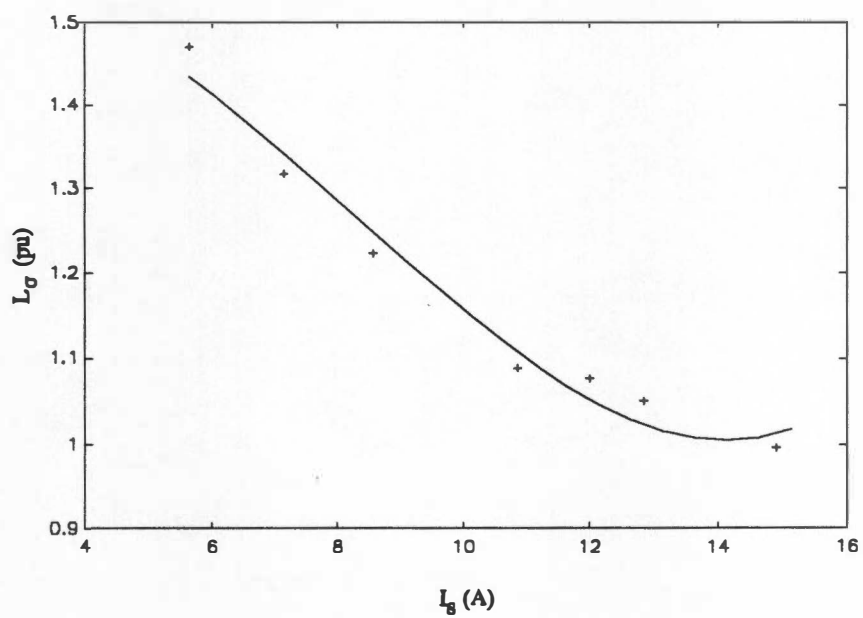


Fig. 5.14 Saturation profile for  $L_\sigma$ .

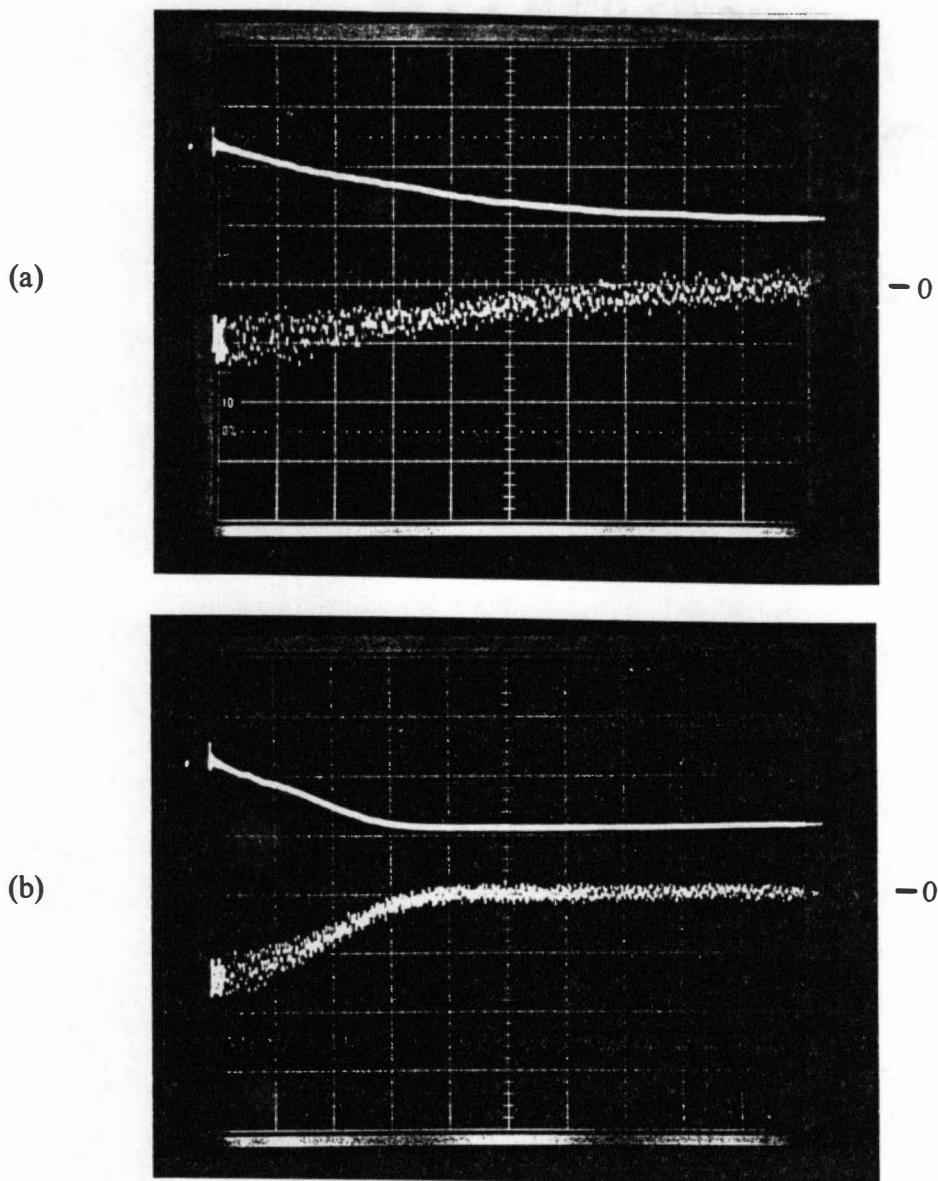


Fig. 5.15 Experimental tuning performance at  $T_L=0.1$  pu and  $K_s/K_{s0}(0)=2$ .

(a)  $\omega_r=0.25$  pu. (b)  $\omega_r=0.50$  pu.

Top trace:  $K_s/K_{s0}$ , 0.84 /div.

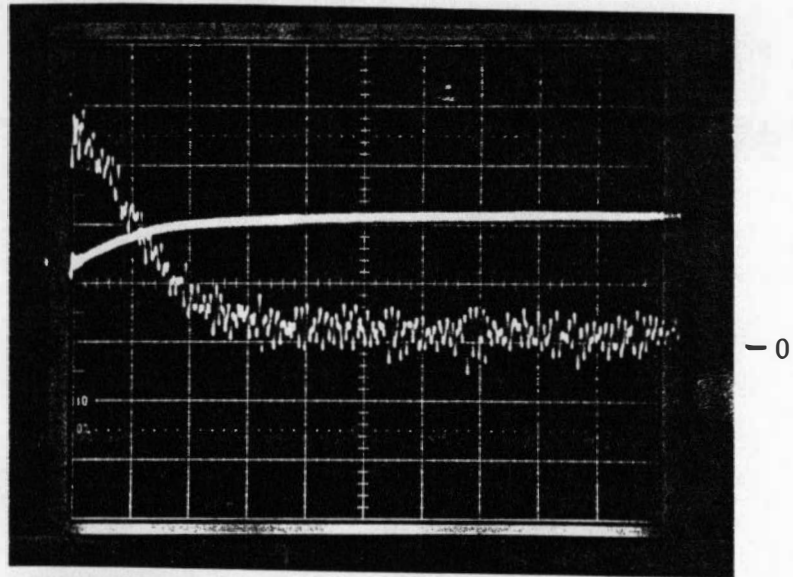
Bottom trace: Error, 0.2 /div.

Time: 1 sec./div.

is enabled at  $t=0$ . In Fig. 5.15(a),  $\omega_r = 0.25$  pu, whereas in Fig. 5.15(b)  $\omega_r = 0.5$  pu. Fig. 5.16 shows similar responses for  $T_L = 0.5$  pu, when  $\hat{K}_s$  is initialized to half  $K_{s0}$ , and converges to a steady-state value in about 2 sec., with an steady-state error smaller than 9.4% in both cases. Further investigation of proper tuning is shown by the no load speed response to a square wave torque command, present in Fig. 5.17. The waveform of Fig. 5.17(a) reflects a tuned condition ( $\hat{K}_s = \hat{K}_{s0}$ ), and it differs slightly from the ideal triangular shape, due to the dragging effect of bearing friction and windage. Fig. 5.17(b) shows similar response to a detuned condition ( $\hat{K}_s = 0.5\hat{K}_{s0}$ ), where the higher order torque dynamics results in speed response degradation, manifested by waveform distortion and amplitude reduction.

In conclusion, a fuzzy logic based tuning method was proposed, that combines the features of MRAC reactive power and d-axis voltage formulations. Fuzzy logic is initially used to determine the dominant method for a given speed and load torque, to ensure a high sensitivity to detuning for the entire torque-speed plane. Next, a second fuzzy controller was used to derive the correcting term  $\Delta K_s$  from the combined error and error change, that results in a fast convergence under various operating conditions. Both simulation and experimental studies were carried out, demonstrating the effectiveness of the method. The algorithm was able to converge to a good estimate of  $K_s$ , with only a small dependency on load torque. However, as the performance of indirect vector control drive systems is insensitive to small slip gain errors [55], this torque dependency does not constitute a practical problem for the application of the proposed technique to actual drive systems.

(a)



(b)

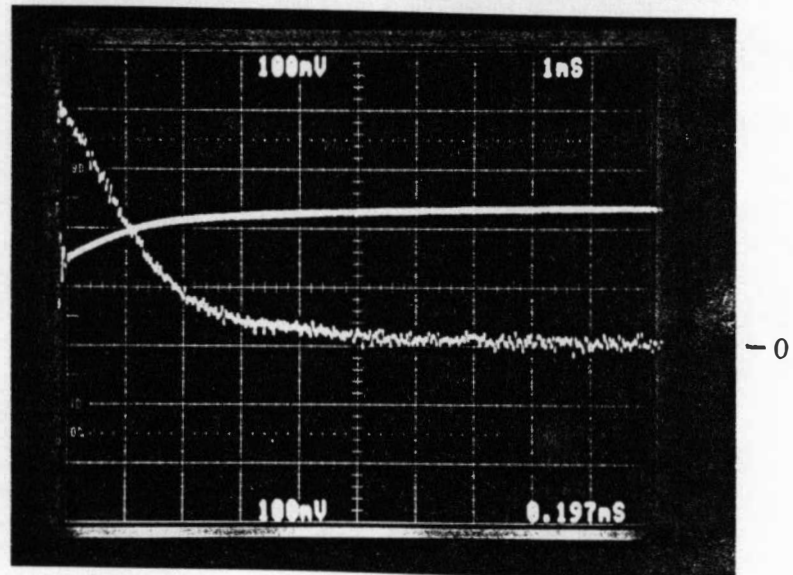


Fig. 5.16 Experimental tuning performance at  $T_L = 0.5$  pu and  $K_s/K_{s0}(0) = 0.5$ .

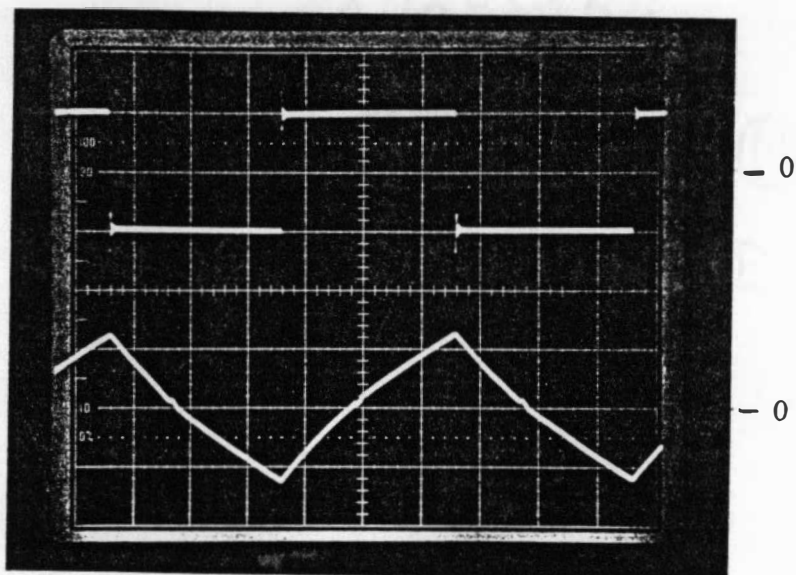
(a)  $\omega_r = 0.25$  pu. (b)  $\omega_r = 0.50$  pu.

Top trace:  $K_s/K_{s0}$ , 0.42 /div.

Bottom trace: Error, 0.1 /div.

Time: 0.5 sec./div.

(a)



(b)

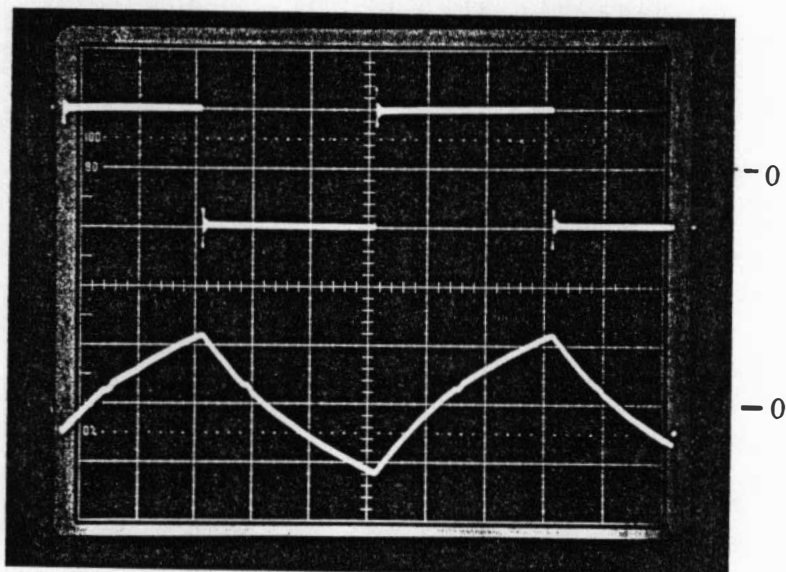


Fig. 5.17 Speed response at no load for a square-wave torque command ( $i_{qs}^*$ ).

(a)  $K_s/K_{s0}=1.0$ .

(b)  $K_s/K_{s0}=0.5$ .

Top trace:  $i_{qs}^*$ , 5 A/div.

Bottom trace:  $\omega_r$ , 286 rpm/div.

Time: 100 msec/div.

## **CHAPTER 6**

### **CONCLUSIONS AND RECOMMENDATIONS FOR FUTURE RESEARCH**

The systematic application of fuzzy logic in the control of both DC and AC drives has been discussed in this dissertation. Several control problems have been addressed, using a methodology that typically involved an initial system analysis, followed by control design and validation through digital simulation. Experimental studies were also conducted in most cases, with results that confirm the feasibility of the proposed schemes.

Fuzzy logic control was initially applied to a phase-controlled converter DC drive system that uses a separately excited DC machine. The contributions for this control system are summarized below:

- . Study of converter transfer characteristics at continuous and discontinuous conduction modes;
- . Development of a fuzzy logic compensation algorithm for the converter system, capable of linearizing converter transfer characteristics during discontinuous conduction mode;
- . Design of fuzzy logic controllers for current and speed loops;
- . Development of a methodology for simulation of fuzzy controllers in PC-



- SIMNON, used in the simulation of fuzzy controllers for both DC and AC drives;
- . SIMNON programs design for phase- controlled converter and DC machine;
- . Comparative simulation study of fuzzy controlled DC drives and those with conventional PI controls.

The application of fuzzy  $\Delta\alpha$  compensation significantly improves the speed of current loop response, particularly when combined with fuzzy current control. Use of fuzzy speed and current controllers in place of conventional PI controllers resulted in a more robust system.

The remaining research effort was devoted to indirect vector controlled induction motor drives. The on-line efficiency optimization via flux control was first considered. In order to validate the control strategy and predict the system performance, a detailed loss model of the converter induction machine system was derived.

The achievements on this subject were:

- . Analysis and modeling of induction machine copper losses, core losses and stray losses, under PWM inverter supply;
- . Inclusion of skin effect on rotor resistance, temperature effects on winding resistances and modeling of saturation for magnetizing inductance;
- . Development of a novel synchronous frame  $D^e$ - $Q^e$  lossy equivalent circuit for the induction machine, capable of representing both the loss phenomenon and its dynamic behavior;
- . Modeling of conduction and switching losses for a converter system, consisting of diode bridge rectifier and PWM transistor inverter;

- . Implementation and testing of machine and converter models in PC-SIMNON, for a 10 hp drive system.

A consistent performance was observed both at steady-state and dynamic conditions. Actual accuracy of lossy models is dependent on the precision with which the machine and converter parameters can be obtained. Currently, one disadvantage of the lossy models is the long simulation time, when using PC-SIMNON. This is especially true when a long term trend is important, such as efficiency optimization studies. Of course, this problem can be minimized by using more powerful computers.

The efficiency optimization study resulted in the following developments:

- . Design of a fuzzy logic controller that adaptively adjusts the magnetizing current on the basis of measured DC link power, until the optimum efficiency is achieved;
- . Introduction of a feedforward torque compensator to suppress the low frequency pulsating torque, due to changes in flux;
- . Development of a criterion for transition between efficiency optimization and transient optimization modes;
- . Comprehensive simulation study of a 5 hp drive system with proposed efficiency and torque compensation controls;
- . Construction of hysteresis band current controller, protection and monitoring circuits, DC link voltage and current sensing interfaces;
- . Design and testing of a speed sensing interface for the TMS320C25 DSP;
- . Development of assembly language software for the vector control system;
- . Design of assembly language programs for efficiency optimization, torque

compensation and transition controls;

- . Experimental evaluation of steady-state and transient performances of proposed control schemes.

The experimental performance correlates well with that predicted by simulation.

The efficiency gains are somewhat smaller than expected, because some practical aspects are difficult to model. For example, actual induction machines have some phase unbalance, that creates torque fluctuations and adversely impacts machine efficiency. Irrespective of these problems, the proposed controller ensures true optimum efficiency operation. The method can be incorporated into an existing vector drive system, with a minimum of extra hardware. In most cases, the added software can be easily implemented by the existing processor, resulting in a very cost effective efficiency optimized drive.

The proposed fuzzy efficiency controller is applicable to a number of practical drive systems. In fact, it is currently being considered for an electrical vehicle drive, as part of a technology transfer project to Delco-Remy company.

Finally, fuzzy logic application to the slip gain tuning of an indirect vector-controlled induction motor drive was considered. The salient contributions of the study are:

- . An initial fuzzy controller was designed, that combines two MRAC models, D-axis voltage and reactive power, to generate the error signal. This ensures good control sensitivity in the entire torque-speed plane;
- . A second fuzzy controller was designed to tune the slip gain based on combined error signal and its slope, resulting in fast convergence at any load condition;

- . Simulation programs were developed for the fuzzy tuning controllers and vector control drive, followed by a comprehensive simulation study;
- . A hardware voltage interface for  $v_{ds}^s$  and  $v_{qs}^s$  sensing was designed and built;
- . Assembly language programs were developed for the fuzzy tuning controllers, and experimental validation carried out, for a 5 hp drive system.

The test results correlate well with the theory and simulation performance. All the tuning controls were executed by the same TMS320C25 DSP, used for the basic vector control function. Therefore, the extra cost involved in the fuzzy slip gain tuning controller implementation is reasonably low.

Further research topics to extend the current work would comprehend:

- . Use of adjustable DC link voltage topologies to minimize machine harmonic losses;
- . Extend the fuzzy tuning control to flux weakening region, along with proper saturation modeling of machine inductances;
- . Integration of slip gain tuning technique to efficiency optimization control, to ensure proper pulsating torque compensation as well as fast torque response;
- . Investigate the potential use of neural networks to the implementation of fuzzy controllers as well as for better representation of saturation effects.

The fuzzy logic control of drive systems has the potential of enhancing system performance, as well as to reduce sensitivity to disturbances and parameter variation effects. Of course, other control techniques such as Model-Reference Adaptive Control (MRAC), variable structure control (VSC) can also be applied to get robust system

performance. Fuzzy control, however, has the advantages of not requiring a mathematical model of the plant and delivering a chatter free system response.

When compared to other AI techniques, fuzzy control shares some common features with both expert systems and neural networks. While expert systems are ideal for structured knowledge representation and symbolic processing, they possess poor numerical capabilities and are not adequate for real time control of fast power electronic systems. On the other side, neural networks are very efficient in processing unstructured knowledge. Typically, a neural network can be trained to implement a desired mapping, such as a non-linear controller, provided that an extensive numerical input/output data is available to train the network. Although the automated training makes it simpler to tune than a heuristic based fuzzy controller, the training process is not always convergent, and in many cases not very precise. Furthermore, neural networks lack the ability to incorporate qualitative knowledge.

Recently, fuzzy neural networks have been considered. Essentially, neural network techniques are applied in the implementation of parts of a fuzzy controller, such as in the representation of more elaborate membership functions. It can be viewed as an attempt to combine the strengths of both technologies, such as the qualitative knowledge representation of fuzzy logic, with the numerical capabilities of neural networks.

In conclusion, it is expected that, as the research on fuzzy control and other emerging technologies evolves, a formal methodology for fuzzy logic control design and analysis will be developed, along with new CAD tools. Then, the full benefit of this new technology will be realized.

## REFERENCES

## REFERENCES

- [1] L. A. Zadeh, "Fuzzy sets", *Information and Control*, Vol. 8, pp. 338-353, 1965.
- [2] L. A. Zadeh, "Outline of a new approach to the analysis of systems and decision processes", *IEEE Trans. Systems, Man and Cybernetics*, Vol. SMC-3-1, pp. 28-44, 1973.
- [3] E. H. Mamdani and Assillian, "An experiment in linguistic synthesis with a fuzzy logic controller", *Int'l. Journal Man-Machine Studies*, Vol. 7, pp. 1-13, 1975.
- [4] R. M. Tong, "A control engineering review of fuzzy systems", *Automatica*, Vol. 13, pp. 559-569, 1977.
- [5] Y. F. Li and C. C. Lau, "Development of fuzzy algorithms for servo systems", *IEEE Control System Magazine*, Vol. 9, no. 3, pp. 65-72, 1989.
- [6] L. E. B. da Silva, G. E. April and G. Oliver, "Real time fuzzy adaptive controller for an asymmetrical four quadrant power converter", *Conf. Rec. IEEE IAS Annual Meeting*, pp. 872-878, 1987.
- [7] R. M. Tong, "An annotated bibliography of fuzzy control", in *Industrial Applications of Fuzzy Control*, M. Sugeno (Ed.), North-Holland, pp. 249-269, 1985.
- [8] K. L. Tong and R. J. Mulholland, "Comparing fuzzy logic with classical controller designs", *IEEE Trans. Systems Man and Cybernetics*, Vol. SMC-17, no. 6, pp. 1085-1087, Nov./Dec. 1987.
- [9] J. A. Bernard, "Use of a rule-based system for process control", *IEEE Control System Magazine*, Vol. 8, no. 5, pp. 3-12, Oct. 1988.
- [10] J. C. Bezdek, "Editorial: Fuzzy models - what are they, and why?", *IEEE Trans. on Fuzzy Systems*, Vol. 1, No. 1, pp. 1-6, Feb., 1993.
- [11] C. C. Lee, "Fuzzy logic in control systems: fuzzy logic controller, Part I", *IEEE Trans. on Systems Man and Cybernetics*, Vol. 20, pp. Mar./April 1990.
- [12] C. C. Lee, "Fuzzy logic in control systems: fuzzy logic controller, Part II", *IEEE*

Trans. Systems Man and Cybernetics, Vol. 20, pp. Mar./April 1990.

- [13] M. Figueiredo, F. Gomide, A. Rocha, and R. Yager, "Comparison of Yager's level set method for fuzzy logic control with Mamdani's and Larsen's methods", IEEE Trans. on Fuzzy Systems, Vol. 1, No. 2, pp. 156-159, May, 1993.
- [14] **G. C. D. Sousa and B. K. Bose, "A fuzzy set theory based control of a phase controlled converter dc machine drive", IEEE IAS Annual Meeting Conf. Rec., pp. 854-861, 1991.**
- [15] T. Ohmae, T. Matsuda, N. Azusawa, K. Kamiyama and T. Konishi, "A microprocessor controlled fast response speed regulator with dual mode current loop for DCM drives", IEEE Trans. on Industry Applications, Vol. IA-16, pp. 388-394, May/June 1980.
- [16] J. S. Mapes and B. K. Bose, "Linearization of the transfer characteristics of a phase-controlled converter under discontinuous conduction", IEEE Trans. on Industry Applications, Vol. IA-14, pp. 559-564, 1978.
- [17] B. K. Bose, Power Electronics and AC Drives, Prentice Hall, 1986.
- [18] P. C. Sen, Thyristor DC Drives, John Wiley, 1981.
- [19] B. K. Bose, "Variable frequency drives - technology and applications", IEEE International Symp. on Industrial Electronics Conf. Rec., pp. 1-18, 1993.
- [20] Y. Dote and B. K. Bose, "Fuzzy CAD for variable structure PID controller", IEEE IECON Conf. Rec., pp. 705-708, 1989.
- [21] J. C. Read, "The calculation of rectifier and inverter performance characteristics", J. IEE, Vol. 92, pp. 495-509, Aug. 1945.
- [22] K. Hirota, "Fuzzy control and its industrial applications in Japan", IEEE IECON Conf. Rec., pp. 826-827, 1990.
- [23] Y. Dote, "Fuzzy and neural network controller", IEEE IECON Conf. Rec., pp. 1314-1343, 1990.
- [24] Togai Infralogic Application Note, April 1990.
- [25] V. B. Honsinger, "Induction motors operating from inverters", IEEE IAS Annual Meeting Conf. Rec., pp. 1276-1285, 1980.
- [26] B. J. Chalmers and B. R. Sarkar, "Induction motor losses due to nonsinusoidal



supply waveforms", Proc. IEEE vol. 115, pp.1777-1782, Dec. 1968.

- [27] M. R. Udayagiri and T. A. Lipo, "Simulation of inverter fed induction motors including core losses", IEEE IECON Conf. Rec., pp. 232-237, 1989.
- [28] D. W. Novotny, S.A. Nasar, B. Jeftenic and D. Maly, "Frequency dependency of time harmonic losses in induction machines", Int'l Conf. on Elec. Machines Conf. Rec., pp. 233-238, 1990.
- [29] F. G. de Buck, P. Gistelinck and D. de Backer, "A simple but reliable loss model for inverter supplied induction motors", IEEE Trans. Industry Applications, vol. 20, pp. 1190-1202, Jan./Feb. 1984.
- [30] E. A. Klingshirn and H. E. Jordan, "Polyphase induction motor performance and losses on nonsinusoidal voltage sources", IEEE Summer Power Meeting Conf. Rec., pp. 624-631, 1967.
- [31] K. Kawagishi, M. Udaka and M. Akamatsu, "Frequency dependency of induction motor parameters and their measuring method", Int'l. Power Electronics Conf. Rec., Tokyo, pp. 202-213, 1983.
- [32] W. McMurray, "Selection of snubbers and clamps to optimize the design of transistor switching converters", IEEE Trans. on Industry Applications, Vol. 16, pp. 513-523, July/Aug. 1980.
- [33] M. M. Jovanovic, F. C. Lee and D. Y. Chen, "Characterization of high power BJT's for motor drive applications", IEEE IAS Annual Meeting Conf. Rec., pp. 440-447, 1986.
- [34] Y. Ikeda, J. Itsumi and H. Funato, "The power loss of a PWM voltage-fed inverter", PESC Conf. Rec., pp. 277-283, 1988.
- [35] P. L. Alger, G. Angst and E. J. Davies, "Stray load losses in polyphase induction machines", AIEE Trans. on Power Apparatus and Systems, Vol. 78, pp. 349-357, 1959.
- [36] TableCurve 3.0 User's Manual, Jandel Scientific, CA, 1991.
- [37] B. W. Williams, Power Electronics, John Wiley, NY, 1987.
- [38] F. J. Nola, "Power factor control system for ac induction motor", US Patent 4,052,648, Oct. 4, 1977.
- [39] P. Famouri and J. J. Cathey, "Loss minimization control of an induction motor

- drive", IEEE Trans. on Industry Applications, Jan-Feb, 1991, Vol. 27, No. 1, pp. 32-37.
- [40] D. S. Kirschen, D. W. Novotny and T. A. Lipo, "On-line efficiency optimization of a variable frequency induction motor drive", 1984 IEEE IAS Annual Meeting Conf. Rec., pp. 488-492, 1984.
  - [41] D. S. Kirschen, D. W. Novotny, and T. A. Lipo, "Optimal efficiency control of an induction motor drive", IEEE Trans. on Energy Conversion, Vol. EC-2, No. 1, March 1987, pp. 70-76.
  - [42] **G. C. D. Sousa, B. K. Bose, J. G. Cleland, R. J. Spiegel and P. J. Chappell, "Loss modeling of converter induction machine system for variable speed drive", IEEE IECON Conf. Rec., pp. 114-120, 1992.**
  - [43] B. K. Bose, "Microcomputer-based efficiency optimization control for an induction motor drive system", U.S. Patent No. 4,450,398, May 22, 1984.
  - [44] J. Cleland, W. Turner, P. Wang, T. Espy, J. Chappell, R. Spiegel and B. K. Bose, "Fuzzy logic control of ac induction motors", IEEE Int'l. Conf. Rec. on Fuzzy Systems (FUZZ-IEEE), pp. 843-850, March 1992.
  - [45] L. J. Garces, "Parameter adaption for the speed controlled static ac drive with squirrel cage induction motor", IEEE Trans. on Industry Applications, Vol. 16, pp. 173-178, Mar./Apr. 1980.
  - [46] R. Gabriel and W. Leonhard, "Microprocessor control of induction motor", IEEE Int'l. Seminar on Power Converter Conf. Rec., 1982, pp. 385-395.
  - [47] J. C. Moreira, K. T. Hung, T. A. Lipo and R. D. Lorenz, "A simple and robust adaptive controller for detuning correction in field oriented induction machines", IEEE Trans. on Industry Applications, Vol. 28, pp. 1359-1366, Nov./Dec. 1992.
  - [48] R. D. Lorenz and D. B. Lawson, "A simplified approach to continuous on-line tuning of field oriented induction machine drives", IEEE IAS Annual Meeting Conf. Rec., pp. 444-449, 1988..
  - [49] T. M. Rowan, R. J. Kerkman and D. Leggate, "A simple on-line adaptation for indirect field orientation of an induction machine", IEEE IAS Annual Meeting Conf. Rec., pp. 579-587, 1989.
  - [50] L. C. Zai and T. A. Lipo, "An extended Kalman filter approach to rotor time constant measurement in PWM induction motor drives", IEEE Trans. Industry Applications, Vol. 28, pp. 96-104, Jan./Feb. 1992.

- [51] C. Wang, D. W. Novotny and T. A. Lipo, "An automated rotor time constant measurement system for indirect field oriented drives", IEEE Trans. on Industry Applications, Vol. 24, pp. 151-159, Jan./Feb. 1988.
- [52] T. Matsuo and T. A. Lipo, "A rotor parameter identification scheme for vector controlled induction motor drives", IEEE Trans. on Industry Applications, Vol. 21, pp. 624-632, May/June 1985.
- [53] H. Sugimoto and S. Tamai, "Secondary resistance identification of an induction motor model reference adaptive system and its characteristics", IEEE Trans. on Industry Applications, Vol. 23, pp. 296-303, Mar./Apr. 1987.
- [54] K. T. Hung and R. D. Lorenz, "A rotor flux error based adaptive tuning approach for feedforward field oriented induction machine drives", IEEE IAS Annual Meeting Conf. Rec., 1990, pp. 589-594.
- [55] K. B. Nordin, D. W. Novotny and D. S. Zinger, "The influence of motor parameter deviations in feedforward field orientation drive systems", IEEE Trans. on Industry Applications, Vol. 21, pp. 1009-1015, July/Aug. 1985.
- [56] J. C. Moreira and T. A. Lipo, "A new method for rotor time constant tuning in indirect field oriented control", IEEE PESC Conf. Rec., pp. 1990.
- [57] Ariel, Operating Manual for the DSP-16 Data Acquisition Processor, Ariel Corp., August 1987.
- [58] Texas Instrument, TMS320C2x User's Guide, Texas Instruments Inc., 1990.
- [59] H. Bausch, B. Lange and D. Sahn, "Experimental investigation of losses in a PWM - inverter/induction machine drive system", Proc. of the International Conf. on Electrical Machines, pp. 195-201, 1990.
- [60] A. Kusko and D. Galler, "Control means for minimization of losses in ac and dc motor drives.", IEEE Trans. on Industry Applications, Vol. IA-19, pp. 651-570, Jul. Aug. 1983.
- [61] Y. Jani, G. C. D. Sousa, W. Turner, R. J. Spiegel and P. J. Chappell, "Fuzzy efficiency optimization of ac induction motors", Proc. of the 3rd Fuzzy Logic Control Symposium, Houston, June 1-3, 1992.
- [62] G. C. D. Sousa, B. K. Bose, J. G. Cleland, R. J. Spiegel and P. J. Chappel, "Fuzzy logic based on-line efficiency optimization control of an indirect vector controlled induction motor drive.", To be presented at the 1993 International Conference on Industrial Electronics, Control, Instrumentation and Automation

**(IECON' 93).**

- [63] G. C. D. Sousa, B. K. Bose and Kyung S. Kim, "Fuzzy logic based on-line MRAC tuning of slip gain for an indirect vector-controlled induction motor drive.", To be presented at the 1993 International Conference on Industrial Electronics, Control, Instrumentation and Automation (IECON' 93).**

## **APPENDICES**

## APPENDIX A

### SIMNON SIMULATION PROGRAMS LISTING

#### A.1 DC Drive Programs

```

" -----
"                               DC MOTOR
" -----
CONTINUOUS SYSTEM DCM

INPUT Vt
OUTPUT W1 Ea X IaI IAPU
TIME T
STATE W Ia IIa
DER DW DIa DIIa

" ----- Define state variables.
DW=(-B/J)*W+(Te-TL)/J      "Speed.
DIa=(-Ra/La)*Ia+(Vt-Ea)/La "Armature current.
DIIa=Ia                    "Integral of Ia, for average computation.
Te=Kt*Ia                   "Eletromagnetic torque.
TL=KL*W*W                  "Load torque.
Ea=KI*W                    "Counter emf.
Eapu=Ea/Vm

"----- Auxiliary variables for OUTPUT.
W1=W                      "Used in FCC.
X=IIa                     "Used in RCFR.
IaI=Ia
Iapu=Ia/53.73

"----- Parameters.
Kt:0.55                   "Torque constant.
KI:0.55                   "Flux constant.
La:0.008                  "Armature inductance.
Ra:0.6                    "Armature resistance.
J:0.0465                  "Inertia.
B:0.004                   "Viscous damping.
Vm:169.7                  "Base value.
KL:2.78E-04              "Load constant.
END

" -----
"                               FUZZY DELTA ALPHA COMPENSATION
" -----
DISCRETE SYSTEM ACOMP
STATE A D                 "A, D Store the previous values of alpha
NEW NA ND                 " and delta alpha , respectively.
INPUT ALPHA Ia Iar

```

OUTPUT ALP1 ALP2 IDN

"Final values of alpha.

TIME T

TSAMP Z

Z = T + DT

ALFA=(ALPHA\*180)/3.1416

"Alpha in degrees.

IDN=IF Ia>0 THEN Ia/Tbase ELSE 0

"PU current.

J=INT((ALFA+10)/20)

"Interval indices.

I=INT((IDN+0.01)/0.01)

" ----- Get degrees of membership and perform rule base evaluation.

MA1=(20\*J+10-ALFA)/20

MID1=(0.01\*I-IDN)/0.01

MRA=MIN(MID1,MA1)

MRB=MIN(MID1,(1-MA1))

MRC=MIN((1-MID1),MA1)

MRD=MIN((1-MID1),(1-MA1))

" ----- Compute value of delta alpha.

IJ=I+J

"Retrieve contribution of first rule.

DAA=IF I<2 THEN C1 ELSE IF I<3 THEN C2 ELSE IF I<4 THEN C3 ELSE T1

T1=IF I<5 THEN C4 ELSE IF I<6 THEN C5 ELSE IF I<7 THEN C6 ELSE T2

T2=IF I<8 THEN C7 ELSE IF I<9 THEN C8 ELSE IF I<10 THEN C9 ELSE 0

"

C1=IF J<3 THEN 30 ELSE IF J<5 THEN 27 ELSE 25

C2=IF J<2 THEN 5 ELSE IF J<3 THEN 16 ELSE 17

C3=IF J<2 THEN 0 ELSE IF J<3 THEN 10 ELSE 12

C4=IF J<2 THEN 0 ELSE IF J<3 THEN 6 ELSE 9

C5=IF J<2 THEN 0 ELSE IF J<3 THEN 2 ELSE 7

C6=IF J<3 THEN 0 ELSE IF J<4 THEN 4 ELSE 6

C7=IF J<3 THEN 0 ELSE IF J<4 THEN 2 ELSE 4

C8=IF J<4 THEN 0 ELSE 2

C9=IF J<4 THEN 0 ELSE 1

"

L=J+1

"Retrieve contribution of second rule.

DAB=IF I<2 THEN D1 ELSE IF I<3 THEN D2 ELSE IF I<4 THEN D3 ELSE T6

T6=IF I<5 THEN D4 ELSE IF I<6 THEN D5 ELSE IF I<7 THEN D6 ELSE T7

T7=IF I<8 THEN D7 ELSE IF I<9 THEN D8 ELSE IF I<10 THEN D9 ELSE 0

"

D1=IF L<3 THEN 30 ELSE IF L<5 THEN 27 ELSE 25

D2=IF L<3 THEN 16 ELSE 17

D3=IF L<3 THEN 10 ELSE 12

D4=IF L<3 THEN 6 ELSE 9

D5=IF L<3 THEN 2 ELSE 7

D6=IF L<3 THEN 0 ELSE IF L<4 THEN 4 ELSE 6

D7=IF L<3 THEN 0 ELSE IF L<4 THEN 2 ELSE 4

D8=IF L<4 THEN 0 ELSE 2

D9=IF L<4 THEN 0 ELSE 1

"

M=I+1

"Retrieve contribution of third rule.

DAC=IF M<3 THEN C2 ELSE IF M<4 THEN C3 ELSE IF M<5 THEN C4 ELSE T9

T9=IF M<6 THEN C5 ELSE IF M<7 THEN C6 ELSE IF M<8 THEN C7 ELSE T10

T10=IF M<9 THEN C8 ELSE IF M<10 THEN C9 ELSE 0

DAD=IF M<3 THEN D2 ELSE IF M<4 THEN D3 ELSE T11

T11=IF M<5 THEN D4 ELSE IF M<6 THEN D5 ELSE T12

T12=IF M<7 THEN D6 ELSE IF M<8 THEN D7 ELSE T13

T13=IF M<9 THEN D8 ELSE IF M<10 THEN D9 ELSE 0

" ----- Test of overflow and underflow.

OV=IF J>9 THEN 0 ELSE IF I>9 THEN 0 ELSE 1

UF=IF IJ<2 THEN 0 ELSE 1

```

COND=OV*UF*FLAG
SUM=MRA+MRB+MRC+MRD
PROD=DAA*MRA+DAB*MRB+DAC*MRC+DAD*MRD

"----- Define final value of alpha depending on sign of E=IAR-IA
ND=DALFA
DK=PROD/SUM
E=Iar-Ia "Current loop error.
DALFA=IF COND<1 THEN 0 ELSE IF E>0 THEN CO1 ELSE CO2
CO1=IF DK<D THEN DK ELSE D
CO2=IF DK>D THEN DK ELSE D
ALP1=IF T>0.0028 THEN AU ELSE ALPHA
AU=ALPHA+(DALFA*3.1416)/180 "Alpha in rad.
NA=ALP1
ALP2=A

" ----- Parameters.
DT:2.778E-03 "Sampling interval.
Ibase:53.73 "Base armature current.
FLAG:1 "FLAG=1: compensation on; =0 compensation off.
A:1.5708 "Initial condition for ALP2.
END

" -----
" FUZZY SPEED CONTROLLER
" -----
DISCRETE SYSTEM FSC2

"NOTE: SEVEN FUZZY SETS ARE USED FOR STATE VARIABLES E AND CE,
" WHILE ELEVEN ARE USED FOR DU.
INPUT W
OUTPUT Iar
STATE X U
NEW NX NU
TIME T
TSAMP TS
TS=T+AT
"
" ----- Compute error FE, change in error FCE.
FE=0.10472*WR-W
FCE=FE-X
NX=FE " X = E(k-1)
E=FE/GEs "Get the PU values E and CE.
C=FCE/GCs

" ----- Compute preliminary values of degree of membership.
A1=MIN(1,(E-Es1)/(1-Es1))
A2=(E-Es2)/(Es1-Es2)
A3=E/Es2
A5=-E/Es2
A6=(-E-Es2)/(Es1-Es2)
A7=(-E-Es1)/(1-Es1)
"
B1=MIN(1,(C-Cs1)/(1-Cs1))
B2=(C-Cs2)/(Cs1-Cs2)
B3=C/Cs2
B5=-C/Cs2
B6=(-C-Cs2)/(Cs1-Cs2)
B7=(-C-Cs1)/(1-Cs1)

```



```

"----- Get interval indices J and I, for E and CE, respectively.
J=IF E<-ES1 THEN 1 ELSE IF E<-ES2 THEN 2 ELSE IF E<0 THEN 3 ELSE T1
T1=IF E<ES2 THEN 4 ELSE IF E<ES1 THEN 5 ELSE 6
I=IF C<-CS1 THEN 1 ELSE IF C<-CS2 THEN 2 ELSE IF C<0 THEN 3 ELSE T2
T2=IF C<CS2 THEN 4 ELSE IF C<CS1 THEN 5 ELSE 6

"----- Compute degree of membership for relevant fuzzy sets.
ME1=IF J<2 THEN MIN(1,A7) ELSE IF J<3 THEN A6 ELSE T3
T3= IF J<4 THEN A5 ELSE IF J<5 THEN 1-A3 ELSE IF J<6 THEN 1-A2 ELSE MIN(1,1-A1)
ME2=1-ME1
MC1=IF I<2 THEN MIN(1,B7) ELSE IF I<3 THEN B6 ELSE IF I<4 THEN B5 ELSE T4
T4=IF I<5 THEN 1-B3 ELSE IF I<6 THEN 1-B2 ELSE MIN(1,1-B1)
MC2=1-MC1

"----- Perform rule base evaluation.
MRA=MIN(ME1,MC1)
MRB=MIN(ME2,MC1)
MRC=MIN(ME1,MC2)
MRD=MIN(ME2,MC2)

"----- Retrieve the control signal for each fired rule.
"----- First rule.
D11=IF J<2 THEN C1 ELSE IF J<3 THEN C2 ELSE IF J<4 THEN C3 ELSE T5
T5=IF J<5 THEN C4 ELSE IF J<6 THEN C5 ELSE C6
L=J+1 "Point to second rule.
D12=IF L<3 THEN C2 ELSE IF L<4 THEN C3 ELSE IF L<5 THEN C4 ELSE T6
T6=IF L<6 THEN C5 ELSE IF L<7 THEN C6 ELSE C7

"----- Ci is the i-th column of the rule base.
C1=IF I<2 THEN -1 ELSE IF I<5 THEN -U1 ELSE IF I<6 THEN -U2 ELSE -U3
C2=IF I<2 THEN -1 ELSE IF I<3 THEN -U1 ELSE IF I<5 THEN -U2 ELSE T6A
T6A=IF I<6 THEN -U3 ELSE 0
C3=IF I<2 THEN -U1 ELSE IF I<3 THEN -U2 ELSE IF I<5 THEN -U3 ELSE T7
T7=IF I<6 THEN 0 ELSE U3
C4=IF I<2 THEN -U1 ELSE IF I<3 THEN -U2 ELSE IF I<4 THEN -U3 ELSE T8
T8=IF I<5 THEN 0 ELSE IF I<6 THEN U3 ELSE U2
C5=IF I<2 THEN -U2 ELSE IF I<3 THEN -U3 ELSE IF I<4 THEN 0 ELSE T9
T9=IF I<6 THEN U3 ELSE U2
C6=IF I<2 THEN -U3 ELSE IF I<3 THEN 0 ELSE IF I<4 THEN U3 ELSE U2
C7=IF I<2 THEN 0 ELSE IF I<3 THEN U3 ELSE IF I<4 THEN U2 ELSE U1
"
M=I+1 "Access third and fourth rules.
D21=IF J<2 THEN V1 ELSE IF J<3 THEN V2 ELSE IF J<4 THEN V3 ELSE T10
T10=IF J<5 THEN V4 ELSE IF J<6 THEN V5 ELSE V6

D22=IF L<3 THEN V2 ELSE IF L<4 THEN V3 ELSE IF L<5 THEN V4 ELSE T11
T11=IF L<6 THEN V5 ELSE IF L<7 THEN V6 ELSE V7

"----- Vi also represent the i-th column of the rule base.
V1=IF M<5 THEN -U1 ELSE IF M<6 THEN -U2 ELSE IF M<7 THEN -U3 ELSE 0
V2=IF M<2 THEN -1 ELSE IF M<3 THEN -U1 ELSE T12
T12= IF M<5 THEN -U2 ELSE IF M<6 THEN -U3 ELSE T12B
T12B= IF M<7 THEN 0 ELSE U3
V3=IF M<3 THEN -U2 ELSE IF M<5 THEN -U3 ELSE IF M<6 THEN 0 ELSE T13
T13=IF M<7 THEN U3 ELSE U2
V4=IF M<3 THEN -U2 ELSE IF M<4 THEN -U3 ELSE IF M<5 THEN 0 ELSE T14
T14=IF M<6 THEN U3 ELSE IF M<7 THEN U2 ELSE U1
V5=IF M<3 THEN -U3 ELSE IF M<4 THEN 0 ELSE IF M<6 THEN U3 ELSE U2
V6=IF M<3 THEN 0 ELSE IF M<4 THEN U3 ELSE IF M<7 THEN U2 ELSE 1
V7=IF M<3 THEN U3 ELSE IF M<4 THEN U2 ELSE IF M<7 THEN U1 ELSE 1

"----- Defuzzification using height method.

```

```
SUM=MRA+MRB+MRC+MRD
PROD=D11*MRA+D12*MRB+D21*MRC+D22*MRD
DU=PROD/SUM
```

```
" ----- Compute the next control signal.
```

```
UK=U+DU*GUs
IAR=IF UK<UMIN THEN UMIN ELSE MIN(UK,UMAX)
NU=IAR
```

```
Wr=IF T<0.8 THEN WR1 ELSE WR2
WR1:1000
WR2:1000
```

```
" ----- Parameters for the fuzzy controller.
```

```
Cs1:0.5
Cs2:0.2
Es1:0.5
Es2:0.2
U1:0.5
U2:0.125
U3:0.05
U4:0.01
UMAX:25
Umin:0
GEs:20
GCs:0.9
GUs:12.5
AT:2.778E-03
END
```

```
" -----
"          FUZZY CURRENT CONTROLLER
" -----
```

```
DISCRETE SYSTEM FCC
```

```
INPUT Iar Ila Ea
OUTPUT ALPHA1 ALPHA2 Ia Vt
STATE X U I A
NEW NX NU NI NA
TIME T
TSAMP TS
TS=T+AT
```

```
NI=Ila
Ia=(Ila-I)/AT          "Compute average Ia.
```

```
" ----- Compute error (FE) and change in error (FCE).
```

```
FE=Iar-Ia
FCE=FE-X
NX=FE          "X = FE(k-1).
E=FE/GEc      "PU values.
C=FCE/GCc
```

```
" ----- Compute preliminary degrees of membership.
```

```
A1=MIN(1,(E-Ec1)/(1-Ec1))
A2=(E-Ec2)/(Ec1-Ec2)
A3=E/Ec2
A5=-E/Ec2
A6=(-E-Ec2)/(Ec1-Ec2)
A7=(-E-Ec1)/(1-Ec1)
```

```

"
B1=MIN(1,(C-Cc1)/(1-Cc1))
B2=(C-Cc2)/(Cc1-Cc2)
B3=C/Cc2
B5= -C/Cc2
B6=(-C-Cc2)/(Cc1-Cc2)
B7=(-C-Cc1)/(1-Cc1)

" -----Get interval indices J and H , for E and C, respectively.
J=IF E<-Ec1 THEN 1 ELSE IF E<-Ec2 THEN 2 ELSE IF E<0 THEN 3 ELSE T1
T1=IF E<Ec2 THEN 4 ELSE IF E<Ec1 THEN 5 ELSE 6
H=IF C<-Cc1 THEN 1 ELSE IF C<-Cc2 THEN 2 ELSE IF C<0 THEN 3 ELSE T2
T2=IF C<Cc2 THEN 4 ELSE IF C<Cc1 THEN 5 ELSE 6

" -----Compute degree of membership for relevant fuzzy sets.
ME1=IF J<2 THEN MIN(1,A7) ELSE IF J=2 THEN A6 ELSE T3
T3= IF J<4 THEN A5 ELSE IF J<5 THEN 1-A3 ELSE T3B
T3B=IF J<6 THEN 1-A2 ELSE MIN(1,1-A1)
ME2=1-ME1
MC1=IF H<2 THEN MIN(1,B7) ELSE IF H<3 THEN B6 ELSE T4
T4= IF H<4 THEN B5 ELSE IF H<5 THEN 1-B3 ELSE T4B
T4B= IF H<6 THEN 1-B2 ELSE MIN(1,1-B1)
MC2=1-MC1

" ----- Perform rule base evaluation.
MRA=MIN(ME1,MC1)
MRB=MIN(ME2,MC1)
MRC=MIN(ME1,MC2)
MRD=MIN(ME2,MC2)

" ----- Retrieve the control signal for each fired rule.
" ----- First rule: (J,H) =(E,C)
D11=IF J<2 THEN C1 ELSE IF J<3 THEN C2 ELSE IF J<4 THEN C3 ELSE T5
T5=IF J<5 THEN C4 ELSE IF J<6 THEN C5 ELSE C6
L=J+1 "Access second rule: (L,H)=(E,C)
D12=IF L<3 THEN C2 ELSE IF L<4 THEN C3 ELSE IF L<5 THEN C4 ELSE T6
T6=IF L<6 THEN C5 ELSE IF L<7 THEN C6 ELSE C7

" ----- Ci is the i-th column of rule base.
C1=IF H<2 THEN -U1 ELSE IF H<3 THEN -U1 ELSE IF H<6 THEN -U2 ELSE -U3
C2=IF H<2 THEN -U1 ELSE IF H<3 THEN -U1 ELSE IF H<5 THEN -U2 ELSE T6A
T6A=IF H<6 THEN -U3 ELSE 0
C3=IF H<2 THEN -U1 ELSE IF H<3 THEN -U2 ELSE IF H<5 THEN -U3 ELSE T7
T7=IF H<6 THEN 0 ELSE U3
C4=IF H<2 THEN -U1 ELSE IF H<3 THEN -U2 ELSE IF H<4 THEN -U3 ELSE T8
T8=IF H<5 THEN 0 ELSE IF H<6 THEN U3 ELSE U2
C5=IF H<2 THEN -U2 ELSE IF H<3 THEN -U3 ELSE IF H<4 THEN 0 ELSE T9
T9=IF H<6 THEN U3 ELSE U2
C6=IF H<2 THEN -U3 ELSE IF H<3 THEN 0 ELSE IF H<4 THEN U3 ELSE U2
C7=IF H<2 THEN 0 ELSE IF H<3 THEN U3 ELSE IF H<4 THEN U2 ELSE U1
"
M=H+1 "Access third and fourth rules
D21=IF J<2 THEN V1 ELSE IF J<3 THEN V2 ELSE IF J<4 THEN V3 ELSE T10
T10=IF J<5 THEN V4 ELSE IF J<6 THEN V5 ELSE V6
"
D22=IF L<3 THEN V2 ELSE IF L<4 THEN V3 ELSE IF L<5 THEN V4 ELSE T11
T11=IF L<6 THEN V5 ELSE IF L<7 THEN V6 ELSE V7

" ----- Vi also represents the i-th column of the rule base.
V1=IF M<5 THEN -U1 ELSE IF M<6 THEN -U2 ELSE IF M<7 THEN -U3 ELSE 0
V2=IF M<2 THEN -U1 ELSE IF M<3 THEN -U1 ELSE T12
T12=IF M<5 THEN -U2 ELSE IF M<6 THEN -U3 ELSE IF M<7 THEN 0 ELSE U3

```

```

V3=IF M<3 THEN -U2 ELSE IF M<5 THEN -U3 ELSE IF M<6 THEN 0 ELSE T13
T13=IF M<7 THEN U3 ELSE U2
V4=IF M<3 THEN -U2 ELSE IF M<4 THEN -U3 ELSE IF M<5 THEN 0 ELSE T14
T14=IF M<6 THEN U3 ELSE IF M<7 THEN U2 ELSE U1
V5=IF M<3 THEN -U3 ELSE IF M<4 THEN 0 ELSE IF M<6 THEN U3 ELSE U2
V6=IF M<3 THEN 0 ELSE IF M<4 THEN U3 ELSE IF M<7 THEN U2 ELSE 1
V7=IF M<3 THEN U3 ELSE IF M<4 THEN U2 ELSE IF M<7 THEN U1 ELSE 1

```

"----- Defuzzification using height method.

```

SUM=MRA+MRB+MRC+MRD
PROD=D11*MRA+D12*MRB+D21*MRC+D22*MRD
DU=PROD/SUM

```

"-----Compute the next control signal.

```

UK=DU*GUc+U
UKE=UK+Ea
Vt=IF UKE<Umin THEN Umin ELSE MIN(UKE,Umax)
NU=UK+Vt-UKE

```

"----- Calculate firing angle by cosine crossing method.

```

ALPHA1=ARCCOS(Vt/(1.35*VL))
NA=ALPHA1
ALPHA2=A

```

"-----Parameters for the fuzzy controller.

```

UMAX:110           "Max. and min. control output.
Umin:-81
AT:2.778E-03       "Sampling interval.
VL:90              "Supply line voltage.
Cc1:0.5            "Change in error fuzzy set definitions.
Cc2:0.2
Ec1:0.5            "Error fuzzy set definitions.
Ec2:0.2
U1:0.5             "Control output fuzzy set definitions.
U2:0.125
U3:0.05
"
GEc:25             "Input and output gains.
GCc:5
GUc:40

```

"-----Initial values

```

A:1.5708
END

```

```

"-----
" PHASE-CONTROLLED RECTIFIER
"-----

```

CONTINUOUS SYSTEM RCFR

```

INPUT ALPHA1 ALPHA2 Ia Ea
OUTPUT Vt IVT VTPU

```

STATE IV "USED TO GENERATE Vdc IN CPI

DER DIV

TIME T

TSH=T-N\*2.778E-03 "Relative time.

N=INT((T-1E-10)/2.778E-03)

"-----DEFINE BASIC VOLTAGES PROFILES.

Vab=Vmax\*SIN(1.0472+W\*TSH)

```

Vcb=Vmax*SIN(2.0944+W*TSH)
Vca=Vmax*SIN(3.1416+W*TSH)
"
" -----FIRING ANGLE REFLECTED IN THE INTERVAL 0 - 60 DEG.
UA=IF ALPHA1<1.0472 THEN ALPHA1 ELSE ALPHA1-1.0472
FT=UA/W "FIRING TIME
Vold= IF ALPHA1<1.0472 THEN Vcb ELSE Vca
Vnew= IF ALPHA1<1.0472 THEN Vab ELSE Vcb
VT1=IF TSH<FT THEN Vold ELSE Vnew
VT=IF VT1>Ea THEN VT1 ELSE CONI "Converter output voltage.
CONI=IF Ia>1E-03 THEN VT1 ELSE Ea "Test for continuous conduction.

" -----EVALUATE INTEGRAL OF VT
Vtpu=Vt /Em
DIV=Vtpu "Vt (pu) integral.
IVT=IV "Electrical frequency.

" -----Parameters.
W=376.99
Vmax:127.28 "Peak line voltage.
END

" -----
" DISCRETE PI CURRENT CONTROLLER
" -----
" Note: INCORPORATES ANTI-WINDUP.
DISCRETE SYSTEM CPI
INPUT Iar Ila II IVT Ea "II is the actual current and Ila is its integral.
OUTPUT ALPHA1 ALPHA2 Ia Vt VDC

STATE X I Vd A " A = ALPHA(k-1)
NEW NX NIN Vd NA
TIME T
TSAMP TS
TS=T+AT

" -----Computation of Idc and Vdc (pu).
NI=IIa
Ia=(IIa-I)/AT
NVd=IVT
Vdc=(IVT-Vd)/AT

" -----COMPUTE ERROR E, CONTROL SIGNAL U
E=Iar-Ia
V=Kpi*E+X+Ea
U=IF V<Umin THEN Umin ELSE IF V>UMAX THEN UMAX ELSE V
NX=X+Kii*E*AT
Vt=U

ALPHA1=ARCCOS(Vt/(1.35*VL)) " Firing angle.
NA=ALPHA1
ALPHA2=A " Alpha(k-1)

" ----- PARAMETERS
UMAX:110 "Max. and min. control output.
Umin:-81
Kpi:1.2 "PI gains.
Kii:80
AT:2.778E-03 "Sampling interval.
VL:90 "Line voltage.
" -----INITIAL VALUES.

```

A:2.094  
END

"120 DEGREES

```
"-----
"          DISCRETE PI SPEED CONTROLLER
"-----
"NOTE: Using anti-windup.
DISCRETE SYSTEM SPI
INPUT W
OUTPUT Iar

STATE X
NEW NX
TIME T
TSAMP TS
TS=T+ADT

"----- COMPUTE ERROR E AND CONTROL SIGNAL U.
E=0.10472*Wr-W
V=Kps*E+X
U=IF V<0 THEN 0 ELSE IF V>UMAX THEN UMAX ELSE V
NX=X+Kis*E*ADT+U-V "WITH ANTI WINDUP
Iar=U                  "Reference current.
Wr=IF T<0.8 THEN Wr1 ELSE Wr2    "Reference speed.

"-----PARAMETERS.
UMAX:25                "Maximum current reference.
Kis:28                 "PI gains.
Kps:2
ADT:2.778E-03          "Sampling interval.
Wr1:1000
Wr2:1000
END
```

## A.2 Loss Modeling and Efficiency Optimization Programs

```
"-----
"          AC POWER SUPPLY
"-----
CONTINUOUS SYSTEM AC
OUTPUT vas vbs vcs we
TIME t

"---Generate 3-phase sinusoidal voltages
vas=Vm*sin(wt)
vbs=Vm*sin(wt-2.0944)
vcs=Vm*sin(wt-4.1888)
wt=we*t
we=377
Vm:187.79
END
```

```

"-----
" LOSSY MODEL OF A THREE-PHASE DIODE BRIDGE RECTIFIER
"-----

CONTINUOUS SYSTEM RCFL
INPUT  Vas Vbs Vcs I2
OUTPUT Vd Pild Pior Piir
STATE Vc I1
DER   DVc DI1
TIME t

"-----GENERATION OF IDEAL RECTIFIER VOLTAGE Vr
Vp = MAX(Vas, MAX(Vbs,Vcs))      "Positive profile,
Vn = MIN(Vas, MIN(Vbs,Vcs))      "Negative profile
Vr = Vp-Vn

"-----EQUATIONS FOR CURRENT AND VOLTAGES
Vdd = Vd0+Cd*ABS(I1)^Ed          "Diode voltage drop
DVc = (I1-I2)/C                  "Capacitor voltage
DI1 = IF I1<0 AND AUX<0 THEN 0 ELSE AUX "Current through L
AUX = (Vr-2*Vdd-Vc)/L            "Voltage across L
Vd = Vc

"-----INSTANTANEOUS POWERS AND LOSSES
Pild = 2*Vdd*abs(I1)             "Instantaneous conduction losses in diodes
Pior = Vd*I1                     "Instantaneous power output of rectifier
Piir = Vr*I1                     "Instantaneous power input of rectifier

"-----INITIAL VALUES
Vc:314
I1:1.57

"-----PARAMETERS FOR POWEREX CD 411230 (30 A/ 1200-1600 V)
C:0.0048                        "DC link capacitor
L:0.001                          "DC link equivalent of AC source inductance
Cd:0.052                         "Volt-ampere coefficient of diode characteristics
Ed:0.585                         "Exponent of diode characteristics
Vd0:0.8                          "Forward voltage drop of diode
END

"-----
" LOSSY MODEL OF A THREE-PHASE HYSTERESIS
" BAND PWM INVERTER
"-----
"

DISCRETE SYSTEM INVL
INPUT Iac Ibc Icc Ia1 Ib1 Ic1 Vd We AT
OUTPUT Va Vb Vc I2 Nsaux Plinv
STATE A B C sl s Sla lav          "Inverter Switching State
NEW NA NB NC Ns1 Ns NSla Nlav      "A=1 -> T1 on, T4 off
STATE Ia Ib Ic
NEW NIa NIb Nic
TIME T                              "A=0 -> T4 on, T1 off
TSAMP Ts
Ts = T + AT

"-----DEFINE AUXILIAR STATE EQUATIONS FOR CURRENT
NIa = Ia1
NIb = Ib1
NIC = Ic1

```

```

"-----DEFINITION OF ERROR = REF-ACTUAL
Iae = Iac-Ia
Ibe = Ibc-Ib
Ice = Icc-Ic

"-----LOGIC TO GENERATE PWM BY HB COMPARISON
NA = IF Iae>HB THEN 1 ELSE IF IAE<-HB THEN 0 ELSE A
NB = IF Ibe>HB THEN 1 ELSE IF IBE<-HB THEN 0 ELSE B
NC = IF Ice>HB THEN 1 ELSE IF ICE<-HB THEN 0 ELSE C

"-----GENERATION OF VOLTAGES (WITH RESPECT TO GROUND)
Vag = IF Ia>0 THEN C1a ELSE C2a
C1a = IF NA>0 THEN Vd-TdropA ELSE -DdropA
C2a = IF NA>0 THEN Vd+DdropA ELSE TdropA
TdropA = ABS(Ia)*Rt + Vt0
DdropA = Vd0 + Cd*ABS(Ia)^Ed

Vbg = IF Ib>0 THEN C1b ELSE C2b
C1b = IF NB>0 THEN Vd-TdropB ELSE -DdropB
C2b = IF NB>0 THEN Vd+DdropB ELSE TdropB
TdropB = ABS(Ib)*Rt + Vt0
DdropB = Vd0 + Cd*ABS(Ib)^Ed

Vcg = IF Ic>0 THEN C1c ELSE C2c
C1c = IF NC>0 THEN Vd-TdropC ELSE -DdropC
C2c = IF NC>0 THEN Vd+DdropC ELSE TdropC
TdropC = ABS(Ic)*Rt + Vt0
DdropC = Vd0 + Cd*ABS(Ic)^Ed

"-----GENERATION OF PHASE VOLTAGES
Va = (2*Vag-Vbg-Vcg)/3
Vb = (2*Vbg-Vag-Vcg)/3
Vc = (2*Vcg-Vbg-Vag)/3

"-----CONDUCTION LOSSES COMPUTATION
Pca = IF NA THEN (Vd-Vag)*Ia ELSE -Vag*Ia
Pcb = IF NB THEN (Vd-Vbg)*Ib ELSE -Vbg*Ib
Pcc = IF NC THEN (Vd-Vcg)*Ic ELSE -Vcg*Ic
Picli = Pca+Pcb+Pcc "Instantaneous conduction losses

"-----CONTABILIZATION OF SWITCHING CYCLES/PERIOD
" FOR UPPER TR OF LEG A. (Nsaux)
RES = SIGN(Iac) "LOGICAL SIGNAL (+1 OR -1)
DRES = DELAY(RES,AT) "DELAYED LOGICAL SIGNAL
PROD = RES*DRES "PULSE FOR RESET (-1 AT RESET INSTANT)
Ns1 = IF PROD>0 THEN (IF A<NA OR A>NA THEN s1+1 ELSE s1) ELSE 0
Ns = IF PROD<0 THEN 2*s1 else s
Nsaux = s

"-----COMPUTE AVERAGE VALUE OF ABS(Ia)
fs = We/pi2
NSIa = IF PROD>0 THEN SIa+ ABS(Ia) ELSE 0 "Integral over half period.
NIav = IF PROD>0 THEN Iav ELSE (2*fs*AT*SIa) "Average over half cycle.

"-----COMPUTATION OF TRs TURN-ON SWITCHING LOSSES
Nif = (Nsaux/2)*Iav*fs
Kon = 1.5*ton*(1-1.333*(t1L/ton)+0.5*(t1L/ton)*(t1L/ton))
Rton = Vd/(Nif*Kon+alpha)
Pton = Vd*Vd/Rton "Turn on losses.
Iton = Vd/Rton "Current component due to Pton

"-----COMPUTATION OF TRs TURN-OFF SWITCHING LOSSES

```



```

Koff = 1.5*toff*(1-1.333*(t1C/toff)+0.5*(t1C/toff)*(t1C/toff))
Rtoff = Vd/(Nif*Koff+alpha)
Ptoff = Vd*Vd/Rtoff
Itoff = Vd/Rtoff                                "Current component due to Ptoff

"-----COMPUTATION OF SNUBBER LOSSES
Rsn = 2/(3*Nsaux*fs*Cs+alpha)
Psn = Vd*Vd/Rsn
Isn = Vd/Rsn                                    "Current component due to Psn

"-----COMPUTATION OF DC LINK CURRENT AND INV. OUTPUT POWER
I2 = NA*Ia+NB*Ib+NC*Ic+ (Ition+Itoff+Isn)
Plinv = Picl + Pton + Ptoff + Psn                "Total inverter losses.

"-----INITIAL VALUES
A:1                                           "Base drive states.
B:1
C:0
s1:1
s:1
Iav:10

"-----PARAMETERS
"Data for POWEREX single darlington TR ks524503 (30 A/ 600 V)
toff: 0.8e-06                                "Turn-off time of TR ( tf )
ton: 0.52e-06                                "Turn-on time of TR ( tr )
Rt: 0.01                                     "Conduction resistance of TR
Vt0: 0.7                                    "Saturated collector-emitter of TR
Vd0: 0.7                                    "Forward voltage drop of freewheeling diode
Cd: 0.051                                   "Coefficient of VxA characteristic of FWD
Ed: 0.671                                  "Exponent of VxA charac. of FWD

"Data related to snubbers
Cs: 0.0068E-06                              "Snubber capacitor
Ls: 0.2e-06                                 "Snubber inductance
t1L:0.11e-06
t1C:0.382e-06

"Other parameters
alpha:1e-07
pi2= 8*atan(1)
HB: 1.5                                     "Hysteresis band
END

" -----
"  INDUCTION MOTOR LOSSY D-Q MODEL IN SYNCHRONOUS FRAME
" -----
" FEATURES INCLUDED IN THIS MODEL
" 1) TEMPERATURE EFFECTS ON BOTH ROTOR AND STATOR
"    RESISTANCES ;
" 2) SATURATION EFFECTS ON MAGNETIZING INDUCTANCE (Lm);
" 3) SKIN EFFECT ON ROTOR RESISTANCE (HARMONIC FREQUENCY);
" 4) STRAY LOSSES (BOTH FUND. AND HARMONICS) ARE INCLUDED;
" 5) FRICTION AND WINDAGE LOSSES ARE CONSIDERED;
" 6) CORE LOSSES ARE SEPARATELY COMPUTED FOR FUND. AND
"    HARMONIC FREQUENCIES AND INTEGRATED IN THE MODEL.
"

CONTINUOUS SYSTEM IMS3
INPUT va vb vc we Nsaux SINWT COSWT
OUTPUT ia ib ic wr Lm Rr po Pin

```

```

STATE iqsl idsl iqsr idsr iqm idm iqr idr
DER diqsl didsl diqsr didsr diqm didm diqr didr
STATE iqrr idrr w Plf fc
DER diqrr didrr dw DPlf dfc
TIME t

"-----DEFINE SOME USEFUL CONSTANTS AND VARIABLES
pi = atan(1)*4
p2 = pi*2
pb2s = p2*p2
sq2 = sqrt(2)
sqr3 = sqrt(3)

tl = kl*wr*wr                                "Load torque
spd = wr*60/p2                               "Speed in rpm
wr=w*2/pole                                  "In mech. rad/s
f = we/p2                                    "Supply frequency
fca = max(f*Nsaux,2500)                     "Harmonic frequency (carrier)
wc = p2*fc                                   "Harmonic frequency (in rad/s)
dfc = (fca-fc)/talt

"-----COMPUTE MACHINE FLUXES
fqls = Lls*iqsl                               "Stator leakage fluxes
fdls = Lls*idsl
fqm = Lm*iqm                                  "Air-gap fluxes
fdm = Lm*idm
fqr = fqm - Llr*iqr                           "Rotor fluxes
fdr = fdm - Llr*idr

"-----DEFINE CURRENTS AND AUXILIAR VARIABLES
iqs = iqsl + iqsr
iqr = -(iqr + iqr)
iqrm = iqs + iqr - iqm
F1q = -vqs + R1*iqs + we*fdls
F2q = (RbL2*iqsr-F1q*Leq2-RbL3*iqrm-we*fdm*Leq3+wsf*idr*Leq4+F2qc)/Leq1
F2qc = (RbL5+RbL6)*iqr-RbL4*iqr
LF2q = Lls*F2q

ids = idsl + idsr
idr = -(idr + idrr)
idrm = ids + idr - idm
F1d = -vds + R1*ids - we*fqls
F2d = (RbL2*idsr-F1d*Leq2-RbL3*idrm+we*fqm*Leq3-wsl*fqr*Leq4+F2dc)/Leq1
F2dc = (RbL5+RbL6)*idr-RbL4*idrr
LF2d = Lls*F2d

"-----STATE EQUATIONS FOR MACHINE DYNAMICS
diqsl = F2q                                    "Q-axis circuit
diqsr = (LF2q - Rssn*iqsr)/Lssn
diqm = (-F1q-LF2q - we*fdm)/Lm
Vlrq = -F1q-LF2q + wsl*idr-we*fdm+Rr*iqr
diqr = Vlrq / Llr
diqrr = (Vlrq - Rrsnp*iqrr)/Lrsn

didsl = F2d                                    "Q-axis circuit
didsr = (LF2d - Rssn*idsr)/Lssn
didm = (-F1d-LF2d + we*fqm)/Lm
Vlrd = -F1d-LF2d -wsl*fqr + we*fqm+Rr*idr
didr = Vlrd / Llr
didrr = (Vlrd - Rrsnp*idrr)/Lrsn

dw = (te-tl-b*wr-Kfw*Wr*Wr)*pole/(j*2) "In elec. rd/s

```

```

"-----VOLTAGE TRANSFORMATIONS
vqss = va                                "abc to d-q stationary
vdss = (vc-vb)/sqr3
Vqs = vqss*coswt-vdss*sinwt            "d-q stationary to synchronous
Vds = vqss*sinwt+vdss*coswt

"-----COMPUTATION OF DEVELOPED TORQUE
te = -(fdr*iqr-fqr*idr)*0.75*pole        "Instantaneous value

"-----CURRENT TRASFORMATIONS
iqss = coswt*iqs+sinwt*ids              "synchronous to stationary
idss = -sinwt*iqs+coswt*ids
ia = iqss                                "d-q stat. to abc
ib = -(0.5*iqss)-(0.5*sqr3*idss)
ic = -(0.5*iqss)+(0.5*sqr3*idss)

"-----CALCULATE THE RMS CURRENT THROUGH Lm
im = sqrt(iqm*iqm+idm*idm)/sq2

"-----COMPUTE TIME DEPENDENT MODEL PARAMETERS
rs = rs0*(1+A1*Dtemp)                    "Resistance values correct
rr = rr0*(1+A2*Dtemp)                    "for temperature
Lm = if im<im0 then lm0 else lm0-m*(im-im0) "Magnetizing ind.
Lr = Lm+Llr

wsl = we-w                                "Slip frequency
s = wsl/we                                "Per unit slip
Rm = pb2s*f/((1+abs(s))*Kh+(1+s*s)*Ke*f) "Core loss resistor (fund.)
Rmc = pb2s*fc/(2*(Kh+Ke*fc))             "Core loss resistor (harm.)
Rtemp = Rm*(Rmc-Rm)
Llm = if Rtemp > 0.18 then sqrt(Rm*(Rmc-Rm))/wc else 10e-06
                                           "Leakage mag. induc.(harm.)

" ----- Parameter for stray loss in stator
Rsl1 = Rslb*(f/fb)*(1+gm*f)/(1+gm*fb)    "Series resist. (fund.)
Cfr = (fc/fcb)*(1+gm*fcb)/(1+gm*fc)      "Correction factor for harm.
Rssn = Rssb*Cfr                          "Stator harm. stray loss res.
Rrc = Rr*Kr*sqrt(fc)                     "Rotor resist. at harm. freq.

" Parameters for stray loss and skin effect in the rotor
Xlrc = Llr*wc                             "Rotor leakage reac. at harm.freq.
Xlrc2 = Xlrc*Xlrc                         "Square of Xlrc
Rrsn = Cfr*Rrsb                           "Rotor harm. stray loss res.
Rrsnb = Xlrc2* Rrsn / (Rrsn*Rrsn+Xlrc2)  "Series eq. of Rrsn (harm. freq.)
Rrle = Rrsnb+(Rrc-Rr)                     "Combined stray + skin res.,series
XbR = Xlrc2/Rrle                          "Aux. variable
SIG = If Xlrc < Rrsn then +1 else -1      "Sign of correct root of quadr. expr.
DLT = max((XbR*XbR - 4*Xlrc2),0)         "Aux. variable
Rrsnp = If DLT>0 then (XbR+SIG*sqrt(DLT))/2 else Xlrc/2
                                           "Parallel combined stray+skin res.

"-----COMPUTE OUTPUT AND INPUT POWERS
po = tl*wr                                "Output power
pin = va*ia+vb*ib+vc*ic                  "Input power, instantaneous
Pl = pin-po                               "Instantaneous overall losses

"-----ESTIMATE TEMPERATURE RISE
DPlf = (Pl-Plf)/Talt                      "Average overall losses
Dtemp = Plf*theta

"-----DEFINE AUXILIAR CONSTANTS
Leq4 = 1/Lrsn + 1/Llr

```

$Leq3 = Leq4 + 1/Lm$   
 $Leq2 = Leq3 + 1/Llm$   
 $Leq1 = (Leq2 + 1/Lssn)*Lls + 1$   
 $RbL2 = Rssn /Lssn$   
 $RbL3 = Rm/Llm$   
 $RbL4 = Rrsnp/Lrsn$   
 $RbL5 = Rr/Llr$   
 $RbL6 = Rr/Lrsn$   
 $Rl = Rs + Rsl1$

"-----CONSTANT MACHINE PARAMETERS

" CLASS B 5 hp machine.

rs0:0.370	"Resistance values at 25C, 60 Hz
rr0:0.436	" " " " ", dc
Rslb:0.1384	"Base value of series fund. stray loss stator res.
Rssb:164.46	"Base value of stator harm. stray loss res. (at fcb=5KHz)
Rrsb:164.46	"Base value of rotor harm. stray loss res. (at fcb)
theta: 0.06319	"Thermal resistance
A1:0.00385	"Temperature coefficient for copper 100
A2:0.00389	" " " for aluminum 60
kh:4.3811	"Hysteresis coefficient
ke:0.0313	"Eddy current coefficient
gm:0.00238	
Kr:0.1371	"Skin effect coef. for 3/8" deep bar
fb:60	"Base frequency (1800 rpm)
lm0:0.06277	"Linear value of magnetizing inductance
im0:3.4	"Linear region breakpoint of Lm
m:0.00366	"Saturation coefficient
Lls:0.00213	"Leakage inductances
Llr:0.00213	
Lssn = 0.05*Lls	
Lrsn = 0.05*Llr	
j:17.5E-03	"Machine inertia
b:4.05e-04	"Viscous damping coefficient
pole:4	
kl = factor*0.5862e-03	"Load constant (Rated = 0.5862e-03)
factor = if t<3 then 0.4 else 2 !	
Kfw:2.248e-06	"Friction and windage coefficient
Tal:0.0004	"Time constant for filters
Talt:0.010	
fcb:5000	"Base carrier frequency

"-----INITIAL CONDITIONS FOR Wref=900 rpm

idsl:9.786	
idm: 9.7	
iqsl:1.6	
iqrl:1.6	
w:188.5	"1800 rpm --> 377 rad/s.
fc:5000	
END	

```

" -----
"      DISCRETE SPEED PI CONTROLLER
" -----
" NOTES:
"      1) ANTI-WINDUP IS USED, AS WELL AS SATURATION FUNCTION
"          TO LIMIT VALUE OF CONTROL VARIABLE iqec;
"      2) GAINS ARE SELECTED FOR A 5 HP MACHINE;

DISCRETE SYSTEM WCTRL
INPUT Wr
OUTPUT E iqecp
STATE X
NEW NX
TIME T
TSAMP TS
TS=T+AT

"-----COMPUTE SPEED ERROR E AND INITIAL CONTROL SIGNAL V
E = 0.1047197*Wref-Wr
V = Kp*E+X
NX = X+Ki*E*AT+kwup*(iqecp-V)

"-----COMPUTE FINAL CONTROL SIGNAL iqec
iqecp = IF ABS(V)<IQM THEN V ELSE SIGN(V)*IQM

"-----PARAMETERS
Wref:2200
IQM:26.7                "Maximum iqec (50% higher Is).
Kp:1.25                 "Proportional gain
Ki:25                   "Integral gain
Kwup:0.02               "Anti-windup coefficient.
AT:1E-03                "Speed sampling time.

"-----INITIAL VALUES
X:5
END

" -----
"      FUZZY EFFICIENCY OPTIMIZATION ROUTINE
" -----
DISCRETE SYSTEM FEOPT
INPUT DWr Wr Pi DT TLest
OUTPUT DIDECD RT FSSA
STATE Po DPi CR DC Dids FSS      " DC=Down Counter
NEW NPo NDPi NCR NDC NDids NFSS
TIME T
TSAMP TS
TS=T+DT

"-----CHECK FOR STEADY STATE (SS) AND DEFINE FLAGS
E1 = DELAY(DWr,TW)
E2 = DELAY(E1,TW)
SUM = ABS(DWr)+ABS(E1)+ABS(E2)
NFSS = IF FSS THEN TOEX ELSE TOST      "FLAG FOR SS CONDITION
TOEX = IF SUM<TOLEX THEN 1 ELSE 0      " -- TEST OF EXIT
TOST = IF SUM<TOLST THEN 1 ELSE 0      " -- TEST OF START
FSSA = FSS      "AVOID SIMNON PROBLEM WHEN EXPORTING FSS
NCR = IF FSS<1 THEN 0 ELSE IF RT THEN CR+1 ELSE CR
NDC = IF DC < 0.99 THEN COUNT ELSE DC-1
RT = IF DC < 0.99 THEN 1 ELSE 0      "FLAG FOR 1ST ITERATION.

```

```

"-----DEFINE BASE VALUE FOR Dids (GID), IMPOSING Min. AND Max.
GIDA = C1*Wr/Wrated + C2*TLest/Trated + C3      "PRELIMINARY VALUE.
GID = IF ABS(GIDA) < TOL4 THEN SIGN(GIDA)*TOL4 ELSE GIDC
GIDC = IF ABS(GIDA) > TOL5 THEN SIGN(GIDA)*TOL5 ELSE GIDA

"-----COMPUTE POWER GAIN (1/Pbase) AND SCALED DELTA Pi (DPi)
GPbA = -0.05*Wr/Wrated + 0.0625
GPb = MIN( GPbmax, MAX(GPBmin,GPbA))

NPo = IF RT THEN Pi ELSE Po                      "Pdc(k-1)
NDPi = IF RT THEN (Pi-Po)*GPb ELSE DPi           "Delta Pdc.

"-----EVALUATION OF Cid (CHANGE IN Dids)
" (A FUZZY RELATION IS USED TO EVALUATE Cid)
" -----PRELIMINARY COMPUTATION OF MEMBERSHIP VALUES
A1 = MIN(1,(-NDPi-P2)/(P1-P2))
A2 = (-NDPi-P3)/(P2-P3)
A3 = (-NDPi/P3)
A5 = NDPi/P3
A6 = (NDPi-P3)/(P2-P3)
A7 = MIN(1,(NDPi-P2)/(P1-P2))

"-----GET INTERVAL INDEX FOR DPi
J = IF NDPi< -P1 THEN 1 ELSE IF NDPi<-P2 THEN 2 ELSE J1
J1 = IF NDPi<-P3 THEN 3 ELSE IF NDPi< 0 THEN 4 ELSE J2
J2 = IF NDPi< P3 THEN 5 ELSE IF NDPi< P2 THEN 6 ELSE J3
J3 = IF NDPi < P1 THEN 7 ELSE 8

"-----EVALUATION OF DEGREES OF MEMBERSHIP FOR DPi
MP1 = IF J<3 THEN A1 ELSE IF J<4 THEN A2 ELSE IF J<5 THEN A3 ELSE T1
T1 = IF J<6 THEN (1-A5) ELSE IF J<7 THEN (1-A6) ELSE (1-A7)
MP2 = 1-MP1

"-----COMPUTES DEGREE OF MEMBERSHIP FOR LAST Dids
MI1 = IF Dids<-L3 THEN 0 ELSE MIN(1,((Dids+L3)/(L2+L3)))      "POSITIVE
MI2 = IF Dids> L3 THEN 0 ELSE MIN(1,((-Dids+L3)/(L2+L3)))     "NEGATIVE

"-----PERFORM RULE BASE EVALUATION
MRA = MIN(MP1,MI1)
MRB = MIN(MP1,MI2)
MRC = MIN(MP2,MI1)
MRD = MIN(MP2,MI2)

"-----GET CONTROL SIGNAL FOR EACH RELEVANT FUZZY RULE
DIA = IF J<3 THEN I1 ELSE IF J<4 THEN I2 ELSE IF J<5 THEN I3 ELSE T2
T2 = IF J<6 THEN 0.0 ELSE -I3
DIB = -DIA                      "FOR THIS SPECIFIC RB
DIC = IF J<3 THEN I2 ELSE IF J<4 THEN I3 ELSE IF J<5 THEN 0.0 ELSE T3
T3 = IF J<7 THEN -I3 ELSE -I2
DID = -DIC                      "FOR THIS SPECIFIC RB

"-----EVALUATE Cid USING HEIGHT DEFUZZIFICATION METHOD
FV = (MRA*DIA+MRB*DIB+MRC*DIC+MRD*DID)/(MRA+MRB+MRC+MRD)
Cid = IF NCR<1 THEN 0 ELSE IF NCR<2 THEN -1.0 ELSE FV

"-----CALCULATION OF NEW Dids
NDids = IF RT THEN Cid ELSE Dids
DAUX = NDIDS*GID
DIDEC = IF ABS(DAUX)<TOL2 THEN SIGN(DAUX)*TOL2*FSS*RT ELSE DAUX

"-----PARAMETERS
"DT:5E-06                      "SAMPLING INTERVAL OF THE DISCRETE SYSTEMS

```

```

TW:1E-03          "PERIOD FOR TEST OF SS CONDITION

TOLST:1           "TOL. TO START STEADY STATE COND. (IN RAD/S)
TOLEX:3           "TOL. TO EXIT STEADY STATE COND.

C1:1.083          "COEFFICIENTS FOR GID COMUTATION
C2:-3.047
C3:1.496

GPbmax:0.05       "MAX AND MIN VALUES FOR POWER GAIN
GPbmin:0.0125

Trated:20.83      "RATED MOTOR TORQUE
Wrated:188.5      "RATED  $W_r$  IN MECH. RAD/S
TOL2:0.1          "MIN. CHANGE FOR  $D_{ids}$  (A)
TOL4:0.5          "MIN. VALUE FOR GID (AMPS)
TOL5:1.5          "MAX. VALUE FOR GID (AMPS)
COUNT=0.5/DT     "DOWN COUNTER INITIAL VALUE (FOR  $T_{eff}=0.5$  S)

"-----PARAMETERS FOR FUZZY SETS
P1:1              "CONSTANTS USED IN DEFINITION OF FUZZY SETS FOR  $D_{Pi}$ 
P2:0.5
P3:0.3
I1:1.0            "CONSTANTS USED IN DEFINITION OF FUZZY SETS FOR  $D_{ids}$ 
I2:0.7
I3:0.40
L1:1.0            "CONSTANT USED IN DEFINITION OF FUZZY SETS FOR  $LD_{ids}$ 
L2:0.1
L3:0.001

"----- INITIAL VALUES
DC:100000         "DOWN COUNTER
END

"
"-----
"          FEED FORWARD TORQUE COMPENSATION ROUTINE
"-----
DISCRETE SYSTEM FFTC

INPUT iqecp  $D_{ids}$  RT FSS AT
OUTPUT  $W_{sl}$   $i_{dec}$   $i_{qec}$   $T_{Lest}$ 
STATE  $i_{dec}$   $f_{dre}$   $i_{qst}$   $i_{qsc}$   $f_{dr}$ 
NEW  $N_{idec}$   $N_{fdre}$   $N_{iqst}$   $N_{iqsc}$   $N_{fdr}$ 
TIME T
TSAMP TS
TS=T+AT

"-----DEFINES  $i_{dec}$ ,  $L_m$  AND STEADY-STATE ESTIMATED D-AXIS FLUX
 $a_{idec} = i_{dec} + D_{ids}$ 
 $L_m = L_{m0} - M_{bs2} * (a_{idec} - i_{dec0})$ 
 $N_{fdre} = \text{if } RT \text{ then } L_m * a_{idec} \text{ else } f_{dre}$ 

"-----COMPUTE  $d_{iqs}$  (DELTA  $i_{qs}$ ) , TEST FOR  $I_{Smax}$ 
"          AND COMPUTE  $i_{qst}$  (STAIR-CASE  $i_{qs}$ )
 $d_{iqsa} = FSS * (f_{dre} - N_{fdre}) * i_{qec} / N_{fdre}$ 
 $a_{iqec} = i_{qecp} + i_{qst} + d_{iqsa}$ 
 $IP2 = a_{idec} * a_{idec} + a_{iqec} * a_{iqec}$           "SQUARE OF NEW STATOR CURRENT VECTOR
 $d_{iqs} = \text{if } IP2 < I_{MAX} \text{ then } d_{iqsa} \text{ else } 0$ 
"          (IMAX IS THE SQUARE OF MAX. STATOR. CURR. VECTOR)
 $N_{iqst} = \text{if } RT \text{ then } i_{qst} + d_{iqs} \text{ else } i_{qst}$           "Accumulated  $d_{iqs}$ .

```

```

"-----COMPUTE iqsc (compensatig signal) and iqec (iqs*)
Ni qsc = iqsc + AT*(iqst-iqsc)/Tl r      "Filter of rotor time constant.
Nidec = if FSS<1 then idecr else if IP2<IMAX and RT then aidec else idec
ideca = Nidec                          "Ids*(k).
iqec = min((iqecp+iqsc),sqrt(IMAX-idec*idec))  "Iqs*(k).

"-----EVALUATE SLIP FREQUENCY Wsl, USING ESTIMATED FLUX
Tl r=Lr/Rr
fdrc = if FSS then fdre else fdr      "Estimate of the new steady state
Nfdr = fdr + AT*(fdrc-fdr)/Tl r      " value of fdr
Wsl=(Lm*Rr*iqec)/(Lr*fdr)

"-----ESTIMATE MACHINE TORQUE
TLest = Kt*iqec*fdr

"-----PARAMETERS
IMAX = if FSS then IMAX1 else IMAX2
Lr=Lm+Llr      "Rotor inductance.
Llr:0.00213    "Rotor leakage inductance.
Rr:0.478       "Rotor resistance.
Lm0:0.06277   "Magnetizing inductance (unsaturated).
Mbs2:2.588e-03 "Saturation coefficient.
idec0:4.8 "
idecr:9.786   "RATED idec
fdr:0.4833    "RATED flux
IMAX1:360     "MAX. STEADY STATE STATOR CURRENT (SQUARED)
IMAX2:808     "MAX. TRANSIENT STATOR CURRENT (SQUARED)
Kt:2.655     "Torque constant.

"-----INITIAL CONDITIONS
fdr:0.4833    "INITIAL CONDITION FOR RATED Ids*.
idec:9.786
fdre:0.4833
END

"-----
" REFERENCE CURRENT GENERATOR AND VECTOR ROTATOR
"-----
"
CONTINUOUS SYSTEM VECROT
INPUT iqec idec Wr Wsl
OUTPUT iac ibc icc We coswt sinwt
STATE TH
DER DTH
"
TIME T
"-----GENERATE UNIT VECTORS
We=(pole/2)*Wr+Wsl
Dth=We
the=MOD(th,p2)
coswt=cos(the)
sinwt=sin(the)

"-----SYNCHRONOUS TO STATIONARY D-Q REF. FRAME
iqsc=iqec*coswt+idec*sinwt
idsc=idec*coswt-iqec*sinwt

"-----STATIONARY TO ABC REF FRAME
iac=iqsc
ibc=-(idsc*sqrt(3)+iqsc)*0.5
icc=-(iac+ibc)

```



"-----DEFINE CONSTANTS

p2=8\*ATAN(1)

pole:4

END

"-----  
" COMPUTATION OF AVERAGE LOSSES, INPUT AND  
" OUTPUT POWERS AND EFFICIENCY  
"

CONTINUOUS SYSTEM ECALC

INPUT Plinv Pild Pin Po Pior Piir

OUTPUT Piav

STATE X1 X2 X3 X4 X5 X6

DER DX1 DX2 DX3 DX4 DX5 DX6

TIME T

"-----COMPUTE AVERAGE (FILTERED) VALUES OF LOSSES AND POWERS

DX1 = X2

DX2 = A21\*X1 + A22\*X2 + Piir

Pair = -A21\*X1

"AVE. INPUT POWER OF DIODE BRIDGE

"

DX3 = X4

"AVE. OUTPUT POWER OF DIODE BRIDGE

DX4 = A21\*X3 + A22\*X4 + Pior

Paor = -A21\*X3

"

DX5 = X6

"AVE. MACHINE INPUT POWER.

DX6 = A21\*X5 + A22\*X6 + Pin

Paim = -A21\*X5

Piav = Paor

Nsys = 100\*Po/Pair

Ndc = 100\*Po/Paor

"Efficiency of IM+INVERTER

Nim = 100\*Po/Paim

"-----PARAMETERS AND INITIAL VALUES.

Tal2:40e-03

A21 = -1/(Tal2\*Tal2)

A22 = -2/Tal2

X1:2.0368

X3:2.0368

X5:2.0368

END

"-----  
" CONNECTING SYSTEM FOR VECTOR CONTROL  
"

CONNECTING SYSTEM CIVCS

"

VAS[RCFL]=VAS[AC]

VBS[RCFL]=VBS[AC]

VCS[RCFL]=VCS[AC]

VA[IMS3]=VA[INVL]

VB[IMS3]=VB[INVL]

VC[IMS3]=VC[INVL]

Vd[INVL]=Vd[RCFL]

"

IA1[INVL]=IA[IMS3]

IB1[INVL]=IB[IMS3]

IC1[INVL]=IC[IMS3]

```

IAC[INVL]=IAC[VECROT]
IBC[INVL]=IBC[VECROT]
ICC[INVL]=ICC[VECROT]
IQECP[FFTC]=IQECP[WCTRL]
IQEC[VECROT]=IQEC[FFTC]
IDEC[VECROT]=IDEC[FFTC]
I2[RCFL]=I2[INVL]
DIDS[FFTC] = DIDEC[FEOPT]
"
We[IMS3] = We[VECROT]
Wr[WCTRL] = Wr[IMS3]
Wsl[VECROT] = Wsl[FFTC]
Wr[VECROT] = Wr[IMS3]
We[INVL] = We[VECROT]
Wr[FEOPT] = Wr[IMS3]
DWr[FEOPT] = E[WCTRL]
"
Nsaux[IMS3] = Nsaux[INVL]
RT[FFTC] = RT[FEOPT]
FSS[FFTC] = FSSA[FEOPT]
TLest[FEOPT] = TLest[FFTC]
"
Pi[FEOPT] = Piav[ECALC]
Pior[ECALC] = Pior[RCFL]
Piir[ECALC] = Piir[RCFL]
Pin[ECALC] = Pin[IMS3]
Po[ECALC] = Po[IMS3]
Plinv[ECALC] = Plinv[INVL]
Pild[ECALC] = Pild[RCFL]
"
SINWT[IMS3]=SINWT[VECROT]
COSWT[IMS3]=COSWT[VECROT]

AT[INVL] = 1E-06                                "SPECIFY THE SAMPLING PERIOD
AT[FFTC] = 1E-06
DT[FEOPT] = 1E-06
END

```

```

" -----
"                MACRO FOR VECTOR CONTROL SYSTEM
" -----
"

MACRO MIVCS
SYST AC RCFL INVL IMS3 WCTRL VECROT FEOPT FFTC ECALC CIVCS
STORE iqec[vecrot] idec[vecrot] spd Po[IMS3] Nsys Ndc[ECALC] Nim
STORE fdr[ims3] fqr[ims3] Paor -ADD

split 2 1
plot idec[vecrot]
axes v 0 10 h -0.3 6
text 'ids* for efficiency optimization'
"

" ----- PARAMETER DEFINITION AND INITIAL VALUES
par wref:900
init w:188.5                                "for IMS3
init x:1.6                                  "for wctrl
init x1:0.3                                "for ecalc
init x3:0.3                                " "
init x5:0.3
SIMU -0.30 4 0.5E-06 / fig9a 0.005

```

```

split 2 1
area 1 1
axes v 0 10 h 0 4
show idec
area 2 1
axes v 0 2000
show Paor
END

```

### A.3 Slip Gain Tuning Programs

```

"-----
"               IDEAL HYSTERESIS BAND PWM INVERTER
"-----
DISCRETE SYSTEM INV
INPUT ia ib ic iac ibc icc
OUTPUT va vb vc
STATE A B C
NEW NA NB NC
TIME T
TSAMP TS
TS=T+AT

"-----GET CURRENT ERRORS
iae=iac-ia
ibe=ibc-ib
ice=icc-ic

"-----CALCULATE NEW STATES OF THE SWITCHES
NA=IF iae>L THEN 1 ELSE IF iae<-L THEN 0 ELSE A
NB=IF ibe>L THEN 1 ELSE IF ibe<-L THEN 0 ELSE B
NC=IF ice>L THEN 1 ELSE IF ice<-L THEN 0 ELSE C
Vd3=Vd/3
va=(2*NA-NB-NC)*Vd3
vb=(2*NB-NA-NC)*Vd3
vc=(2*NC-NB-NA)*Vd3

" ----- PARAMETERS AND INITIAL STATES.
AT:2E-06           "Sampling interval.
L:1.2              "Hysteresys band.
Vd:310             "Assumed dc link voltage
A:1
B:1
C:0
END

"-----
"               SYNCHRONOUS REFERENCE FRAME D-Q MODEL OF
"               AN INDUCTION MACHINE IN TERMS OF CURRENT
"-----
CONTINUOUS SYSTEM machine
INPUT  va vb vc we coswt sinwt
OUTPUT ia ib ic wr Vds Vqs
STATE iqs ids iqr idr w x
DER   diqs dids diqr didr dw dx
TIME t

```

```

pi = atan(1)*4
p2 = pi*2
sqr3 = sqrt(3)
spd = w/pole/pi*60

"----- STATE EQUATIONS
diqs = (lr*(vqs-rs1*iqs)-fse*ids+lm*rr*iqr-lrm*w*idr)/k1
dids = (fse*iqs+lr*(vds-rs1*ids)+lrm*w*iqr+lm*rr*idr)/k1
diqr = (lm*(rs1*iqs-vqs)+w*ism*ids-iqr*rr*ls+fre*idr)/k1
didr = (-w*ism*iqs+lm*(ids*rs1-vds)-fre*iqr-ls*rr*idr)/k1
dw = (te-tl-b*w*2/pole)/j*pole/2

tl=kl*wr*wr
wr=w*2/pole " SPEED IN MECH. RAD./S

"----- VOLTAGE TRANSFORMATIONS
vqss = va "Stationary frame.
vdss = (vc-vb)/sqr3
vqs = vqss*coswt-vdss*sinwt "Synchronous frame.
vds = vqss*sinwt+vdss*coswt

delw = we-w "Slip frequency.
fse = lsr*we-delw*lm "Auxiliary expressions.
fre = we*lm-delw*lsr
te = 0.75*pole*lm*(idr*iqs-iqr*ids) "Developed torque.

"----- NEW VARIABLES BEING INTRODUCED
DX = (Te - X)/TAL
Tefpu = X/Tb "Per-unit filtered torque.

fdr = Lr*idr+Lm*ids "D and Q axis rotor flux.
fqr = Lr*iqr+Lm*iqs
frpu = sqrt(fdr*fdr+fqr*fqr)/frb "Per-unit rotor flux.

" ----- GET MACHINE PARAMETERS
ls = (xm+xs)/wb "Stator and rotor inductances.
lr = (xm+xr)/wb
lm = xm/wb "Magnetizing inductance.
lrm = lr*lm "Auxiliary parameters.
ism = ls*lm
lsr = ls*lr
lmm = lm*lm
kl = lsr-lmm

"----- CURRENT TRANSFORMATIONS
iqss = iqs*coswt+ids*sinwt "Stationary D-Q frame.
idss = ids*coswt-iqs*sinwt
ia = iqss "ABC frame.
ib = -(0.5*iqss)-(0.5*sqr3*idss)
ic = -(0.5*iqss)+(0.5*sqr3*idss)

"----- PARAMETERS: FOR 5 HP IM OF AC 200 SYSTEM
wb:377 "Rated frequency (rad./sec.)
rs1:0.177 "Stator and rotor resistances.
rr:0.099
xs:0.8068 "Stator and rotor reactances.
xr:0.5127
xm:12.8105 "Magnetizing inductance.
j:6.58E-03 "Machine inertia
b:6.58E-04 "Viscous damping coefficient
pole:4

```

```

kl1=kfactor*3.2027e-04      "At rated speed and torque, kl1=3.2027e-04
kfactor:1                  "Rated conditions
lds:9.216                  "Initial value at rated flux.

TAL:50e-06                 "Filter time constant.
frb:0.3132                 "Base flux
Tb:17                      "Base torque

END

```

```

" -----
"                      FUZZY SLIP GAIN TUNER
" -----
" NOTE: USE E AND CE AS INPUT VARIABLES
"
DISCRETE SYSTEM FSGT
INPUT DQ DVd Wr Iqec
OUTPUT Kslip                      "Kslip = slip gain

STATE Ks Err X1 X2
NEW NKs NErr NX1 NX2
TIME T
TSAMP TS
TS = T + AT

" ----- FUZZY CONTROL 1 - Kf COMPUTATION
MHWr = Min(1,ABS(Wr)/Wb)          "D.M. for HIGH Wr
MLWr = 1 - MHWr                  "      LOW

Iqecpu = Iqec/Iqrated
MHIq = Min(1,ABS(Iqecpu))         "D.M. for HIGH Iqe
MLIq = 1 - MHIq                  "      LOW

" ----- PERFORM RULE BASE EVALUATION - FUZZY CONTROLLER I
MRA1 = Min(MHWr,MHIq)
MRBI = Min(MLWr,MHIq)
MRC1 = Min(MHWr,MLIq)
MRD1 = Min(MLWr,MLIq)

" ----- COMPUTE VALUE OF Kf, USING HEIGHT DEFUZZ. METHOD
PROD = MRA1*Kf2 + MRBI*Kf3 + MRC1*Kf1 + MRD1*Kf2
SUM = MRA1 + MRBI + MRC1 + MRD1
Kf = PROD / SUM

" ----- COMPUTE Error AS A COMBINATION OF DQ AND DVd
NErr = -1*(Kf*DQ + (1-Kf)*DVd)
AUX = NErr*GE                    "Normalized error
E = IF AUX<e1 THEN e1 ELSE IF AUX>e6 THEN e6 ELSE AUX "Impose bounds

" ----- COMPUTE CHANGE IN ERROR (ABSOLUTE VALUE)
DE = (NErr-Err)*GC               "Delta E
NX1 = X1 + (DE - X1)*AT/TAL      "Filtered DE
NX2 = X2 + (X1 - X2)*AT/TAL      "2nd order filter
CE = MIN(c3,ABS(X2))             "Impose c3 as upper bound for CE

" ----- DEFINE INTERVAL INDEX (I) AND D.M. FOR CE
I = IF CE<c1 THEN 3 ELSE IF CE<c2 THEN 2 ELSE 1
ci = FUNC(4,I)                   "D.M is obtained by using a function of I
cil = FUNC(5,I)
MC1 = (ci - CE) / (ci - cil)     "Left M.F. for error
MC2 = 1 - MC1                   "Right M.F. for error

```

```

"----- GET INTERVAL INDEX FOR E
J = IF E< e2 THEN 1 ELSE IF E< e3 THEN 2 ELSE J1
J1 = IF E< 0 THEN 3 ELSE IF E< e4 THEN 4 ELSE J2
J2 = IF E< e5 THEN 5 ELSE 6

" ----- DEFINE M.F. FOR E
ei = FUNC(2,J)           "M.F. definition is given by functions of J
eil = FUNC(3,J)

ME1 = (ei - E) / (ei - eil)      "Left M.F. for error
ME2 = 1 - ME1                  "Right M.F. for error

"-----PERFORM RULE BASE EVALUATION - FUZZY CONTROL 2
MRA = MIN(MC2,ME1)
MRB = MIN(MC2,ME2)
MRC = MIN(MC1,ME1)
MRD = MIN(MC1,ME2)

" ----- GET Delta Ks VALUES FROM FUNCTION
IJ = (I-1)*7 + J              "FUNC position of the rule A consequent

DKA = FUNC(1,IJ)              "Retrieve values of delta Ks, for
DKB = FUNC(1,IJ+1)            " the relevant rules.
DKC = FUNC(1,IJ+7)
DKD = FUNC(1,IJ+8)

" ----- EVALUATE DKs USING HEIGHT DEFUZZIFICATION METHOD
SUM = MRA+MRB+MRC+MRD
DKs = (MRA*DKA+MRB*DKB+MRC*DKC+MRD*DKD)/SUM

" ----- GET NEW VALUE FOR DELTA Ks
NKs = IF T<0 THEN Ks ELSE Ks+DKs*GKs      "New slip gain
Kslip = Ks

" ----- PARAMETERS FOR 5 HP MACHINE
Ls: 36.12E-03
Lsig: 3.45E-03
Rs: 0.177
Wb:230.383           "Wb==2200 RPM
Iqrated:19.11

"----- FUZZY CONTROLLER PARAMETERS
e1:-0.6              "Define M.F. for Error (E)
e2:-0.3
e3:-0.06
e4:0.1
e5:0.5
e6:1.0
c1:0.2
c2:0.6
c3:1

Kf1:0.8              "Define M.F. for Kf
Kf2:0.9
Kf3:0.98

GE:0.5               "Input gain for Err
GC:200               "Input gain for change in error
GKs:2.5e-03          "Output gain for DKs

" ----- INITIAL VALUES
Ks:0.608

```

AT:1E-03  
TAL:50E-03  
END

"Sampling interval  
"For CE filter

"-----  
" COMPUTATION OF FUNDAMENTAL DELTA Q, DELTA Vd  
"-----

CONTINUOUS SYSTEM ECOMP  
INPUT We Vds Vqs Idéc Iqec  
OUTPUT DQE DVdE  
STATE XI X2 X3  
DER DX1 DX2 DX3  
TIME T

"-----COMPUTE FILTERED VALUES

DX1 = (Vds - X1)/TAL "X1 = Vds filtered  
DX2 = (Vqs - X2)/TAL "X2 = Vqs filtered  
DX3 = (X1 - X3)/TAL "X3 = 2nd order filtered Vds

QE = X2\*Idéc-X3\*Iqec "Estimated Q, from Idéc, Iqec  
QEC = We\*(Ls\*Idéc\*Idéc+Lsig\*Iqec\*Iqec)"Reference from command signals  
Qb = 0.5 + QEC "Base value

"----- COMPUTE DELTA REACTIVE POWER  
DQE = (QEC - QE)/Qb "Delta Q

"----- COMPUTE DELTA Vd  
VdEC = rs\*Idéc - We\*Lsig\*Iqec "Command Vds  
Vb = 0.1 + ABS(We)\*Lsig\*ABS(Iqec) "Base Vds  
DVdE = -(VdEC - X3)/Vb "Delta Vds.

"-----PARAMETERS

Tal:3e-03 "Filter time constant.  
Ls: 34.877E-03 "Stator inductance.  
Lsig: 3.2975E-03 "Modified leakage inductance  
Rs: 0.177 "Stator resistance.  
END

"-----  
" CONNECTING SYSTEM FOR SLIP GAIN TUNING  
"-----

CONNECTING SYSTEM CMACH

VA[MACHINE]=VA[INV]  
VB[MACHINE]=VB[INV]  
VC[MACHINE]=VC[INV]  
Vds[ecalc]=Vds[MACHINE]  
Vqs[ecalc]=Vqs[MACHINE]

IA[INV]=IA[MACHINE]  
IB[INV]=IB[MACHINE]  
IC[INV]=IC[MACHINE]  
IAC[INV]=IAC[VECROT]  
IBC[INV]=IBC[VECROT]  
ICC[INV]=ICC[VECROT]  
IQEC[VECROT]=IQECP[WCTRL]  
Iqec[FSGT]=Iqecp[WCTRL]  
IDEC[VECROT]=IDEC[WCTRL]  
IQEC[ECALC]=IQECP[WCTRL]

```

IDEC[ECALC]=IDEC[WCTRL]
"
We[MACHINE]=We[VECROT]
We[ECALC]=We[VECROT]
Wr[WCTRL]=Wr[MACHINE]
Wr[VECROT]=Wr[MACHINE]
Wr[FSGT] = Wr[MACHINE]
Wsl[VECROT]=Wsl[WCTRL]
"
SINWT[MACHINE]=SINWT[VECROT]
COSWT[MACHINE]=COSWT[VECROT]

DQ[FSGT] = DQE[ECALC]
DVd[FSGT] = DVdE[ECALC]
Ks[WCTRL] = Kslip[FSGT]
"
END

```

```

"-----
"                               MACRO FOR SLIP GAIN TUNING
"-----
MACRO MMACH
SYST INV MACHINE WCTRL VECROT ECOMP FSGT CMACH
STORE iqecpu Tefpu frpu spd
PLOT fct

error 0.0001
IMPORT MYFUNC < MYFUNC /2
par AT[INV]:5E-06
split 3 2

INIT Ks:0.304
par wref:1100

par kfactor:4.0
par GC:500
par GKs:0.3e-03

AREA 1 1
axes h -0.5 2 v 0 2
TEXT 'Ks/Kso'
SIMU -0.50 2 /fig11B 0.001 //MYFUNC

area 1 1
ashow 0 2 iqecpu
TEXT 'iqs*(pu)'
area 2 1
ashow 0 2 tefpu
text 'Te (pu)'
area 3 1
ashow 0 2 frpu
text 'Fr (pu)'

END

```



## APPENDIX B

### TMS320C25 ASSEMBLY PROGRAMS LISTING

#### B.1 Efficiency Optimization and Vector Control Programs

```
-----
;  INDIRECT VECTOR CONTROL WITH FUZZY LOGIC
;  EFFICIENCY OPTIMIZATION PROGRAM
;-----
;  GILBERTO C. D. SOUSA
;  UNIVERSITY OF TENNESSEE, KNOXVILLE.
;
;  THIS PROGRAM INCLUDES:
;      1 - VECTOR CONTROL FUNCTIONS
;      2 - SPEED COMPUTATION ROUTINE
;      3 - PI SPEED CONTROL
;      4 - ADC ISR FOR TWO CHANNELS
;      5 - DAC ISR
;      6 - DC LINK POWER CALCULATION
;      7 - SLIP GAIN COMPUTATION FOR VARIABLE FLUX
;      8 - FEED-FORWARD TORQUE COMPENSATION
;      9 - FUZZY EFFICIENCY OPTIMIZATION CONTROLLER
;     10 - TRANSITION CONTROL
;
;NOTE: USING DATA FROM 5 hp CLASS B MACHINE.
;
;-----
;          I/O PORT ADDRESS
;-----
MCNT:      EQU    0      ;Encoder pulse count.
TCNT:      EQU    1      ;Clock pulse count.
INSTU:     EQU    2      ;Inverter status READ.
INCOM:     EQU    2      ;Inverter command WRITE.
DATA:      EQU    8      ;Buffer data port.
ADDR:      EQU    9      ;Buffer address port.
READHOST:  EQU    10     ;Host read port.
REFRESH:   EQU    11     ;Enable buffer refresh.
DAC:       EQU    13     ;DAC latch.
HOSTSTAT:  EQU    14     ;Host status.
WRITEHOST: EQU    15     ;Host write port.
;
;-----
;          CONSTANTS
;-----
PRDC:      EQU    2000   ;Main sampling time (=0.2 msec).
Iderated:  EQU    12826  ;Rated Ids = 9.786 A (= 12826).
SLIPGAIN:  EQU    810    ;Rated slip gain.
NUMKSLC:   EQU    179    ;Numerator of SG (=LmRr/Lr).1 PU = 179
DT:        EQU    4000   ;Delta t for theta calculation.
TBL90:     EQU    512    ;90 degree offset.
SSAMPC:    EQU    5      ;Speed sampling time counter. (=1msec.)
```

```

STMAXC:      EQU      25          ;Max. speed sampling time. (5 ms)
DELWRCC:     EQU      32767-100 ; Max speed variation in 1 ms.

; ----- MEMORY MAPPED REGISTERS (ALREADY DEFINED IN RESMON)
;DRR:        EQU      0          ;A/D input data register
;TIM:        EQU      2          ;Timer.
;PRD:        EQU      3          ;Period register.
;IMR:        EQU      4          ;Interrupt mask register.
;GREG:       EQU      5          ;Global memory allocation register.
;
; ----- DEFINE CONSTANTS FOR PI CONTROLLER
K1C:         EQU      3929        ;3935 ;For kp=0.4 and ki=0.8: K1C=3935
K2C:         EQU      -3920       ;          ; K2C=-3927
IQMV:        EQU      322        ;|Iqe| limit / 64 = 322
;Maximum value of Iqs*=16.228 A (= 21270)

; ----- DEFINE CONSTANTS FOR FIRST ORDER FILTER1 (FOF)
;          FOR SLIP GAIN COMPUTATION AND FFTC.
;          CURRENTLY USING Tr = 0.10778 s.
A1C:         EQU      32465
B1C:         EQU      504
C1C:         EQU      19570
D1C:         EQU      151

; ----- DEFINE CONSTANTS FOR FOF OF Iqs*, for FFTC only!
A2C:         EQU      32442
B2C:         EQU      503
C2C:         EQU      21127
D2C:         EQU      163

; ----- DEFINE CONSTANTS FOR FOF OF Pdc.
A3C:         EQU      32702
B3C:         EQU      307
C3C:         EQU      6983
D3C:         EQU      32

; ----- CONSTANTS FOR FFTC ROUTINE.
Ideco:       EQU      6302        ;Linear region breakpoint.
Mbs2c:       EQU      21200       ;Coefficient for Lm computation (1.216e-03).
Lm0c:        EQU      20568       ;Linear value of Lm (0.06277 H).
Idmaxc:      EQU      17038       ;(32767-Idmax), Idmax=15729 (12A).
Idminc:      EQU      18350       ;(32768+Idmin)/2, Idmin=3932 (3A).
IMAX:        EQU      18830       ;Square of max. stator cur.(Imax=18.95^2).

; ----- CONSTANTS FOR TRANSITION CONTROL.
TOLex:       EQU      300         ;Limit to exit eff. opt. mode.
TOLst:       EQU      100        ;Limit to start eff. opt. mode.

; ----- DEFINE CONSTANTS FOR FEOPT ROUTINE.
I1:          EQU      32767       ;Definition of fuzzy sets for DIds (Delta
I2:          EQU      22938       ; Ids* ).
I3:          EQU      13107
L3:          EQU      328         ;Def. of fuzzy sets for LDIds (Last DIds).
P1:          EQU      2154        ;Def. of fuzzy sets for DPi (Delta Pi).
P2:          EQU      1077
P3:          EQU      646

DPimaxc:     EQU      32767-100   ;Used to clamp (Pi(k)-Pi(k-1) to 100
; (43W).
L2limc:      EQU      32767-3277 ;Clamp LDIds to 3277.

CG1C:        EQU      2955        ;C1, C2 and C3 coef. for GID comp.

```

CG2C:	EQU	-31827	
CG3C:	EQU	1961	
G1C:	EQU	-3438	;Coefficients for GPb computation.
G2C:	EQU	5408	
GIDMAXC:	EQU	32767-1966	;Const. for max and min GID values.
GIDMINC:	EQU	16580	; == (32768+393)/2, min GID = 393.
GPBMAXC:	EQU	32767-6760	; Const. for max and min GPb comp.
GPBMINC:	EQU	18356	; == (32768+3943)/2, min GPb=3943.
Dldminc:	EQU	131	;Min. value for DIdc (==0.1 A).
RP12C:	EQU	7606	;1/(P1-P2).
RP23C:	EQU	19007	;1/(P2-P3).
RP3C:	EQU	12681	;1/P3.
RL23C:	EQU	9089	;1/(L2+L3).

```

;-----
;
;      DEFINE DATA RAM
;-----

```

```

;----- PAGE 0   SSV0 and SSVI must be in PAGE 0 !

```

	ORG	061H	
SSV0:	DS	1	
SSV1:	DS	1	
SSTEMP:	DS	1	

```

;----- PAGE 6

```

	ORG	00H	;On-board data RAM (Block B1).
OUTBFA:	DS	1	;Channel A output buffer.
OUTBFB:	DS	1	;Channel B output buffer.
COMMAND:	DS	1	;Host command word.
COMMAND2:	DS	1	;Value passed to TMSC25.
DISP:	DS	1	;Value passed to HOST.
HOSTBUF:	DS	1	;Buffer host status.
DUMMY:	DS	1	;Dummy register.

Vd:	DS	1	;DC link voltage.
Id:	DS	1	;DC link current.

```

;----- MAIN INTERRUPT (0.2 ms) ROUTINE.

```

THETA1:	DS	1
THETAH:	DS	1
We:	DS	1
Kslip:	DS	1
SIN:	DS	1
COS:	DS	1
Iqs:	DS	1
Ids:	DS	1
Ias:	DS	1
Ibs:	DS	1
RT34:	DS	1
TEMP0:	DS	1

```

;----- DATA BUFFER STORAGE VARIABLES.

```

BUFAL:	DS	1
BUFAH:	DS	1
COL:	DS	1
LOW:	DS	1
BFADATA:	DS	1
BFBDATA:	DS	1
TEMP2:	DS	1
SACCH:	DS	1
SACCL:	DS	1
ZERO:	DS	1

```

ONE:          DS      1

; ----- FEEDBACK SPEED COMPUTATION ROUTINE.
Wrst:         DS      1
STP:          DS      1
SSAMP:        DS      1
MNEW:         DS      1
MOLD:         DS      1
TNEW:         DS      1
TOLD:         DS      1
Wr1:          DS      1
WORLD:        DS      1
DELM:         DS      1
DELT:         DS      1
DELRWC:       DS      1

;----- DEFINE VARIABLES FOR PI CONTROLLER
IQH:          DS      1
IQL:          DS      1
ILIM:         DS      1      ;Limit for test of iqs*max (32767-IQMAX).
EK:           DS      1      ;Speed error e(k).
EK1:          DS      1      ;e(k-1).
WREF:         DS      1      ;Speed reference.
KWREF:        DS      1      ;Constant for RPM-->decimal conversion.
KBR:          DS      1      ; " " decimal -->RPM conversion.
IQMAX:        DS      1      ;IQMAX location.
K1:           DS      1      ;Modified PI gains.
K2:           DS      1

; ----- VARIABLES FOR HOST/DSP COMMUNICATION.
INCOMDATA:    DS      1
MSTEP:        DS      1      ;Main routine step.
VAR1:         DS      1      ;Buffer storage var. 1 (Ch. A).
VAR2:         DS      1      ;Buffer storage var. 2 (Ch. B).

; ----- VARIABLES FOR TRANSITION CONTROL.
FSS:          DS      1      ;Flag for steady state (1=ss, 0=dyn.mode).
CSS:          DS      1      ;Counter for state transition.
EOM:          DS      1      ;User defined Eff. Opt. Mode start/stop.

; ----- VARIABLES FOR NEW ADC.
PHIGH:        DS      1
PLOW:         DS      1
TREG:         DS      1
Idc:          DS      1
SPdH:         DS      1      ;Sum of Vd(k)*Idc(k)
SPdL:         DS      1

; ----- VARIABLES FOR Pdc COMPUTATION
SWT0:         DS      1      ;S/W timer 0: variable Ts, for Buffer storage
SWT1:         DS      1      ;S/W timer 1: 1 ms for PI speed and FFTC filter
SWT2:         DS      1      ;S/W timer 2: 50 ms for Pdc ave comp.
SWT3:         DS      1      ;S/W timer 3: 0.5 s for FEOPT, FFTC
Pdc:          DS      1      ;Pdc average over 50 ms
Pdck:         DS      1      ;Instantaneous Pdc(k)
TEMP:         DS      1      ;Used in ADCGIL
PTEMP:        DS      1      ;Used in computation of Pdck

; ----- VARIABLES FOR SLIP GAIN COMPUTATION (VARIABLE FLUX)
Idef:         DS      1      ;Filtered value of Ide (=flux/Lm)
xks:          DS      1      ;State variable for filter 1
A1:           DS      1      ;Constants for filter 1

```

```

B1:          DS      1
C1:          DS      1
D1:          DS      1
NUMKSL:      DS      1      ;Numerator for slip gain computation

; ----- VARIABLES FOR FFTC
DIde:        DS      1      ;Delta Ide
Alde:        DS      1      ;Auxiliary Ide
Ide:         DS      1      ;Ids*
Lm:          DS      1      ;Magnetizing inductance
Mbs2:        DS      1      ;Coefficient for Lm computation
Nfdre:       DS      1      ;New steady state estimate of rotor flux
fdre:        DS      1      ;Current value of flux estimate
DIqe:        DS      1      ;Delta Iqe
Iqep:        DS      1      ;Iqs*, from PI speed controller
AIqe:        DS      1      ;Actual Iqs*, including compensation
Iqe:         DS      1      ;Auxiliary variable (=Iqe)
SDIqe:       DS      1      ;Sum of Delta Iqs. Staircase shape
SDIqf:       DS      1      ;Output of 1st order filter (filtered SDIqe)
Idmax:       DS      1      ;(32767-Idmax)
Idmin:       DS      1      ;(32768-Idmin)/2
IP2:         DS      1      ;Is**2
Lm0:         DS      1      ;Linear value of Lm
xkf:         DS      1      ;State variable for 1st order filter FOFT
TLest:       DS      1      ;Torque estimate

; ----- VARIABLES FOR FEEDBACK SPEED SIGNAL
A2:          DS      1      ;Coefficients for filter FOFW
B2:          DS      1
C2:          DS      1
D2:          DS      1
XWK:         DS      1      ;State variable
Wr:          DS      1      ;Filtered speed signal
XKL:         DS      1      ;16 lsb of xkw (Speed fb)
XKLS:        DS      1      ;      xks      (Slip gain)
XKLT:        DS      1      ;      xkf      (Torque comp.)

; ----- TEST VARIABLES.
SWeH:        DS      1      ;Average computation of Wr
SWeL:        DS      1
Iqave:       DS      1
SPdH2:       DS      1
SPdL2:       DS      1

; ----- VARIABLES FOR Pdc FILTER
Pdc1:        DS      1      ;Original Pdc
Pd16:        DS      1      ;Pd ave. over 8 samples
Poffset:     DS      1
A3:          DS      1      ;Coefficients for filter FOFp
B3:          DS      1
C3:          DS      1
D3:          DS      1
xpk:         DS      1      ;State variable
XPL:         DS      1      ;16 lsb of xpk (Pdc filter)

; ----- DEFINE VARIABLES AND ADJUSTABLE CONSTANTS FOR FEOPT.
; ----- PAGE 7.
ORG          30h      ;Use data page 7 for FEOPT variables.

TLest2:      DS      1      ;Load torque estimate, dp 7.
Wr2:         DS      1      ;Speed, dp7.
DPi:         DS      1      ;DPi = Pi(k)-Pi(k-1).

```

CG1:	DS	1	;Coef. for GID computation
CG2:	DS	1	
CG3:	DS	1	
G1:	DS	1	;Coef. for GPb computation
G2:	DS	1	
GID:	DS	1	;Scale factor for Dids
GIDMAX:	DS	1	;Impose max. value to GID (32767-1966)
GIDMIN:	DS	1	;Impose min. value to GID (32767+655)/2
GPb:	DS	1	;Scale factor for DPi
GPbMAX:	DS	1	;Impose max. value to GPb (32767-17564)
GPbMIN:	DS	1	;Impose min. value to GPb (32767+4378)/2
Dldmin:	DS	1	;Dldmin is the min. value for DIdc
JP:	DS	1	;Interval index for DPi
MP1:	DS	1	;Degree of membership for DPi (Left)
MP2:	DS	1	;Same (right)
MI1:	DS	1	;Degree of membership for last Dids (Pos.)
MI2:	DS	1	;Same (Neg.)
MRA:	DS	1	;Truth value for rule A
MRB:	DS	1	; B
MRC:	DS	1	; C
MRD:	DS	1	; D
DIA:	DS	1	;Control signal due to rule A
DIB:	DS	1	; B
DIC:	DS	1	; C
DID:	DS	1	; D
Dids:	DS	1	;Per-unit value of delta Ids
DMONE:	DS	1	;Degree of membership value of one
RP12:	DS	1	; 1/(P1-P2)
RP23:	DS	1	; 1/(P2-P3)
RP3:	DS	1	; 1/P3
RL23:	DS	1	; 1/(L2+L3)
Pik:	DS	1	; Pdc(k)
Pik1:	DS	1	; Pdc(k-1)
DPimax:	DS	1	
L2lim:	DS	1	
SUMMR:	DS	1	; Sum of truth values of fired rules
SUMPROD:	DS	1	; Sum of products (sum of MRi*Dli, i=A,B,C,D)
TEMPi:	DS	1	; Temporary variable

```

;-----
;      RESET AND INTERRUPT VECTORS
;-----
;      ORG      0
;RESET:  B      INIT      ;Reset vector:currently in RESMON
;      ORG      4
INT1:    B      AINT      ;Channel A service interrupt routine
;      ORG      6
INT2:    B      BINT      ;Channel B service interrupt routine
;      ORG     24
INTT:    B      TINT      ;MAIN INTERRUPT (TIMER)
;      ORG     26
RCV:     B      ININT     ;ADC service interrupt routine

```

```

;-----
;      INITIALIZE PROCESSOR
;-----
;      ORG     1024      ;WITH RESMON ORG MUST BE 1024
INIT:    LDPK      0

```

```

LALK  PRDC
SACL  PRD          ;SET TIMER PERIOD
SOVM
SSXM          ;Set sign extension mode.
SPM  0          ;No shift in product register output
FORT  0          ;Configure for 16 bit word serial data
SXF          ;Set output channel flag
LACK  30        ;Enable RINT(16), AINT(2), BINT(4),TIMER(8)
SACL  IMR        ;Set interrupt mask register
LDPK  6
LACK  1
SACL  INCOMDATA
OUT   INCOMDATA,INCOM      ;Clear M and T counters

; ----- CONSTANT INITIALIZATION.
ZAC
SACL  SSAMP
LALK  DELWRCC
SACL  DELWRC

; ----- Initialization of task handler and speed computation
LDPK  6
IN    MOLD,MCNT      ;Initialize MOLD=MCOUNT
IN    TOLD,TCNT      ; "   TOLD=TCOUNT
ZAC
SACL  Wr1
SACL  Wr
SACL  Wref
SACL  TLest
SACL  WROLD
SACL  OUTBFA
SACL  OUTBFB
SACL  STP
LALK  SLIPGAIN
SACL  Kslip
LALK  28377
SACL  RT34

; ----- BUFFER INITIALIZATION
LACK  3
SACL  BUFAH
LALK  0FE00H
SACL  BUFAL
ZAC
SACL  VARI          ;Selection of variable to be stored
SACL  VAR2
SACL  ZERO
LACK  1
SACL  ONE

; ----- FILTER 1 INIT.: SLIP GAIN COMPUTATION UNDER VAR. FLUX
LALK  A1C          ;Initialize coefficients
SACL  A1
LALK  B1C
SACL  B1
LALK  C1C
SACL  C1
LALK  D1C
SACL  D1

LALK  A2C          ;Initialize coefficients for Wr filter
SACL  A2

```

```

LALK    B2C
SACL    B2
LALK    C2C
SACL    C2
LALK    D2C
SACL    D2

LALK    A3C           ;Initialize coefficients for Pdc filter
SACL    A3
LALK    B3C
SACL    B3
LALK    C3C
SACL    C3
LALK    D3C
SACL    D3

LALK    Iderated       ;Initialize Idef (always to rated value)
SACL    Idef
LALK    20133          ;Initialize xks to rated value (due to Ider)
SACL    xks
LALK    NUMKSLC        ;Initialize numerator of slip gain fraction
SACL    NUMKSL

; ----- INITIALIZE VARIABLES FOR PI CONTROLLER AND SPEED FILTER
ZAC
SACL    WR1            ;Original feedback speed
SACL    WR             ;Filtered feedback speed
SACL    XWK
SACL    WREF
SACL    Iqep
SACL    Iqe
SACL    IQH
SACL    IQL
SACL    EK1
LALK    K1C
SACL    K1
LALK    K2C
SACL    K2
LALK    IQMV
SACL    IQMAX          ;Store iqmv into IQMAX
LALK    32767
SUB     IQMAX ;
SACL    ILIM           ;ILIM = 32767 - IQMAX

; ----- INITIALIZE VARIABLES FOR Pdc COMPUTATION
LALK    5              ;Multiple of 0.2ms (50 <--> 10 ms)
SACL    SWT0           ;Counter for Buffer storage (variable)
LACK    5
SACL    SWT1           ;Counter for PI speed ctrl and FOF for FFTC
LALK    1000
SACL    SWT2           ;Counter for Pdc ave. computation
LALK    1000           ; 1000bits or 2 sec.
SACL    SWT3           ;Counter for FEOPT AND FFTC
ZAC
SACL    FSS            ;Initially FSS=0 (dynamic mode)
SACL    CSS            ;Counter for transition control
SACL    EOM            ;Eff. Opt. Mode (user defined)
SACL    Pd16           ;8 samples average
LARK    AR5,7          ;Counter for Pd16 average computation

; ----- INITIALIZE VARIABLES AND CONSTANTS FOR HOST/DSP COMM.
LALK    29320

```



```

SACL  KWREF  ;rpm to binary coef.
LALK  4578
SACL  KBR      ;Binary to rpm coef.

; ----- INITIALIZE VARIABLES AND CONSTANTS FOR FFTC
LALK  Mbs2c
SACL  Mbs2
LALK  Idmaxc    ;Current limits: Idmax = 12 A
SACL  Idmax     ;DIdmax=32767-Idmax
LALK  Idminc    ;      Idmin = 3 A
SACL  Idmin     ;DIdmin=(32768-Idmin)/2
LALK  Iderated  ;Rated Ide = 9.216 A for 5 hp m/c.
SACL  Ide
SACL  AIdc     ;AIdc is also initialized to Iderated
LALK  6335     ;Rated flux is 0.4833 Wb (=6335)
SACL  Nfdre
SACL  fdre     ;Both fdre and Nfdre are init. to rated values.
LALK  16340    ;Rated Lm (49.38 mH or 16340 bits)
SACL  Lm
LALK  Lm0c
SACL  Lm0

ZAC
SACL  SDIqc    ;Initialize to zero the remaining variables
SACL  SDIqf    ;Sum of delta Iqs*
SACL  DIde     ;Filtered version of SDIqc
SACL  DIqe     ;Delta Ide
SACL  xkf      ;Delta Iqe
SACL  TLest    ;State variable for FOFT
SACL  DISP     ;Torque estimate

SACL  XKL      ;Lsb of fof, speed, slip gain , torque comp.
SACL  XKLS
SACL  XKLT

; ----- INITIALIZE VARIABLES AND ADJUSTABLE CONST. FOR FEOPT
LDPK  7
LALK  CG1C     ;Coef. for GID computation
SACL  CG1
LALK  CG2C
SACL  CG2
LALK  CG3C
SACL  CG3

LALK  GIDMAXC  ;Max and min values for GID
SACL  GIDMAX
LALK  GIDMINC
SACL  GIDMIN

LALK  G1C      ;Coef. for GPb computation
SACL  G1
LALK  G2C
SACL  G2

LALK  GPbMAXC  ;Max and min values for GPb
SACL  GPbMAX
LALK  GPbMINC
SACL  GPbMIN

LALK  DIdmnc   ;Min value for DId
SACL  DIdmin

```

```

LALK    1000
SACL    DMONE           ;Value for degree of membership one
LALK    DPimaxc         ;Value used in the DPi max computation
SACL    DPimax
LALK    L2limc          ;Used for max LDIds computation
SACL    L2lim
ZAC
SACL    GID

; ----- Initialize constants for evaluation of degree of memb.
LALK    RP12C
SACL    RP12
LALK    RP23C
SACL    RP23
LALK    RP3C
SACL    RP3
LALK    RL23C
SACL    RL23

; -----
; BACKGROUND LOOP - HOST COMMUNICATION AND IDLE TIME
; -----
MAIN:    EQU    $
        EINT
        LDPK    6           ;Write selected variable to HOST
        OUT     DISP,WRITEHOST ;VAR ---> WRITEHOST (PA15)

; -----
; HOST/DSP16 COMMUNICATION ROUTINE
; -----
NCLUD HOSTDSP.ASM

; -----
; MAIN INTERRUPT ROUTINE
; -----
; ----- CONTEXT SAVE
; AR7 IS THE STACK POINTER ( AR7=124!)
TINT:    LARP    AR7
        LARK    AR7,124
        MAR     *-
        SSTI    *-
        SST     *-
        EINT
        SACH    *-
        SACL    *-
        SPH     *-
        SPL     *-
        MPYK    1
        SPL     *-
        LDPK    6

; -----
; PERFORM FEEDBACK SPEED COMPUTATION
; -----
        CALL    SPEED
        LAC     Wrl
        SACL    Wr

; -----
; PI SPEED CONTROL
; FIRST ORDER FILTERS FOR SLIP GAIN AND FFTC
; TRANSITION CONTROL ROUTINE
; -----

```

```

TS1MS: LDPK    6           ;1 ms sampling time routines
        LAC     SWT1       ;Check for the sampling time
        SUBK    1
        SACL    SWT1       ;Decrement counter SWT1
        BGZ     TS1RET
        LACK    5           ;5<-->1ms
        SACL    SWT1       ;Reload counter if zero
        CALL    PI          ;PI speed controller
        CALL    FOF1       ;Compute estimate of "flux" (Idef).
        CALL    FOFT       ;Get compensated Iqe, for FFTC
        CALL    FOFW       ;Filter for Iqs* (FFTC use only).
        CALL    TRCTL      ;Execute transition control routine
        CALL    FOFP       ;Compute filtered Pdc.
        CALL    AVE16      ;Average variables for monitoring only.
TS1RET: EQU     $

```

```

;-----
;      PERFORM BASIC VECTOR CONTROL FUNCTIONS
;-----
        CALL    VECROT      ;Original program: slip calc. + v.r

```

```

;-----
;      OUTPUT VARIABLES (FOR DAC)
;-----
        SPM     1
        LT      las         ;Compensates for DAC gain mismatches
        MPYK    203
        PAC
        ADDH    las
        SACH    las
        LAC     las

        ADDK    90          ;Offset compensation for DAC A
        SACL    OUTBFA      ;Channel A of DAC

        LT      lbs         ;Compensates for DAC gain mismatches
        MPYK    128
        PAC          ;PAC is the correct command here.
        ADDH    lbs
        SACH    lbs
        LAC     lbs
        ADDK    120         ;Offset compensation for DAC B
        SACL    OUTBFB      ;Channel B of DAC

```

```

;-----
;      COMPUTATION OF Pdc AVERAGE
;-----
        LDPK    6
        LAC     SWT2       ;Check for the sampling time of Pdc comput.
        SUBK    1
        SACL    SWT2       ;Decrement counter SWT2
        BGZ     PDCRET
        LALK    1000       ;SWT2 = 200 ms (1000 x 0.2 ms)
        SACL    SWT2       ;Reload counter if zero and
        CALL    PDCAVE      ;Compute Pdc ave.
PDCRET: EQU     $

```

```

;-----
;      FUZZY EFFICIENCY OPTIMIZATION AND
;      FEED-FORWARD TORQUE COMPENSATION
;-----
        LAC     FSS        ;Test operating mode

```

```

        BGZ      SSMD      ;If FSS = 1, go to steady state mode
        ZAC      ;Dyn. mode. Make SDIqe = 0
        SACL     SDIqe    ; ... and bypass FFTC and FEOPT
        B        FRET

SSMD:    LAC      SWT3      ;Check for the sampling time of FFTC AND FEOPT
        SUBK     1
        SACL     SWT3      ;Decrement counter SWT3
        BGZ      FRET
        LALK     10000     ;TIMER = 2 S (10000*0.2ms)
        SACL     SWT3      ;Reload counter if zero and
        CALL     FEOPT     ;Calculate DIde by fuzzy logic
        CALL     FFTC      ;Compute value of DIqe
FRET:    EQU      $

; -----
;          BUFFER STORAGE
; -----
; ----- SELECT THE VARIABLE TO BE STORED IN CHANNEL A
        SPM      1
        LDPK     6
        LAC      VAR1      ;*****
        SUBK     1          ;Case VAR1 = 1      ;*          VAR1 = 1  STORE:  Ide      *
        BNZ      VA2        ;*                  2          Iqe      *
        LAC      Ide        ;*                  3          Pdc      *
        SACL     DISP      ;*****
        B        VAEND

VA2:     SUBK     1          ;Case VAR1 = 2
        BNZ      VA3
        LAC      Iqe,1
        SACL     DISP
        B        VAEND

VA3:     SUBK     1          ;Case VAR1 = 3
        BNZ      VBSTART    ;Wrong value for VAR1; check VAR2
        LAC      Pd16       ;Pd16 is the 1.6 s average of Pdc
        SACL     DISP

VAEND:   SACL     BFADATA    ;Store selected variable into CH. A

; ----- SELECT THE VARIABLE TO BE STORED IN CHANNEL B
VBSTART:
        LDPK     6
        LAC      VAR2      ;*****
        SUBK     1          ;Case VAR2 = 1      ;*          VAR2 =      1          Pdc      *
        BNZ      VB2        ;*                  2          SDIqf   *
        LAC      Pdc        ;*                  3          Wr       *
        SUB      Poffset    ;*****
        SACL     DISP,5
        LAC      DISP
        B        VBEND

VB2:     SUBK     1          ;Case VAR2 = 2
        BNZ      VB3
        LAC      SDIqf,1    ;Torque compensating signal.
        SACL     DISP
        B        VBEND

VB3:     SUBK     1          ;Case VAR2 = 3
        BNZ      VAREND     ;Value of VAR2 is not valid; ignore it.

```

```

        LAC      Wr1,1      ;Speed.
        SACL     DISP
VBEND:  SACL     BFBDATA

;-----
;  BUFFER STORAGE SUBROUTINE
;-----
VAREND:  LDPK     6
        LAC      SWT0      ;Check for the sampling time of Buffer Storage.
        SUBK     1
        SACL     SWT0      ;Decrement counter SWT0
        BGZ      BUFRET    ;By-pass if not required
        LALK     100       ;SWT0 = 10 ms (variable) 50 x 0.2ms = 10ms
        SACL     SWT0      ;Reload counter if zero and
        CALL     BUFSTR    ;Perform buffer storage
BUFRET:  EQU     $

;----- CONTEXT RESTORE
        LARP          AR7
        MAR           *+
        MAR           *+
        LT            *-
        MPYK     1
        LT           *+
        MAR           *+
        LPH           *+
        ZALS          *+
        ADDH     *+
        DINT
        LDPK          0
        SST1          SSTEMP
        BIT           SSTEMP,0bh
        BBNZ     PPPP
        LDPK     6
        LST           *+
        EINT
        RET
PPPP:   LDPK     6
        LST           *+
        EINT
        RET

;-----
;  LIST OF INCLUDED SUBROUTINES
;-----
NCLUD  ADC.ASM      ;ADC interrupt service subroutine.
NCLUD  BUFSTO.ASM   ;Buffer storage subroutine
NCLUD  DAC.ASM      ;DAC interrupt service subroutine.
NCLUD  PI.ASM       ;PI speed controller.
NCLUD  SPEED.ASM    ;Feedback speed computation.
NCLUD  PDCOMP.ASM   ;Average DC link power computation.

NCLUD  FFTC.ASM     ;Feedforward pulsating torque compensation.
NCLUD  FEOPT.ASM    ;Fuzzy efficiency optimization controller.
NCLUD  FOFSG.ASM    ;First order filter for slip gain computation
NCLUD  FOFT.ASM     ;First order filter for Iqe compensation, FFTC
NCLUD  FOFW.ASM     ;First order filter for Iqs* (Use in FFTC only)
NCLUD  FOPP.ASM     ;First order filter for Pdc.
NCLUD  TRNCTRL.ASM  ;Transition control.
NCLUD  SIN.ASM      ;Table for sin/cos theta computation.
NCLUD  VR.ASM       ;Vector rotation.
NCLUD  AVE16.ASM    ;Average Pdc computation over 1.024 s.

```

```

;----- END OF PROGRAM -----
;
;-----
;      ADC INTERRUPT SERVICE ROUTINE
;-----
;      AR6 IS USED HERE TO STORE DRR CONTENT
;
ININT: EQU      $
          BIOZ    CHB          ;If channel B jump to CHB
;      ----- CONTEXT SAVE AND INPUT DRR CONTENT
          SST1    SSV1          ;SST1 and SST instr. always load into page 0!
          SST     SSV0
          LDPK    0
          LAR     6,DRR          ;Note that DRR is in DATA PAGE 0
          LDPK    6              ;Remaining of ISR are in DATA PAGE 6
          SACH    SACCH          ;Save ACC
          SACL    SACCL
          SPM     0
          SPH     PHIGH          ;Save P register
          SPL     PLOW
          MPYK    1              ;Save T register (PR=TR)
          SPL     TREG

CHA:     SAR     6,Vd
          B       CHEXT

CHB: SST1    SSV1          ;SST1 and SST instr. always load into page 0!
          SST     SSV0
          LDPK    0
          LAR     6,DRR          ;Note that DRR is in DATA PAGE 0
          LDPK    6              ;Remaining of ISR are in DATA PAGE 6
          SACH    SACCH          ;Save ACC
          SACL    SACCL
          SPM     0
          SPH     PHIGH          ;Save P register
          SPL     PLOW
          MPYK    1              ;Save T register (PR=TR)
          SPL     TREG
          SAR     6,Idc

;----- Compute Spd = sum of Vd(k)*Idc(k)
          LT      Vd
          MPY     Idc
          PAC
          SACH    TEMP,I          ;Now this LS of 1 is for product mode only!
          ZALH    SPdH
          ADDS    SPdL
          ADD     TEMP
          SACL    SPdL          ;SPdL and SPdH are in DATA PAGE 6
          SACH    SPdH

;      ----- CONTEXT RESTORE
CHEXT: ZALS    SACCL
          ADDH    SACCH          ;Restore ACC
          SPM     0
          LT      PLOW          ;Restore low P register
          MPYK    1              ;(TR)-->PRL
          LT      TREG          ;Restore T reg.
          LPH     PHIGH          ;Restore High P reg.
          LDPK    0
          LST1    SSV1          ;Restore status regs.
          LST     SSV0

```

```

        EINT                      ;Enable interrupts
        RET

;-----
;          AVERAGE COMPUTATION
;-----
; AVERAGE OF SELECTED VARIABLES OVER 1024 SAMPLES
AVE16:  LARP      5                ;Select AR5, down counter of 16
        BANZ      NZERO1          ;AR5=AR5-1, and test if AR5>0
        LALK      1024
        SACL      TEMP0
        LAR       AR5,TEMP0       ;Case AR5 = 0; Reinitialize to 1024
        ZALH      SWeH            ; and get average of We
        ADDS      SWeL
;        SACH      lqave,6         ;lqave, average over 1024 samples (1.024 s)

        ZALH      SPdH2           ; Also get average of Pdc
        ADDS      SPdL2
        SACH      Pd16,6         ;Pd16, average over 1024 samples (1.024 s)
        ZAC                      ;Reset summation.
        SACL      SWeH
        SACL      SWeL
        SACL      SPdH2          ;Reset summation
        SACL      SPdL2

; ----- Case AR5>0: Accumulate lqs (lqe) , Pdc (Ptemp)
NZERO1: ZALH      SWeH            ;Uses double precision to compute average.
        ADDS      SWeL
        ADD       lqe
        SACL      SWeL
        SACH      SWeH

        LALK      14062          ;Convert Pdc1 into Watts
        SACL      PTEMP
        LT        Pdc1
        MPY       PTEMP
        PAC
        SACH      PTEMP          ;New Pdc in WATTS.
        ZALH      SPdH2          ;Uses double precision to compute average.
        ADDS      SPdL2
        ADD       PTEMP          ;Add Pdc1(WATTS) to summation, SPd (H,L).
        SACL      SPdL2
        SACH      SPdH2
        RET

;-----
;          BUFFER STORAGE SUBROUTINE
;-----
; ----- DATA STORAGE CH-A
BUFSTR: ZALS      BUFAL
        ADDH      BUFAH
        ADDK      2
        SACH      BUFAH
        SACL      BUFAL
        SACH      TEMP0,7
        ANDK      1FEH
        SACL      LOW
        LAC       TEMP0
        ANDK      1FFH
        SACL      COL

        OUT       ONE,11

```

```

IN      TEMP0,8
OUT     LOW,ADDR
OUT     COL,ADDR
OUT     BFADATA,DATA ;White line in GRAPH
OUT     ZERO,11

; -----DATA STORAGE CH-B
LALK    1FFH
SUB     COL
BGZ     JMPFUL
LALK    0FE00H
SACL    BUFAL
LACK    3
SACL    BUFAH
JMPFUL: LAC    LOW
ADDK    1
SACL    LOW

OUT     ONE,11
IN      TEMP0,8
OUT     LOW,ADDR
OUT     COL,ADDR
OUT     BFBDATA,DATA ;Red line in GRAPH
OUT     ZERO,11
RET

; -----
; OUTPUT INTERRUPT SERVICE ROUTINE
; -----
; ----- Channel A
AINT:   EQU    $
SST     SSV0
LDPK    6
OUT     OUTBFA, DAC ;Load DAC LATCH
NOP
SXF                                ;Set output channel flag
LDPK    0
LST     SSV0
EINT                                ;Enable interrupts
RET                                ;Return from interrupt

; ----- Channel B
BINT:   EQU    $
SST     SSV0
LDPK    6
OUT     OUTBFB, DAC
NOP
RXF                                ;Reset output channel flag
LDPK    0
LST     SSV0
EINT                                ;Enable interrupts
RET                                ;Return from interrupt

; -----
; FUZZY EFFICIENCY OPTIMIZATION ROUTINE - FEOPT
; -----
; ----- START FEOPT
FEOPT:  SOVM                                ;Use overflow mode troughout FEOPT
SPM     1

```



```

; ----- Move some data from dp6 to dp7
LDPK    6
LAR     AR1,Wr
LAR     AR2,Pdc
LAR     AR3,TLest
LDPK    7
SAR     AR1,Wr2
SAR     AR2,Pik
SAR     AR3,TLest2

; ----- Compute GID, the scale factor for Dlds
LT      TLest2
ZALH    CG3          ;ACCH = C3
MPY     CG2          ;P = C2*TLest
LTA     CG1
MPY     Wr2          ;ACCH = C2*TLest+C3
APAC                    ;ACCH = C1*Wr+C2*TLest+C3 = GIDA

; ----- Perform test for max |GID|
ADDH    GIDMAX      ;Use saturation features to find max |GID|
SUBH    GIDMAX
SUBH    GIDMAX
ADDH    GIDMAX

; ----- Perform test for min |GID|
BGEZ    GGEZ        ;ACCH = GID
ADDH    GIDMIN      ;Case GID < 0
ADDH    GIDMIN
SUBH    GIDMIN      ;Use saturation features to find min |GID|
SUBH    GIDMIN      ;Actually GIDmin=(32768+minGID)/2
B       GIDEND
GGEZ: SUBH    GIDMIN      ;Case GID >= 0
SUBH    GIDMIN
ADDH    GIDMIN
ADDH    GIDMIN
GIDEND: SACH    GId      ;Final value for GId
;

; ----- Compute scale factor for DPi (GPb)
ZALH    G2          ;ACCH = G2, DP = 7
LT      G1
MPY     Wr2
APAC                    ;ACCH = G1*Wr + G2

; ----- Test for max and min GPb
ADDH    GPbmax      ;Max
SUBH    GPbmax
SUBH    GPbmin      ;Min
SUBH    GPbmin
ADDH    GPbmin
ADDH    GPbmin
SACH    GPb          ;Final value for GPb

; ----- Compute DPi (Pdc(k)-Pdc(k-1))*GPb
ZALH    Pik
SUBH    Pik1          ;ACCH = Pi(k)-Pi(k-1)
ADDH    DPimax        ;Clamp |DPi| to DPimax
SUBH    DPimax
SUBH    DPimax        ;DPimax = 32767 - max DPi
ADDH    DPimax

SACH    TEMPi,7      ;Now TEMPi = (Pi(k)-Pi(k-1)) 2**7
LT      GPb
MPY     TEMPi        ;P=(Pi(k)-Pi(k-1)) 2**7 GPb
PAC

```

```

SACH  DPi          ;Final value for DPi
DMOV  Pik          ;Pi(k)--> Pi(k-1)

; ----- Compute Degree of Membership for DPi
LAC   DPi
BGEZ  DPiGEZ
ADLK  P3           ;----- Case DPi<0
SACL  TEMPi       ;Check if it is in the interval 0, -P3
BLZ   NP1
LT    RP3         ;Case -P3<DPi<0
LACK  4           ;Interval index J = 4
SACL  JP
B      DPdone

NP1:   LAC   DPi          ;Compare DPi with -P2
ADLK  P2
BLZ   NP2
LT    RP23        ;Case -P2 < DPi < -P3
SACL  TEMPi
LACK  3           ;Interval index J = 3
SACL  JP
B      DPdone

NP2:   LAC   DPi
ADLK  P1
LT    RP12        ;Case -P1<DPi<-P2
SACL  TEMPi
LACK  2           ;Interval index J = 2
SACL  JP
B      DPdone

DPiGEZ: SBLK  P2          ;----- Case DPi > 0
BLZ   POS1        ;Test if P2 < DPi < P1
SACL  TEMPi       ;Case P2 < DPi < P1
LACK  7
SACL  JP          ;Interval index J = 7
LT    RP12
B      DPdone

POS1:  LAC   DPi
SBLK  P3
BLZ   POS2        ;Test if P3 < DPi < P2
SACL  TEMPi       ;Yes
LACK  6
SACL  JP          ;Interval index J = 6
LT    RP23
B      DPdone

POS2:  LACK  5          ;Case 0 < DPi < P3
SACL  JP          ;Interval index J = 6
LT    RP3
LAC   DPi
SACL  TEMPi

DPdone: MPY   TEMPi          ;ACC = MP2, D.M. of right MF for DPi
PAC
SACH  MP2,2
LAC   DMONE
SUB   MP2          ;ACC = 1 - MP2 = MP1
SACL  MP1

;
; ----- Compute DM for LDIds (=DIds, up to this point)

```

	ZALH	Dlds	
	ADDH	L2lim	;Limit  LDlds  to L2
	SUBH	L2lim	
	SUBH	L2lim	
	ADDH	L2lim	
	SACH	Dlds	;Now  Dlds <= L2
	LAC	Dlds	;Get DM for Positive MF
	ADLK	L3	
	SACL	TEMPi	;ACC = LDlds + L3
	LT	RL23	
	MPY	TEMPi	
	PAC		
	SACH	MII	;MII is the Positive MF of LDlds
	BGEZ	NEGMF	
	ZAC		
	SACL	MII	;MII = 0, since DPi < -L3
NEGMF:	ZAC		;Get DM for Negative MF
	SUB	Dlds	;ACC = -Dlds
	ADLK	L3	
	SACL	TEMPi	;ACC = -Dlds+L3
	MPY	TEMPi	;T = RL23, unchanged
	PAC		
	SACH	MI2	
	BGEZ	IDONE	;If MI2 > 0, the value is valid
	ZAC		
	SACL	MI2	;MI2 = 0, since computed DM<0
IDONE:	EQU	\$	
; ----- Perform rule base evaluation (Min operator)			
	LAC	MP1	;MRA = MIN(MP1,MI1)
	SACL	MRA	;Assume MRA = MP1
	SUB	MII	;ACC = MP1-MII
	BLEZ	NXT1	;Assumption is correct if ACC<=0
	LAC	MII	;No: MP1>MI1. Make MRA=MI1
	SACL	MRA	
NXT1:	LAC	MP1	;MRB = MIN(MP1,MI2)
	SACL	MRB	;Assume MRB = MP1
	SUB	MI2	;ACC = MP1-MI2
	BLEZ	NXT2	;Assumption is correct if ACC<=0
	LAC	MI2	;No: MP1>MI2. Make MRB=MI2
	SACL	MRB	
NXT2:	LAC	MP2	;MRC = MIN(MP2,MI1)
	SACL	MRC	;Assume MRC = MP2
	SUB	MII	;ACC = MP2-MII
	BLEZ	NXT3	;Assumption is correct if ACC<=0
	LAC	MII	;No: MP2>MI1. Make MRC=MI1
	SACL	MRC	
NXT3:	LAC	MP2	;MRD = MIN(MP2,MI2)
	SACL	MRD	;Assume MRD = MP2
	SUB	MI2	;ACC = MP2-MI2
	BLEZ	NXT4	;Assumption is correct if ACC<=0
	LAC	MI2	;No: MP2>MI2. Make MRD=MI2
	SACL	MRD	
NXT4:	EQU	\$	
; ----- Get control signal for each of the 4 fired rules			

```

; ----- Rule A
LAC    JP
SUBK   2           ;ACC = JP-2 (table offset)
ADLK   EFTBL       ;Points to Eff. Optimization Table
TBLR   DIA         ;Read DIA from table
ADDK   1           ;Change pointer to read DIC
TBLR   DIC         ;ACC = JP-1
; ----- Compute remaining control signals (DIB, DID)
LALK   DMONE
SUB     DIA
SACL   DIB         ;DIB = 1 - DIA, for this RB
LALK   DMONE
SUB     DIC
SACL   DID         ;DID = 1 - DIC, for this RB

; -----
; ----- DEFUZZIFICATION BY HEIGHT METHOD
; -----
; ----- Get sum of truth value of fired rules (MRA+MRB+MRC+MRD)
LAC     MRA
ADD     MRB
ADD     MRC
ADD     MRD
SACL   SUMMR       ;SUMMR = MRA+MRB+MRC+MRD

; ----- Get sum of products: MRi*Dli, i=A,B,C,D
LT      MRA
MPY     DIA
LTP     MRB         ;ACC = MRA*DIA
MPY     DIB
LTA     MRC
MPY     DIC
LTA     MRD
MPY     DID
APAC
SACH   SUMPROD     ;SUMPROD=MRA*DIA+....+MRD*DID

; ----- Divide SUMPROD BY SUMMR do get Dlds (Fractional division)
; Here, the sign of the result is defined by SUMPROD only
; since SUMMR is by def. always positive
ZALH   SUMPROD
ABS           ;Make numerator positive
RPTK   14
SUBC   SUMMR ;Result is in low ACC
SACL   Dlds

;
LAC     SUMPROD
BGEZ   DIVDONE   ;Done if sign is positive
ZAC
SUB     Dlds
SACL   Dlds       ;Negate quotient if negative

; ----- GET VALUE OF Dld IN AMPS
DIVDONE: LT      GID
MPY     Dlds
PAC
SACH   TEMPi     ;TEMPi = Dld

; ----- Impose minimum value for Dld to keep search active
ABS           ;ACCH = |Dlds|
SUBH   Dldmin
BGEZ   FEND

```

```

    LAC    TEMPi          ;Case |DId| < DIdmin. Make DId=DIdmin
    BGEZ   POSId
    ZAC                                ;Case DId < 0.
    SUB     DIdmin
    SACL    TEMPi          ;DId = -DIdmin
    LALK    -L3
    SACL    DId            ;Prevents |DId| < L3
    B       FEND

POSId: LAC    DIdmin          ;Case DId >= 0
    SACL    TEMPi          ;DId = +DIdmin
    LALK    L3
    SACL    DId            ;Prevents |DId| < L3

FEND:  ROVM
    LAC     TEMPi
    LDPK    6
    SACL    DId            ;Store new DId into dp 6
    RET

;
; -----
; ----- DEFINE THE TABLE FOR DM's FOR DId
EFTBL: DW     11,      12,      13,      0,      -13,      -12,      -12

;
; -----
; FEED FORWARD TORQUE COMPENSATOR
; -----
; ----- NEW VALUE FOR Ide = AId (Preliminary value)
FFTC:  LDPK    6 ;Select DP 6
    SPM        1          ;For product shift correction
    LAC        Ide
    ADD        DId        ;DId from FEOPT
    SACL       AId        ;Preliminary value of new Ide

;
; ----- CHECK FOR MAX AND MIN Ide (SAFETY REASONS)
SOVM          ;Use saturation features for test purpose
ZALH         AId        ;Idmax=15729 (== 12 A), Idmin=3932 (== 3 A)
ADDH         Idmax      ;Idmax = 32767-max Id
SUBH         Idmax      ;End of MAX test

SUBH         Idmin      ;Test for MIN Ide
SUBH         Idmin      ;Subtract and add twice since
ADDH         Idmin      ; ... Idmin = 0.5*(32768+Idmin)
ADDH         Idmin      ;End of MIN test
SACH         AId        ;AId now is between Idmin and Idmax
SUBH         Ide        ;Corrects DId in case AId violates limits
SACH         DId        ;DId = AId-Ide

; ----- COMPUTE ESTIMATE OF Lm
LAC          AId
ADLK         -Idc0      ;Idc0 is the linear region breakpoint
BGZ          GTRL
LALK         Lm0c       ;Case Ide<Idc0, linear region
SACL         Lm          ;Lm = Lm0
B            ENDL
GTRL:  SACL    TEMP      ;Case Ide>= Idc0, saturation region
    ZALH     Lm0        ;ACCH = Lm0
    LT       Mbs2
    MPY      TEMP        ;TEMP=Ide-Idc0
    SPAC     ACC         ;ACC = Lm0-Mbs2*(Ide-Idc0)
    SACH     Lm

```

```

; ----- ESTIMATE NEW VALUE OF ROTOR FLUX
ENDL:  LT      Lm
      MPY      Alde
      PAC
      ABS      ;ACC = Lm*Alde
      SACH     Nfdre      ;Flux has to be always positive (Safeguard for div.)
                        ;New steady state value of flux

; ----- COMPUTE DIqe - STEP SIZE FOR Iqe
;      IMPEMETATION: DIqe = 2 * {(fdre/2)/Nfdre - 1/2} * Iqe
; ----- DIVIDE NUMERATOR (NUMKSL=Rr/Lr) BY Idef TO GET Kslip
      ZALH     fdre      ;Numerator is placed in High ACC
      RC      ;0 --> C , Carry bit in ST1, before Rotation
      ROR      ;Devide numerator by 2 (fdre/2)
; ----- START FRACTIONAL DIVISION ROUTINE (Positive numbers only)
      RPTK     14
      SUBC     Nfdre      ;ACC = (fdre/2) / Nfdre
      ADLK     -16384      ;ACC = (fdre/2) / Nfdre - 1/2
      SACL     TEMP,1      ;TEMP = 2 * {(fdre/2) / Nfdre - 1/2 }, 1 LSHIFT = x 2
      LT      TEMP
      MPY      Iqave
      PAC
      SACH     DIqe      ;

; ----- GET NEW Iqe AND TEST FOR MAX STATOR CURRENT
      ADDH     Iqe      ;ACC=Iqe+DIqe
      SACH     AIqe
      SQRA     AIqe      ;Get AIqe**2
      ZAC
      SQRA     AIde      ;Get AIde**2; ACC=AIqe**2
      APAC     ;ACC = AIde**2 + AIqe**2 = Is**2
      SACH     IP2      ;IP2 = Is**2
      LAC      IP2
      ADLK     -IMAX      ;IMAX is the square of max. stator current
      BGZ      GTRIS      ;Branch if Is**2 > IMAX
      LAC      SDIqe      ;Case Is**2 < IMAX
      ADD      DIqe      ; Update SDIqe, sum of DIqe
      SACL     SDIqe
      DMOV     AIde      ;AIde --> Ide
      DMOV     Nfdre      ;Nfdre --> fdre for next iteration
      B        ENDIS

GTRIS: ZAC      ;Case Is**2 > IMAX, neglect changes
      SACL     DIqe

ENDIS: SPM      0      ;Restore for compatibility with old routines
      RET

```

```

; -----
;      FIRST ORDER FILTER FOR Pdc SIGNAL
; -----
;      TAL = 500 ms
;      Tsamp = 1 ms
; *****
;      * y(k) = c x(k) + d u(k) *      * y<==>Pdc  u<==>PdcI *
;      * x(k+1) = a x(k) + b u(k) *      * a<==>A3  b<==>B3 *
;      * c<==>C3  d<==>D3 *
;      * x(k)<==>xpk x(k+1)<==>xpkI *
;      * *****
; ----- COMPUTE Pdc - Filtered version of PdcI
FOFP:  LDPK     6

```

```

SPM      1
ZAC
LT       xpk
MPY      C3
LTA      Pdc1      ;ACC = c x(k) , T = u(k)
MPY      D3
APAC     ;ACC = c x(k) + d u(k)
SACH     Pdc
ZAC
MPY      B3      ;T = u(k) has not changed
LTA      xpk      ;ACC = b u(k) , T = x(k)
MPY      A3
APAC     ;ACC = a x(k) + b u(k)
ADDS     XPL      ;Add 16 lsb from last iteration
SACH     xpk      ;Actually x(k+1) --> x(k) for next iteration
ANDK     65280     ;Get upper half of ACCL
SACL     XPL      ;Save 16 lsb for next iteration
RET

```

---

SLIP GAIN COMPUTATION, INCLUDING FIRST ORDER FILTER

---

Tr = 0.1073s (Rotor time constant)

Tsamp = 1 ms

```

*****
*      y(k) = c x(k) + d u(k)*      * y<==>Idef  u<==>Nfdre      *
*      x(k+1) = a x(k) + b u(k)*      * a<==>A1    b = 1          *
*****                                * c<==>C1    d<==>D1          *
*      x(k)<==>xks x(k+1)<==>xk1s *
*****

```

```

FOF1:  SPM      1
ZAC
LT      xks
MPY      C1
LTA      Nfdre      ;ACC = c x(k) , T = u(k)
MPY      D1
APAC     ;ACC = c x(k) + d u(k)
SACH     Idef
ZAC
MPY      B1      ;T = u(k) has not changed
LTA      xks      ;ACC = b u(k) , T = x(k)
MPY      A1
APAC     ;ACC = a x(k) + b u(k)

ADDS     XKLS      ;Add 16 lsb from last iteration
SACH     xks      ;Actually x(k+1) ---> x(k) for next iteration
ANDK     65280     ;Take upper half of ACCL (65280=FF00h)
SACL     XKLS      ;Save 16 lsb for next iteration

```

; -----DIVIDE NUMERATOR (NUMKSL=Rr/Lr) BY Idef TO GET Kslip

```

LAC      Idef
ABS      ;Get abs of Idef to avoid error (Idef>0 always)
SACL     Idef
ZALH     NUMKSL      ;Numerator is placed in High ACC

```

; ----- START DIVISION ROUTINE (Positive numbers only)

```

RPTK     14
SUBC     Idef
SACL     Kslip
RET

```

```

;-----
; FIRST ORDER FILTER FOR FFTC - COMPUTATION OF SDIqf
;-----
; Tr = 0.1819s (Rotor time constant)
; Tsamp = 1 ms
;*****
; * y(k) = c x(k) + d u(k) * * y<==>Idef u<==>SDIqe *
; * x(k+1) = a x(k) + b u(k) * * a<==>A1 b = B1 *
;*****
; * c<==>C1 d<==>D1 *
; * x(k)<==>xkf x(k+1)<==>xk1f *
;*****
;----- COMPUTE SDIqf - Filtered version of SDIqe
FOFT: LDPK 6
      SPM 1
      ZAC
      LT xkf
      MPY C1
      LTA SDIqe ;ACC = c x(k) , T = u(k)
      MPY D1
      APAC ;ACC = c x(k) + d u(k)
      SACH SDIqf
      ZAC
      MPY B1 ;T = u(k) has not changed
      LTA xkf ;ACC = b u(k) , T = x(k)
      MPY A1
      APAC ;ACC = a x(k) + b u(k)

      ADDS XKLT ;Add 16 lsb from last iteration
      SACH xkf ;Actually x(k+1) ----> x(k) for next iteration
      ANDK 65280 ;Take upper half of ACCL (65280=ff00h)
      SACL XKLT ;Save 16 lsb for next iteration

;----- GET COMPENSATED Iqe
      LAC Iqep ;Iqep from PI speed controller
      ADD SDIqf ;Iqe = Iqep + SDIqf
      SACL Iqe

;----- COMPUTE TORQUE ESTIMATE, TLest
      LT Iqave ; As FEOPT is called before FFTC, we use
      MPY fdre ; Iqave(Iqs*) and fdre to estimate TL
      PAC
      SACH TLest
      RET

;-----
; FIRST ORDER FILTER FOR Iqs* (Used in FFTC only)
;-----
; TAL = 0.1 sec
; Tsamp = 1 ms
;*****
; * y(k) = c x(k) + d u(k) * * y<==>Iqave u<==>Iqe *
; * x(k+1) = a x(k) + b u(k) * * a<==>A2 b<==>B2 *
;*****
; * c<==>C2 d<==>D2 *
; * x(k)<==>xwk x(k+1)<==>xwk1f *
;*****
;----- COMPUTE Iqave, filtered version of Iqs*
FOFW: LDPK 6
      SPM 1
      ZAC

```



```

LT      xwk
MPY     C2
LTA     Iqe      ;ACC = c x(k) , T = u(k)
MPY     D2
APAC
SACH    Iqave    ;ACC = c x(k) + d u(k)
ZAC     ;Correct result before storing ( * 2 )
MPY     B2      ;T = u(k) has not changed
LTA     xwk      ;ACC = b u(k) , T = x(k)
MPY     A2
APAC    ;ACC = a x(k) + b u(k)
ADDS    XKL      ;Add 16 lsb from last iteration
SACH    xwk      ;Actually x(k+1) --> x(k) for next iteration
ANDK    65280    ;Get upper half of ACCL
SACL    XKL      ;Save 16 lsb for next iteration
RET

; -----
;   HOST COMMUNICATION ROUTINE
; -----
LAC     MSTEP
BZ      SBF0      ;MSTEP=0
SUBK    I
BZ      SBF1      ;MSTEP=1
SUBK    1
BZ      SBF2      ;MSTEP=2
ZAC     ;MSTEP value is incorrect, make MSTEP=0
SACL    MSTEP

; ----- CASE MSTEP=0 : READ FIRST VALUE FROM HOST (Code)
SBF0:   IN      HOSTBUF, HOSTSTAT;Read host status
DINT
BIT     HOSTBUF, 15      ;Test host status
BBZ     MAIN            ;Loop if no data is available
EINT
IN      COMMAND, READHOST ;Read host 1st data (COMMAND)
CALL    CASEA           ;Single command functions
B       MAIN

; ----- CASE MSTEP=1 : READ SECOND VALUE FROM HOST (Par. value)
SBF1:   IN      HOSTBUF, HOSTSTAT ;Read host status
DINT
BIT     HOSTBUF, 15      ;Test host status
BBZ     MAIN            ;Loop if no data is available
EINT
IN      COMMAND2, READHOST ;Read host 2nd data (COMMAND2)
LACK    2              ;Make MSTEP=2
SACL    MSTEP
B       MAIN

; ----- CASE MSTEP=2 : FUNCTIONS THAT REQUIRE 2 COMMANDS.
;   IDENTIFY AND STORE INFORMATION IN PROPER PARAM./VAR.
SBF2:   ZAC     ;Set MSTEP=0
SACL    MSTEP

; ----- S0 THROUGH S6 TEST FOR EACH PARTICULAR COMMAND(INSTRUCTION)
S0:     LAC     COMMAND
SUBK    2              ;COMMAND=2? (Wref input)
BNZ     S1            ;NO: Test next condition

SPM     2
ZAC

```

	LT	COMMAND2	;YES: Read Wref (in rpm)
	MPY	KWREF	; and convert it to software value
	APAC		
	SACH	WREF	;Now Wref is correct software value
	SPM	0	
	B	CMDEND	
S1:	LAC	COMMAND	
	SUBK	6	
	BNZ	S2	;COMMAND=6 (Def. Buffer A var.)
	LAC	COMMAND2	
	SACL	VAR1	;VAR1 is the code for 1st var.
	B	CMDEND	
S2:	LAC	COMMAND	
	SUBK	7	;COMMAND=7 (Def. Buffer B var.)
	BNZ	S3	
	LAC	COMMAND2	
	SACL	VAR2	;VAR2 is the code for 2nd var.
	B	CMDEND	
S3:	LAC	COMMAND	
	SUBK	8	
	BNZ	S4	;COMMAND=8 (Input Poffset)
	LAC	COMMAND2	; Offset value for Pdc.
	SACL	Poffset	
	B	CMDEND	
S4:	LAC	COMMAND	
	SUBK	9	;COMMAND=9 (Input K1 of PI
	BNZ	S5	; speed controller)
	LAC	COMMAND2	
	SACL	K1	
	LDPK	6	
	B	CMDEND	
S5:	LAC	COMMAND	
	SUBK	10	;COMMAND=10 (Input K2 of PI
	BNZ	S6	; speed controller)
	LAC	COMMAND2	
	SACL	K2	
	B	CMDEND	
S6:	LAC	COMMAND	;DEBUG FUNCTION
	SUBK	11	;COMMAND=11 (Input lde (ids*))
	BNZ	CMDEND	; set S/W timer 3 to 2500 and
	LAC	COMMAND2	; reset buffer storage
	SACL	lde	
	LALK	10000	
	SACL	SWT3	
	B	CMDEND	
CMDEND:	ZAC		;If the instruction was acknowledged
	SACL	MSTEP	; set MSTEP=0 and loop again
	B	MAIN	
; ----- RESET BUFFER STORAGE SUBROUTINE			
BUFSTO:	DINT		
	ZAC		
	SACL	BUFAH	
	SACL	BUFAL	
	SACL	COL	

```

SACL    LOW
EINT
RET

; ----- CASE A: Single instruction routines

CASEA:  LAC      COMMAND      ;COMMAND=0 :Stop system
        BNZ      CMD1
        LACK     1
        SACL     INCOMDATA
        OUT      INCOMDATA,INCOM
        B        AEND        ;INCON=1: Disable inverter gate

CMD1:   LAC      COMMAND      ;COMMAND=1 : Set rated flux
        SUBK     1
        BNZ      CMD2
        LACK     3
        SACL     INCOMDATA
        OUT      INCOMDATA,INCOM
        B        AEND        ;INCON=3 : Enable inverter gate

CMD2:   LAC      COMMAND      ;COMMAND=3: Start Eff. Opt. mode
        SUBK     3            ; with Buffer storage
        BNZ      CMD3
        LACK     1
        SACL     EOM          ;Set Efficiency Optimiz. Mode (=1)
        CALL     BUFSTO
        LALK     10000        ;Load S/W TIMER 3 for 0.5 s period
        SACL     SWT3
        B        AEND

CMD3:   LAC      COMMAND      ;COMMAND=4: Enter dynamic mode
        SUBK     4
        BNZ      CMD4
        ZAC
        SACL     EOM          ;Reset Efficiency Optimiz. Mode (=0)
        B        AEND

CMD4:   LAC      COMMAND      ;COMMAND=5: Start buffer storage
        SUBK     5            ; VAR1 and VAR2 define the vars.
        BNZ      CMD5        ; being stored
        CALL     BUFSTO
        B        AEND

CMD5:   LALK     1            ;Case of 2 instr. commands
        SACL     MSTEP        ; Make MSTEP=1 and return
        RET

AEND:   ZAC
        SACL     MSTEP        ;If the instruction was acknowledged
        RET                  ; set MSTEP=0 and return

```

```

; -----
; ROUTINE FOR Pdc (average) COMPUTATION
; -----

```

```

; NOTES: 1) AVERAGE IS COMPUTED EVERY 200 ms INTERVAL;
;         2) SPd=(SPH,SPdL) IS THE SUM OF Vd(k)*Idc(k) OVER 200 ms
;           (TRAPEZOIDAL RULE OF INTEGRATION), FROM ADC ISR
;         3) THE AVERAGE IS COMPUTED BY MAKING
;           SUM OF Vd(k)*Idc(k) FOR k = 1,10000} * {1/10000}
;         4) TO INCREASE RESOLUTION, THE SUM IS FIRST MULTIPLIED BY 2^3
;           AND THEN DIVIDED BY 2**16 (TAKING THE ACCH)

```



	SACL	SSAMP	
	LAC	STP	;STP = 0 --> Read M, T counts
	BZ	STP0	
	SUBK	1	
	BZ	STP1	;STP = 1 --> Compute new Wr
	ZAC		
	SACL	STP	;If STP not 0 or 1, reset to 0
STP0:			; STEP 0 : Read M (P.G.) and T (Clock)
	LAC	SSAMP	
	SBLK	SSAMPC	; =1msec
	BLZ	SFEXIT	
	IN	MNEW,MCNT	;Input M, T counters content
	IN	TNEW,TCNT	
	IN	TEMP0,MCNT	;Read MCNT again for security reasons
	LAC	TEMP0	
	SUB	MNEW	
	BNZ	SFEXIT	;If TEMP0 not = MNEW, neglect readings
	LAC	MNEW	; New data has been latched?
	SUB	MOLD	
	BZ	STP02	; No: Check if max Ts has elapsed.
; -----	Case	MNEW not= MOLD	
	LAC	SSAMP	; Greater than max sampling time?
	SBLK	STMAXC	
	BGZ	STP01	; Yes: speed is close to 0. Branch to STP01
			; No: Data is valid; proceed.
			; calc. delta M
	LAC	MNEW	
	SUB	MOLD	
	SACL	DELM,6	; dM=32*(MNEW-MOLD ) FOR CLASS B
	LALK	18641	; USE NEW PULSE ENCODER
	SACL	TEMP0	; FACTOR = 0.5689
	LT	TEMP0	; Overall: 1/7.0313 = 1/4 * 0.5689
	MPY	DELM	
	PAC		
	SACH	DELM,1	
	LAC	TNEW	
	SUB	TOLD	
	SACL	DELT	;DELT = TNEW - TOLD
	LACK	1	; Next iteration execute STP1
	SACL	STP	
	B	SFEXIT	
STP01:	ZAC		; SSAMP = 0, Wr = 0
	SACL	SSAMP	
	SACL	DELM	
	DMOV	MNEW	; MOLD <-- MNEW
	DMOV	TNEW	; TOLD <-- TNEW
	DMOV	Wr1	
	B	SFEXIT	
STP02:	LAC	SSAMP	
	SBLK	STMAXC	
	BLZ	SFEXIT	
	LACK	STMAXC	; SSAMP = Stmax, Wr = 0
	SACL	SSAMP	
	ZAC		
	SACL	DELM	; Originally was Wr
	B	SFEXIT	
STP1:	EQU	\$	; Compute new speed value

```

        LAC      DELM,15      ; WRTEMP = DELM / DELT
        ABS
        LARP     1
        LARK     1,15

STP11: SUBC      DELT
        BAZ      STP11

DTST: IN TEMP0,INSTU      ;Direction check.
        BIT      TEMP0,15
        BBZ      STP12
        NEG
        ;Negative speed.

; ----- SPEED VAR. LIMIT
STP12: SOVM      ; Set overflow mode to use saturation feature

        SUB      WROLD
        SACL     TEMP0      ;TEMP0 = Wmew - Wrold
        ZALH     TEMP0
        ADDH     DELWRC      ;Test for DELWRC > +DELWRC
        SUBH     DELWRC
        SUBH     DELWRC      ;Test for DELWRC < -DELWRC
        ADDH     DELWRC
        ADDH     WROLD
        SACH     Wr1      ;New value of Wr1, within limits of DELWRC
        ZAC      ;Reset counters
        SACL     SSAMP
        SACL     STP
        DMOV     MNEW      ; MOLD <-- MNEW
        DMOV     TNEW      ; TOLD <-- TNEW
        DMOV     Wr1      ; WROLD <-- Wr

SFEXIT: RET

; -----
;          TRANSITION CONTROL SUBROUTINE
; -----
TRCTL: LAC      FSS
        BGZ      FSS1      ;FSS=1 --> Steady state mode.
FSS0:   LAC      EK      ;EK = Wref-Wr
        ABS
        SBLK     TOLst
        BLEZ     CSST1
        RET      ;If EK> TOLst, stay in Dyn. mode

CSST1: LAC      CSS      ;EK<TOLst
        ADDK     1      ;Increment counter for steady state (ss) test
        SACL     CSS
        SUBK     3      ;CSS-3 >= 0 ?
        BGEZ     SS
        RET      ;No: stay in dynamic mode

SS:     LACK     1      ;Yes: ss mode has been detected.
        AND      EOM      ;AND with EOM flag, to allow operator control
        SACL     FSS      ;FSS = 1 indicates ss mode
        BZ       RTN      ;If FSS = 0, it is because EOM=0!

; ----- Initialize Pik1 and DIDs for the first iteration
        LDPK     6
        LALK     10000
        SACL     SWT3

```

```

        LALK    1400
        ADD     Pdc
        LDPK    7
        SACL    Pik1           ;Initialize Pik1 to Pdc+1400, such that DPi=NB
        LALK    -32767
        SACL    Dlds           ;Initialize LDlds to NB

RTN:    ZAC
        SACL    CSS           ;Reset counter
        RET

;----- Case FSS = 1. Check if a dyn. mode has come
FSS1:   LAC     EOM           ;Check if operator has terminated eff. opt. mode
        BZ      DYN           ;If EOM = 0, exit eff. opt mode, regardless of EK
        LAC     EK
        ABS
        SBLK    TOLex
        BGZ     CSST2         ;EK > TOLex ?
        RET          ;No: stay in ss mode

CSST2:  LAC     CSS           ;Yes: Make futher tests.
        ADDK    1             ;Increment counter, for dynamic test
        SACL    CSS
        SUBK    3             ;CSS >= 3 ?
        BGEZ    DYN           ;No: stay in ss mode
        RET

DYN:    ZAC                 ;Yes: make transition to dynamic mode
        SACL    FSS           ;FSS = 0 indicates ss mode
        SACL    CSS           ;Reset counter
        LALK    Iderated      ;Restore rated flux
        SACL    Ide
        LALK    6335          ;Rated flux for 5 hp class B m/c.
        SACL    fdre          ;Reset flux to rated value
        RET

```

```

;-----
;   PERFORM BASIC VECTOR CONTROL FUNCTIONS
;-----
VECROT: SPM    0
        LDPK    6
        ZALH    Wr           ;We computation. We = Wr + Kslip*Iqe
        LT      Kslip        ;As PM=0, net effect is Wr+(Kslip/2)*Iqe
        MPY     Iqe
        APAC
        APAC
        SACH    We

;----- Calc. angle theta
BP1:    ROVM                ;Reset overflow mode
        ZALH    THETAH
        ADDS    THETAL
        LT      We
        MPYK    DT
        APAC
        SACL    THETAL
        SACH    THETAH

;----- Get SIN(theta), COS(theta) from look-up table
SSXM    ;Set sign extension
LT      THETAH

```

```

        MPYK    2048
        PAC
        SACH    TEMP0
        LAC     TEMP0
        BGEZ    POSIN
        ADLK    1024          ;If negative, add 180 degrees
        ANDK    1023
;
NESIN: SOVM
        ADLK    SINTBL
        TBLR    SIN
        ADLK    TBL90
        TBLR    COS
        LAC     SIN
        NEG
        SACL    SIN
        LAC     COS
        NEG
        SACL    COS
        B       SINEND

POSIN: SOVM          ;Set overflow mode
        ADLK    SINTBL
        TBLR    SIN
        ADLK    TBL90
        TBLR    COS
SINEND: EQU    $

; ----- Synchronous to stationary conversion
;      Iqs= Iqe*cos+Ide*sin
;      Ids=-Iqe*sin+Ide*cos
        ZAC
        LT      SIN
        MPY     Ide
        LTA     COS
        MPY     Iqe
        APAC
        SACH    Iqs,l
        ZAC
        MPY     Ide
        LTA     SIN
        MPY     Iqe
        SPAC
        SACH    Ids,l
;
; ----- 2 TO 3 Phase conversion
        LAC     Iqs
        SACL    Ias
        ZAC
        SUB     Iqs,l4
        LT      Ids
        MPY     RT34
        SPAC
        SACH    Ibs,l
        LAC     Ibs
        RET          ; ----- End of vector rotation

```



## B.2 Slip Gain Tuning Assembly Programs.

```

;-----
; FUZZY LOGIC BASED SLIP GAIN TUNING
; FOR VECTOR CONTROL AC200 SYSTEM
;-----
;
; GILBERTO C. D. SOUSA
; UNIVERSITY OF TENNESSEE, KNOXVILLE.
;
;THIS VERSION INCLUDES:
;
; 1 - VECTOR CONTROL FUNCTIONS
; 2 - SPEED COMPUTATION ROUTINE
; 3 - PI SPEED CONTROL
; 4 - ADC ISR FOR TWO CHANNELS
; 5 - DAC ISR
; 6 - REVERSE VECTOR ROTATION FOR Vds AND Vqs
; 7 - FILTER FOR Vds AND Vqs
; 8 - DELTA Q, DELTA Vd COMPUTATION
; 9 - RULE BASE I - Kf COMPUTATION
; 10 - RULE BASE II - DELTA Ks COMPUTATION
;-----
;
; I/O PORT ADDRESS
;-----
;
MCNT: EQU 0 ;pulse cnt. read
TCNT: EQU 1 ;clock cnt. read
INSTU: EQU 2 ;inverter status READ
INCOM: EQU 2 ;inverter command WRITE

DATA: EQU 8 ;Buffer data port
ADDR: EQU 9 ;Buffer address port
READHOST: EQU 10 ;Host read port
REFRESH: EQU 11 ;Enable buffer refresh
DAC: EQU 13 ;DAC latch
HOSTSTAT: EQU 14 ;Host status
WRITEHOST: EQU 15 ;Host write port

;-----
;
; CONSTANTS
;-----
;
PRDC: EQU 2000 ;MAIN SAMPLING TIME=.2msec
Iderated: EQU 12080 ;RATED Ids = 9.216 A (= 12080)
SLIPGAIN: EQU 244 ;UNDER RATED Ids, SLIPGAIN==244
DT: EQU 4000 ; FOR THETA CALC.
TBL90: EQU 512 ;90 DEGREE
SSAMPC: EQU 5 ;SPEED SAMPLING=1msec
STMAXC: EQU 10 ;15=3msec MAX. SPEED SAMP. TIME
DELWRCC: EQU 32767-100 ; Max speed VARIATION IN 1 MS

;----- MEMORY MAPPED REGISTERS (ALREADY DEF. IN RESMON
;DRR: EQU 0 ;A/D Input data register
;TIM: EQU 2 ;TIMER
;PRD: EQU 3 ;PERIOD REG.
;IMR: EQU 4 ;Interrupt mask register
;GREG: EQU 5 ;Global memory allocation register
;
;----- DEFINE CONSTANTS FOR PI CONTROLLER
K1C: EQU 19637 ;For kp=2 and ki=0.2: K1C=19637
K2C: EQU -19635 ; : K2C=-19635
IQMV: EQU 391 ;|Iqe| limit / 64 == 391
;Maximum value of Iqs*=19.11 A == 25047

```

```

; ----- DEFINE CONSTANTS FOR FIRST ORDER FILTER: Vds, Vqs.
;      CURRENTLY USING TAL = 2 ms, fsamp = 25 KHz.
A1C:      EQU      29647
B1C:      EQU      3121
C1C:      EQU      31208
D1C:      EQU      1560

; ----- DEFINE CONSTANTS FOR FOF OF FEEDBACK SPEED
A2C:      EQU      31357
B2C:      EQU      2048
C2C:      EQU      22090
D2C:      EQU      706

; ----- DEFINE CONSTANTS FOR FIRST ORDER FILTER: CE
;      CURRENTLY USING TAL = 30 ms, Ts = 1ms.
A3C:      EQU      31694
B3C:      EQU      1074
C3C:      EQU      32231
D3C:      EQU      537

; ----- CONSTANTS FOR RULE BASE II, DKs COMPUTATION.
e1:      EQU      -19660 ;Membership functions for Error
e2:      EQU      -9830
e3:      EQU      -1966
e4:      EQU      3277
e5:      EQU      16384
e6:      EQU      32767

ce1:      EQU      6553 ;Membership function for CE.
ce2:      EQU      19660
ce3:      EQU      32767

dk1:      EQU      -32767 ;Rule base for DKs.
dk2:      EQU      -19660
dk3:      EQU      -13107
dk4:      EQU      -1311
dk5:      EQU      4915
dk6:      EQU      9830
dk7:      EQU      19660
dk8:      EQU      32767

; -----
;      DEFINE DATA RAM
; -----
;PAGE 0      SSV0 and SSV1 must be in PAGE 0!
ORG      061H
SSV0:      DS      1
SSV1:      DS      1
SSTEMP:    DS      1
; -----

;PAGE 6
ORG      00h ;Start of on-board data RAM (PAGE6)
OUTBFA:    DS      1 ;Channel A output buffer
OUTBFB:    DS      1 ;Channel B output buffer
COMMAND:    DS      1 ;Host command word
COMMAND2:   DS      1 ;Value passed to TMSC25
DISP:      DS      1 ;Value passed to HOST
HOSTBUF:    DS      1 ;Buffer host status

;----- MAIN INT.
THETAL:    DS      1

```

THETAH:	DS	1
We:	DS	1
Kslip:	DS	1
SIN:	DS	1
COS:	DS	1
Iqs:	DS	1
Ids:	DS	1
Ias:	DS	1
Ibs:	DS	1
RT34:	DS	1

;----- DATA SAVE

BUFAL:	DS	1
BUFAH:	DS	1
COL:	DS	1
LOW:	DS	1
BFADATA:	DS	1
BFBDATA:	DS	1
TEMP2:	DS	1
SACCH:	DS	1
SACCL:	DS	1
ZERO:	DS	1
ONE:	DS	1

; ----- SPEED FEEDBACK

STP:	DS	1
SSAMP:	DS	1
MNEW:	DS	1
MOLD:	DS	1
TNEW:	DS	1
TOLD:	DS	1
Wr1:	DS	1
WROLD:	DS	1
DELM:	DS	1
DELT:	DS	1
DELWRC:	DS	1

; ----- VECTOR CONTROL VARIABLES

Ide:	DS	1
Iqe:	DS	1
PHIGH:	DS	1
PLOW:	DS	1
TREG:	DS	1

;----- DEFINE VARIABLES FOR PI CONTROLLER

IQH:	DS	1	
IQL:	DS	1	
ILIM:	DS	1	;Limit for test of iqs*max (32767-IQMAX)
EK:	DS	1	;Speed error e(k)
EK1:	DS	1	;e(k-1)
WREF:	DS	1	;Speed reference
KWREF:	DS	1	;Constant for RPM-->decimal conversion
KBR:	DS	1	; " " decimal -->RPM conversion
IQMAX:	DS	1	;IQMAX location
K1:	DS	1	;PI gains (derived from, but not equal, kp,ki).
K2:	DS	1	

; ----- VARIABLES FOR HOST/DSP COMMUNICATION

INCOMDATA:	DS	1	
MSTEP:	DS	1	;MAIN ROUT. STEP
VAR1:	DS	1	;Buffer storage var. 1 (Ch. A)
VAR2:	DS	1	;Buffer storage var. 2 (Ch. B)

```

; ----- TIMERS FOR REAL TIME SCHEDULER
SWT0:      DS      1      ;S/W timer 0: variable Ts, for Buffer storage
SWT1:      DS      1      ;S/W timer 1: 1 ms for PI speed and SGT.
SWT2:      DS      1      ;Test of speed response

; ----- VARIABLES FOR FEEDBACK SPEED SIGNAL
A2:        DS      1      ;Coefficients for filter FOFW
B2:        DS      1
C2:        DS      1
D2:        DS      1
XWK:       DS      1      ;State variable
Wr:        DS      1      ;Filtered speed signal
XKL:       DS      1      ;16 lsb of xkw      (Speed fb)

; -----
; ----- VARIABLES FOR SLIP GAIN ROUTINES
; PAGE 6, CONTINUED.

; ----- VARIABLES FOR IVR.ASM: INVERSE VECTOR ROTATION
SVdH:      DS      1
SVdL:      DS      1
SVqH:      DS      1
SVqL:      DS      1
AV:        DS      1      ;Coefficients for temp. compensation
BV:        DS      1      ; of Vds and Vqs sensing.
RT123:     DS      1      ;1 / sqrt(3).
Talv:      DS      1      ;Tal for phase shift correction.

FSG:       DS      1      ;Flag for slip gain process.
Vds :      DS      1      ;Stationary frame D-Q voltages.
Vqs:       DS      1
Vde:       DS      1      ;Synchronous frame D-Q voltages
Vqe:       DS      1
TEMP0:     DS      1      ;Auxiliary variable
SIND:      DS      1      ;Unit vector with phase shift compensation.
COSD:      DS      1

; ----- VARIABLES FOR FILTER.ASM, Vde AND Vqe FILTER.
xkd1:      DS      1      ;Vde state variable for 1st filter.
xkd2:      DS      1      ;Vde state variable for 2nd filter.
Vde1:      DS      1      ;Output of first Vde filter.
Vdef:      DS      1      ;Final Vde, after 2nd filter.
xkq:       DS      1      ;Vqe state variable.
Vqef:      DS      1      ;Filtered Vqe.
xd1l:      DS      1      ;16 lsb of xkd1
xd2l:      DS      1      ;16 lsb of xkd2
xql:       DS      1      ;16 lsb of xkq
A1:        DS      1      ;Constants for filter Vde, Vqe filters
B1:        DS      1
C1:        DS      1
D1:        DS      1

; ----- VARS. FOR DELTAC.ASM, DELTA Q AND DELTA Vd COMP.
QE:        DS      1      ;Actual Q.
QEC:       DS      1      ;Command Q.
Qb:        DS      1      ;Base Q (= Kq+QEC).
Vdec:      DS      1      ;Command Vd.
Vqec:      DS      1
Vb:        DS      1      ;Base Vd.
TEMP1:     DS      1      ;Auxiliary variable.
KQ:        DS      1      ;Epson for Qb.
KV:        DS      1      ;Epson for Vd.

```

Lsb8:	DS	1	;Stator inductance (Lls+Lm)/4
Lsig:	DS	1	;Combined inductance with sat. (appr. Lls+Llr)
Lsigr:	DS	1	;Rated Lsig.
Rs:	DS	1	;Stator resistance.
NUM:	DS	1	;Auxiliary variable.
Asb2:	DS	1	
Cs:	DS	1	

; ---- Page 6, test variables

Iqave:	DS	1	;Average Iqe
SIqH:	DS	1	
SIqL:	DS	1	
Weave:	DS	1	;Average We
SWeH:	DS	1	
SWeL:	DS	1	
FLAG:	DS	1	;Speed response to square wave comm.
Vs:	DS	1	;Stator voltage magnitude.

; ----- RULE BASE 1 - Kf COMPUTATION, E AND CE COMPUTATION

; USING P. 7!

	ORG	0	
DVb4:	DS	1	;Delta Vd/4.
DEMAX:	DS	1	; = 32767 - 1024, Max. DE.
Wmax:	DS	1	;Upper bound for We (32767 - Wb)
Imax:	DS	1	;Upper bound for Iqe (32767 - Iqmax)
Wea:	DS	1	;Wea is the auxiliar We (bounded)
Iqea:	DS	1	;Iqea is the auxiliar Iqe (bounded)
RWb:	DS	1	;1/Wb, scaled
MWH:	DS	1	;Degree of membership HIGH for Wea.
MWL:	DS	1	;Degree of membership LOW for Wea.
DMONE:	DS	1	;Degree of membership one.
RIqr:	DS	1	;1/Iqr, scaled.
MIH:	DS	1	;Degree of membership HIGH for Iqea.
MIL:	DS	1	;Degree of membership LOW for Iqea.
MRA:	DS	1	;= MIN(MWH,MIH)
MRB:	DS	1	;= MIN(MWL,MIH)
MRC:	DS	1	;= MIN(MWH,MIL)
MRD:	DS	1	;= MIN(MWL,MIL)
Kf1:	DS	1	;Membership functions for Kf.
Kf2:	DS	1	
Kf3:	DS	1	
SUMPROD:	DS	1	;Sum of product: MRi*Kfn
SUMMR:	DS	1	;Sum of D.M.'s:MRA+...+MRD
Kf:	DS	1	;Weight factor between Q and Vd errors.
DQE:	DS	1	;Delta Q (error from Q model)
Err:	DS	1	;Combined error.
e1min:	DS	1	; -32766 + e1
EkcH:	DS	1	;Clamped Error at time k
Ekc_1H:	DS	1	
EkcL:	DS	1	
Ekc_IL:	DS	1	; " " from time k-1
GC:	DS	1	;Input gain for change in error.
DE:	DS	1	;Original delta error.
A3:	DS	1	;Coefficients for CE filters.
B3:	DS	1	

```

C3:          DS      1
D3:          DS      1

xkc1:        DS      1      ;State variables for CE filter.
xkc2:        DS      1
xcl1:        DS      1      ;16 lsb of xkc1
xcl2:        DS      1      ;16 lsg of xkc2
CE:          DS      1      ;Filtered change in error, bounded by c3.
TEMP3:       DS      1      ;Auxiliary variable for p. 7.

; ----- Rule base II variables and adjustable constants.
RE21:        DS      1      ; 1/(e2-e1), scaled.
RE32:        DS      1
RE3b2:       DS      1
RE4:         DS      1
RE54:        DS      1
RE65:        DS      1
RC1:         DS      1      ; 1/c1, scaled.
RC21:        DS      1
RC32:        DS      1
Ksmax:       DS      1      ;32767 - MaxKs (520) = 32247.
Ksmin:       DS      1      ;(32767 + MinKs(130))/2 = 16449
DKA:         DS      1      ;Rule A value.
DKB:         DS      1
DKC:         DS      1
DKD:         DS      1

ME1:         DS      1      ;Error membership value (left).
ME2:         DS      1
MC1:         DS      1      ;Change in error memb. value (left).
MC2:         DS      1
IJ:          DS      1      ;Offset for rule base look-up table.
IC:          DS      1      ;Row index.
JE:          DS      1      ;Column index.
DKs:         DS      1      ;Delta Ks.
TEMPi:       DS      1      ;Auxiliary variable.
GKs:         DS      1      ;Output gain.
KsH:         DS      1      ;High byte for slip gain.
KsL:         DS      1      ;Low byte for slip gain.

```

```

; -----
;          RESET AND INTERRUPT VECTORS
; -----
;          ORG      0
;RESET:    B        INIT      ;Reset vector:currently in RESMON
;          ORG      4
INT1:      B        AINT      ;Channel A service interrupt routine
;          ORG      6
INT2:      B        BINT      ;Channel B service interrupt routine
;          ORG      24
INTT:      B        TINT      ;MAIN INTERRUPT (TIMER)
;          ORG      26
RCV:       B        ININT     ;ADC service interrupt routine

; -----
;          INITIALIZE PROCESSOR
; -----
;          ORG      1024      ;WITH RESMON ORG MUST BE 1024

INIT:      LDPK      0
           LALK      PRDC

```

```

SACL   PRD           ;SET TIMER PERIOD

SOVM
SSXM           ;set sign extension mode
SPM   0           ;No shift in product register output
FORT   0           ;Configure for 16 bit word serial data
SXF           ;Set output channel flag
LACK   30          ;Enable RINT(16), AINT(2), BINT(4),TIMER(8)
SACL   IMR          ;Set interrupt mask register
LDPK   6
LACK   1
SACL   INCOMDATA
OUT    INCOMDATA,INCOM      ;Clear M and T counters

; ----- CONSTANT INITIALIZATION
ZAC
SACL   SSAMP
LALK   DELWRCC
SACL   DELWRC
LALK   5
SACL   SWT1
LACK   50
SACL   SWT0
LALK   300
SACL   SWT2
ZAC
SACL   FLAG

; ----- Initialization of task handler and speed computation
LDPK   6
IN      MOLD,MCNT      ;Initialize MOLD=MCOUNT
IN      TOLD,TCNT      ; "   TOLD=TCOUNT
ZAC
SACL   DELWr0          ;Case of constant acceleration.
SACL   Wr1
SACL   Wr
SACL   Wref
SACL   WROLD
SACL   OUTBFA
SACL   OUTBFB
SACL   STP
LALK   SLIPGAIN
SACL   Kslip
LALK   28377
SACL   RT34

; ----- BUFFER INITIALIZATION
LACK   3
SACL   BUFAH
LALK   0FE00H
SACL   BUFAL
ZAC
SACL   VAR1            ;Selection of variable to be stored
SACL   VAR2
SACL   ZERO
LACK   1
SACL   ONE

; ----- FILTER 1 INIT.: SLIP GAIN COMPUTATION UNDER VAR. FLUX
LALK   A1C            ;Initialize coefficients
SACL   A1
LALK   B1C

```

```

SACL BI
LALK CIC
SACL CI
LALK DIC
SACL DI

LALK A2C           ;Initialize coefficients for Wr filter
SACL A2
LALK B2C
SACL B2
LALK C2C
SACL C2
LALK D2C
SACL D2
LALK Iderated       ;Initialize Ide (always to rated value)
SACL Ide

; ----- INITIALIZE VARIABLES FOR PI CONTROLLER AND SPEED FILTER
ZAC
SACL WR1           ;Original feedback speed
SACL WR            ;Filtered feedback speed
SACL XWK
SACL WREF
SACL Iqe
SACL IQH
SACL IQL
SACL EKI
LALK K1C
SACL K1
LALK K2C
SACL K2
LALK IQMV
SACL IQMAX         ;Store iqmv into IQMAX
LALK 32767
SUB IQMAX          ;
SACL ILIM          ;ILIM = 32767 - IQMAX

; ----- INITIALIZE VARIABLES AND CONSTANTS FOR HOST/DSP COMM.
LALK 29320
SACL KWREF         ;rpm to binary coef.
LALK 4578
SACL KBR           ;Binary to rpm coef.

; ----- INITIALIZE VARS AND CONSTANTS FOR SLIP GAIN PROJECT
; ----- DELTAC ROUTINE (p. 6)
LALK 3224          ;Coefficients for temp. compensation
SACL AV            ; in Vds and Vqs sensing.
LALK -465
SACL BVs
LALK 18919
SACL RTI23         ;RTI23 = I / SQRT(3).
LALK 17731
SACL Lsb8
LALK 13548
SACL Lsigr         ;Rated Lsig.
SACL Lsig          ;Actual Lsig.
LALK 725
SACL Rs
LALK 4
SACL KQ            ;KQ = 0.5 VA or 4 bits.
LALK 131           ;KV = 1.6 V or 262 bits.
SACL KV            ;KV = 0.1 V or 16 bits.

```



```

LALK 24363 ;Coefficients for Lsig saturation effect.
SACL Asb2
LALK -31147
SACL Bsb2
LALK 20096
SACL Cs

; ----- FILTER ROUTINE (Vds AND Vqs FILTERS)
ZAC
SACL FSG ;Flag for slip gain process.
SACL xkd1
SACL xkd2
SACL xkq
SACL xd11
SACL xd21
SACL xql
LALK 12000 ;Now using isolation amp. circuit.
SACL Talv ;Measured time delay = 72.2 Micro sec.
LALK 10000 ;Stator voltage magnitude (Vs(0)).
SACL Vs

; ----- VARIABLES AND CONSTANTS FOR RULE BASE I
LDPK 7 ;Uses page 7
LALK 17019
SACL Wmax ;Wmax = 32767 - Wb(=15748).
LALK 7720
SACL lmax ;lmax = 32767 - lqrated (=25047).
LALK 3270
SACL DMONE ;DMONE = degree of membership 1.
LALK 6804
SACL RWb ;RWb = 1/Wb, scaled.
LALK 4278
SACL RIqr ;RIqr = 1/Iqrated.
LALK 26214
SACL Kf1 ;Kf1 = 0.8 (26214)
LALK 29490
SACL Kf2 ;Kf2 = 0.9 (29490)
LALK 32112
SACL Kf3 ;Kf3 = 0.98 (32112)
LALK -13107
SACL elmin ;elmin = -32768 - elmin (= -0.6*32768)
LALK 18431 ; For GC = 400, 18431.
SACL GC ;GC = remainder of 400/256.
LALK 31743 ;32686 ;
SACL DEMAX ;DEMAX = 32767 - max DE ( = 1024).

LALK A3C ;Initialize coefficients for CE filter
SACL A3
LALK B3C
SACL B3
LALK C3C
SACL C3
LALK D3C
SACL D3

ZAC
SACL xkc1 ;State var. for CE filter.
SACL xkc2
SACL xcl1
SACL xcl2 ;16 slb of xkc1, xkc2.

; ----- VARIABLES AND CONSTANTS FOR RULE BASE II.

```

```

LALK    10900          ;REmn = I / (em - en)
SACL    RE21
LALK    13625
SACL    RE32
LALK    27250
SACL    RE3b2
LALK    32700
SACL    RE4
LALK    8175
SACL    RE54
LALK    6540
SACL    RE65

LALK    16350          ;RCmn = I / (cm - cn).
SACL    RC1
LALK    8175
SACL    RC21
LALK    8175
SACL    RC32

LALK    32247
SACL    Ksmax          ;Ksmax = 32767 - maxKs.
LALK    16449
SACL    Ksmin          ;Ksmin = (32767+Ksmin)/2.

LALK    12452          ;Original gain = 82.
SACL    GKs            ;Output gain.

LALK    SLIPGAIN       ;Initialize Ksh with rated slip gain.
SACL    KsH
ZAC
SACL    KsL

;-----
; BACKGROUND LOOP - HOST COMMUNICATION AND IDLE TIME
;-----
MAIN:   EQU    $
        EINT
        LDPK    6          ;Write selected variable to HOST
        OUT     DISP,WRITEHOST ;VAR ----> WRITEHOST (PA15)

;-----
;          HOST/DSP16 COMMUNICATION ROUTINE
;-----
NCLUD  HOSTDSP.ASM

;-----
;          MAIN INTERRUPT ROUTINE
;-----
;----- CONTEXT SAVE
;          AR7 IS THE STACK POINTER ( AR7=124!)

TINT:   LARP    AR7
        LARK    AR7,124
        MAR     *.
        SSTI    *.
        SST     *.
        EINT
        SACH    *.
        SACL    *.
        SPH     *.

```

```

SPL      *.
MPYK     1
SPL      *.
LDPK     6

;-----
; PERFORM SLIP GAIN TUNING ROUTINES WITH Ts = 0.2 ms.
;-----
CALL     IVR          ;Reverse vector rotation (Vde, Vqe comp.)
CALL     FILTER       ;Vde and Vqe filters.

;-----
; PERFORM FEEDBACK SPEED COMPUTATION
;-----
CALL     SPEED
LAC      Wr1
SACL     Wr

;-----
; PI SPEED CONTROL
;-----
TSIMS:   LDPK         6          ;1 ms sampling time routines
          LAC          SWT1      ;Check for the sampling time
          SUBK         1
          SACL         SWT1      ;Decrement counter SWT1
          BGZ          TS1RET
          LACK         5          ;5<-->1ms
          SACL         SWT1      ;Reload counter if zero
          CALL         PI        ;PI speed controller

;-----
; PERFORM SLIP GAIN TUNING ROUTINES WITH Ts = 1 ms.
;-----
          LAC          FSG
          BZ           TS1RET     ;Slip gain tuning is active if FSG = 1.
          CALL         DELTAC     ;Delta Q and delta Vd computation.
          CALL         RBI        ;KF, E and CE computation.
          CALL         RBII       ;DKs, Ks computation.
TS1RET:   EQU          $

;-----
; PERFORM BASIC VECTOR CONTROL FUNCTIONS
;-----
CALL     VECROT ;Original program: slip calc. + v.r

;-----
; OUTPUT VARIABLES (FOR DAC)
;-----
SPM      1
LT       Ias          ;Compensates for DAC gain mismatches
MPYK     203
PAC
ADDH     Ias
SACH     Ias
LAC      Ias
ADDK     64          ;Offset compensation for DAC A
SACL     OUTBFA      ;Channel A of DAC

LT       Ibs          ;Compensates for DAC gain mismatches
MPYK     139
PAC
ADDH     Ibs

```

SACH	Ibs	
LAC	Ibs	
ADDK	115	;Offset compensation for DAC B
SACL	OUTBFB	;Channel B of DAC
CALL	AVE16	;1.024 sec average for Vdef, Vqef (monitoring ).

```

;-----
;          BUFFER STORAGE
;-----
;----- SELECT THE VARIABLE TO BE STORED IN CHANNEL A
;
SPM      1
LAC      VAR1
LDPK     6
SUBK     1          ;Case VAR1 = 1
BNZ      VA2
LDPK     7
LAC      Ekch
NEG
B        VAEND
;*****
;*****VAR1 = 1 STORE: Ekch *
;*****
;*****      2      Iqe      *
;*****      3      Wref      *
;*****

VA2:     SUBK     1          ;Case VAR1 = 2
BNZ      VA3
LAC      Iqe
NEG
B        VAEND

VA3:     SUBK     1          ;Case VAR1 = 3
BNZ      VBSTART          ;Wrong value for VAR1; check VAR2
Wref

VAEND:   LDPK     6
SACL     DISP
SACL     BFADATA          ;Store selected variable into CH. A

;----- SELECT THE VARIABLE TO BE STORED IN CHANNEL B
;
VBSTART: LDPK     6
LAC      VAR2
SUBK     1          ;Case VAR2 = 1
BNZ      VB2
LAC      Kslip,5
NEG
B        VBEND
;*****
;*****VAR2 = 1 STORE: Kslip *
;*****
;*****      2      CE      *
;*****      3      Iqe      *
;*****

VB2:     SUBK     1          ;Case VAR2 = 2
BNZ      VB3
LDPK     7
LAC      CE
B        VBEND

VB3:     SUBK     1          ;Case VAR2 = 3
BNZ      VAREND          ;Value of VAR2 is not valid; ignore it.
LDPK     6
LAC      Iqe

VBEND:   LDPK     6
SACL     BFBDATA
SACL     DISP

;-----
;          BUFFER STORAGE SUBROUTINE
;-----

```

```

VAREND:      LDPK      6
;-----
      LAC      SWT0      ;Check for the sampling time of Buffer Storage.
      SUBK     1
      SACL     SWT0      ;Decrement counter SWT0
      BGZ      BUFRET    ;By-pass if not required
      LACK     50        ;SWT0 = 10 ms (variable) 50 x 0.2ms = 10ms
      SACL     SWT0      ;Reload counter if zero and
      CALL     BUFSTR     ;Perform buffer storage
BUFRET: EQU   $

;----- CONTEXT RESTORE
      LARP     AR7
      MAR      *+
      MAR      *+
      LT       *-
      MPYK     1
      LT       *+
      MAR      *+
      LPH      *+
      ZALS     *+
      ADDH     *+

      DINT
      LDPK     0
      SST1     SSTEMP
      BIT      SSTEMP,0bh
      BBNZ     PPPP
      LDPK     6
      LST      *+
      EINT
      RET
PPPP:  LDPK     6
      LST      *+
      EINT
      RET

;-----
; LIST OF INCLUDED SUBROUTINES
;-----
NCLUD ADCSG.ASM      ;ADC INTERRUPT SERVICE ROUTINE
NCLUD BUFSTO.ASM     ; BUFFER STORAGE SUBROUTINE
NCLUD DAC.ASM        ;OUTPUT INTERRUPT SERVICE ROUTINE
NCLUD PICOMP.ASM     ;PI SPEED CONTROLLER
NCLUD SPEED.ASM      ; SPEED FEEDBACK SUBROUTINE
NCLUD FOFW.ASM       ;First order filter for speed, FOFW
NCLUD SIN.ASM        ;TABLE FOR SIN/COS COMPUTATION
NCLUD VR.ASM         ; BASIC VECTOR CONTROL FUNCTIONS

;-----
; SLIP GAIN TUNING FUNCTIONS
;-----
NCLUD IVR.ASM        ;Reverse vector rotation.
NCLUD FILTER.ASM     ;Vde and Vqe filters.
NCLUD DELTAC.ASM     ;Delta Q and delta Vd computation.
NCLUD RBI.ASM        ;Kf, E and CE computation.
NCLUD RBIL.ASM       ;DKs, Ks computation.
NCLUD AVE16.ASM      ;16 ms average for Vdef and Vqef.
NCLUD VSMOD.ASM      ;Stator voltage amplitude computation.
;----- END OF PROGRAM -----

```

```

; -----
;      Computation of DELTA Q and DELTA Vd
; -----
;
DELTAQ: SPM      1
        LDPK      6
        SOVM

; ----- Compute QE, actual Q from measurements
        LT        Vqef
        MPY        Ide
        LTP        Vdef          ;ACC = Vqef*Ide; TR = Vdef
        MPY        Iqe
        SPAC
        SACH      QE

; ----- Compute QEC, command Q from reference model
        SQRA      Ide
        LTP        Lsb8          ;TR = Ls/8, ACCH = Ide^2
        SACH      TEMP0          ;TEMP0 = Ide^2
        MPY        TEMP0
        PAC
        SACH      TEMP0,3        ;TEMP0 = 8* Ls/8 *Ide^2
        SQRA      Iqe
        LTP        Lsig          ;TR = Lsig, ACC = Iqe^2
        SACH      TEMP1          ;TEMP1 = Iqe^2
        MPY        TEMP1
        PAC
        ADDH      TEMP0          ;ACCH = Ls*Ide^2+Lsig*Iqe^2
        SACH      TEMP1
        LT        We
        MPY        TEMP1
        PAC
        SACH      QEC          ;QEC = We*(Ls*Ide^2+Lsig*Iqe^2)

        ADDH      KQ          ;Qb = QEC + KQ ;KQ = constant
        SACH      Qb

; ----- Compute DELTA Q, by division
        LAC        QEC
        SUB        QE
        SACL      NUM          ;NUM = QEC-QE

; ----- Clamp |QEC - QE| to Qb
        LALK      32767
        SUB        Qb
        SACL      TEMP1
        ZALH      NUM
        ADDH      TEMP1
        SUBH      TEMP1
        SUBH      TEMP1
        ADDH      TEMP1

; ----- Divide NUM BY Qb to get DQE (Fractional division)
;      Here, the sign of the result is given by NUM only,
;      since Qb is always positive
DST1:  ZALH      NUM
        ABS          ;Make numerator positive
        RPTK      14
        SUBC      Qb          ;Result is in low ACC
        SACL      TEMP1
        LAC      NUM

```

```

    BGEZ    DONE1      ;Done if sign is positive
    LAC     TEMPI
    NEG
    SACL    TEMPI      ;Negate quotient if NUM is negative

DONE1:  LAC     TEMPI
    LDPK    7
    SACL    DQE        ;DQE is now in p. 7!

    LDPK    6

; ----- Introduce saturation effect on Lsig.
;          xsr = A Is^4 + B Is^2 + C.
;          Lsig = Lsigr + xsr*Lsigr
    SQRA    Ide
    ZAC                                           ;PR = Ide^2.
    SQRA    Iqe                                           ;ACCH = Ide^2, PR = Iqe^2.
    APAC
    SACH    TEMP0                                           ;Is2 = Ide^2 + Iqe^2 = TEMP0.
    SQRA    TEMP0
    PAC
    SACH    TEMP1                                           ;Is4 = Is^4 = TEMP1.

    ZALH    Cs
    MPY     Bsb2                                           ;TR = Is2 has not changed.
    APAC                                           ;PR = (Bs/2) Is^2.
    LTA     TEMP1                                           ;ACCH = B*Is^2 + C.
    MPY     Asb2                                           ;TR = Is4.
    APAC                                           ;PR = (As/2) Is^4.
    LTA     Lsigr                                           ;ACCH = A Is^4 + B Is^2 + C = xsr = TEMP2.
    SACH    TEMP2
    ZALH    Lsigr                                           ;TR = Lsigr.
    MPY     TEMP2
    APAC                                           ;ACCH = Lsigr + xsr*Lsigr = Lsig.
    SACH    Lsig                                           ;Saturation compensated Lsig.

; ----- Perform computation of Vdec, commanded Vd
    LT      We
    MPY     Lsig                                           ;TR = We.
    LTP     Iqe                                           ;TR = Iqe, ACC = We*Lsig
    SACH    TEMP0                                           ;TEMP0 = We*Lsig
    MPY     TEMP0
    LTP     Ide                                           ;ACCH = We*Lsig*Iqe = TEMP0; TR = Ide
    SACH    TEMP0
    MPY     Rs
    PAC                                           ;ACCH = Rs*Ide
    SUBH    TEMP0
    SACH    Vdec                                           ;Vdec = Rs*Ide - TEMP0
    LAC     TEMP0
    ABS
    ADD     KV                                           ;KV is a constant
    SACL    Vb,2                                           ;Vb = 4*(KV + ABS(We*Lsig*Iqe))

; ----- Compute DELTA Vd, by division
    LAC     Vdef
    SUB     Vdec                                           ;Sign reversal is intentional!
    SACL    NUM                                           ;NUM = Vdef - Vdec
    LALK    32767
    SUB     Vb                                           ;Clamp |NUM| to 4*Vb
    SACL    TEMP1                                           ; to ensure proper fractional division.
    ZALH    NUM
    ADDH    TEMP1

```

```

SUBH    TEMP1
SUBH    TEMP1
ADDDH   TEMP1
SACH    NUM

; ----- Divide NUM BY Vb(x4) to get DVb4 (Fractional division)
; Here, the sign of the result is given by NUM only,
; since Vb is always positive
ZALH    NUM
ABS                                           ;Make numerator positive
RPTK    14
SUBC    Vb                                   ;Result is in low ACC
SACL    TEMP1
LAC     NUM
BGEZ    DONE2                               ;Done if sign is positive
LAC     TEMP1
NEG
SACL    TEMP1                               ;Negate quotient if NUM is negative

DONE2:  LAC     TEMP1
        LDPK    7
        SACL    DVb4
        LDPK    6
        RET

; -----
; FILTER FOR Vde AND Vqe
; -----
; fcf = 53.05 Hz (TAL = 3 ms) , fsamp = 5 KHz
;  $y(k) = c x(k) + d u(k)$ 
;  $x(k+1) = a x(k) + b u(k)$ 
;
; . Two cascade first order filters are used for Vde
; . One filter is used for Vqe
; . Discrete version of ECALC (first part of)
; -----
FILTER: SPM    1
        LT      xkd1
        MPY     C1
        LTP     Vde                               ;ACC = c x(k) , T = u(k)
        MPY     D1
        APAC                                         ;ACC = c x(k) + d u(k)
        SACH    Vde1                               ;Vde after first filter
        MPY     B1                                   ;T = u(k) has not changed
        LTP     xkd1                               ;ACC = b u(k) , T = x(k)
        MPY     A1
        APAC                                         ;ACC = a x(k) + b u(k)
        ADDS    xdl1                               ;Add 16 lsb from last iteration
        SACH    xkd1                               ;Actually x(k+1) --> x(k) for next iteration
        ANDK    65280                             ;Get upper half of ACCL
        SACL    xdl1                               ;Save 16 lsb for next iteration.

; ----- Get filtered version of Vde
        LT      xkd2
        MPY     C1
        LTP     Vde1                               ;ACC = c x(k) , T = u(k)
        MPY     D1
        APAC                                         ;ACC = c x(k) + d u(k)
        SACH    Vdef
        MPY     B1                                   ;T = u(k) has not changed
        LTP     xkd2                               ;ACC = b u(k) , T = x(k)

```



```

MPY      A1
APAC                                           ;ACC = a x(k) + b u(k)
ADDS     xd2l                                ;Add 16 lsb from last iteration
SACH     xkd2                                ;Actually x(k+1) ---> x(k) for next iteration
ANDK     65280                               ;Get upper half of ACCL.
SACL     xd2l                                ;Save 16 lsb for next iteration.

; ----- Get filtered Vqe (1st order only)
LT        xkq
MPY       C1
LTP       Vqe                                ;ACC = c x(k) , T = u(k)
MPY       D1
APAC                                           ;ACC = c x(k) + d u(k)
SACH     Vqef                                ;Filtered Vqe
MPY       B1                                ;T = u(k) has not changed
LTP       xkq                                ;ACC = b u(k) , T = x(k)
MPY       A1
APAC                                           ;ACC = a x(k) + b u(k)
ADDS     xql                                ;Add 16 lsb from last iteration
SACH     xkq                                ;Actually x(k+1) ---> x(k) for next iteration
ANDK     65280                               ;Get upper half of ACCL.
SACL     xql                                ;Save 16 lsb for next iteration.
RET

; -----
; REVERSE VECTOR ROTATOR FOR Vds AND Vqs COMPUTATION
; -----
; ----- Correct phase-shift due to analog filters
IVR:      SPM      0
; -----
LDPK      6
ROVM
ZALH      THETAH                                ;Angle from forward vector rotator
ADDS      THETAL
LT         We
MPY       Talv                                ;Correcting angle is proportional
SPAC                                           ; to We, when phase shift is small.
SACH      TEMP0                                ;Current Taleq = 9145 bits (457.3 Ms)

; ----- Compute shift-compensated unit vectors
SSXM
LT         TEMP0                                ;TEMP0 = Corrected angle
MPYK      2048
PAC
SACH      TEMP0                                ;Scaling to access SIN table
LAC       TEMP0
BGEZ      POSIND
ADLK      1024                                ;If negative, add 180 degrees
ANDK      1023                                ;Extract the first seven bits only.

NESIND:   SOVM
ADLK      SINTBL                                ;Add address offset
TBLR      SIND                                ;Retrieve sin(thetac)
ADLK      TBL90
TBLR      COSD                                ;Retrieve cos(thetac)
LAC       SIND
NEG
SACL      SIND                                ;Reverse sign of vectors
LAC       COSD

```

```

        NEG
        SACL    COSD
        B       SINED

POSIND: SOVM                      ;Case of positive angle
        ADLK    SINTBL
        TBLR    SIND
        ADLK    TBL90
        TBLR    COSD

SINED:  EQU     $

; ----- Make ADC offset corrections and temp. compensation
;         for Vds and Vqs sensing.
        SPM     1                  ;From this point on, use PM = 1.
        LAC     Vqs
        ADLK    164
        SACL    TEMP1              ;Offset compensation.
        LAC     Vds
        SUBK    40
        SACL    TEMP2

        LT      AV                  ;Temperature effect compensation.
        MPY     We
        PAC
        ADDH    BVs
        SACH    TEMP0              ;TEMP0 = Coefficient of correction for
                                   ;      temp. effect on Vds and Vqs.

        LT      TEMP0              ;TR = temp. coeff.
        MPY     TEMP1
        PAC
        ADDH    TEMP1
        SACH    TEMP1              ;TEMP1 = Vqs*(1 + coeff)
        MPY     TEMP2              ;TR = temp. coeff.
        PAC
        ADDH    TEMP2
        SACH    TEMP2              ;TEMP2 = Vds*(1 + coeff)

; ----- Stationary to synchronous frame conversion
;         Vqe= Vqs*COS-Vds*SIN
;         Vde= Vqs*SIN+Vds*COS
        LT      COSD
        MPY     TEMP1
        LTP     SIND              ;ACC = Vqs*COSD
        MPY     TEMP2
        SPAC                    ;ACC = Vqs*COSD - Vds*SIND = Vqe
        SACH    Vqe,l            ;Uses a new scale for voltage.!
        MPY     TEMP1            ;TR = SIND
        LTP     COSD              ;ACC = Vqs*SIND; TR = COSD
        MPY     TEMP2
        APAC                    ;ACC = Vqs*SIND + Vds*COSD
        SACH    Vde,l            ;Using new scale for voltage.
        RET

; -----
;         RULE BASE I - Kf COMPUTATION
;         ALSO E (Error) AND CE (Change in Error) COMPUTATION
; -----
;         NOTE: VARIABLES ARE DEFINED IN P. 7
RBI:    SPM     1
        LDPK    6

```

LAR	AR1,We	;Copy We and Iqe from p. 6 into p. 7.	
LAR	AR2,Iqe		
LDPK	7		
SAR	AR1,Wea		
SAR	AR2,Iqea		
SOVM		;Use overflow mode to clamp We, Iqe	
ZALH	Wea		
ABS		;Only module of We is relevant.	
ADDH	Wmax	;Clamp We to Wb = 2200 rpm.	
SUBH	Wmax		
SACH	Wea	;Wea is the auxiliar We	
ZALH	Iqea		
ABS		;Only module of Iqe is relevant.	
ADDH	Imax	;Clamp Iqe to Iqrated = 19.2 A.	
SUBH	Imax		
SACH	Iqea	;Iqea is the auxiliar Iqe	
; ----- Get degree of membership for Wea and Iqea			
LT	Wea		
MPY	RWb	;RWb is 1/Wb, scaled.	
PAC		;ACC = MWH, D.M. HIGH for Wea.	
SACH	MWH		
LAC	DMONE		
SUB	MWH	;ACC = 1 - MWH = MWL	
SACL	MWL		
LT	Iqea		
MPY	RIqr	;RIqr is 1/Iqr, scaled.	
PAC		;ACC = MIH, D.M. of right MF for Iqea	
SACH	MIH		
LAC	DMONE		
SUB	MIH	;ACC = 1 - MIH = MIL	
SACL	MIL		
; ----- Perform rule base evaluation (Min operator)			
LAC	MWH	;MRA = MIN(MWH,MIH)	
SACL	MRA	;Assume MRA = MWH	
SUB	MIH	;ACC = MP1-MIH	
BLEZ	NXT1	;Assumption is correct if ACC<=0	
LAC	MIH	;No: MP1>MIH. Make MRA=MIH	
SACL	MRA		
NXT1:	LAC	MWL	;MRB = MIN(MWL,MIH)
	SACL	MRB	;Assume MRB = MWL
	SUB	MIH	;ACC = MWL-MIH
	BLEZ	NXT2	;Assumption is correct if ACC<=0
	LAC	MIH	;No: MWL>MIH. Make MRB=MIH
	SACL	MRB	
NXT2:	LAC	MWH	;MRC = MIN(MWH,MIL)
	SACL	MRC	;Assume MRC = MWH
	SUB	MIL	;ACC = MWH-MIL
	BLEZ	NXT3	;Assumption is correct if ACC<=0
	LAC	MIL	;No: MWH>MIL. Make MRC=MIL
	SACL	MRC	
NXT3:	LAC	MWL	;MRD = MIN(MWL,MIL)
	SACL	MRD	;Assume MRD = MWL
	SUB	MIL	;ACC = MWL-MIL
	BLEZ	NXT4	;Assumption is correct if ACC<=0
	LAC	MIL	;No: MWL>MIL. Make MRD=MIL

```

NXT4:  SACL  MRD
      EQU   $

; -----
; ----- DEFUZZIFICATION BY HEIGHT METHOD
; ----- Get sum of truth value of fired rules (MRA+MRB+MRC+MRD)
      LAC   MRA
      ADD   MRB
      ADD   MRC
      ADD   MRD
      SACL  SUMMR          ;SUMMR = MRA+MRB+MRC+MRD

; ----- Get sum of products: MRi*Kfn, i=A,B,C,D, n=1,2,3
      LT    MRA
      MPY   Kf2
      LTP   MRB          ;ACC = MRA*Kf2, TR = MRB
      MPY   Kf3
      LTA   MRC
      MPY   Kf1
      LTA   MRD
      MPY   Kf2
      APAC
      SACH  SUMPROD       ;SUMPROD=MRA*Kf2+....+MRD*Kf2

; ----- Divide SUMPROD BY SUMMR do get Kf (Fractional division)
; ----- Here, the sign of the result is defined by SUMPROD only
; ----- since SUMMR is by def. always positive
      ZALH  SUMPROD
      ABS
      RPTK  14          ;Make numerator positive
      SUBC  SUMMR       ;Result is in low ACC
      SACL  Kf
      LAC   SUMPROD
      BGEZ  DIVDONE     ;Done if sign is positive
      ZAC
      SUB   Kf
      SACL  Kf          ;Negate quotient if negative
DIVDONE:EQU $

; ----- Compute Error (E) and Change in Error (CE).
      SPM   0          ;PM = 0 introduces GE = 0.5 automatically!
      LALK  -32767
      ADD   Kf
      SACL  TEMP3,2     ;TEMP3 = -4*(1 - Kf). As (1 - Kf)<0.2
                        ; no overflow occurs.

      LT    Kf
      MPY   DQE
      ZAC
      LTS   TEMP3       ;ACC = -0.5*Kf*DQE, TR = -4*(1 - Kf).
      MPY   DVb4        ;DVb4 = DVde / 4.
      APAC
      SACH  Err         ;Err = -0.5*(Kf*DQ + 4*(1-Kf)*DVb4)
      SPM   1          ;Restores PM to its normal value.

; ----- Now impose lower (e1) bound to Err
; ----- (Upper bound e6 has been enforced by OVM = 1)
      SUBH  elmin       ;elmin = -32767 + e1.
      ADDH  elmin
      SACH  EkcH        ;Ekc = Err, if Err > e1.
      SACL  EkcL        ;Stores in 32 bit to improve precision.

; ----- Compute Change in Error

```

```

SUBS    Ekc_1L
SUBH    Ekc_1H           ;Get delta error in extended precision.
ADDDH   DEMAX            ;Use saturation features to clamp DE to 1024
SUBH    DEMAX            ;DEMAX = 32767 - 1024 = 32665
SUBH    DEMAX
ADDDH   DEMAX
SACH    DE,5             ;Define DE = (Ekc - Ekc_1)*2^5.
DMOV    EkcH             ;Ekc --> Ekc_1.
DMOV    EkcL             ;Ekc --> Ekc_1.

; ----- Pass DE through filters to get CE (final change in error)
LT      xkc1
MPY     C3
LTP     DE                ;ACC = c x(k) , T = u(k)
MPY     D3
APAC                                         ;ACC = c x(k) + d u(k)
SACH    TEMP3            ;DE after first filter
MPY     B3                ;T = u(k) has not changed
LTP     xkc1             ;ACC = b u(k) , T = x(k)
MPY     A3
APAC                                         ;ACC = a x(k) + b u(k)
ADDD    xcl1             ;Add 16 lsb from last iteration
SACH    xkc1             ;Actually x(k+1) --> x(k) for next iteration
ANDK    65280            ;Get upper half of ACCL.
SACL    xcl1             ;Save 16 lsb for next iteration.

; ----- Second filter for DE
LT      xkc2
MPY     C3
LTP     TEMP3            ;ACC = c x(k) , T = u(k)
MPY     D3
APAC                                         ;ACC = c x(k) + d u(k) = filtered DE
ABS                                           ;Only module of DE is relevant.
SACH    CE,5             ;CE is the filtered version of DE * 2^5.
                                ;CE = 1024 * (E(k) - E(k-1))
MPY     B3                ;T = u(k) has not changed
LTP     xkc2             ;ACC = b u(k) , T = x(k)
MPY     A3
APAC                                         ;ACC = a x(k) + b u(k)
ADDD    xcl2             ;Add 16 lsb from last iteration
SACH    xkc2             ;Actually x(k+1) --> x(k) for next iteration
ANDK    65280            ;Get upper half of ACCL.
SACL    xcl2             ;Save 16 lsb for next iteration.
RET

; -----
; RULE BASE II - DELTA Ks COMPUTATION
; -----
RBII:   SOVM              ;Use overflow mode throughout RBII
        SPM               1
        LDPK              7           ;Uses page 7 throughout.

; ----- Compute Degree of Membership for ERROR (E)
LAC     EkcH
BGEZ    EGEZ
SBLK    e3                ;----- Case E<0
SACL    TEMPi,1           ;Check if it is in the interval (e3,0).
BLZ     NE1               ;Here TEMPi = 2 * (E - e3) to compensate for RE3b2.
LT      RE3b2             ;Case e3<E<0
LACK    3                 ;Interval index J = 3
SACL    JE

```

	B	Edone	
NE1:	LAC	EkcH	;Compare E with e2
	SBLK	e2	
	BLZ	NE2	
	LT	RE32	;Case e2 < E < e3
	SACL	TEMPi	
	LACK	2	;Interval index J = 2.
	SACL	JE	
	B	Edone	
NE2:	LAC	EkcH	
	SBLK	e1	
	LT	RE21	;Case e1 < E < e2
	SACL	TEMPi	
	LACK	1	;Interval index J = 1
	SACL	JE	
	B	Edone	
EGEZ:	SBLK	e5	;----- Case E > 0
	BLZ	POS1	;Test if e5 < E < e6
	SACL	TEMPi	;Case e5 < E < e6
	LACK	6	
	SACL	JE	;Interval index J = 6
	LT	RE65	
	B	Edone	
POS1:	LAC	EkcH	
	SBLK	e4	
	BLZ	POS2	;Test if e4 < E < e5
	SACL	TEMPi	;Yes
	LACK	5	
	SACL	JE	;Interval index J = 5
	LT	RE54	
	B	Edone	
POS2:	LACK	4	;Case 0 < E < e4
	SACL	JE	;Interval index J = 4
	LT	RE4	
	LAC	EkcH	
	SACL	TEMPi	
Edone:	MPY	TEMPi	
	PAC		;ACC = ME2, D.M. of right MF for E
	SACH	ME2	
	LAC	DMONE	
	SUB	ME2	;ACC = 1 - ME2 = ME1
	SACL	ME1	
; ----- Compute DM for Change in Error (CE).			
	LAC	CE	
	SBLK	ce2	;CE > 0 by definition.
	BLZ	PCE1	;Test if ce2 < CE < ce3
	SACL	TEMPi	;Case e5 < E < e6
	LACK	1	
	SACL	IC	;Interval index I = 1.
	LT	RC32	
	B	CEdone	
PCE1:	LAC	CE	
	SBLK	ce1	

```

        BLZ      PCE2      ;Test if ce1 < CE < ce2
        SACL     TEMPi     ;Yes
        LACK     2
        SACL     IC        ;Interval index I = 2
        LT       RC21
        B        CEdone

PCE2:   LACK     3          ;Case 0 < CE < ce1
        SACL     IC        ;Interval index I = 3
        LT       RC1
        LAC      CE
        SACL     TEMPi

CEdone: MPY      TEMPi
        PAC
        SACH     MC2      ;ACC = MC2, D.M. of right MF for CE.
        LAC      DMONE
        SUB      MC2
        SACL     MC1      ;ACC = 1 - MC2 = MC1

; ----- Perform rule base evaluation (Min operator)
        LAC      ME1      ;MRA = MIN(ME1,MC2)
        SACL     MRA      ;Assume MRA = ME1
        SUB      MC2      ;ACC = ME1-MC2
        BLEZ     NXK1     ;Assumption is correct if ACC<=0
        LAC      MC2      ;No: ME1>MC2. Make MRA=MC2
        SACL     MRA

NXK1:   LAC      ME2      ;MRB = MIN(ME2,MC2)
        SACL     MRB      ;Assume MRB = ME2
        SUB      MC2      ;ACC = ME2-MC2
        BLEZ     NXK2     ;Assumption is correct if ACC<=0
        LAC      MC2      ;No: ME2>MC2. Make MRB=MC2
        SACL     MRB

NXK2:   LAC      ME1      ;MRC = MIN(ME1,MC1)
        SACL     MRC      ;Assume MRC = ME1
        SUB      MC1      ;ACC = ME1-MC1
        BLEZ     NXK3     ;Assumption is correct if ACC<=0
        LAC      MC1      ;No: ME1>MC1. Make MRC=MC1
        SACL     MRC

NXK3:   LAC      ME2      ;MRD = MCN(ME2,MC1)
        SACL     MRD      ;Assume MRD = ME2
        SUB      MC1      ;ACC = ME2-MC1
        BLEZ     NXK4     ;Assumption is correct if ACC<=0
        LAC      MC1      ;No: ME2>MC1. Make MRD=MC1
        SACL     MRD

NXK4:   EQU      $

; ----- Get control signal for each of the 4 fired rules
; ----- Compute offset for look-up table. (IJ)
        LAC      IC,3     ;ACC = 8*IC
        SUB      IC       ;ACC = 7*IC
        ADD      JE
        SUBK     8        ;ACC = 7*IC+JE-8 = IJ
        SACL     IJ

        ADLK     SGTBL    ;Points to slip gain table
        TBLR     DKA      ;Read DKA from table
        ADDK     1        ;Change pointer to read DKB
        TBLR     DKB      ;ACC = IJ+1

```

```

        ADDK    6                ;Change pointer to read DKC
        TBLR    DKC              ;ACC = IJ+7
        ADDK    1                ;Change pointer to read DKD
        TBLR    DKD              ;ACC = IJ+8

; -----
; ----- DEFUZZIFICATION BY HEIGHT METHOD
; ----- Get sum of truth value of fired rules (MRA+MRB+MRC+MRD)
        LAC     MRA
        ADD     MRB
        ADD     MRC
        ADD     MRD
        SACL    SUMMR            ;SUMMR = MRA+MRB+MRC+MRD

; ----- Get sum of products: MRi*DKi, i=A,B,C,D
        LT      MRA
        MPY     DKA
        LTP     MRB            ;ACC = MRA*DKA
        MPY     DKB
        LTA     MRC
        MPY     DKC
        LTA     MRD
        MPY     DKD
        APAC
        SACH    SUMPROD         ;SUMPROD=MRA*DKA+....+MRD*DKD

; ----- Divide SUMPROD BY SUMMR do get DKs (Fractional division)
; ----- Here, the sign of the result is defined by SUMPROD only
; ----- since SUMMR is by def. always positive.
        ZALH    SUMPROD
        ABS
        RPTK    14              ;Make numerator positive
        SUBC    SUMMR           ;Result is in low ACC
        SACL    DKs

;
        LAC     SUMPROD
        BGEZ    DDONE2          ;Done if sign is positive
        ZAC
        SUB     DKs
        SACL    DKs            ;Negate quotient if negative

; -----
; ----- GET NEW VALUE OF Ks (SLIP GAIN)
; -----
DDONE2:
        LDPK    6
        LAC     SWT2            ;Introduce a delay after FSG is set,
        BZ      PROC
        SUBK    1                ; to store rated condition into buffer.
        SACL    SWT2            ;Decrement counter SWT2
        BGZ     QUIT

PROC:   LDPK    7
        LT      GKs
        MPY     DKs
        PAC
        SACH    TEMPi
        ZALH    KsH            ;Use double precision to compute Ks.
        ADDS    KsL
        ADD     TEMPi          ;Add to low ACC since GKs = 0.64 bit.

```



```

; ----- Impose min and maximum values for Ks, for safety reasons.
ADDH Ksmax ;Ksmax = 32767 - maxKs (maxKs = 2Kso = 520)
SUBH Ksmax
SUBH Ksmin ;Use saturation features to enforce min Ks.
SUBH Ksmin ;Actually Ksmin = (32768+minKs)/2
ADDH Ksmin ;Currently, minKs = 0.5 Kso = 130.
ADDH Ksmin

SACH KsH
SACL KsL
LDPK 6
SACH Kslip ;Kslip is the value used to get Wsl
QUIT: RET
;
; -----
; ----- DEFINE THE TABLE FOR DM's FOR Delta Ks
SGTBL: DW dk2, dk3, 0, 0, dk5, dk7, dk8
        DW dk1, dk2, 0, 0, dk5, dk7, dk8
        DW dk1, dk2, dk4, 0, dk5, dk8, dk7
        DW dk1, dk1, dk2, 0, dk5, dk8, dk8

```

## **VITAE**

Gilberto Costa Drumond Sousa was born in Faria Lemos, MG, Brazil on October 5, 1958. He attended city elementary and middle schools and went to the Federal Technical School of Espirito Santo, Vitoria, ES, finishing his High School studies in 1976. He received a B.S. degree in Electrical Engineering from the Federal University of Espirito Santo, (UFES) in 1981. He joined the faculty of UFES as an Auxiliary Professor in 1982. Then he went to the Federal University of Santa Catarina for his Master studies and received a M.Sc degree in Electrical Engineering in 1986. He returned to UFES as an Assistant Professor and from 1986 to 1989 taught several undergraduate courses at the Electrical Engineering Department. In 1989 he received a four-year scholarship from the National Research Council and joined the University of Tennessee, Knoxville, for his doctoral studies. He received his Ph.D. degree in Electrical Engineering in December 1993.

The author has been involved in research areas including Power Systems and Industrial Controls, and more recently, Fuzzy Logic applications to Power Electronics and Drives. He has published several papers on the areas listed above.